

SANDIA REPORT

SAND86-1745 • UC-66c

Unlimited Release

Printed September 1987

RS-8232-2/66289

C1

Development of a Method for Predicting the Performance and Wear of PDC Drill Bits



8232-2/066289



00000001 -

David A. Glowka

Prepared by
Sandia National Laboratories
Albuquerque, New Mexico 87185 and Livermore, California 94550
for the United States Department of Energy
under Contract DE-AC04-76DP00789

Issued by Sandia National Laboratories, operated for the United States Department of Energy by Sandia Corporation.

NOTICE: This report was prepared as an account of work sponsored by an agency of the United States Government. Neither the United States Government nor any agency thereof, nor any of their employees, nor any of their contractors, subcontractors, or their employees, makes any warranty, express or implied, or assumes any legal liability or responsibility for the accuracy, completeness, or usefulness of any information, apparatus, product, or process disclosed, or represents that its use would not infringe privately owned rights. Reference herein to any specific commercial product, process, or service by trade name, trademark, manufacturer, or otherwise, does not necessarily constitute or imply its endorsement, recommendation, or favoring by the United States Government, any agency thereof or any of their contractors or subcontractors. The views and opinions expressed herein do not necessarily state or reflect those of the United States Government, any agency thereof or any of their contractors or subcontractors.

Printed in the United States of America
Available from
National Technical Information Service
U.S. Department of Commerce
5285 Port Royal Road
Springfield, VA 22161

NTIS price codes
Printed copy: A10
Microfiche copy: A01

SAND86-1745
Unlimited Distribution
Printed June 1987

DEVELOPMENT OF A METHOD FOR PREDICTING
THE PERFORMANCE AND WEAR OF PDC DRILL BITS

David A. Glowka

Geotechnical Design Division 6314
Sandia National Laboratories
Albuquerque, New Mexico 87185

ABSTRACT

A method is developed for predicting cutter forces, temperatures, and wear on PDC bits as well as integrated bit performance parameters such as weight-on-bit, drilling torque, and bit imbalance. A computer code called PDCWEAR has been developed to make this method available as a tool for general bit design and analysis †. The method uses single-cutter data to provide a measure of rock drillability and employs theoretical considerations to account for interaction among closely spaced cutters on the bit. Experimental data are presented to establish the effects of cutter size and wearflat area on the forces that develop during rock cutting. Waterjet assistance is shown to significantly reduce cutting forces, thereby potentially extending bit life and reducing weight-on-bit and torque requirements in hard rock. The effects of several other design and operating parameters on bit life and drilling performance are also investigated.

† This code and sample problem input data are available from:

National Energy Software Center
Argonne National Laboratory
9700 South Cass Avenue
Argonne, IL 60439

TABLE OF CONTENTS

	<u>Page</u>
1.0 Introduction	1
2.0 Development of a PDC Cutting Force Model	7
2.1 Experimental Set-up, Procedures, and Conditions	10
2.2 Test Results: Dry, Non-Interacting Cuts	18
2.3 Test Results: Non-Interacting Cuts with Waterjet Assistance	21
2.4 Test Results: Interacting Cuts	29
2.5 Analysis of Cutter Interaction Effects	29
2.6 Other Observations	33
3.0 Development of the Computer Code, PDCWEAR	39
3.1 Cutter Interaction Theory	39
3.2 Forces and Moments Acting on the Bit	48
3.3 Cutter Wearflat Temperatures	51
3.4 Cutter Wear Rates	53
4.0 Demonstration of the Use of PDCWEAR	59
4.1 Input Parameters	62
4.2 Running the Program	65
4.3 Tabulated Program Output	68
4.4 Discussion of Baseline Analysis Results	69
4.5 Other Program Features	80
5.0 Predicted Effects of Design and Operation on Bit Performance	81
5.1 Effects of Bit Profile	81
5.2 Effects of Cutter Placement Density	81
5.3 Effects of Bit Rotary Speed	88
5.4 Effects of Waterjet Assistance	88
5.5 Effects of Wear Mode	91
5.6 Discussion	93
6.0 Conclusions	95
7.0 Nomenclature	97
8.0 Acknowledgment	101
9.0 References	103

	<u>Page</u>
Appendix A - Experimental Single-Cutter Data	109
Appendix B - Listing of Fortram Program PDCWEAR	125
Appendix C - Thermal Numerical Modeling of a 0.75-Inch PDC Cutter	149
Appendix D - PDCWEAR Input Guide	153
Appendix E - Listing of Fortran Program FORMAT	165
Appendix F - Listing of PDCWEAR Input Files Used in Demonstration Analysis	169
Appendix G - Partial PDCWEAR Output Listing for Demonstration Analysis	173
DISTRIBUTION LIST	189
List of Tables	iv
List of Figures	v

LIST OF TABLES

<u>Table No.</u>	<u>Title</u>	<u>Page</u>
I	Coefficients in Equations 38 and 39	55
II	Cutter Positions in Demonstration Analysis	60
III	Bit Operating Conditions in Demonstration Analysis	61
A-1	Description of PDC Cutters Used in Laboratory Tests	110
A-2	Dry, Non-Interacting Cut Test Data for Berea Sandstone	111
A-3	Dry, Non-Interacting Cut Test Data for Sierra White Granite	116
A-4	Dry, Non-Interacting Cut Test Data for Tennessee Marble	119
A-5	Waterjet-Assisted, Non-Interacting Cut Test Data for Sierra White Granite	121
A-6	Dry, Interacting Cut Test Data for Berea Sandstone	122
A-7	Dry, Interacting Cut Test Data for Sierra White Granite	123
C-1	Computed Thermal Response Function for 0.75-Inch and 0.5-Inch Cutters	151
D-1	Measured PDC/Rock Friction Coefficients	162
F-1	PDCWEAR Input File Containing Bit Design Data for Demonstration Analysis (BITDES.DAT)	170
F-2	PDCWEAR Input File Containing Initial Wear Configuration Data for Demonstration Analysis (WEARCF.DAT)	171
F-3	PDCWEAR Input File Containing Operating Conditions for Demonstration Analysis (OPCOND.DAT)	172

LIST OF FIGURES

	Title	Page
Figure 1 -	Collection of 8-1/2 inch PDC bits, showing variations in bit shape and location and number of cutters.	2
Figure 2 -	Single PDC cutter, showing front and side view.	3
Figure 3 -	Schematic of a single PDC cutter mounted on the leading face of a bit and experiencing interaction with nearby cutters.	8
Figure 4 -	Cutting edge profiles for sharp cutters on the leading face of a PDC bit.	9
Figure 5 -	Milling machine used for linear single-cutter tests.	12
Figure 6 -	Geometry of single-cutter tests with waterjet assistance.	13
Figure 7 -	Vertical milling machine used for wearing PDC cutters in the laboratory.	15
Figure 8 -	Cutting pattern used in non-interacting single-cutter tests.	16
Figure 9 -	Cutting patterns used to simulate cutter interaction in single-cutter tests.	17
Figure 10 -	Measured penetrating stresses with various wearflat configurations in dry, non-interacting cuts.	19
Figure 11 -	Measured penetrating stresses with various wearflat configurations in dry, non-interacting cuts.	20
Figure 12 -	Measured penetrating forces with sharp cutters in dry, non-interacting cuts.	22
Figure 13 -	Measured drag coefficients with various wearflat configurations in dry, non-interacting cuts.	23
Figure 14 -	Measured drag coefficients with various wearflat configurations in dry, non-interacting cuts.	24
Figure 15 -	Measured drag coefficients with sharp cutters in dry, non-interacting cuts.	25
Figure 16 -	Measured penetrating stresses in non-interacting cuts made with waterjet assistance.	26
Figure 17 -	Measured drag coefficients in non-interacting cuts made with waterjet assistance.	28
Figure 18 -	Measured penetrating stresses in dry, interacting cuts.	30

	<u>Page</u>
Figure 19 - Interacting cut patterns with large and small lateral spacing between cuts.	31
Figure 20 - Typical cutting pattern for a worn cutter on the leading face of a PDC bit.	32
Figure 21 - Computed effective depth of cut as a function of lateral distance to adjacent cuts in interacting cut tests.	34
Figure 22 - Predicted and measured penetrating stresses for dry, interacting cut tests.	35
Figure 23 - Circumferential wear angle found to develop on field worn cutters.	36
Figure 24 - Cut and cutter profiles for a general PDC cutter mounted on a bit.	40
Figure 25 - Schematic of the four coordinate systems used to describe cut and cutter profiles.	41
Figure 26 - Detailed definition of several points used in cutter geometry analysis.	43
Figure 27 - Schematic of algorithm used in PDCWEAR to compute z-coordinates of cutting profiles at each value of x.	46
Figure 28 - Schematic showing how cutter forces are integrated to produce bit performance parameters.	50
Figure 29 - Finite element mesh used to compute thermal response of 0.75-inch cutters.	52
Figure 30 - Schematic of 8-1/2 inch bit design used in the demonstration analysis.	59
Figure 31 - Definition of several bit design parameters required as input for PDCWEAR.	63
Figure 32 - Predicted wearflat growth of cutter with highest wear rate in the demonstration analysis.	70
Figure 33 - Predicted wear distribution across bit in the demonstration analysis at designated stages of bit wear.	71
Figure 34 - Predicted cutter penetrating forces in the demonstration analysis.	72
Figure 35 - Predicted cutter wear ratios in the demonstration analysis.	73

	<u>Page</u>
Figure 36 - Predicted cutter wearflat temperatures in the demonstration analysis.	74
Figure 37 - Predicted WOB at specified penetration rates in the demonstration analysis.	75
Figure 38 - Predicted drilling torque at specified penetration rates in the demonstration analysis.	76
Figure 39 - Predicted resultant bit side force at specified penetration rates in the demonstration analysis.	77
Figure 40 - Predicted resultant bit bending moment at specified penetration rates in the demonstration analysis.	78
Figure 41 - Schematic of bullet-nose bit design used in modified analysis to illustrate the effects of bit profile.	82
Figure 42 - Predicted cutter wear distribution across bit, showing the effects of bit profile.	83
Figure 43 - Specified penetration rate plotted as a function of predicted WOB to illustrate the effects of bit profile.	84
Figure 44 - Schematic of bit design used in modified analysis to illustrate the effects of cutter placement density.	86
Figure 45 - Predicted cutter wear distribution across bit, showing the effects of cutter placement density.	87
Figure 46 - Predicted cutter wear distribution across bit, showing the effects of rotary speed.	89
Figure 47 - Predicted cutter wear distribution across bit, showing the effects of waterjet assistance for selected cutters (13-16).	90
Figure 48 - Predicted cutter wear distribution across bit, showing the effects of wear mode.	92
Figure D-1 - Measured heat transfer coefficients for various locations on a stud-mounted 0.5-inch diameter compact cutter due to a uniform flow of water past the cutter.	156
Figure D-2 - Measured heat transfer coefficients for various locations on a stud-mounted 0.5-inch diameter compact cutter due to impingement of a low-pressure (80 psi) waterjet.	157
Figure D-3 - Mean PDC cutter heat transfer coefficients under typical air and water drilling conditions.	158

1.0 INTRODUCTION

Research has been conducted for several years at Sandia National Laboratories to foster the development of PDC bits for geothermal drilling. This work, sponsored by the Geothermal Technologies Division of the U. S. Department of Energy, has been directed toward the high-temperature, hard-rock drilling environment that is typically found near geothermal resources. We have strived, however, to interpret the results to make them applicable to drilling environments of interest to the petroleum industry as well.

In high-temperature, hard-rock drilling environments, roller bits suffer extremely short lives and are a significant contributing factor to the high costs associated with geothermal drilling [1-4]. The primary cause of this short bit life is rapid wear of the bearings that support the roller cones. Loose bearings help accelerate gage wear on the bits, thereby leading to undergauge holes. High downhole temperatures play a major role in accelerating roller bit wear because of: (1) temperature limitations on the effectiveness of elastomeric seals that might be used to seal the bearings from the abrasive drilling fluid; and (2) the adverse effects of frictional temperatures on the wear of rubbing surfaces.

A potential alternative to roller bits in many drilling applications is the type of bit known as the polycrystalline diamond compact (PDC) bit. This type of bit consists of a solid bit head onto which are attached multiple PDC cutters. A photograph of several PDC bit designs is shown in Figure 1. Note that the configuration of a PDC bit can vary in shape, size, number and placement of cutters, and hydraulic design. These and other variables determine the performance of a bit in a given application.

Shown in Figure 2 is a single stud-mounted PDC cutter. The thin black layer of material on the leading face of the cutter is the artificial-diamond compact, which provides the wear resistance that makes this type of cutter effective in drilling rock. The PDC layer is bonded to a tungsten carbide-cobalt (WC-Co) compact, which in turn is mounted to a WC-Co stud. The entire cutter assembly is then pressed into holes machined in the head of the bit. Some PDC bits are also made with matrix-mounted cutters. In this case, the WC-Co compacts with the PDC layers are brazed directly onto flat surfaces cast into the head of the bit.

The mechanical simplicity of PDC bits, particularly the associated advantage of no moving parts, led to Sandia's interest in this technology for geothermal drilling. Our earliest efforts concentrated on developing technology for effectively mounting PDC cutters to the bit body. Developments included: (1) a design for a more fracture-resistant cutter stud [5-7]; (2) test results that helped establish optimal cutter rake angles [8]; and (3) a diffusion bonding technique for attaching the WC-Co compact with its PDC layer to the stud for high-temperature applications [8-11].

Field and laboratory drilling tests in geothermal and other hard-rock formations helped identify the potential limitations of PDC bits under severe conditions [5,6,10,12-20]. Although PDC bits were found capable of drilling most formations as fast or faster than roller bits, bit life was found to be extremely formation-dependent. Field tests in the soft shales and sandstones of geothermal wells in the Imperial Valley demonstrated PDC



Figure 1 - Collection of 8-1/2 inch PDC bits, showing variations in bit shape and location and number of cutters.

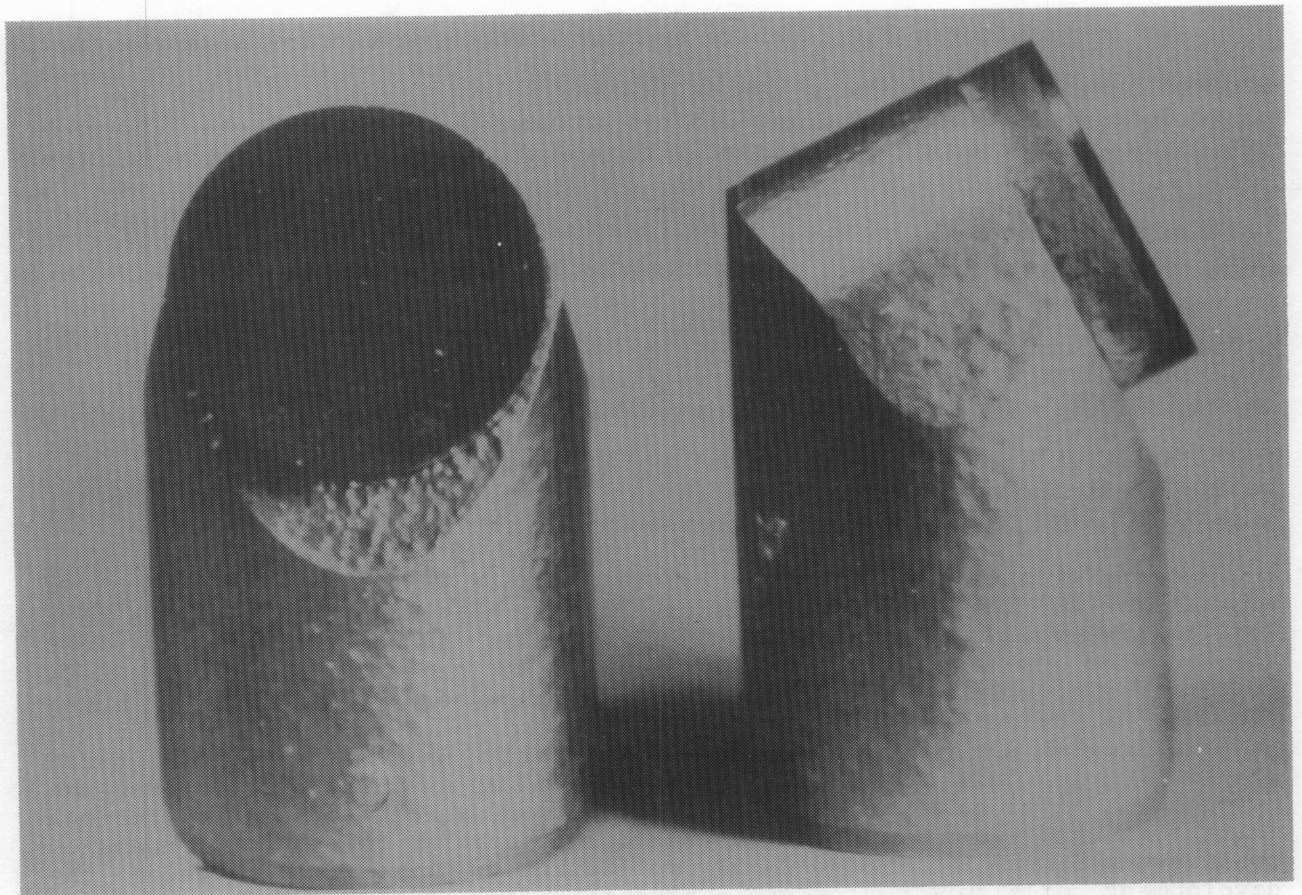


Figure 2 - Single PDC cutter, showing front and side view. Circular diamond compact on this cutter is 0.5 inch in diameter.

bit lives and penetration rates two to three times those of roller bits in the same wells [17,20]. Laboratory tests in formations such as Sierra White granite and Nugget sandstone demonstrated that harder formations accelerate PDC cutter wear, although rapid penetration can be achieved before the cutters wear out [10,15,16,19]. Field tests drilling with air in Franciscan graywacke in the Geysers were largely unsuccessful because of problems with cutter studs fracturing off the bit body [15,17]. Because of its fractured nature, elevated temperature, and high compressive strength, Franciscan graywacke may be inherently too severe for drilling with WC-Co-backed PDC cutters.

Our later efforts [19-32] have concentrated on developing an analytical understanding of the PDC rock drilling process. Our objectives in these studies have been: (1) to determine the inherent limitations of PDC cutters in various applications, which would help us determine whether the hard-rock geothermal environment is inherently too severe for PDC bits or whether the question of success in drilling long intervals in such applications is merely one of proper design and operation; and (2) to develop procedures for designing PDC bits to operate efficiently and wear evenly in suitable applications.

The development of an analytical model [22,26,27] for predicting cutter wearflat temperatures in a given drilling environment has allowed experimental data [19,33] to be correlated in a manner that indicates a strong effect of wearflat temperature, T_w , on cutter wear rates [27,29]. The correlation suggests that above a critical temperature of approximately 350°C, cutters comprised of PDC and WC-Co undergo thermally-accelerated wear. Under these conditions wear rates increase by one or two orders of magnitude, leading to similar-scale reductions in bit life.

Finite element thermal stress calculations of PDC cutters were made in an effort to identify the reasons behind the apparent existence of a critical wearflat temperature [27,29]. It was found that at elevated temperatures, several possible wear mechanisms inherent with the PDC-WC-Co combination come into play. When drilling with water or water-based muds, the results indicate the possibility of compressive yielding occurring in the wearflat region due to a combination of thermally- and mechanically-induced stresses. In hard metals such yielding, even on a small scale, causes the development of microvoids in the grain structure, which act as microcrack initiators and lead to increased wear. Furthermore, the thermal expansion coefficient of the PDC and WC-Co is sufficiently different to cause the development of significant tensile stresses along the face of the cutter in the polycrystalline diamond layer. This leads to an increased potential for cracking along the leading face of the cutter. Portions of this face eventually become the cutting edge, where micro-fractures greatly accelerate material wear rates.

When drilling with air, as is sometimes required in geothermal formations due to underpressured conditions, the convective cooling rate of the cutters is greatly reduced, and the temperature distribution is radically changed. The thermal stress field during air drilling places the wearflat under significant tensile stresses, promoting more rapid microfracturing and wear of the WC-Co and PDC [29].

The effects of intermittent contact between the cutter and the rock were assessed in order to estimate the effects of conditions such as: 1) pulling the bit off-bottom suddenly before adding a length of drill pipe; and 2) bit bounce caused by drill string dynamics or fractured formations. It was found that thermal shock of the hot wearflat, caused by rapid quenching with the drilling mud, can produce significant tensile stresses in the cutter wearflat region. Fractures initiated in the abrasion process can then be propagated more easily. It is therefore desirable to maintain constant contact between the cutters and the rock surface, and the use of shock subs is recommended to maintain a steady weight-on-bit (WOB) under severe conditions [29]. Results of the finite element analyses also show that when lifting a bit off-bottom, reducing WOB slowly (over a period of about 30 seconds) may have significant advantages over pulling the bit off-bottom suddenly. By maintaining some mechanically-induced compressive loading while the cutters slowly cool, thermally induced tensile stresses are suppressed, thereby alleviating some of the wear caused by thermal cycling of the cutters.

The above results have implications for the cutting limitations imposed by the strength of the rock. The thermal model developed in our previous analyses [22,26,27] predicts wearflat temperatures to be directly proportional to the penetrating stress, i.e., the ratio of penetrating force, F , to wearflat area, A_w . There thus exists a critical penetrating stress at which the wearflat temperature reaches 350°C and thermally-accelerated wear begins. This provides an estimate of the upper limit on cutter penetrating stress that can be safely used in a given application.

The minimum penetrating stress that a cutter must impose on a rock surface is related to the strength of the rock. Experimental single-cutter test data indicate that cutter penetrating stresses must reach values on the order of the compressive rock strength before significant penetration of the rock occurs [20,28,31]. This suggests that there exists a threshold penetrating stress, equal to the compressive rock strength, that the cutter must impose in order to effectively drill.

A PDC cutter operating envelope between the threshold and critical penetrating stresses has been suggested [20,28]. As rock strength increases, this operating envelope shrinks and eventually vanishes. Under these conditions, PDC bits cannot achieve significant rock penetration without experiencing thermally-accelerated wear, and bit life is virtually non-existent. The temperature and wear models that have been developed are useful in estimating these wear limitations under different combinations of downhole conditions. Knowledge of these limitations is helpful in bit design because it can be used to help optimize various design parameters, such as bit profile and cutter placement, for different applications.

Use of the temperature and wear models in bit design requires an estimate of cutter penetrating forces during drilling. If an accurate model of cutter forces is available, the following bit performance parameters can also be determined by summing forces and moments acting on the bit: weight on bit, drilling torque, side force, and bending moments. Optimal placement of cutters on the face of a bit to promote uniform cutter wear and to balance the loads and prevent bit wobble should then be possible.

This report deals with the development of a model for estimating cutter forces and the development of a computer code that implements the model to provide an analytical tool for general PDC bit design. The use of the computer program is demonstrated, and some general conclusions derived from its use are identified and discussed.

The potential for using moderate-pressure waterjets to extend the range of application of PDC cutters is also explored. Previous work by Hood [34,35] and Dubugnon [36] with large WC-Co cutters used in hard-rock mining applications has shown that cutter forces can be significantly reduced if waterjets are directed onto the rock surface immediately ahead of the cutter. Penetrating force reductions of 50% with 2500 psi jets and 75% with 9,000 psi jets have been reported. Our previous analysis [28] indicates that if such reductions could also be achieved with PDC cutters, these cutters could operate under more severe conditions and in significantly harder rocks, thereby extending the applicability of PDC bits to more types of formations. This report presents new data obtained with PDC cutters and cavitating jets that support that conclusion. The application of the cutter/waterjet technique to PDC bit design is also discussed.

2.0 DEVELOPMENT OF A PDC CUTTING FORCE MODEL

We seek a model of the PDC cutting process that will allow us to determine the penetrating and drag forces acting on each cutter located on the bit face. The primary parameters that affect these forces include the rock type, cutter design and wear state, position on the bit, cutter interaction, cutting speed, rock stress state, and fluid environment. Some of these parameters are illustrated in Figure 3.

It is possible to duplicate many of these parameters in laboratory single-cutter tests. Most of the cutting conditions encountered by a single cutter in full-scale, atmospheric-pressure, laboratory bit tests can be duplicated by using a modified milling machine and relatively small rock samples. Similarly, deep-hole drilling conditions can, to a large degree, be duplicated in single-cutter tests in the laboratory. Test cells exist that measure single-cutter forces under elevated hydrostatic, confining, and pore pressures [37-40]. Typical downhole rock types, cutter configurations, and cutting speeds can also be duplicated with these test cells.

A more difficult simulation is the cutter interaction that occurs on full-scale bits, where cutting forces on each cutter are reduced by the presence of previous cuts made by adjacent cutters. We have found in unconfined rock tests at atmospheric pressure that interaction does not occur unless the previous cuts are laterally close enough that they actually remove rock that would otherwise be removed by the test cutter. The cross-sectional area of rock removed by each cutter, therefore, seems to be the parameter that characterizes cutter interaction and controls cutter forces.

Our experience with single-cutter tests is that for reasonable depths of cut, PDC cutters do not cause much rock breakage outside the projected area of the cutter profile. Even in coarse-grained and brittle rock such as Sierra White granite at atmospheric pressure, the profile of a cut made with a PDC cutter closely matches the profile of the cutter itself. An even closer match between cut and cutter profiles should be obtained under the elevated hydrostatic and confining stresses found downhole, since a transition from brittle to more ductile rock breakage mechanisms occurs [37,41].

Shown in Figure 4 is a typical sequence of cutting edge profiles for several sharp (i.e. unworn) cutters on the leading flat face of a PDC bit. These profiles are obtained during two bit revolutions as the cutters pass through a radial plane containing the longitudinal axis of the bit. The shaded areas represent the steady-state cross-sectional areas of cut for each cutter. Since the centers of the cutters are all assumed to lie in the same plane normal to the longitudinal axis of the bit, the downward vertical displacement of one cutter profile relative to a preceding one is due entirely to the advancement of the bit as it rotates. The shapes of the cross-sectional areas of cut are seen to be quite complex, even for simple bit geometries. In an arbitrary bit design, the cross-sectional areas of cut are functions of the radial, circumferential, and longitudinal distribution of cutters on the bit face as well as the wear state of the cutters and the penetration rate of the bit. Although it is possible to duplicate some interaction patterns in the laboratory [40], it is clearly

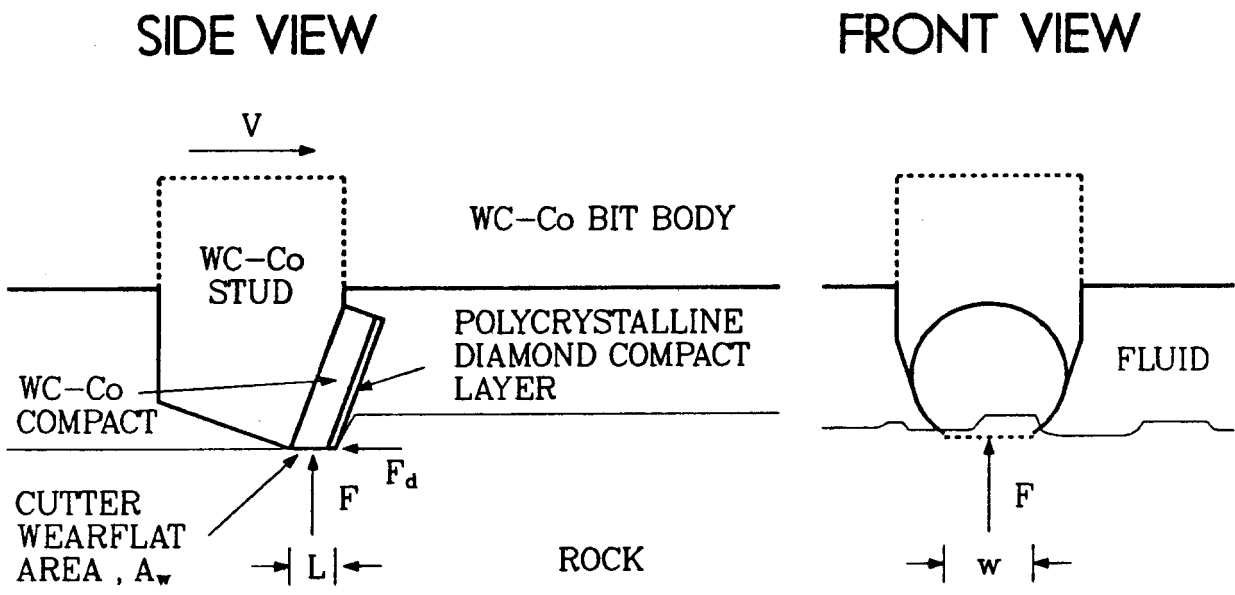


Figure 3 - Schematic of a single PDC cutter mounted on the leading face of a bit and experiencing interaction with nearby cutters.

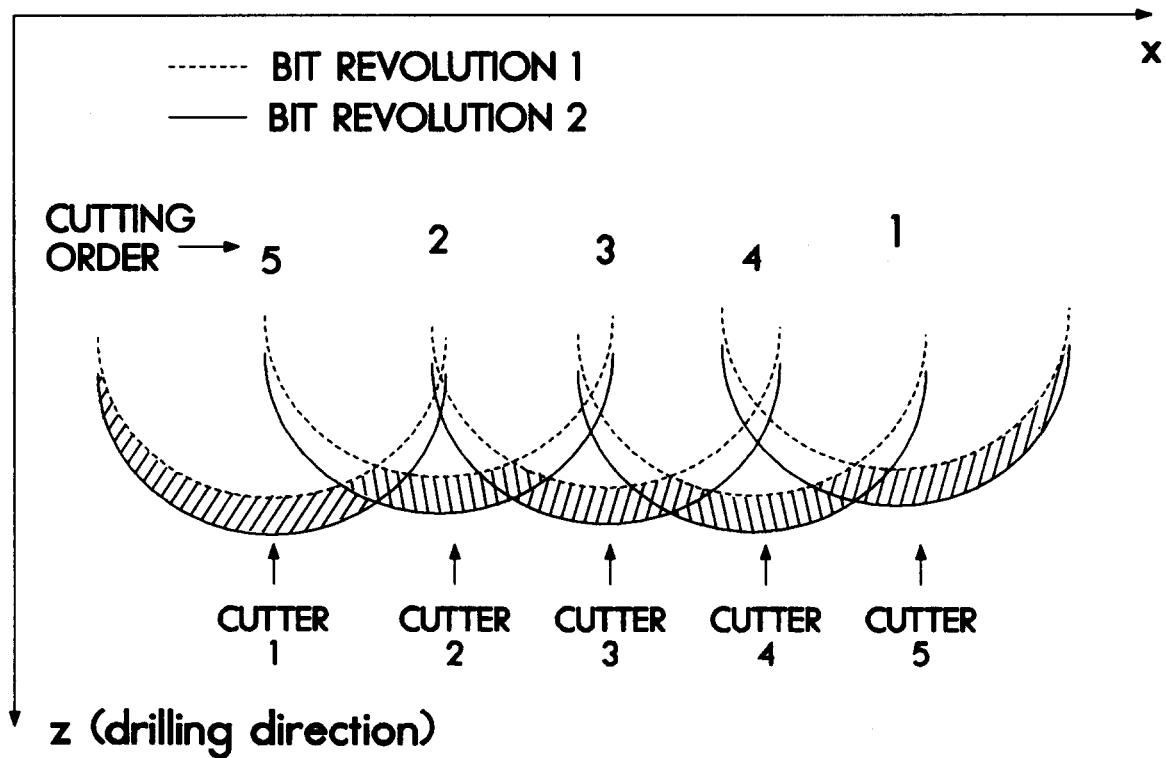


Figure 4 - Cutting edge profiles for sharp cutters on the leading face of a PDC bit. Shaded areas represent cross-sectional areas of cut.

impractical in single-cutter tests to duplicate all the degrees of interaction that could be experienced by cutters in a given bit design.

We, therefore, seek to separate the effects of cutter interaction from the effects of intrinsic drillability of the cutter/rock combination under the imposed conditions. Intrinsic drillability under any set of laboratory conditions can then be determined by conducting single-cutter tests using a standard cut geometry; and an analytical model can be employed to account for cutter interaction.

We choose the simplest geometry possible for the standard cut geometry, that of a single cut on a flat rock surface with no adjacent cuts that might interact with the test cut. The depth to which the cutter penetrates the flat rock surface is a function of the stresses imposed in the rock by the cutter. In the case of worn cutters, the penetrating stress is defined as the average normal stress imposed on the rock surface; thus

$$F/A_w = fct(\delta) \quad (1)$$

In the case of a sharp cutter, the wearflat area is very close to zero. Yet a finite penetrating force is still required to cause penetration of the rock [31]. The reason for this is that the crushed rock zone directly beneath the cutting edge acts to distribute the force over a finite area. For such cases, we seek in our tests to simply define the functional dependence,

$$F = fct(\delta) \quad (2)$$

The following subsections describe the procedures used to obtain experimental data that define Eqs. 1 and 2, and a method is developed for using these correlations to determine cutter performance during interacting cuts.

2.1 Experimental Set-up, Procedures, and Conditions

Rock-cutting tests were conducted in three rock types with PDC cutters having various amounts of wear. Berea sandstone, Tennessee marble, and Sierra White granite were used in order to cover a wide range of rock properties such as strength, composition, and ductility.

Berea sandstone is a relatively soft rock with a measured uniaxial compressive strength, S_c , of 7,100 psi [31]. Tennessee marble, also known as Holton limestone, is a much harder rock, with $S_c = 17,800$ psi. Sierra White granite, $S_c = 21,500$ psi, is somewhat harder than the marble, but its composition is quite different. The granite has a high quartz content (39% by weight) and thus causes cutters to wear at a higher rate.

Two milling machines were used in the test program. The end-mill shown in Figure 5 was used for obtaining quantitative data. The fixed head on the mill was instrumented with a triaxial force transducer, to which the cutter was mounted. Rock samples ranging in length from 12 to 18 inches and in width from 5.0 to 9.75 inches were placed on the milling table and secured with clamps. Linear, parallel cuts in the top surface of a rock sample were made by moving the table at a fixed speed of 2.2 in/sec, the table's maximum speed. Cuts were made in the rock samples under dry cutting conditions at depths ranging from 0.010-0.100 inch, which covers the range generally encountered by a single cutter on a bit downhole.

The milling machine table was later fitted with a steel enclosure and a waterjet nozzle holder mounted ahead of the cutter. A profile of the nozzle holder and its relationship to the cutter are shown in Figure 6. The nozzle holder was designed so that the nozzle standoff distance, d_s , inclination angle, ϕ_n , and jet impingement distance, d_i , could be adjusted over limited ranges. Only one set of these parameters was used in the test program currently reported: $d_s = 1.6$ inches, $\phi_n = 45^\circ$, and $d_i = 0.1$ inch. These values were chosen because they represent practical values that might be used in an actual PDC bit design.

The nozzles used in the test program were self-resonating, cavitating jet nozzles designed and fabricated by Tracor Hydronautics, Inc. under contract to Sandia National Laboratories. These nozzles are the product of several years of research aimed at optimizing nozzle designs that erode rock effectively using drilling mud pressures available on conventional drill rigs (< 5000 psi) [42-46]. They are designed to produce jets that cavitate under higher ambient pressures, and hence at greater hole depths, than conventional nozzles. The cavities produced in these jets are created by vaporization of the liquid in the center of high velocity vortices that form in the jet shear zone. When these cavities collapse near a rock surface, high-speed microjets impact the rock surface with pressures of up to 200,000 psi [47], substantially increasing the rock erosion rate. Two nozzles were fabricated for the single-cutter tests: one optimized for a pressure drop of 2000 psi and the other for a pressure drop of 4500 psi. Both had orifice diameters of 0.1 inches. A more complete description of the specific nozzles fabricated for this test program is given in Ref. 46. Cuts made with PDC cutters assisted by the high-pressure waterjets produced with these nozzles were compared with identical cuts made with 80 psi waterjets and cuts made with no jets at all.

A computerized data acquisition system was used to sample three components of cutter force during a cut on the rock sample: a vertical or penetrating force, a horizontal drag force, and a horizontal side force. The nominal sampling rate of 75 Hz allowed several hundred samples of each force channel to be made for each cut. At the end of each cut, the computer averaged the data and recorded the forces along with other pertinent test data on floppy disk. These other data include rock type, cutter wearflat area, depth of cut, lateral distances to adjacent cuts, and their depths.

Cutters in various stages of wear were used in an effort to determine the effects of wear on cutter forces. New PDC cutters with sharp edges were

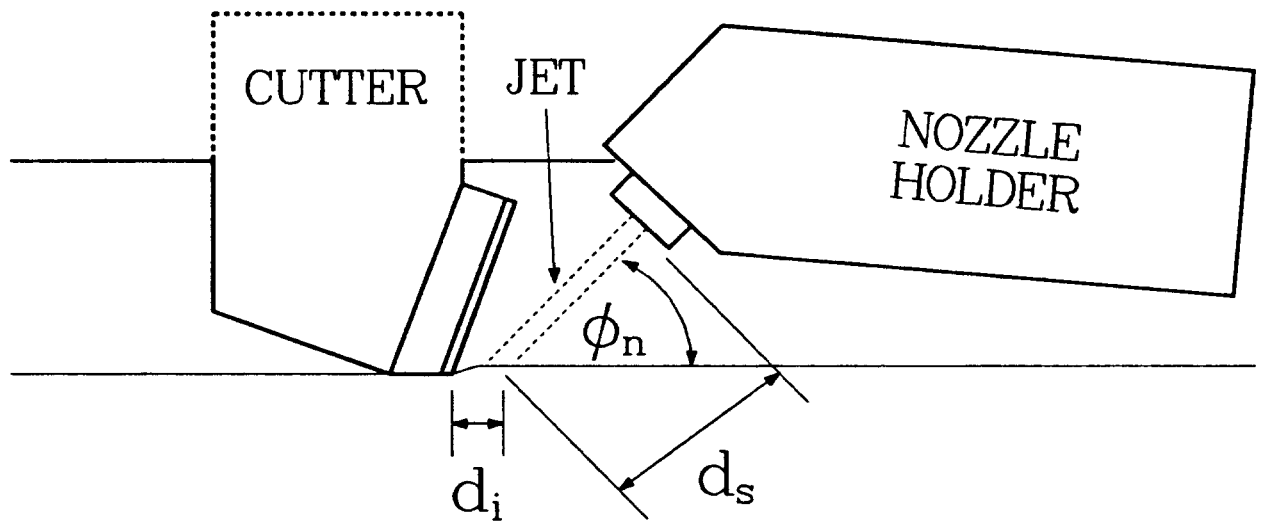


Figure 6 - Geometry of single-cutter tests with waterjet assistance.

used, as were cutters with machine-ground, laboratory-worn, and field-worn wearflats. The machine-ground wearflats were produced by grinding new cutters in a direction parallel to the direction of cutter travel. Cutters with field-worn wearflats were removed from commercial bits that had been run in oil and gas wells.

Laboratory-worn wearflats were obtained with the vertical milling machine, as shown in Figure 7. A cubical specimen of Sierra White granite, 3 ft X 3 ft X 3 ft, was placed on the mill table. The cutter/dynamometer system was attached to a moving head on the vertical mill that traversed the top face of the rotating rock specimen. Because of the slow maximum feed rate of the traversing head (.06 inch/table revolution), the resulting spiral cuts had significant overlap. This provided a means for rapidly wearing the cutters in the laboratory.

Cutter wearflats were measured as follows. A piece of carbon paper was placed between two sheets of plain paper, and the three sheets were then placed between the cutter and the flat rock surface. The cutter was then vertically loaded to a static penetrating force level typical of the level encountered in cutting tests with the same cutter and rock. The portion of the cutter wearflat that contacted the rock left a carbon impression on the plain paper. This impression was overlain with a fine rectangular grid (1 mm x 1mm) and the area calculated by counting shaded blocks. Cutters with measured wearflats ranging from 0.016 to 0.040 in² were tested in this study. Cutter wearflat characteristics are listed in Tables A-1 through A-7 (Appendix A).

Two sizes of cutter were tested. Most cutters had compact diameters of 0.5 inch, the size that has been traditionally used in PDC bits. Also tested, both new and laboratory-worn, was a cutter having a compact diameter of 0.75 inch. All cutters had backrake angles of 20°.

Finally, two types of cut were used: non-interacting cuts and interacting cuts. Non-interacting cuts, as illustrated in Figure 8, are cuts where the lateral spacing, d , between cuts is large enough that forces in a given test cut are not affected by the presence of previous, laterally-adjacent cuts. It was found that previous cuts do not affect the forces in a given test cut unless those previous cuts remove rock that otherwise would be removed in the test cut.

The geometry of interacting cuts designed to simulate the interaction typical of PDC bits is illustrated in Fig. 9. The test cut here is the 0.080-inch cut, which was made after the adjacent 0.040-inch cuts. The interaction shown in the symmetric case, for example, would be encountered with a bit on which two cutters near the same radial location are circumferentially located 180° from the test cutter. In the one-half rotation of the bit between the time the adjacent cutters pass through a given radial plane and the time the test cutter passes through the same radial plane, the bit advances so that the test cut is at a lower level in the rock. A wide range of interaction was achieved by varying the lateral distance, d , over a range of 0.050 to 1.25 inches, in both the symmetric pattern (two adjacent cuts) and the asymmetric pattern (one adjacent cut).

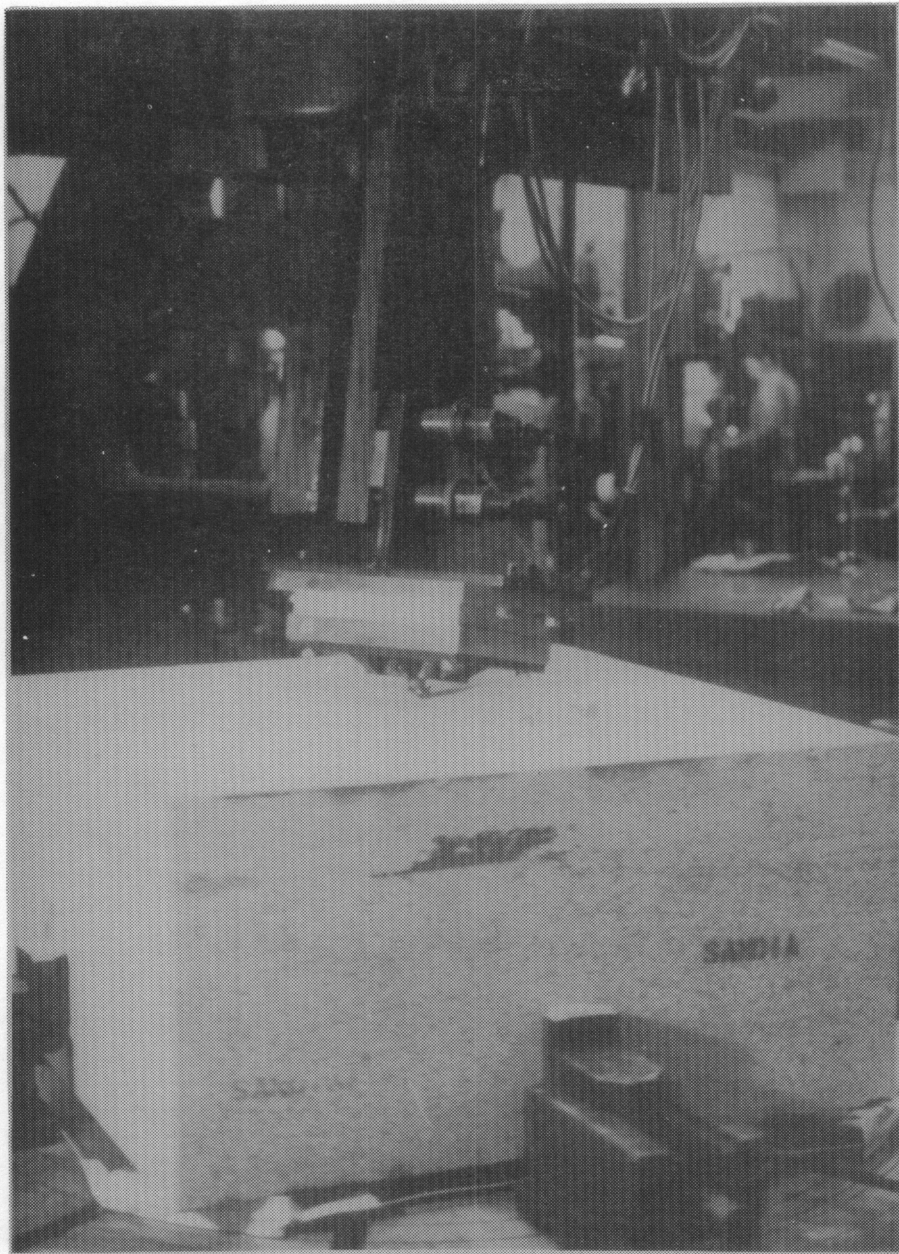


Figure 7 - Vertical milling machine used for wearing PDC cutters in the laboratory.

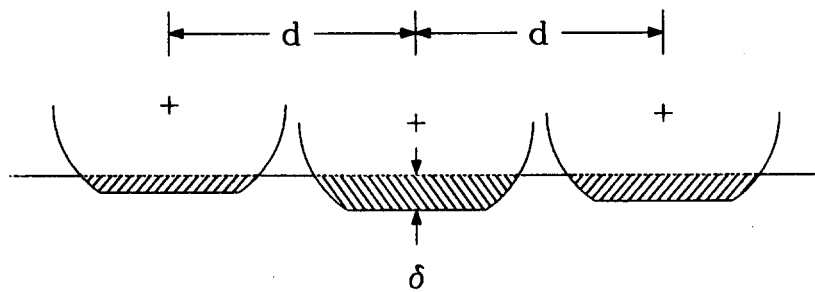


Figure 8 - Cutting pattern used in non-interacting single-cutter tests. Shaded areas are cross-sectional areas of cut.

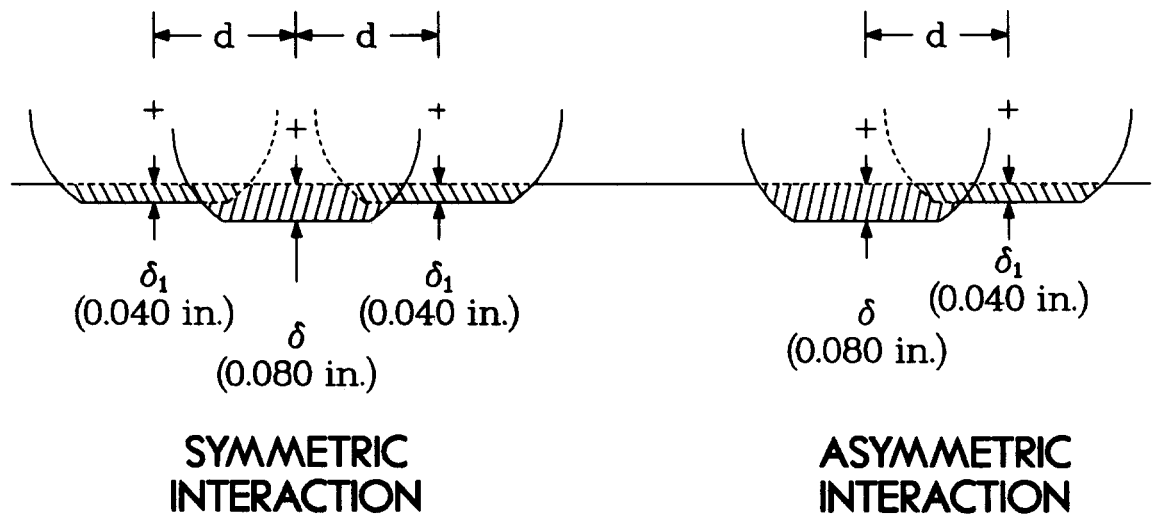


Figure 9 - Cutting patterns used to simulate cutter interaction in single-cutter tests. Test cut is the 0.080-inch cut in each pattern.

2.2 Test Results: Dry, Non-Interacting Cuts

Penetrating and drag forces measured in dry, non-interacting cut tests with the various cutters and rock types are tabulated in Tables A-2 through A-4 (Appendix A).

Shown in Figures 10 and 11 are the measured penetrating stresses, F/A_w , plotted as a function of depth of cut for the worn cutters. The behavior of the data for each rock type suggests correlations of the form

$$F/A_w = C_1 \delta^{n_1} , \quad (3)$$

where the constants C_1 and n_1 are determined from a least squares fit of the data in log-log space. The curves drawn in Figures 10 and 11 show the values of C_1 and n_1 calculated for each rock type. This simple form of correlation equation provides an adequate fit of the data.

The most significant result is that all the data for a given rock type collapse to approximately the same curve, regardless of the size or shape of the wearflat or the diameter of the cutter compact. This suggests two important conclusions:

- (1) The penetrating force on a worn cutter for a given depth of cut is directly proportional to the wearflat area. This implies that for a given rock and set of operating conditions the values of C_1 and n_1 can be determined with any cutter having a measurable wearflat, and those values should also be valid for other stages of wear with the same type cutter.
- (2) For a given depth of cut and a given wearflat area, a large worn cutter requires no greater penetrating force than a small cutter, yet the large cutter does remove more rock. This suggests an improved cutting efficiency with increased cutter size, at least within the range of cutter sizes considered.

The results shown in Figures 10 and 11 for Sierra White granite and Tennessee marble confirm that for these hard rocks, penetrating stresses on the order of the compressive rock strength must be imposed on the rock surface before significant penetration of the rock occurs. This supports the idea of a threshold penetrating stress discussed earlier and suggests that the penetrating force component is important in crushing the surface of hard rocks, leading to cutter penetration. With the softer, more plastic Berea sandstone, however, significant rock penetration can be achieved with penetrating stresses significantly lower than the compressive rock strength. This suggests that crushing of the rock surface is less important with soft rocks and that the drag force component plays a greater role in machining, rather than crushing, the rock surface.

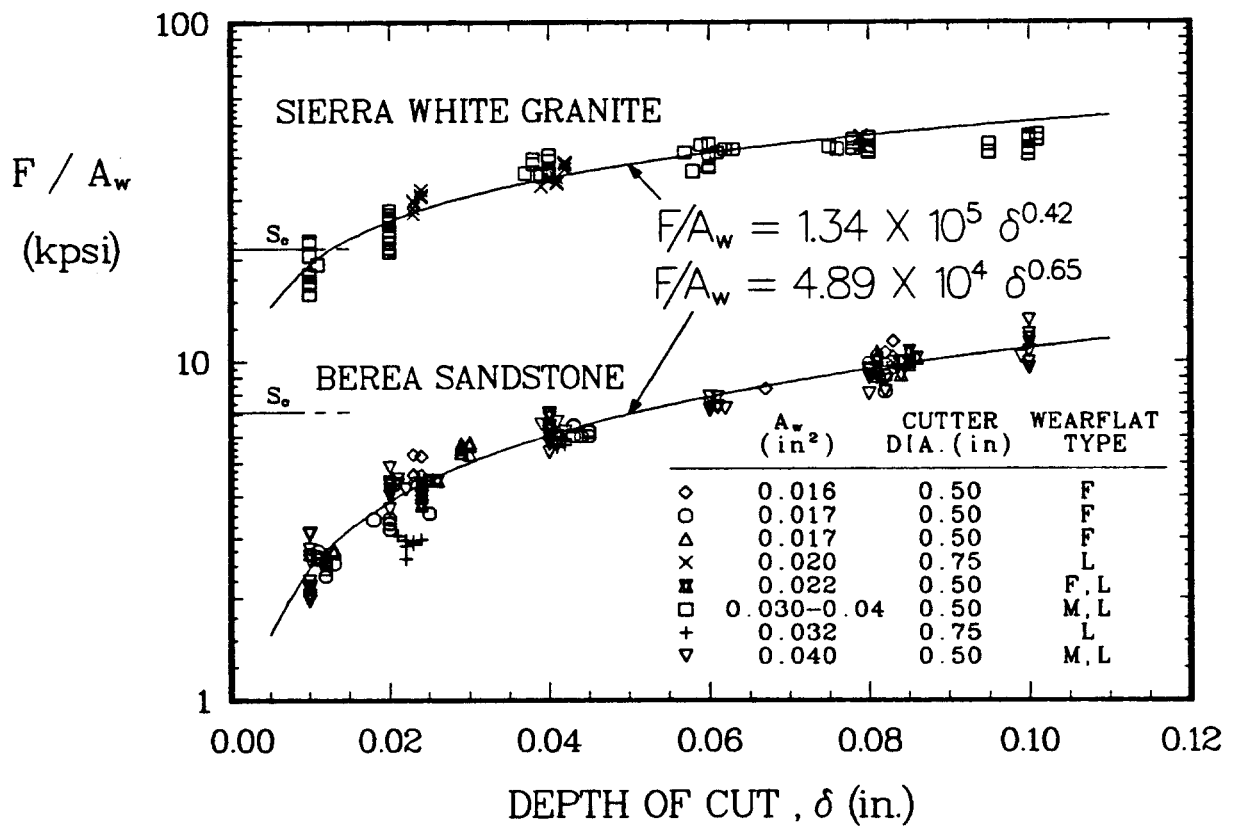


Figure 10 - Measured penetrating stresses with various wearflat configurations in dry, non-interacting cuts. Wearflat type: F=field worn; L=laboratory worn; M=machine ground.

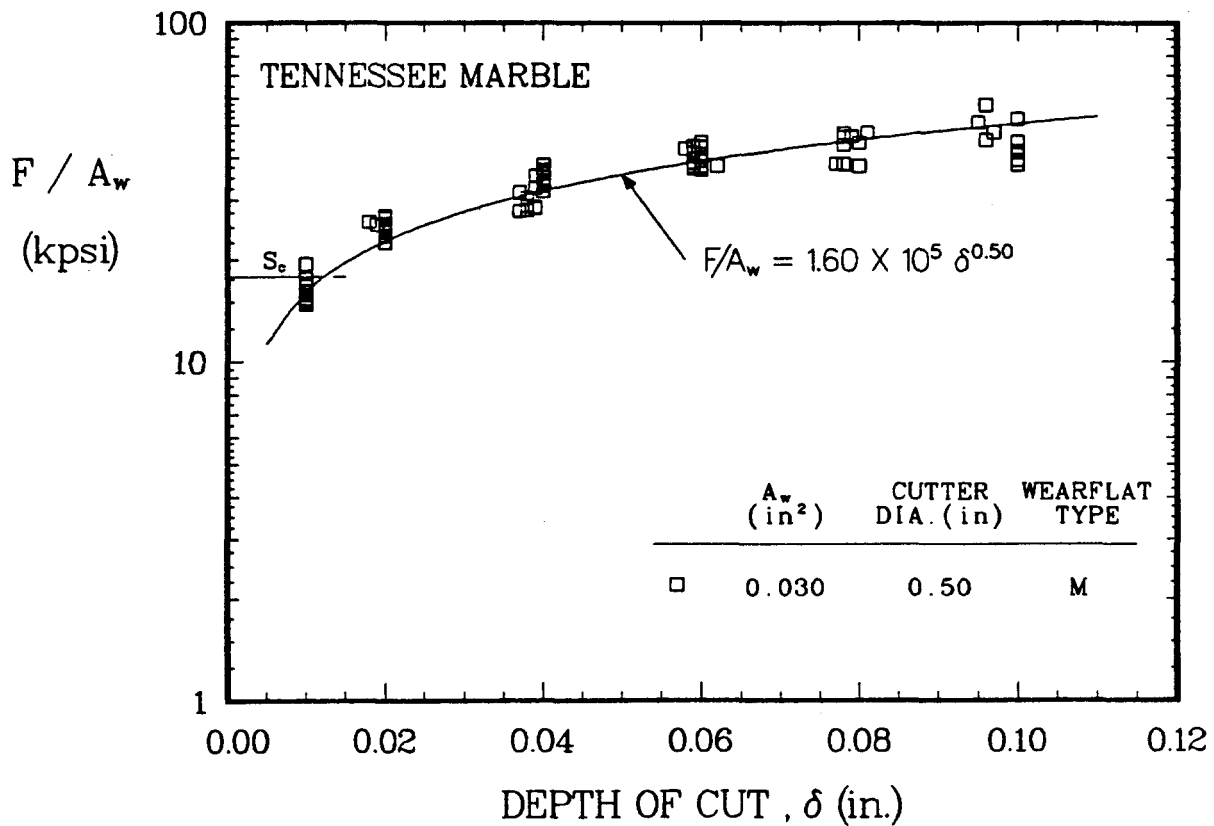


Figure 11 - Measured penetrating stresses with various wearflat configurations in dry, non-interacting cuts. Wearflat type: F=field worn; L=laboratory worn; M=machine ground.

Penetrating forces measured with sharp cutters in dry, non-interacting cuts are shown in Figure 12. Correlations of the form

$$F = C_2 \delta^{n_2} \quad (4)$$

were determined, and the resulting values of C_2 and n_2 are shown in Figure 12. These data indicate another surprising result: even in the sharp condition, the larger cutter requires no larger penetrating force than the smaller cutter. In fact, in the tests with Berea sandstone at 0.08 inch, the larger cutter actually required slightly lower penetrating forces than the smaller cutter.

The cutter drag forces, F_d , measured in the dry, non-interacting cuts with worn cutters are shown in Figures 13 and 14, plotted as a ratio with the penetrating force, F . We define this ratio as the cutter drag coefficient,

$$\mu_d = F_d/F \quad (5a)$$

We see that the drag coefficient is a function of the rock type, but it is relatively independent of the depth of cut and wearflat area. If a model is available to predict F , it is then possible to estimate F_d :

$$F_d = \mu_d F \quad (5b)$$

where, for instance, $\mu_d = 0.64$ for worn cutters in Sierra White granite and Tennessee marble and $\mu_d = 0.95$ in Berea sandstone. The higher drag coefficient for Berea sandstone agrees with the conclusion that the drag force component is more important with this rock type than with the harder rock types.

Drag coefficients for sharp cutters are shown in Figure 15. When compared with the results for worn cutters, as represented by the curves, it is seen that sharp cutters have consistently higher drag coefficients. The larger cutter has slightly higher drag coefficients than the smaller cutter in deep cuts.

2.3 Test Results: Non-Interacting Cuts with Waterjet Assistance

Shown in Figure 16 are the penetrating stresses measured with waterjets impinging on the rock surface ahead of the cutter. These data are tabulated in Table A-5 (Appendix A). Note that the stresses obtained with 80 psi jets are similar to those measured in the dry cuts, as represented by the upper curve in Figure 14. The jet velocity with this nozzle pressure is not sufficient to affect penetrating stresses, and the simple presence of water at the cutter/rock interface also seems to have little effect. At elevated

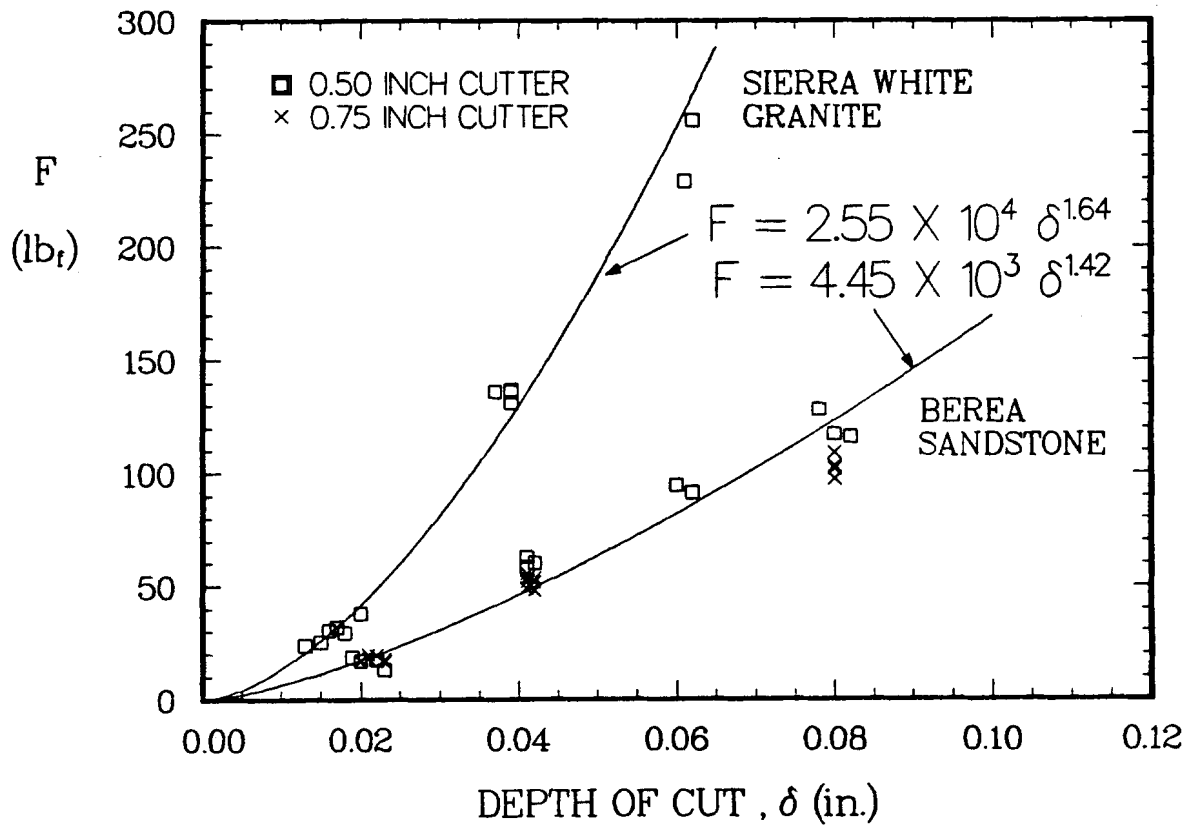


Figure 12 - Measured penetrating forces with sharp cutters in dry, non-interacting cuts.

CUTTER DRAG
COEFFICIENT,
 $\mu_d = F_d/F$

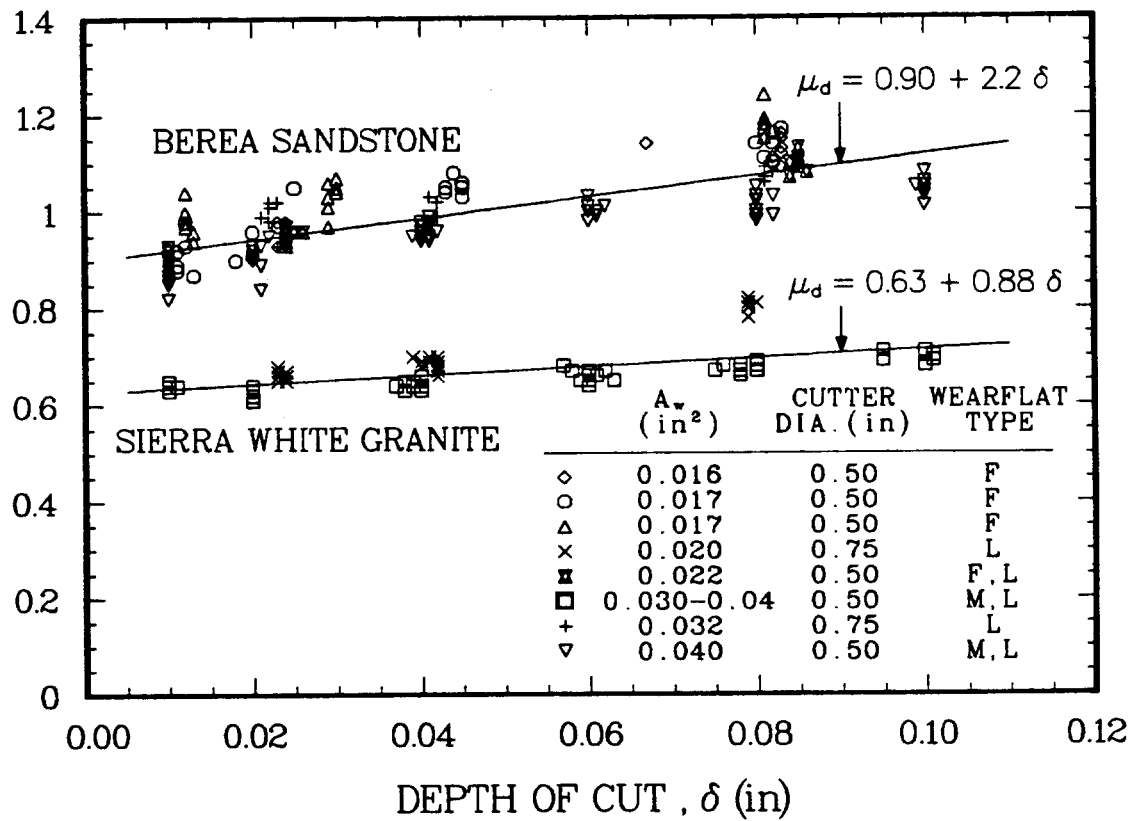


Figure 13 - Measured drag coefficients with various wearflat configurations in dry, non-interacting cuts. Wearflat type: F=field worn; L=laboratory worn; M=machine worn.

CUTTER DRAG
COEFFICIENT,
 $\mu_d = F_d/F$

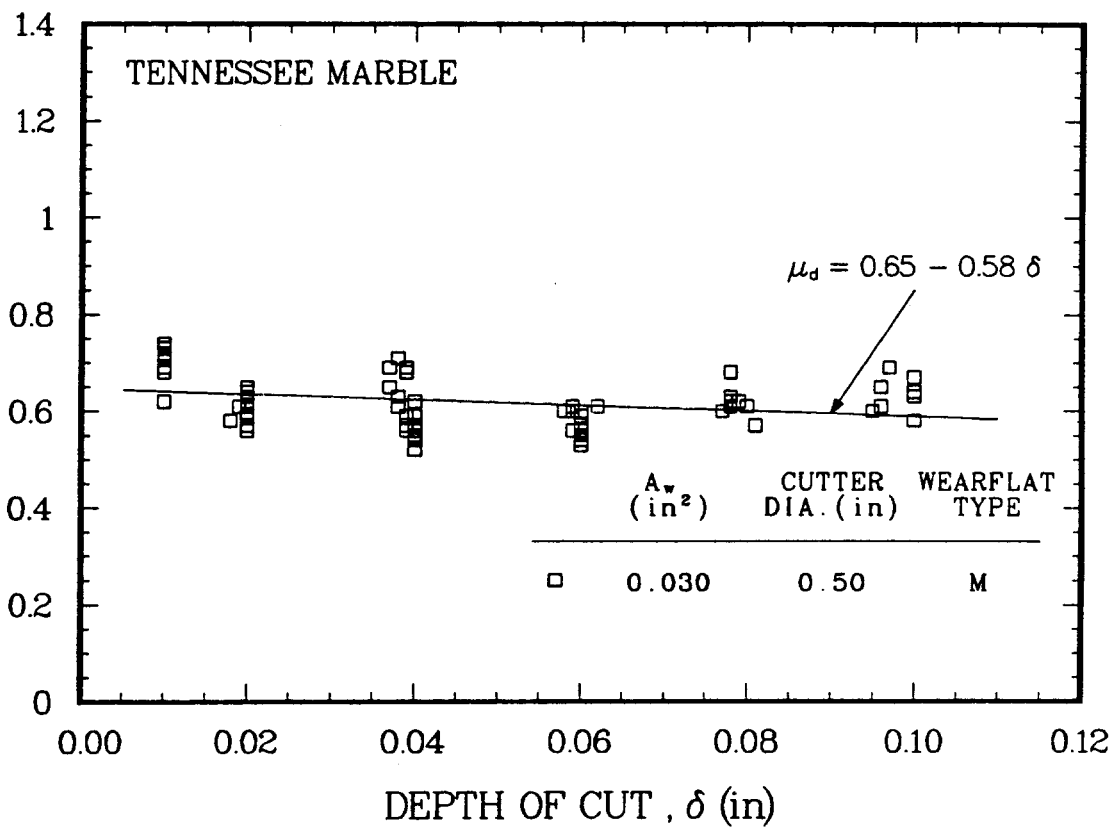


Figure 14 - Measured drag coefficients with various wearflat configurations in dry, non-interacting cuts. Wearflat type: F=field worn; L=laboratory worn; M=machine worn.

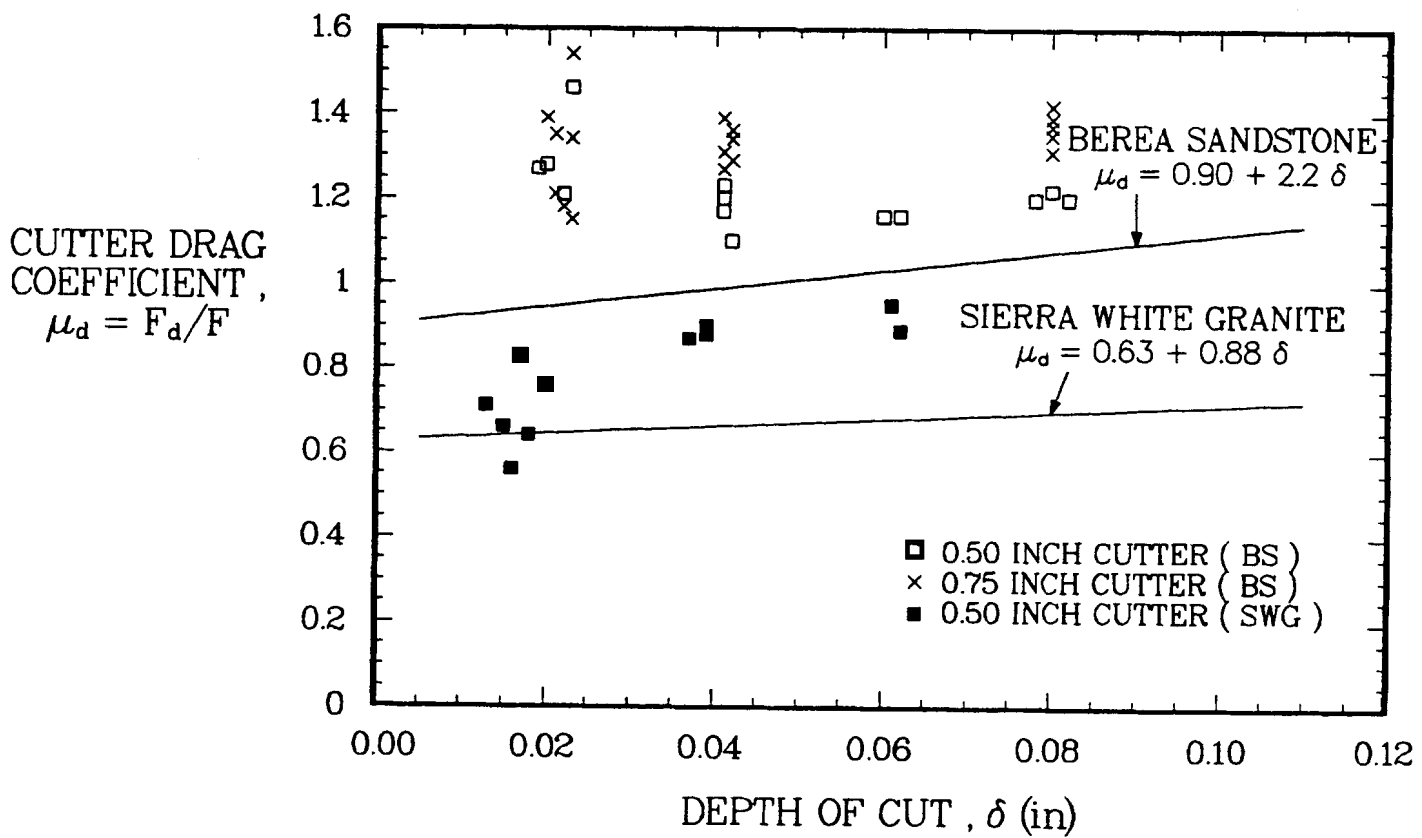


Figure 15 - Measured drag coefficients with sharp cutters in dry, non-interacting cuts. Curves represent mean data obtained with worn cutters (Fig. 13).

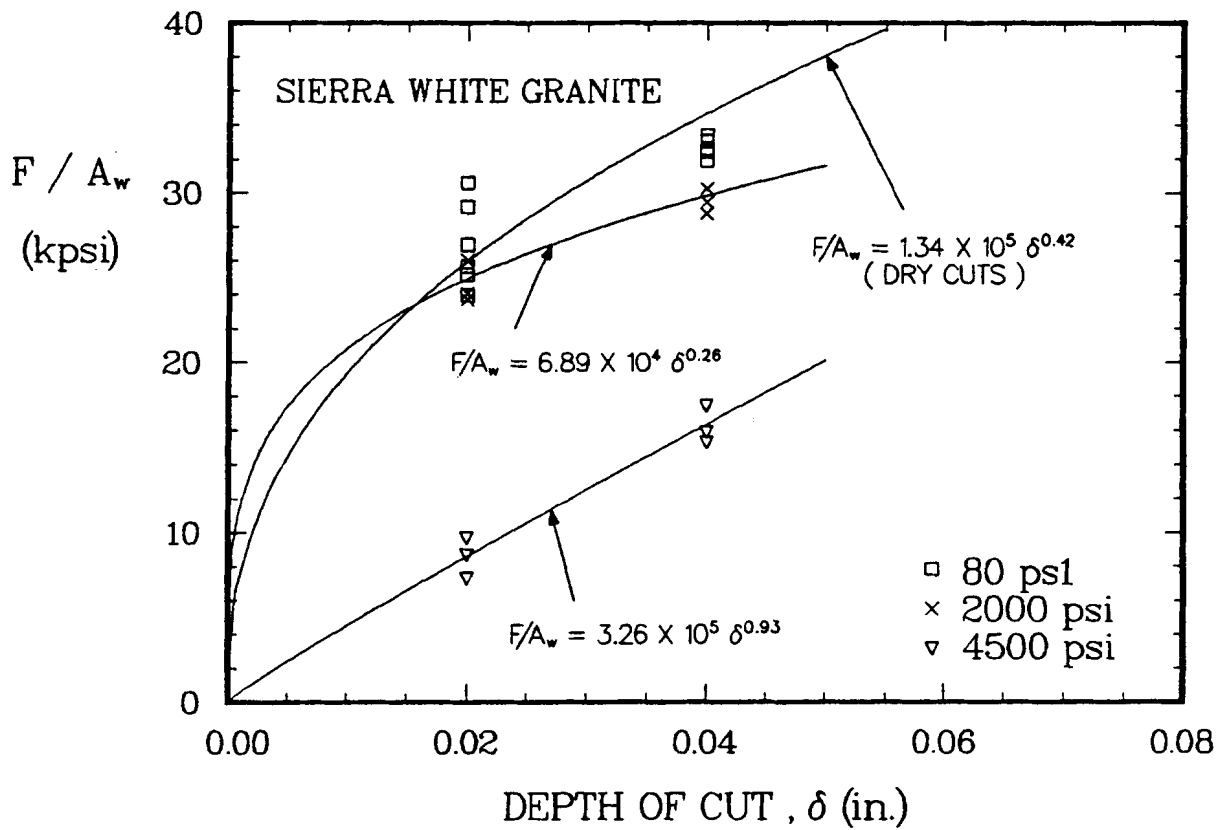


Figure 16 - Measured penetrating stresses in non-interacting cuts made with waterjet assistance. Upper curve represents mean data from dry cuts (Fig. 10).

nozzle pressures, however, penetrating stresses are significantly reduced. With jet pressures of 2,000 psi, the penetrating stresses required to cut Sierra White granite to a given depth are reduced by 10 to 15%. With assistance from 4,500 psi waterjets, cutter penetrating stresses are reduced by 50 to 65%.

Passes made over the rock surface without actual contact between the cutter and the rock revealed that the 2,000 psi jet alone did not cause visible damage to the rock surface. The observed reductions in penetrating stresses in this case are probably due to improved cleaning at the cutter/rock interface. Efficient removal of cutting fines helps maintain greater stress concentration in the rock at the cutting edge.

In contrast, the 4,500 psi jet alone caused considerable damage to the rock surface, even though the nozzle standoff distance was greater than 1.5 inches. Though not a continuous cut, the path left by the jet in the granite resembled a series of closely-spaced irregular holes, some of which were up to 0.08 inch deep. The assistance given to the cutter by the jet in this case was due in large part to a reduction in the cutter cross-sectional area of cut and in the strength of the remaining rock surface.

The drag coefficients measured with the jet-assisted, non-interacting cuts are shown in Figure 17, where they are compared with the results for the dry cuts. The drag forces are seen to be reduced by the presence of water, but they are not greatly affected by jet pressure. This suggests that the reduction in drag coefficient is caused by the lubrication effect of water, which reduces the friction component of the drag force. This supports a model for the drag force which considers the force to be the sum of two components [29]:

$$F_d = F_c + F_f, \quad (6)$$

where F_c is the cutting force and F_f is the friction force. We may divide Eq. 6 by F_c and recognize that the friction coefficient, μ , is defined as the ratio F_f/F_c . The result is then

$$\mu_d = F_c/F + \mu. \quad (7)$$

We thus see that a reduction in friction coefficient results in an equal reduction in drag coefficient.

Measured friction coefficients between PDC cutters and Sierra White granite are approximately 0.16 under dry cutting conditions and 0.07 when cutting with low-pressure waterjets directed at the cutter/rock interface [19]. The difference in friction coefficient of about 0.09 between the wet and dry cutting conditions is apparently translated to a comparable difference in drag coefficient between the two conditions, as predicted by Eq. 7 and confirmed in Figure 17.

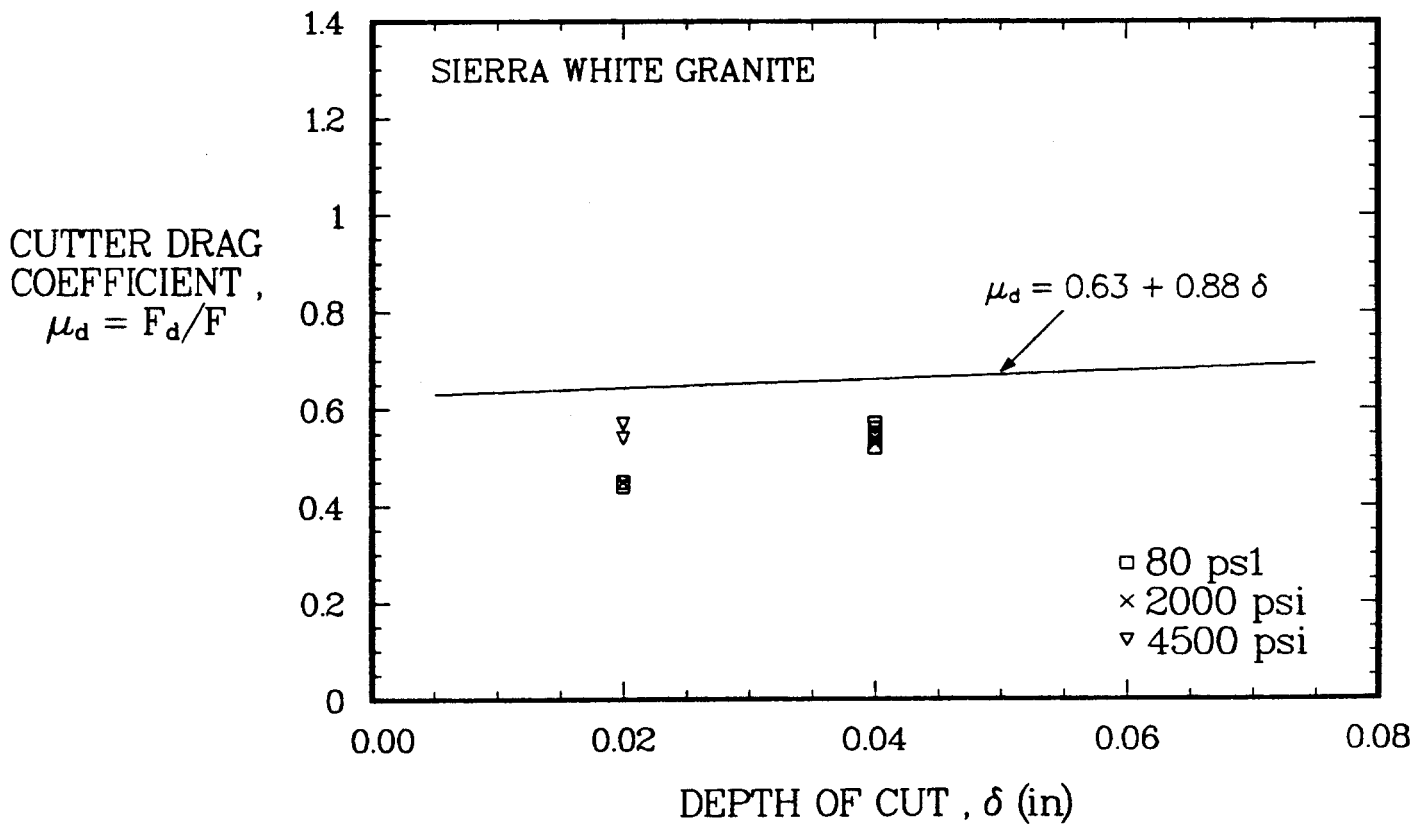


Figure 17 - Measured drag coefficients in non-interacting cuts made with waterjet assistance. Curve represents mean data from dry cuts (Fig. 13).

2.4 Test Results: Interacting Cuts

All interacting cuts were done dry. The data are tabulated in Tables A-6 and A-7 (Appendix A). These data are summarized in Figure 18. Shown here are the measured penetrating stresses as a function of the lateral distance to adjacent, pre-existing cuts. For comparison, the upper and lower dashed lines on the figures represent the penetrating stresses obtained with the dry non-interacting cuts at depths of 0.080 inch and 0.040 inch, respectively.

At large lateral distances to adjacent cuts, the geometry of the center test cut approaches that of a single, non-interacting cut of 0.080 inch depth, as seen in Figure 19. As the pre-existing adjacent cuts are placed closer together, cutter interaction reaches the level where the cross-sectional area of rock removed by the center test cut is the same as that removed in a single, non-interacting cut of 0.040 inch depth. We should, therefore, expect the penetrating stress data of Figure 18 to approach the lower dashed line at small values of d for each rock type and to approach the upper dashed line for each rock type at large values of d , as they do.

The drag coefficients measured in the interacting cut tests are tabulated in Tables A-4 and A-5 (Appendix A). These results are comparable to those obtained in the non-interacting cut tests. This indicates that the cutter drag coefficient is independent of cutter interaction. In other words, although both the penetrating force and the drag force are strongly affected by cutter interaction, the ratio of the two forces is relatively unaffected.

2.5 Analysis of Cutter Interaction Effects

A typical cutting pattern for a cutter on the leading face of a PDC bit is shown in Figure 20. This cutting pattern imposes a given penetrating and drag force on the cutter, depending on the type of rock, the wearflat area, and the cutting conditions. It has been shown that the ratio of drag to penetrating force in a given rock type is not heavily dependent on the depth of cut or degree of cutter interaction. There should then exist an equivalent non-interacting cut that would impose the same forces on the cutter as the actual cutting profile seen in Figure 20. The profile of the flat rock surface in such an equivalent cut is shown as the heavy dashed line in the figure. The location of the equivalent surface relative to the bottom of the cut is δ_e , which is defined as the effective depth of the equivalent non-interacting cut. By definition, the penetrating stress of the equivalent cut is equal to the penetrating stress of the actual cut. Since the geometry of the equivalent cut is the same as that of a non-interacting cut, the effective depth of cut is then related to the actual penetrating stress, as in Eq. 3:

$$F/A_w = C_1(\delta_e)^{n1} \quad (8a)$$

or, in the case of a sharp cutter, to the penetrating force, as in Eq. 4:

$$F = C_2(\delta_e)^{n2} \quad (8b)$$

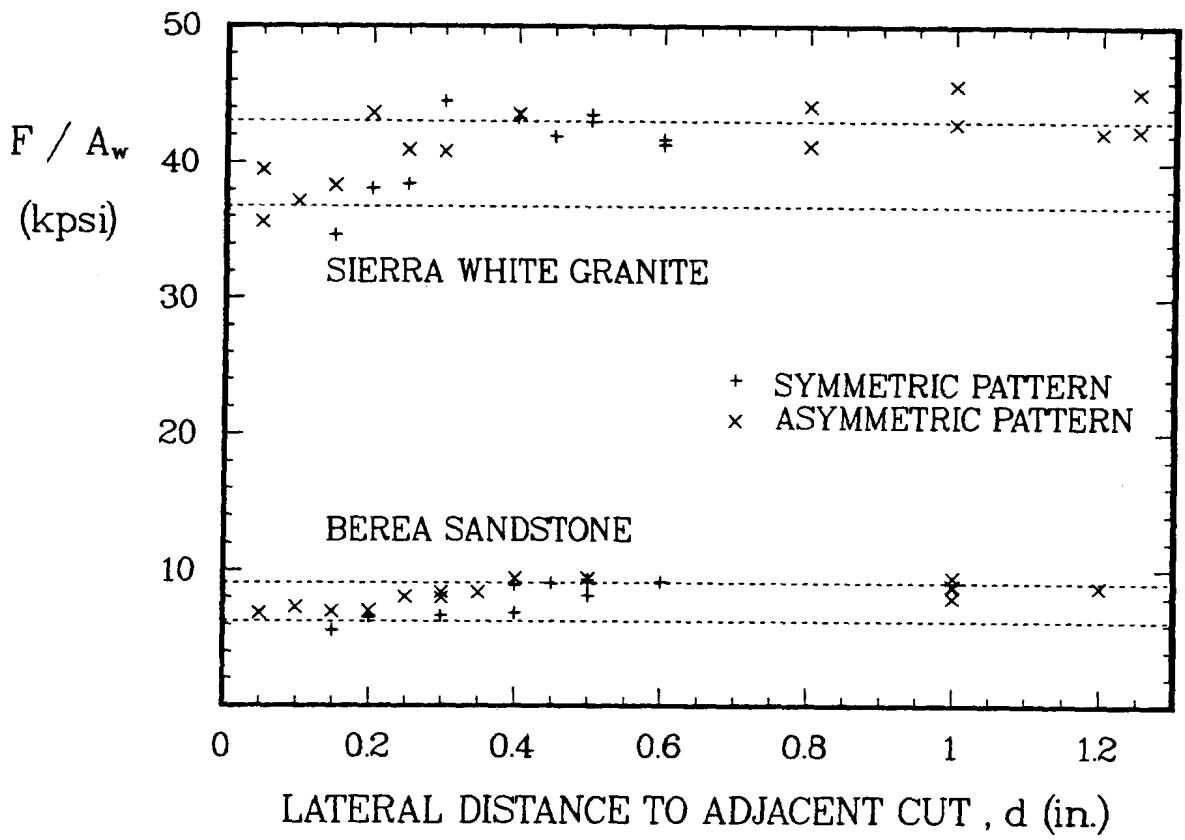


Figure 18 - Measured penetrating stresses in dry, interacting cuts. Upper dashed line for each rock type represents mean penetrating stresses measured at 0.080 inch depth of cut in dry, non-interacting cuts. Lower dashed line for each rock type represents values measured at 0.040 inch depth of cut in dry, non-interacting cuts.

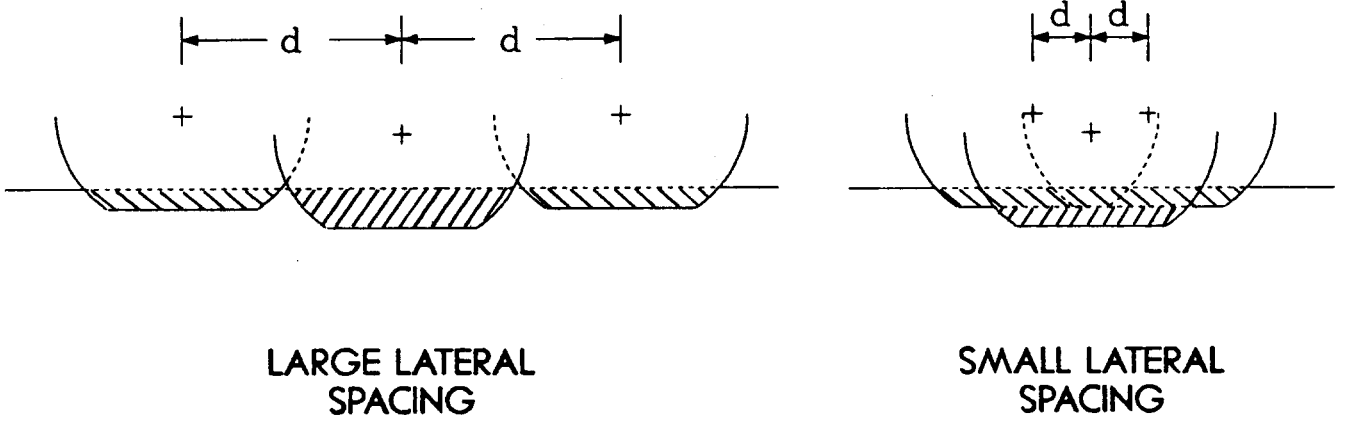


Figure 19 - Interacting cut patterns with large and small lateral spacing between cuts. Center cut is test cut in both cases.

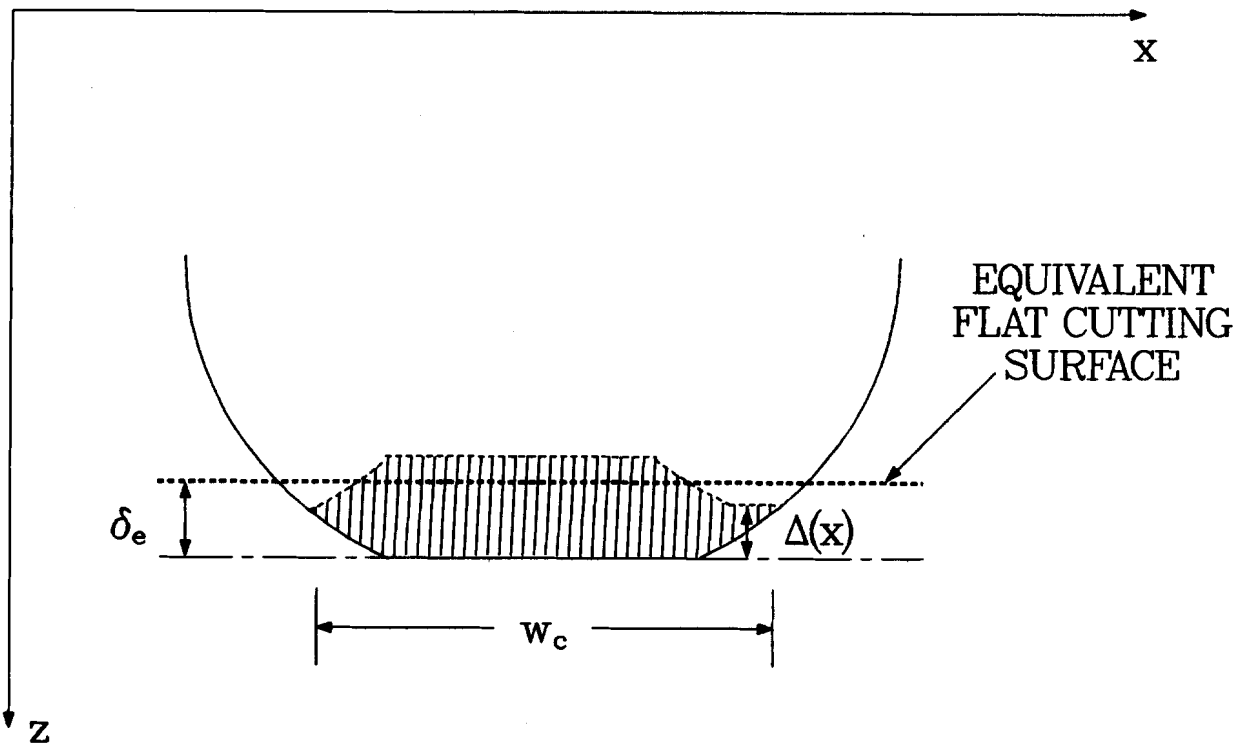


Figure 20 - Typical cutting pattern for a worn cutter on the leading face of a PDC bit. Shaded area is the actual cross-sectional area of cut.

Inspection of Figure 20 shows that the location of the equivalent flat surface would probably be at a midpoint location between the high and low points on the actual rock cutting profile, as shown. A simple estimate of δ_e would then be the mean height of the actual profile:

$$\delta_e \cong \frac{1}{w_c} \int \Delta(x) dx \quad (9)$$

A computer program described in Section 3.0 was written to integrate Eq. 9 numerically for the interacting test cut configurations shown in Figure 9. The results of the integrations for both the symmetric and asymmetric interaction patterns are shown in Figure 21. Note that for these tests, δ_e tends toward 0.040 inch at a small lateral distance to an adjacent cut; at a large lateral distance to an adjacent cut, δ_e approaches 0.080 inch.

The measured penetrating stresses associated with the computed effective depths of cut for the interacting cut tests are shown as the data points in Figure 22. The curves in these figures represent the predicted penetrating stresses given by Eq. 8a for the interacting test cuts, based on the non-interacting cut test data (Figure 10) and the described algorithm for estimating δ_e . The good agreement between the predicted and measured penetrating forces provides the basis for developing a computer code that uses this procedure for estimating δ_e and, subsequently, cutter forces in arbitrary bit designs.

2.6 Other Observations

Considerable scatter exists in the data of Figures 10-22. Since these tests were conducted under carefully controlled and monitored conditions, it is reasonable to assume that the scatter is inherent to the rock cutting process itself. For this reason, tests were generally conducted at least five times at each depth of cut and degree of cutter interaction. This ensured that the average effects of these parameters could be determined.

With the field-worn wearflats, the diamond and part of the WC-Co portion of the wearflat wore parallel to the cutting direction, as shown in Figure 23. The majority of the WC-Co portions of the wearflats, however, were generally inclined at angles of 5-10° with respect to the cutting direction. This angle is defined as the circumferential wear angle. These cutters were field-worn in relatively soft formations. The relative wear resistance of PDC and WC-Co apparently dominated the wear process. The WC-Co wore at a higher rate, thereby tending to keep only a small length, L, of the total wearflat length, L_c , in contact with the rock. This tends to maintain the cutter in a sharper condition. The WC-Co wear along the angled surface is attributable mostly to contact with ground rock particles passing beneath this surface.

The wearflats worn in the laboratory against Sierra White granite, on the other hand, wore nearly parallel to the cutting direction (within 1°).

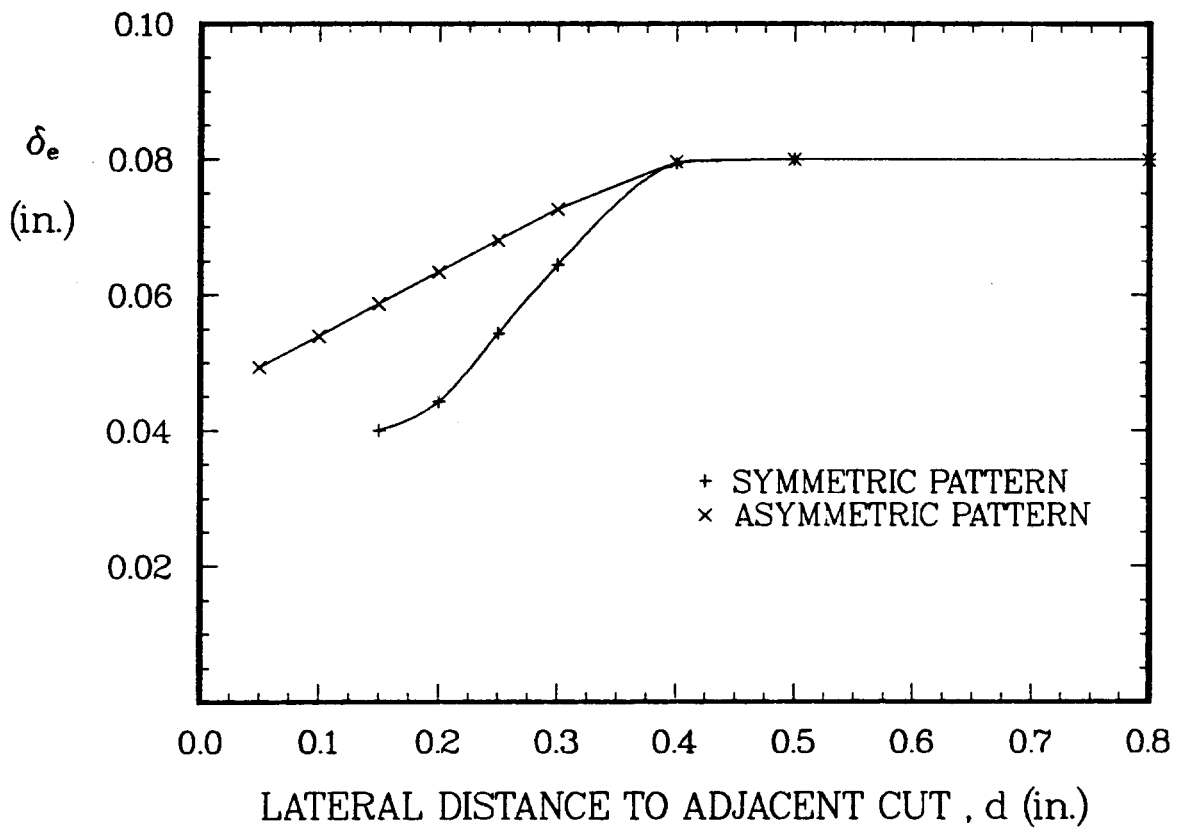


Figure 21 - Computed effective depth of cut as a function of lateral distance to adjacent cuts in interacting cut tests.

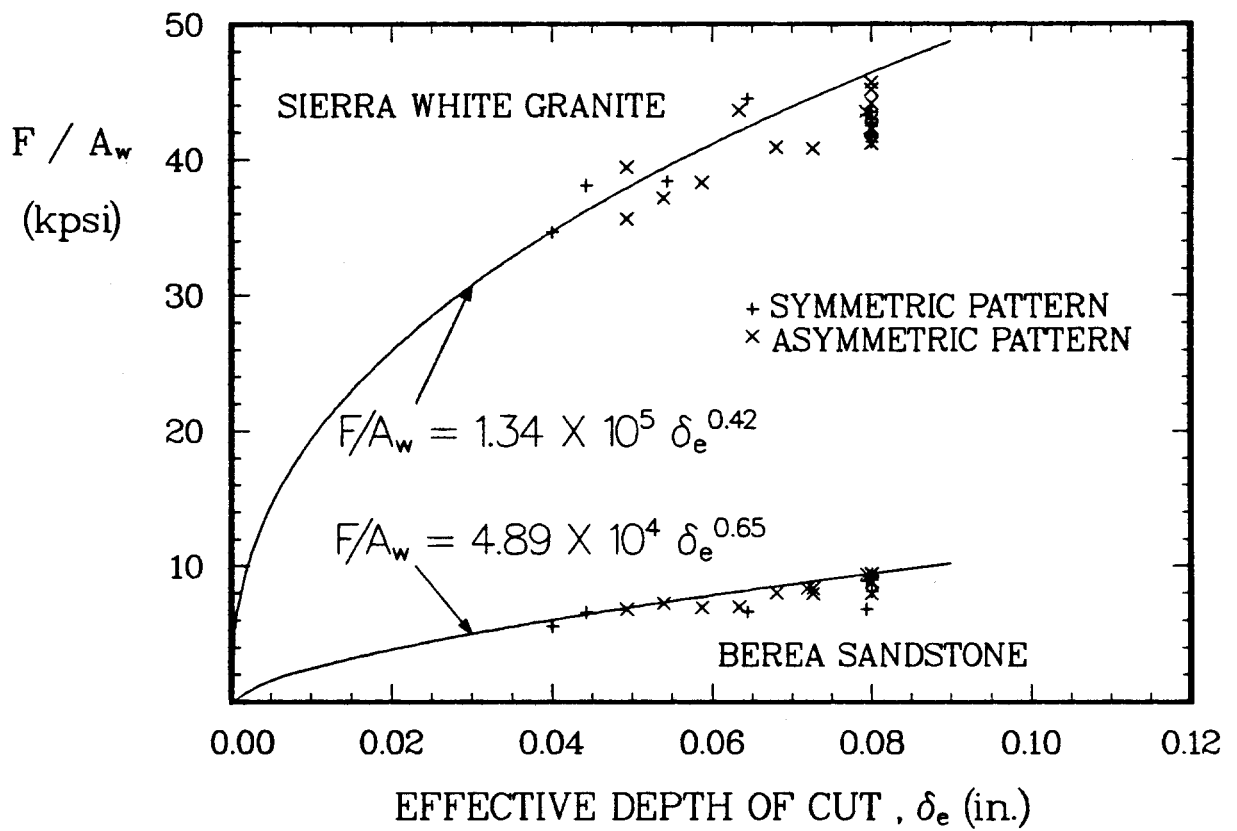


Figure 22 - Predicted and measured penetrating stresses for dry, interacting cut tests.

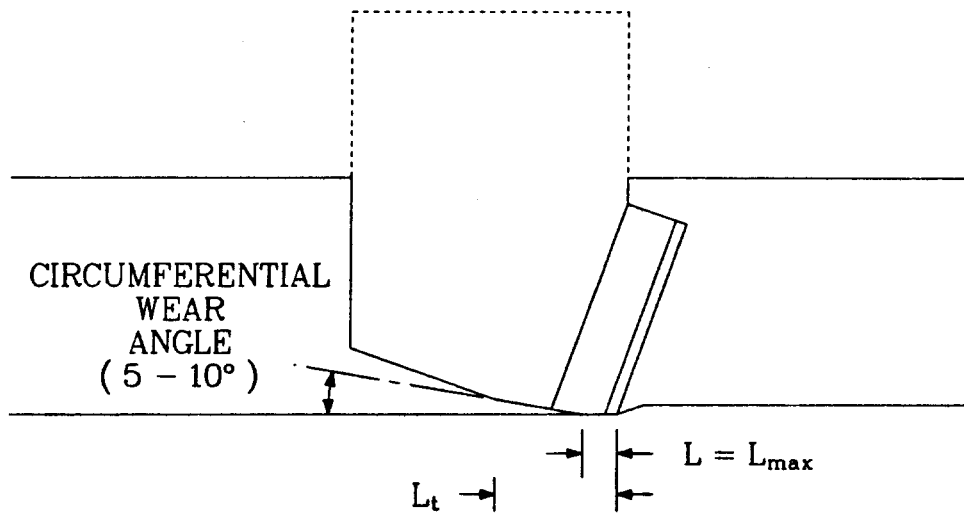


Figure 23 - Circumferential wear angle found to develop on field worn cutters.

Field-worn cutters worn further in the laboratory against granite exhibited the same behavior. This indicates perhaps that the greater impact loading associated with hard-rock drilling, particularly in quartz-rich rock, tends to fracture off any PDC layers that are not fully supported by the WC-Co backup material. This tends to keep more of the WC-Co in contact with the rock, creating a duller cutter condition. This wear mechanism could be a major contributor to poor bit life in hard or fractured rock.

3.0 DEVELOPMENT OF THE COMPUTER CODE, PDCWEAR

This section describes development of a computer code that uses the single-cutter test results as a basis for predicting bit performance. The code also uses PDC cutter wear models developed in our earlier work [31] to predict the wear of the bit and the effects of that wear on subsequent bit performance. Accordingly, the code is named PDCWEAR.

The source code for PDCWEAR is listed in Appendix B. PDCWEAR is written in FORTRAN 77, which complies with the American National Standards Institute (ANSI) standard. It was developed on a VAX 8650 computer.

The origin of the algorithm used in PDCWEAR for cutter geometry calculations is a previous computer code published by Sandia in 1982 [48]. That code, STRATAPAX, computes cross-sectional areas and volumes of cut for each cutter in an arbitrary bit design. STRATAPAX has an optimization routine that adjusts cutter radial placement in order to equalize either cutting volumes or cross-sectional areas, as specified by the user. Extensive modifications to the algorithm have been made in developing PDCWEAR code to account for the effects of wear and to calculate quantities needed to compute cutter forces, temperatures, and wear rates.

3.1 Cutter Interaction Theory

The geometry of a single cutter and cut profile are shown in Figure 24. The cutter inclination angle, ϕ_c , defines the tilt of the cutter longitudinal axis with respect to the longitudinal axis of the bit. The radial wear angle, ϕ_w , defines the location and radial inclination of the wearflat on the cutter profile. It also defines the direction of the cutter penetrating force, because the penetrating force acts normal to the wearflat.

Four coordinate systems are used to describe the cut and cutter profiles, as shown in Figure 25. The hole coordinate system is a non-rotating cartesian coordinate system whose z-axis is parallel to the longitudinal axis of the hole. The bit coordinate system is a cartesian coordinate system that rotates and advances with the bit and has a z'-axis parallel to the longitudinal axis of the bit and parallel to the z-axis of the hole coordinate system. The cutter coordinate system is a two-dimensional, rectangular coordinate system that lies in the plane of the diamond face of the cutter. The cutter profile coordinate system is the projection of the cutter coordinate system onto a radial plane running through the longitudinal axis of the bit.

A point (x'_0, z'_0) in the cutter coordinate system is projected into the cutter profile coordinate system (x_0, z_0) as

$$x_0 = x'_0 \quad (10a)$$

$$z_0 = z'_0 \cos \beta, \quad (10b)$$

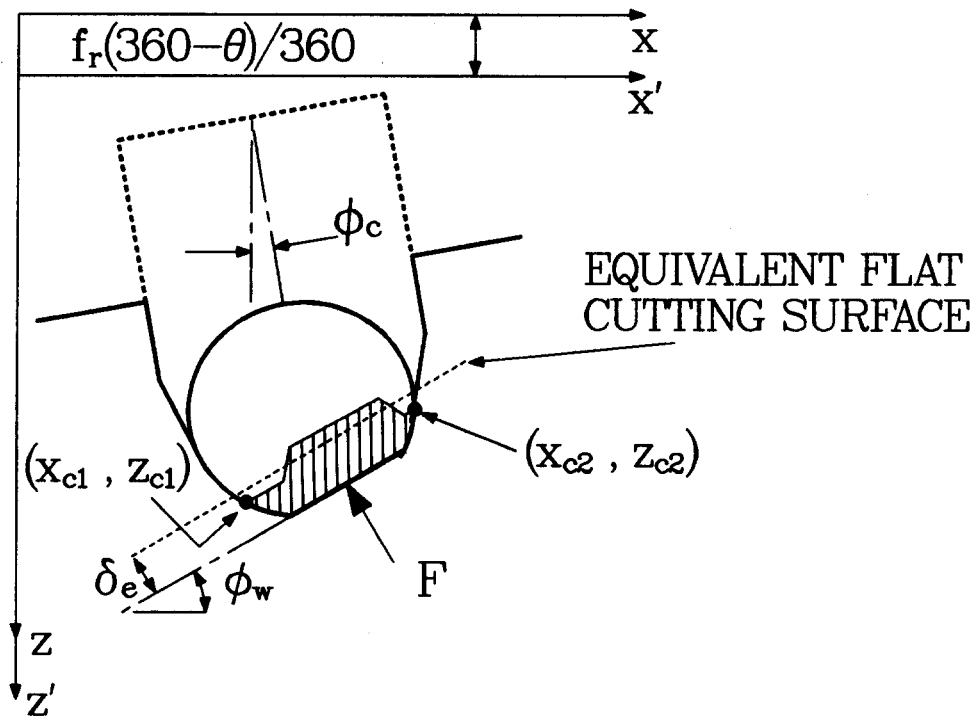


Figure 24 - Cut and cutter profiles for a general PDC cutter mounted on a bit. (x, y, z coordinate system is stationary; x', y', z' coordinate system travels with the bit.)

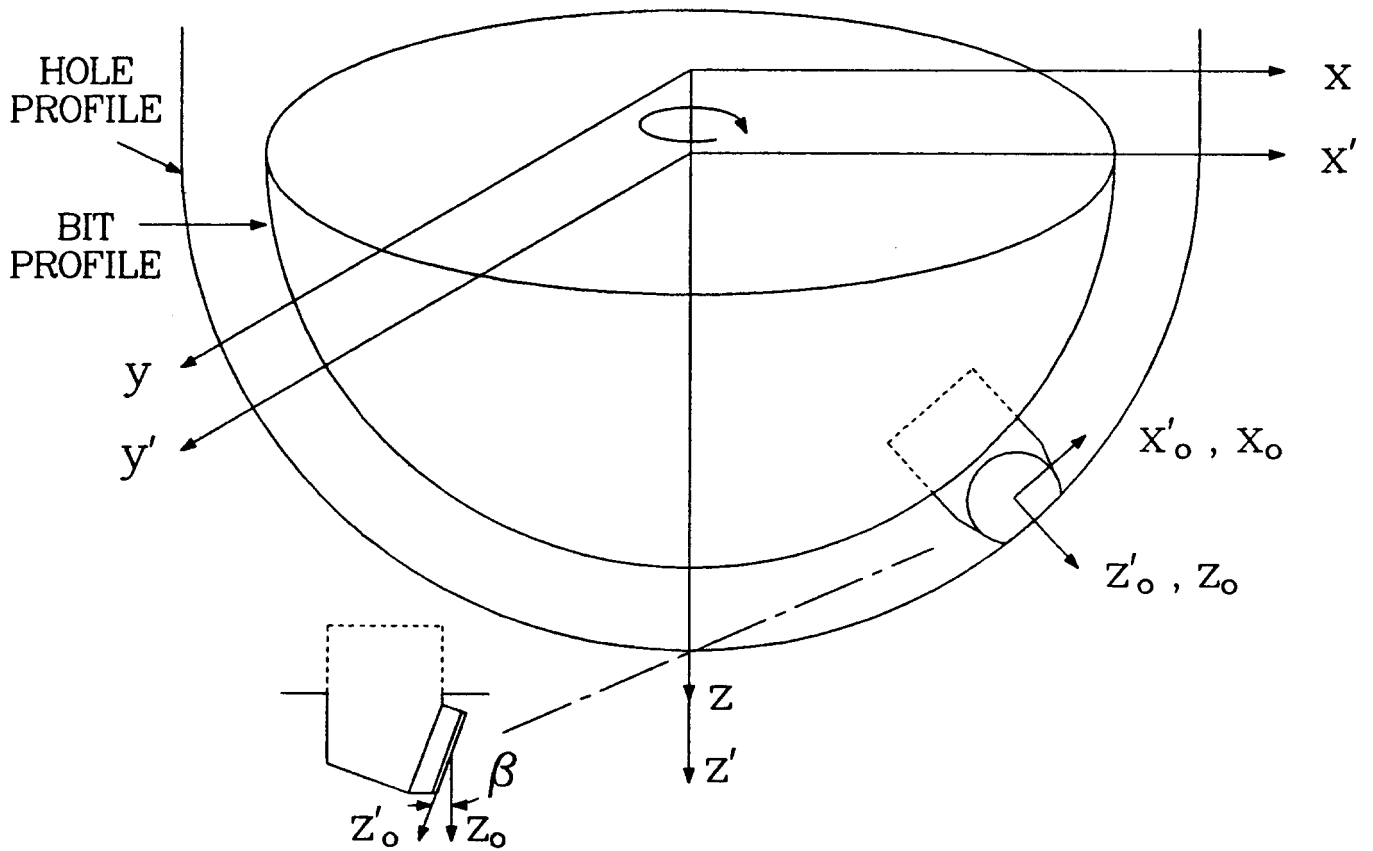


Figure 25 - Schematic of the four coordinate systems used to describe cut and cutter profiles. Hole (x, y, z) , bit (x', y', z') , cutter (x'_o, z'_o) , and cutter profile (x_o, z_o) coordinate systems.

where β is the cutter backrake angle. The circular edge of a sharp cutter in the cutter coordinate system is described by the equation:

$$\left(\frac{x'_o}{r}\right)^2 + \left(\frac{z'_o}{r}\right)^2 = 1, \quad (11)$$

where r is the radius of the circular cutter compact. Transforming this equation to the cutter profile coordinate system, the cutter profile proves to be one of an ellipse:

$$\left(\frac{x_o}{r}\right)^2 + \left(\frac{z_o}{b}\right)^2 = 1, \quad (12a)$$

where
$$b = r \cos \beta. \quad (12b)$$

During one revolution of the bit, each cutter passes through the x - z plane of the hole coordinate system. As each cutter passes through this plane, the transformation equations between the hole coordinate system (x, y, z) and that cutter's profile coordinate system (x_o, z_o) are (see Figure 26):

$$x = R + x_o \cos \phi_c + z_o \sin \phi_c, \quad (13a)$$

and
$$y = 0, \quad (13b)$$

$$z = H - x_o \sin \phi_c + z_o \cos \phi_c, \quad (13c)$$

where
$$H = H' + f_r(360 - \theta)/360. \quad (13d)$$

Here R and H' are the radial and longitudinal locations, respectively, of the center of the cutter compact on the bit body. The quantity H , defined as the cutting height of the cutter, accounts for the fact that the bit advances in the z -direction as it rotates. This height, which is the z -coordinate of the center of each cutter as it passes through the x - z plane of the hole coordinate system is a function of the feed per revolution, f_r , and the angular position, θ , of the cutter on the bit face. The angular position (in degrees) is defined as positive in the counterclockwise direction (looking at the face of the bit). The feed rate is related to the rate of penetration, ROP, and the bit rotary speed, N :

$$f_r = \text{ROP}/N. \quad (13e)$$

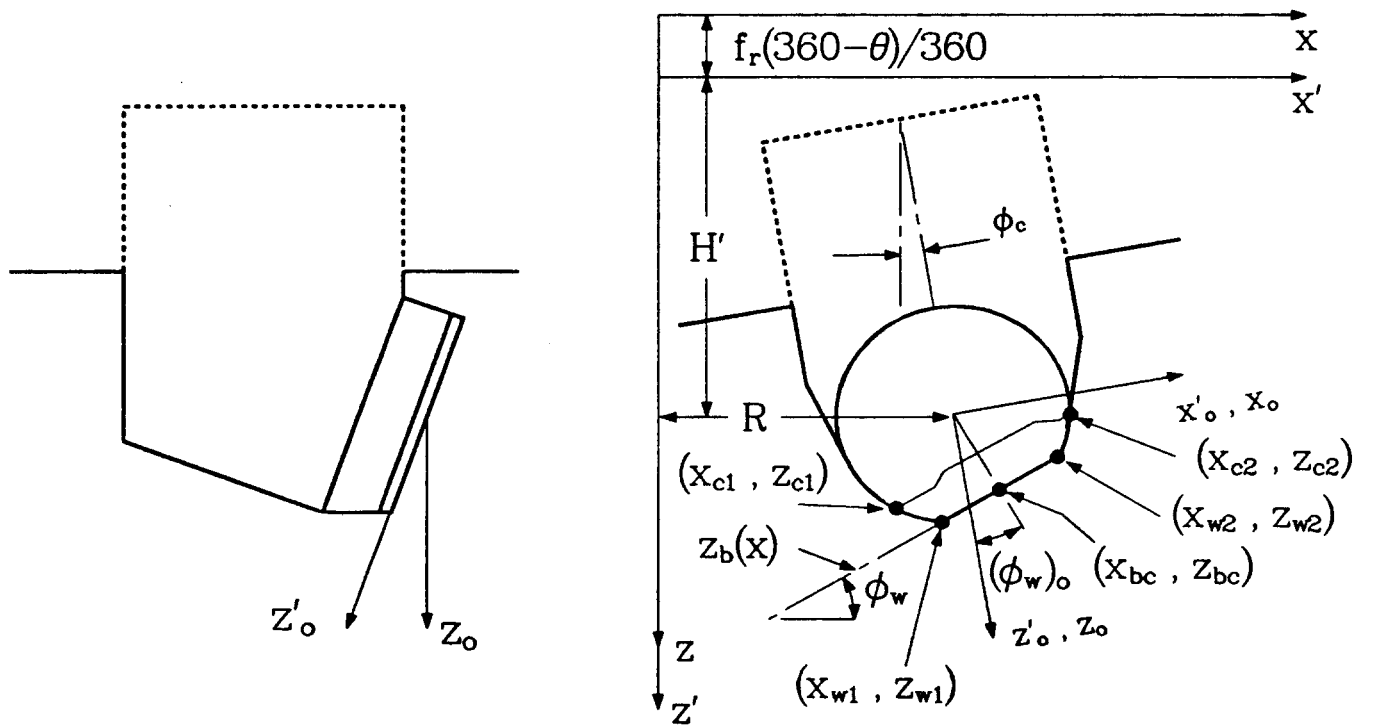


Figure 26 - Detailed definition of several points used in cutter geometry analysis.

Combining Eqs. 12 and 13 we obtain the cutting profile (x,y,z) of a sharp cutter in terms of the hole coordinate system:

$$z = C_3 [D(x - R) \pm \sqrt{E - (x - R)^2}] + H , \quad (14a)$$

$$y = 0 , \quad (14b)$$

where

$$C_3 = \frac{rb}{E} \quad (14c)$$

$$D = -\sin \phi_c \cos \phi_c (r^2 - b^2)/rb \quad (14d)$$

$$E = r^2 \cos^2 \phi_c + b^2 \sin^2 \phi_c . \quad (14e)$$

At any point on the x-axis, these equations define the z-coordinate of the cutting edge of each sharp cutter as it passes through the vertical plane.

Wear modifies the cutting profile according to the wearflat width, w, and the radial wear angle, ϕ_w . An algorithm in the program iterates upon the wear angle by initially assuming $\phi_w = \phi_c$. The wearflat geometry of each cutter is then computed based on this initial guess. The cut profile for each cutter is determined using the algorithm described below. New estimates of ϕ_w are then made for each cutter by assuming that the wearflat of a cutter develops parallel to the overall radial slope of the rock surface encountered by that cutter, as shown in Figure 24. In other words,

$$\phi_w = \tan^{-1} \left[\frac{z_{c1} - z_{c2}}{x_{c2} - x_{c1}} \right] . \quad (15)$$

Since the new estimate of ϕ_w may be different from the initial guess, the wearflat locations on the cutters may change from the previous iteration, which in turn changes the cut profiles. The process is repeated until the solution converges for all cutters.

As suggested by Eq. 15, the location of the wearflat on the cutting profile is a function of the interaction experienced by that cutter. The wearflat modifies the cutter profile over the range

$$x_{w1} < x < x_{w2} \quad (16)$$

seen in Figure 26, and for values of x in this range, Eq. 14 is not valid. Instead, the cutter profile within this range is described by the line,

$$z = z_{w1} + \left[\frac{x - x_{w1}}{x_{w2} - x_{w1}} \right] (z_{w2} - z_{w1}) \quad (17)$$

We must, therefore, derive expressions for (x_{w1}, z_{w1}) and (x_{w2}, z_{w2}) .

The cutter wearflat is easiest described in the cutter coordinate system. In this system, the wear angle $(\phi_w)'_o$ is related to the wear angle in the hole coordinate system with the equation

$$(\phi_w)'_o = \tan^{-1} \left[\frac{(z_{c1})'_o - (z_{c2})'_o}{(x_{c2})'_o - (x_{c1})'_o} \right] = \tan^{-1} \left[\frac{((z_{c1})'_o - (z_{c2})'_o) / \cos \beta}{(x_{c2})'_o - (x_{c1})'_o} \right]$$

or

$$(\phi_w)'_o = \tan^{-1} [\tan(\phi_w)_o / \cos \beta] \quad (18a)$$

where

$$(\phi_w)_o = \phi_w - \phi_c \quad (18b)$$

The wearflat width, w , is measured in the cutter coordinate system. In the circular geometry of this system, geometry considerations give the results,

$$(x_{w1})'_o = r_w \sin(\phi_w)'_o - \frac{w}{2} \cos(\phi_w)'_o \quad (19a)$$

$$(z_{w1})'_o = r_w \cos(\phi_w)'_o + \frac{w}{2} \sin(\phi_w)'_o \quad (19b)$$

$$(x_{w2})'_o = r_w \sin(\phi_w)'_o + \frac{w}{2} \cos(\phi_w)'_o \quad (19c)$$

$$(z_{w2})'_o = r_w \cos(\phi_w)'_o - \frac{w}{2} \sin(\phi_w)'_o \quad (19d)$$

where

$$r_w = \sqrt{r^2 - \left(\frac{w}{2}\right)^2} \quad (19e)$$

The profile of a worn cutter can now be determined by using Eqs. 14-19.

The computer algorithm that implements the above equations is illustrated in Figure 27. The x-axis is divided into a number of equal-sized elements of length Δx . At each value of x corresponding to the midpoint of these elements, a procedure determines which cutters interact at that cutting radius. For each of these cutters, the program tests whether

$$x_{w1} < x < x_{w2} \quad (20)$$

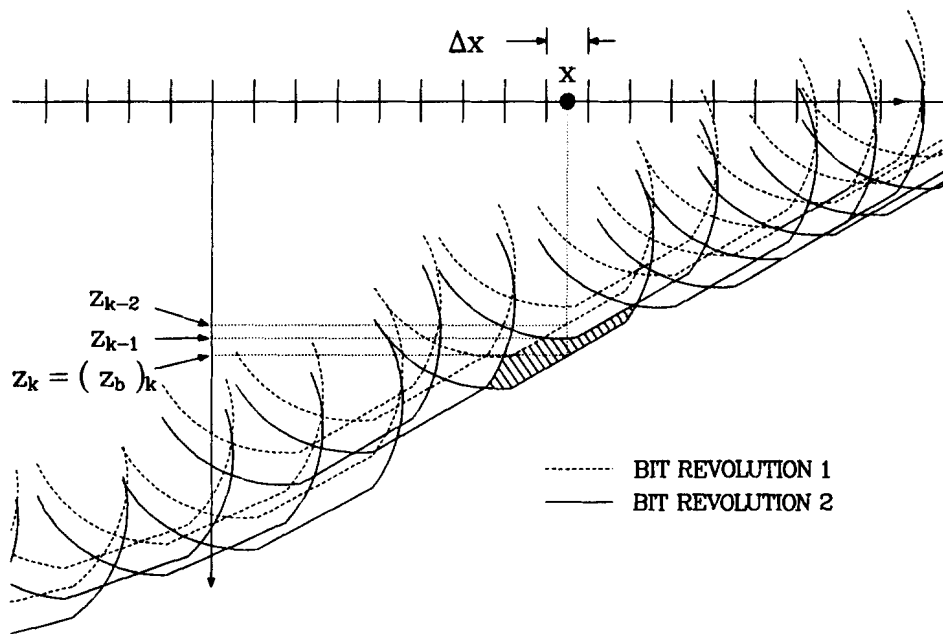


Figure 27 - Schematic of algorithm used in PDCWEAR to compute z-coordinates of cutting profiles at each value of x.

If x falls within this range, Eq. 17 is used to determine z_k , the z -coordinate of the k th cutter profile encountered at that radial position x . If x is not in this range for a given interacting cutter, Eq. 14 is used to determine z_k . In either case, the incremental cross-sectional area of cut,

$$\Delta A_r = \Delta x (z_k - z_{k-1}) , \quad (21)$$

is assigned to the k th cutter. The incremental volume of cut,

$$\Delta V_r = 2\pi x (\Delta A_r) , \quad (22)$$

is assigned to the same cutter. This procedure is repeated for the $k-1$ cutter encountered at x , then the $k-2$ cutter, etc.

By definition, the equivalent cutting surface in the cutter interaction model is inclined at the radial wear angle, ϕ_w . Since the penetrating force is normal to the wearflat, this implies^w that the penetrating force is directed at the angle ϕ_w with respect to the longitudinal axis of the bit. Depending on cutter interaction, ϕ_w may not equal ϕ_c , and the penetrating force may not develop parallel to the longitudinal axis of the cutter, resulting in a cutter side force.

The effective depth of cut must be computed in the same direction as the penetrating force vector. The equivalent bottom of each cut is described by the line (see Fig. 26):

$$z_b = z_{bc} + (x_{bc} - x) \tan \phi_w \quad (23a)$$

where
$$z_{bc} = H - (x_{bc})_o \sin \phi_c + (z_{bc})_o \cos \phi_c \quad (23b)$$

$$x_{bc} = R + (x_{bc})_o \cos \phi_c + (z_{bc})_o \sin \phi_c \quad (23c)$$

$$(z_{bc})_o = [r_w \cos (\phi_w)_o'] \cos \beta \quad (23d)$$

$$(x_{bc})_o = r_w \sin (\phi_w)_o' \quad (23e)$$

and $(\phi_w)_o'$ and r_w are given by Eqs. 18 and 19e, respectively. At each point x , the z -location of the bottom of the k th cut, $(z_b)_k$, is given by Eq. 23. The effective depth of cut for each cutter is then

$$\delta_e = \frac{1}{n_x} \sum_{i=1}^{n_x} \Delta_i \quad (24a)$$

where
$$\Delta_i = [(z_b)_k - (z)_{k-1}] \cos \phi_w \quad (24b)$$

and n_x is the number of Δx elements over which a given cutter interacts with the rock formation.

3.2 Forces and Moments Acting on the Bit

Once the effective depths of cut are computed, the cutter penetrating force can be estimated using Eq. 8b for sharp cutters and Eq. 8a for worn cutters. The algorithm used in PDCWEAR computes penetrating forces based on both equations and uses the larger of the two computed values. This logic is based on the fact that Eq. 8a is not valid with very small wearflat areas because the crushed rock beneath the cutter wearflat tends to distribute the penetrating force over an area larger than the small wearflat area. Since the lowest penetrating force possible is the one obtained with a sharp cutter, it is evident that Eq. 8b is more accurate than Eq. 8a in cases where Eq. 8b predicts higher forces.

It should be noted that in cases where the wearflat develops on the side of the cutter (i.e., $\phi_w \neq \phi_c$), some inaccuracies in computed cutter forces will occur. This is caused by the fact that in such cases, the angular transformation converts some of the cutter backrake to a small effective siderake angle. This factor is not significant for the relatively small backrake angles generally used in PDC bits (5-20°).

As seen in Section 2.3, the cutter correlation constants C_1 , n_1 , C_2 , and n_2 can be significantly affected by waterjet assistance. The effects of other factors that control inherent drillability, such as backrake angle, are also implicitly contained within the values used for these parameters. As a result, PDCWEAR is written so that two different types of cutter can be specified, each with its own set of correlation constants. In this way, the effects of different design options, such as providing waterjet assistance to selected cutters on a bit face, can be assessed.

After the penetrating force is computed using the appropriate correlation constants, it may be resolved into radial and longitudinal (vertical) components in the bit coordinate system:

$$F_r = -F \sin \phi_w \quad (25)$$

and

$$F_v = -F \cos \phi_w \quad (26)$$

The drag force on each cutter is estimated using Eq. 5b. This force is directed opposite to the direction of the cutter velocity vector. In terms of the bit coordinate system, each drag force is a circumferential force about the longitudinal axis.

The resultant bit forces and moments arising from the cutter forces can now be determined. The total weight on bit (WOB) is simply the sum of the longitudinal components, as depicted in Figure 28:

$$WOB = \sum_{j=1}^{n_c} (-F_v)_j , \quad (27)$$

where n_c is the number of cutters on the bit. The drilling torque is the sum of the moments caused by the circumferential drag forces:

$$T = \sum_{j=1}^{n_c} (F_d)_j (x_{bc})_j , \quad (28)$$

where x_{bc} is defined in Eq. 23.

Unless the cutters are placed such that the cutting forces balance each other, there will be a net side force acting on the bit. The component of the side force in the x' -direction is

$$F'_x = \sum_{j=1}^{n_c} [(F_r)_j \cos(\theta)_j + (F_d)_j \sin(\theta)_j] . \quad (29a)$$

Likewise, in the y' -direction,

$$F'_y = \sum_{j=1}^{n_c} [(F_r)_j \sin(\theta)_j - (F_d)_j \cos(\theta)_j] , \quad (29b)$$

giving a resultant side force of

$$F_s = \sqrt{(F'_x)^2 + (F'_y)^2} . \quad (29c)$$

A different mode of bit imbalance is the net bending moment about the x' and y' axes:

$$M'_x = \sum_{j=1}^{n_c} [-(F_r)_j \sin(\theta)_j (z'_{bc})_j + (F_v)_j (x_{bc})_j \sin(\theta)_j + (F_d)_j \cos(\theta)_j (z'_{bc})_j] , \quad (30a)$$

$$M'_y = \sum_{j=1}^{n_c} [(F_r)_j \cos(\theta)_j (z'_{bc})_j - (F_v)_j (x_{bc})_j \cos(\theta)_j + (F_d)_j \sin(\theta)_j (z'_{bc})_j] , \quad (30b)$$

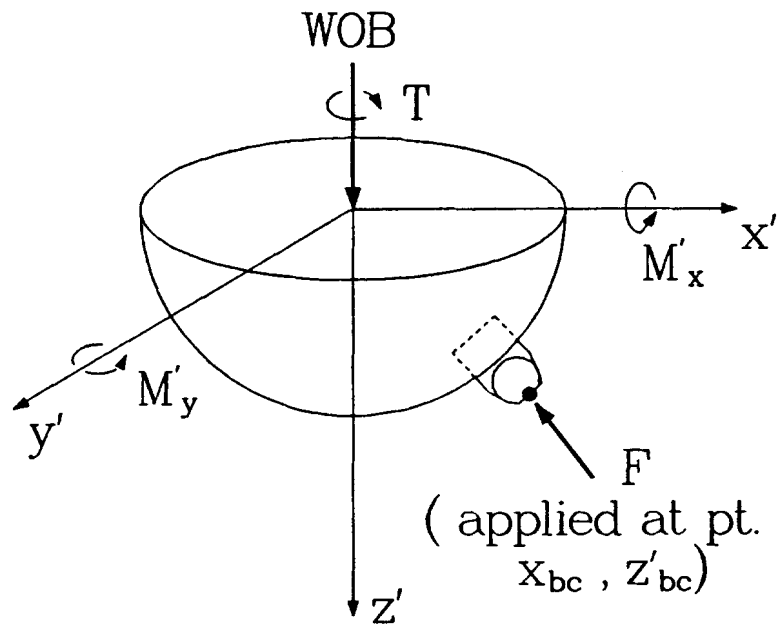
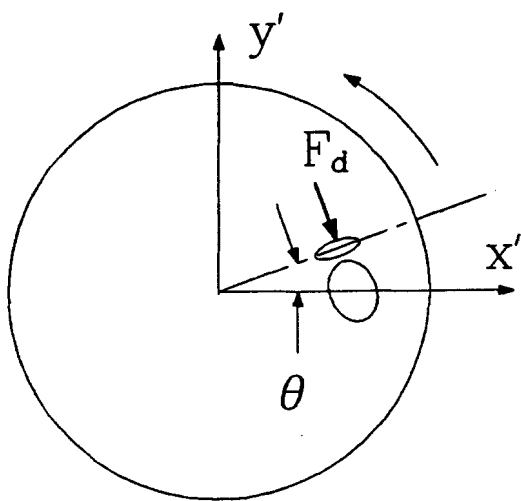


Figure 28 - Schematic showing how cutter forces are integrated to produce bit performance parameters.

where
$$z'_{bc} = z_{bc} - f_r (360 - \theta)/360 \quad (30c)$$

and x_{bc} and z_{bc} are defined in Eq. 23.

3.3 Cutter Wearflat Temperatures

The cutter wearflat temperatures are calculated using an equation developed in our earlier work [22,26,27]:

$$\bar{T}_w = T_f + \frac{\mu F V f}{A_w} \left[1 + \frac{3\sqrt{\pi}}{4} f k_2 \left(\frac{V}{L \chi_2} \right)^{1/2} \right]^{-1} \quad (31)$$

where T_f is the downhole fluid temperature; μ is the cutter/rock friction coefficient; V is the cutting speed; f is the thermal response function; L is the wearflat length in the cutting direction; k_2 is the thermal conductivity of the rock; and χ_2 is the thermal diffusivity of the rock. The cutting speed of each cutter is dependent on the rotary speed, N , of the bit and the radial location of the wearflat, x_{bc} :

$$V = 2\pi N x_{bc} \quad (32)$$

The thermal response function, f , is defined in our earlier work as the temperature rise of the cutter wearflat per unit frictional heat flowing into the cutter at the cutter/rock interface. The numerical value of f depends on the geometry of the cutter, material properties of the cutter and rock, and the cutter convective cooling coefficient, h . In our earlier work [27], we used a finite element thermal model to compute values of f for several different combinations of these parameters with a stud-mounted cutter employing 0.5-inch diameter PDC compacts. In the present study, we have obtained values of f for 0.75-inch diameter compacts, using the same approach.

Shown in Figure 29 is the finite element mesh used for one of the 0.75-inch cutter configurations assumed in this study. Shown here is a cutter with a severely worn compact. In addition to its larger compact size, this cutter also has a larger stud than has been traditionally used with the smaller compacts: 1.0 inch, compared with 0.625 inch, respectively. Because of the larger compact diameter, it is considered desirable to countersink the cutter to prevent the bit body-rock surface standoff distance from becoming excessive. Excessive standoff can reduce drilling fluid velocities across the face of the bit to levels below those required for proper cutter cooling and bottomhole cleaning [23,27].

The results for the severely worn compact and the other wear configurations considered in this study are presented in Appendix C, which also describes the thermal analysis in more detail. The results indicate that for most drilling conditions of interest, larger cutters generally have

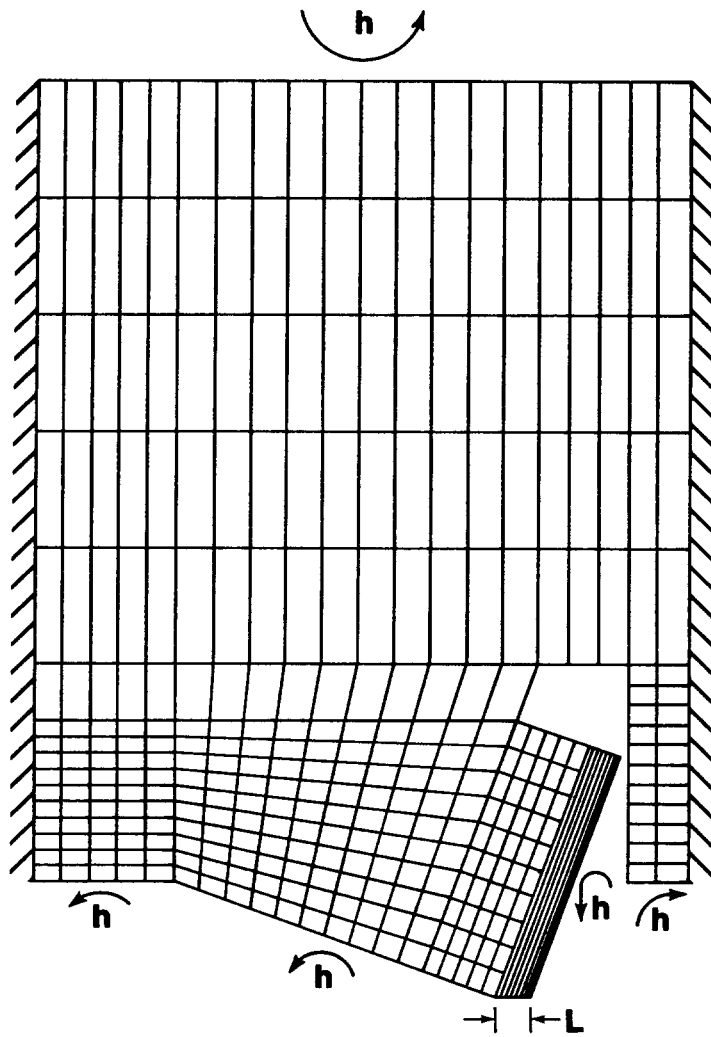


Figure 29 - Finite element mesh used to compute thermal response of 0.75-inch cutters.

larger values of f and thus run hotter than smaller cutters. This is caused by the longer mean path through the cutter for heat being conducted from the wearflat to a cooling surface. The higher temperatures, however, are relatively insignificant and are compensated for by the improved cutting efficiency inherent with larger cutters.

PDCWEAR uses an interpolation scheme to determine f for any given combination of cutter compact radius, r , wearflat length, L , and convective cooling coefficient, h . The range in cooling coefficient for which the computed value of f is backed by numerical results is 1.76 to 1.76×10^4 Btu/hr ft² °F. The range in cutter radius that is backed by numerical results is only 0.25 to 0.375 inch (0.5- to 0.75-inch diameter). All values of f computed by the program assume stud-mounted PDC cutters with a 20° backrake, conventional cutter materials, and a 0.025-inch thick diamond layer on the PDC face. Thermal effects related to parameters such as cutter material thermal conductivity, diamond layer thickness, and bit balling can be assessed for 0.5-inch cutters by replacing the base values of f tabulated in the program with values reported in Ref. 27 for those different conditions.

3.4 Cutter Wear Rates

To prevent thermally-accelerated wear, which is one to two orders of magnitude more rapid than ordinary abrasive wear, wearflat temperatures must be kept below 350°C. At temperatures below this critical value, ordinary abrasive wear will occur. For this type of wear, a model developed in our earlier work [31] concludes that the volume of cutter material, V_w , worn away per unit length of hole drilled, l_h , is related to several design and operating parameters:

$$\frac{dV_w}{dl_h} = \frac{2\pi F_{x_{bc}} C_6 N}{ROP} \quad (33)$$

where the constant C_6 is defined as the abrasive wear constant and is a function of the abrasiveness of the rock and the abrasion-resistance of the drag cutter materials. We may now define a wear ratio (WR) that describes the volumetric wear rate of each cutter relative to that of cutter 1 nearest the center of the bit. Thus

$$WR = \frac{(dV_w/dl_h)}{(dV_w/dl_h)_1} = \frac{F_{x_{bc}}}{(F_{x_{bc}})_1} \quad (34)$$

This quantity provides a measure of wear uniformity among cutters that is independent of the abrasive wear constant C_6 .

A goal of any bit design should be to have uniform wear. If a given cutter wears significantly faster than the other cutters, it could prematurely reach the point where thermally-accelerated wear begins. Once this occurs, the cutter will rapidly attain a wearflat large enough to affect bit performance, i.e. cause greater drilling torque or bit imbalance due to larger cutter forces. Excessive forces can also cause the cutter to fracture off the bit body, which could have a catastrophic effect on bit life. More uniform wear helps ensure that no single cutter affects bit life through premature failure. If all cutters wear at the same rate, the

utilization of expensive cutting materials is also maximized, and the efficiency of refitting bits with new cutters is improved.

The existence of a wear ratio also suggests the possibility of estimating relative cutter wear and modifying cutter geometries to determine the effects of wear on bit performance. As a bit drills a distance from point 1 to point 2, the volume of material worn from the cutter changes from $(V_w)_1$ to $(V_w)_2$, where

$$(V_w)_2 = (V_w)_1 + \frac{dV_w}{d\ell_h} \Delta\ell_h \quad (35)$$

as long as $dV_w/d\ell_h$ is constant over the drilling distance. We may then divide Eq. 35 by the same equation evaluated for a reference cutter (r) and define

$$\Delta V_w = (V_w)_2 - (V_w)_1 \quad (36a)$$

to get

$$\frac{\Delta V_w}{(\Delta V_w)_r} = \frac{dV_w/d\ell_h}{(dV_w/d\ell_h)_r} \quad (36b)$$

or, using Eqs. 33 and 34,

$$\Delta V_w = \frac{WR}{(WR)_r} (\Delta V_w)_r \quad (36c)$$

Thus, if we specify the change in the wear volume for the reference cutter, $(\Delta V_w)_r$, the wear volumes of the other cutters can also be determined using the computed wear ratios. If the value of the abrasive wear constant C_6 is known for the rock of interest, the distance $\Delta\ell_h$ drilled in wearing away the volume $(\Delta V_w)_r$ of reference cutter material can be determined. Combining Eqs. 32 and 34, we obtain the result

$$\Delta\ell_h = \frac{(\Delta V_w)_r \text{ ROP}}{2\pi (F_{x_{bc}})_r C_6 N} \quad (37)$$

It is more convenient to express cutter wear in terms of dimensions that can be readily measured. It is, therefore, necessary to determine the relationships between cutter wear volume and the other wearflat dimensions. These relationships are functions of the wear mode. As discussed previously, two distinct wear modes seem to occur. Accordingly, two separate wear models are developed, one for each mode.

Hard-Rock Wear Mode

In hard, brittle rock, the wearflat tends to develop parallel to the cutting direction. In our previous work, we showed that the length of such a wearflat may be expressed as a simple function of the wear volume [31]:

$$L = C_4 V_w^{n4} \quad (38)$$

or, alternatively, as a function of the wearflat area [27]:

$$L = C_5 A_w^{n5} \quad (39)$$

where C_4 , $n4$, C_5 , and $n5$ are functions of the cutter compact radius and backrake angle. Values of these parameters have been determined for 20° backrake cutters with 0.5-inch and 0.75-inch diameter compacts, as listed in Table I. This analysis assumes that the wearflat is in the center of the cutting profile, i.e. $\phi_w = \phi_c$, but the error for cutter side wear is not large with the backrake angles generally used in PDC bit design (5-20°).

TABLE I
COEFFICIENTS IN EQUATIONS 38 AND 39

COMPACT DIAMETER (in.)	C_4 (in ¹⁻³ⁿ⁴)	$n4$	C_5 (in ¹⁻²ⁿ⁵)	$n5$
0.50	2.94	0.40	1.59	0.68
0.75	2.72	0.40	1.38	0.68

The width of the wearflat, measured at the diamond face, is

$$w = 2\sqrt{r^2 - (r - L \sin \beta)^2} \quad (40)$$

For the hard-rock wear mode, we may now specify a new wearflat area for the reference cutter, compute the associated new wear volume using Eqs. 38 and 39 and compare this with the old wear volume to determine $(\Delta V_w)_r$ according to Eq. 36a. Eqs. 34 and 36c can then be used to compute the new wear volume, $(V_w)_2$, for every other cutter on the bit. From these volumes, the new wearflat length, area, and width for each cutter can be calculated using Eqs. 38-40. Re-running the program with the new wear configuration

then allows the user to assess the effects of the predicted wear pattern on bit performance.

Soft-Rock Wear Mode

In the early stages of wear in the soft-rock wear mode, the wearflat develops parallel to the cutting direction, and the wear model can therefore be assumed to be identical to that of the hard-rock wear mode. At some point, however, the length of the wearflat, L , reaches some maximum value, L_{\max} , and further wear occurs by wearing the WC-Co at an angle with respect to L_{\max} the cutting direction (see Figure 23). Since this angle is relatively small (only 5-10°), the total length of the wearflat, L_t , including the portion not contacting the rock, is given approximately by the equation

$$L_t \cong C_4 (V_w)_t^{n4} \quad (41)$$

which follows from Eq. 38. Under these conditions, the total wearflat area, $(A_w)_t$, including the portion not contacting the rock, is related to L_t by the equation

$$L_t \cong C_5 (A_w)_t^{n5} \quad (42)$$

which follows from Eq. 39.

The parameter needed for the cutting force correlation is A_w , which is the portion of the wearflat in contact with the rock. This parameter can be determined by recognizing that

$$(A_w)_t = A_w + (A_w)_{nc} \quad (43)$$

where $(A_w)_{nc}$ is the portion of the total wearflat that does not contact the rock. The geometry considerations discussed in Ref. 27 suggest that such a portion of the total wearflat area is simply a function of the length of that portion; i.e.,

$$(A_w)_{nc} = [(L_t - L_{\max})/C_5]^{1/n5} \quad (44)$$

Inserting Eqs. 42 and 44 into 43 gives the result

$$A_w = (L_t/C_5)^{1/n5} - [(L_t - L_{\max})/C_5]^{1/n5} \quad (45)$$

For the purpose of developing a preliminary model for the soft-rock wear mode, it is now assumed that $L_{\max} = 0.09$ inch, which is the maximum length of the portion of the wearflat in contact with the rock that was measured in the experimental cutter test program with field-worn cutters.

The wear procedure for the soft-rock wear mode then is to specify a new wearflat area, A_w , for the reference cutter and calculate L_t with Eq. 45, using an iterative procedure. If $L < L_{max}$, then V_w is calculated using Eq. 41, and the new wear volume is compared with the old wear volume to determine $(\Delta V_w)_r$ according to Eq. 36a.

Eqs. 34 and 36c are next used to determine the new wear volume for each cutter, and Eq. 41 is used to determine the new total wearflat length, L_t . For those cutters with $L_t < L_{max}$, the new length of the wearflat portion in contact with the rock, L , is set to L_t , and the procedure described for the hard-rock wear mode is used to determine the new wearflat area and width in the advanced wear state. For cutters with $L_t > L_{max}$, Eq. 45 is used to determine the new wearflat area A_w . The length of the wearflat portion in contact with the rock for such cutters is

$$L = L_{max} \quad , \quad (46)$$

and the width of the wearflat at the diamond face is

$$w \approx 2 \sqrt{r^2 - (r - L_t \sin \beta)^2} \quad . \quad (47)$$

A loop is written in the program to allow the user to repeat the wear process described above for either wear mode as many times as desired. The user can run the program for multiple bit wear states ranging from sharp to severely worn. This provides a means for obtaining predicted results necessary for assessing drilling performance over the life of the bit.

More familiarity with the computer code can be attained by studying the comment statements contained in the code listing in Appendix B. The remainder of the text of this report concentrates on demonstrating the use of the code and drawing some general conclusions based on the predictions of the code.

4.0 DEMONSTRATION OF THE USE OF PDCWEAR

In this section, the use of PDCWEAR is demonstrated by analyzing the bit design shown in Figure 30. This design is for an 8.5 inch-diameter PDC bit with 21 cutters having 0.75-inch diameter compacts. The design is intended for hard-rock drilling, so the bit consequently has a relatively flat profile. The positions of the cutters assumed for this analysis are listed in Table II. Assumed operating conditions for the demonstration analysis are listed in Table III.

The following subsections describe the input parameters required by the code, steps required to run the program, program output, and the results obtained with the demonstration analysis.

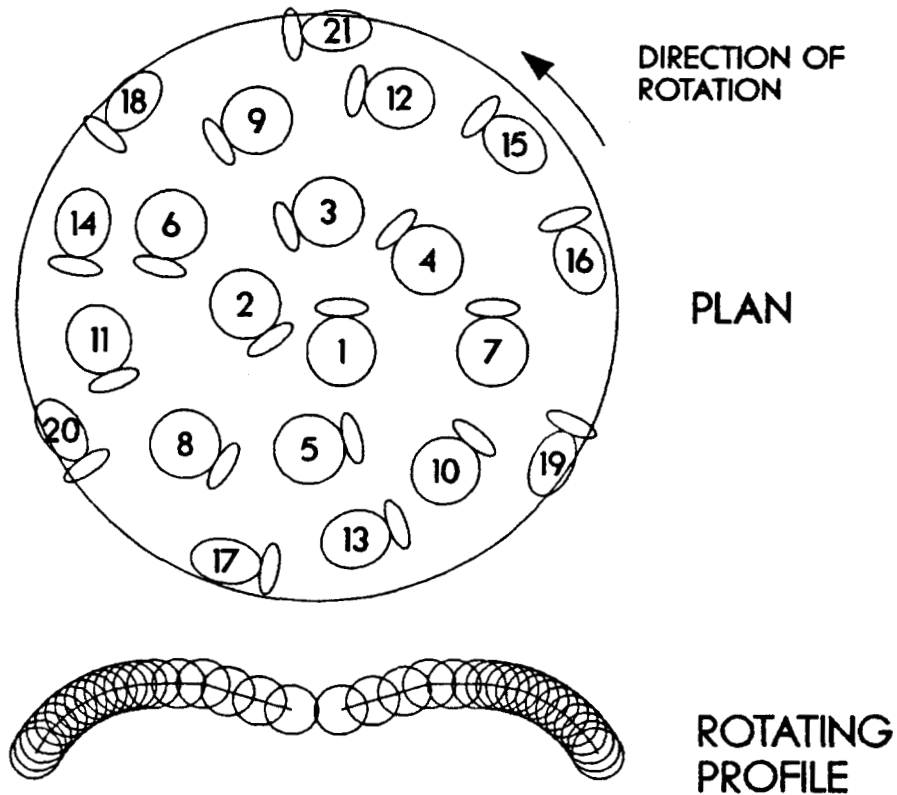


Figure 30 - Schematic of 8-1/2 inch bit design used in the demonstration analysis.

TABLE II
CUTTER POSITIONS IN DEMONSTRATION ANALYSIS *

CUTTER	R (in)	θ (deg)	H' (in)	ϕ_c (deg)
1	0.350	0.0	0.625	-15.0
2	0.800	215.0	0.760	-10.0
3	1.250	110.0	0.895	-5.0
4	1.600	45.0	1.000	-2.0
5	1.950	285.0	1.000	0.0
6	2.300	165.0	1.000	2.0
7	2.495	0.0	0.990	5.0
8	2.635	240.0	0.970	10.0
9	2.775	120.0	0.940	15.0
10	2.915	320.0	0.898	20.0
11	3.055	200.0	0.844	25.0
12	3.195	80.0	0.776	30.0
13	3.335	290.0	0.694	35.0
14	3.475	170.0	0.594	40.0
15	3.615	50.0	0.473	45.0
16	3.735	20.0	0.347	47.5
17	3.835	260.0	0.222	50.0
18	3.915	140.0	0.104	52.5
19	3.975	335.0	0.000	55.0
20	3.975	215.0	0.000	55.0
21	3.975	95.0	0.000	55.0

* See Figure 31 for definition of cutter position parameters.

TABLE III
BIT OPERATING CONDITIONS IN DEMONSTRATION ANALYSIS

<u>PARAMETER</u>	<u>VALUE</u>
Rock thermal conductivity, k_2	1.300 Btu/hr ft °F
Rock thermal diffusivity, χ_2	0.033 ft ² /hr
Rock/cutter friction coefficient,	0.070
Worn cutter drag coefficient,	0.550
Sharp cutter drag coefficient,	0.750
Worn Type A cutter (no jets) correlation constant, C_1	1.34×10^5 psi/in ^{0.42}
Worn Type A cutter (no jets) correlation exponent, n_1	0.42
Worn Type B cutter (w/jets) correlation constant, C_1	3.26×10^5 psi/in ^{0.93}
Worn Type B cutter (w/jets) correlation exponents, n_1	0.93
Sharp Type A cutter (no jets) correlation constant, C_2	2.55×10^4 lbf/in ^{1.64}
Sharp Type A cutter (no jets) correlation exponent, n_2	1.64
Sharp Type B cutter (w/jets) correlation constant, C_2	2.55×10^4 lbf/in ^{1.64}
Sharp Type B cutter (w/jets) correlation exponent, n_2	1.64
Abrasive Wear constant, C_6	6.89×10^{-13} in ² /lbf
Bit rotary speed, N	100 RPM
Downhole cooling fluid temperature, T_f	80°F
Specified bit penetration rates, ROP f	10,20,30,40,50 ft/hr

4.1 Input Parameters

Input parameters are contained in three data files: bit design data, initial cutter wear configurations, and operating conditions. This segregation allows flexibility in running the code. For example, it is possible to run different bit designs for different sets of wear and operating conditions by simply specifying different combinations of input files.

The input guide presented in Appendix D details the input parameters and their required formats, and it also provides guidance for determining appropriate input values. To aid in properly formatting the data, a utility program, FORMAT, has been written and is listed in Appendix E. When this interactive program is run, the user is requested to enter values for the various cutter parameters, and the data are written to files in the proper format. For the demonstration analysis, the input files are named BITDES.DAT, WEARCF.DAT, and OPCOND.DAT.

The bit design data file, BITDES.DAT, requires the following information for each cutter: cutter compact radius, radial position, angular position, longitudinal position, inclination angle, backrake angle, convective cooling coefficient, and type of cutter. For the demonstration bit design, these parameters are listed in Appendix F, Table F-1, in the proper format. Some of these parameters are defined in Figure 31.

The cutter positions for the demonstration bit design are chosen such that the cutters lie in three spiral rows on the bit face, as shown in Figure 30. The specified inclination angles allow the cutters to be mounted in holes drilled roughly perpendicular to the bit body at each cutter location. Cutter radii, backrake angles, and convective cooling coefficients are entered for each cutter as values relative to nominal values, which are also specified by the user. For the demonstration bit design, we specify 0.75-inch diameter (0.375-inch radius) cutters, all employing a 20_8 backrake angle and having convective cooling coefficients of 1700 Btu/hr ft²F, a value typical for water-based mud drilling.

The sign of the relative convective cooling coefficient is used to identify the type of each cutter. A positive value of the relative convective cooling coefficient indicates that the cutter is of type A and is governed by the penetrating stress and force correlations specified for that type cutter. A negative value of the relative cooling coefficient indicates that the cutter is of type B and is governed by a different set of input correlation constants. For the demonstration bit, we initially set all cutters to type A and assume that type A cutters are cutters without waterjet assistance. We later examine the effects of waterjet assistance for selected cutters, defining the type B correlation constants as those measured in the laboratory with waterjet assistance.

The second input data file for this analysis is WEARCF.DAT. This file contains information describing the initial state of wear assumed for each cutter. The area, width, and length of each cutter wearflat must be specified. The user may specify new cutters, where all three parameters for each cutter are zero; or finite values of the wear dimensions may be entered

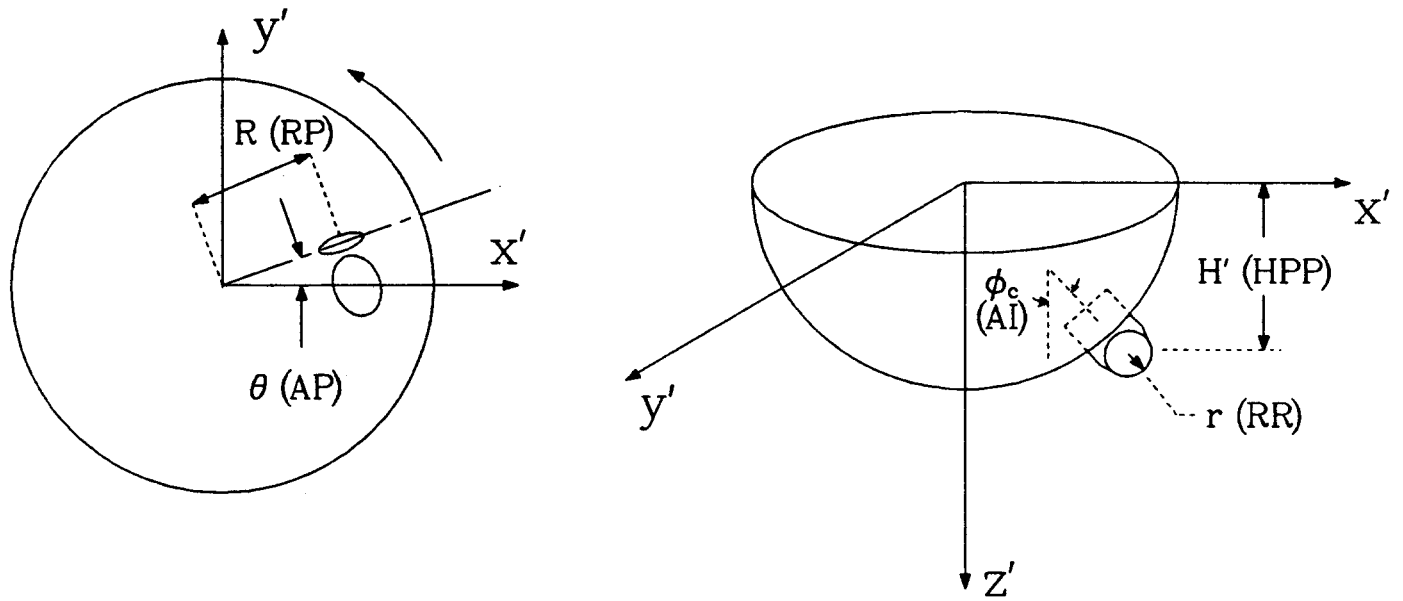


Figure 31 - Definition of several bit design parameters required as input for PDCWEAR. Each analysis variable name is followed by the computer code variable name in parentheses.

to simulate drilling with a worn bit. These wearflat dimensions may result from specific wear models, or the user may wish to use measurements of wearflats on an actual bit. In any case, the three dimensions refer to the portion of the wearflat in direct contact with the rock surface being cut.

For the demonstration bit, we specify initially sharp cutters, as shown in the proper format in Table F-2 of Appendix F. The use of worn cutters is demonstrated by allowing the cutters to wear according to the wear model and algorithm incorporated into the computer program.

The final input data file, OPCOND.DAT, contains data describing the intrinsic drillability of the rock and the assumed operating conditions. The values chosen for the demonstration bit analysis are shown in the proper format in Table F-3.

The rock being drilled is Sierra White granite. In a water-based fluid environment, the friction coefficient between the cutter and this type of rock has been measured as 0.07, compared with a value measured under dry conditions of 0.16 [19]. We wish to simulate a water-drilling environment, so we choose 0.07 for the demonstration analysis.

The data of Figures 13 and 15 suggest an average drag coefficient of about 0.64 for worn cutters and 0.84 for sharp cutters when cutting dry Sierra White granite. We may estimate the drag coefficients for both cutter types when cutting Sierra White granite under wet conditions by reducing the dry values by the same amount as the friction coefficient is reduced by the presence of water (Eq. 7). We thus arrive at the drag coefficients of 0.55 and 0.75 used in the demonstration analysis.

The cutter penetrating stress and force correlation constants and exponents listed in Tables III and F-3 are taken from Figures 10, 12, and 16 for worn type A, sharp type A, and worn type B cutters, respectively. No data have been obtained in this study with sharp cutters and waterjet assistance since cutter forces are already very small with sharp cutters. Accordingly, the constant and exponent for sharp type B cutters are assumed to be the same as those for sharp type A cutters.

Data with which to determine the abrasive wear constant, C_6 , for Sierra White granite were not available. As a result, the abrasive wear constant used in the demonstration analysis was derived from data for Jack Fork and Nugget sandstones [19,33], using Eq. 33. Although both of these sandstones are relatively hard and abrasive, it is unlikely that they are as abrasive as Sierra White granite. As a result, the predicted length of hole drilled in reaching a given wear configuration in the demonstration analysis is probably greater than that which would actually be achieved with Sierra White granite.

We choose for the demonstration bit analysis a rotary speed of 100 RPM. We wish to simulate drilling under atmospheric laboratory conditions, so we assume a cooling fluid temperature of only 80°F. Five penetration rates are specified for the demonstration analysis: 5, 10, 20, 40, and 50 ft/hr. These rates cover the practical range of interest for this type of rock.

4.2 Running the Program

PDCWEAR is run interactively, with the user specifying the files to be read, files to be written, and length of borehole drilled during the analytical simulation. A general description of the session for the demonstration analysis is provided below.

The first request from PDCWEAR is the name of the input file containing the bit design data. File names up to 11 characters in length, including the file extension, can be used. When an acceptable name has been entered, the program reads the file and stores the bit design data. It then gives the user the opportunity to display the input data at the user's terminal.

A similar pattern is repeated for the cutter wear configuration data file and the operating parameter data file. As the data are read from the specified files, the program checks the data to determine whether they are within expected ranges for each variable. If any data are out of range, the program notifies the user, requests that corrections be made, and terminates the session. Once all input data have been accepted by the program, it requests the name of the output file for storing results.

The program then requests the user to specify the value of the parameter NRAY. This parameter determines the precision to which the program calculates the results. NRAY determines the number of elemental lengths Δx into which the x-axis is divided by the numerical integration routine that computes cutter interaction. To ensure an adequately fine division of the x-axis for even the smallest cutter used in any given bit design, NRAY is defined as the number of elemental lengths used over the width of the smallest cutter. Based on the specified value of this parameter and the diameter of the smallest cutter, the program calculates a value of Δx and uses this value at all x across the face of the bit. A value of 100 is a reasonable value for NRAY. Lower values may be used to speed up calculations at the expense of precision. Values of NRAY larger than 100 may be used for final analysis of a bit design in order to confirm that greater precision would not change the results. For the demonstration analysis, a value of 100 was initially used for NRAY. The program was then re-run using a value of 500, but the difference in results was insignificant.

After specification of NRAY by the user, the program begins the calculations. For the initial wear configuration specified in WEARCF.DAT and the first penetration rate specified in OPCOND.DAT, the program iterates on the radial wear angle for each cutter until convergence. If convergence is not attained within 30 iterations, the program displays the latest two iteration values for each cutter wear angle and gives the user the opportunity to proceed with the latest values or to terminate the program. Generally a failure to converge indicates that the user has not used a sufficiently large value of NRAY. In most cases, however, continuing with the non-converged wear angles will not cause significant inaccuracies in the algorithms used to compute total bit performance parameters.

Following the radial wear angle determinations, the program computes the rock removal volume, cross-sectional area of cut, effective depth of cut, penetrating force, drag force, wearflat temperature, and wear ratio for

each cutter. These detailed data are written to the specified output file. In addition, the following data are computed and written to both the output file and the user's terminal: weight-on-bit, drilling torque, bit side forces, bit bending moments, maximum wearflat temperature, and maximum wear ratio across the bit.

Before repeating the calculations for the next specified penetration rate, the program allows the user to open several files into which data are written in a format suitable for plotting. Cutter plot files are formatted as shown below:

```
Bit Design Data File Name
Wear Configuration Data File Name
Operating Conditions Data File Name
ROP
1,Q(1)
2,Q(2)
3,Q(3)
.
.
.
nc,Q(nc)
```

where Q(j) represents the computed quantity associated with the jth cutter. The following cutter plot files may be saved on disk:

- (1) FVSCN.DAT contains the penetrating force for each cutter for the current ROP (i.e., Q(1) = F for cutter 1, etc.);
- (2) DEFVSCN.DAT contains the effective depth of cut for each cutter;
- (3) TWVSCN.DAT contains mean wearflat temperatures for each cutter;
- (4) WRVSCN.DAT contains the wear ratio for each cutter;
- (5) VRVSCN.DAT contains the rock cutting volume for each cutter; and
- (6) ARVSCN.DAT contains the cross-sectional area of cut for each cutter.

After data have been written to the cutter plot files, the program repeats the calculations for the next specified penetration rate. Data are again written to the cutter plot files, and the process is repeated for the next specified penetration rate. (The program is written such that once a cutter plot file is opened, the appropriate data are automatically written to the opened plot file for each subsequent penetration rate.)

After results have been computed for all specified penetration rates, the program writes summary data to the output file for the current wear configuration and displays the same summary data at the user's terminal. It then gives the user the opportunity to write this data to bit plot files. The format of these files is:

Bit Design Data File Name
Wear Configuration Data File Name
Operating Conditions Data File Name
ROP(1),Q(1)
ROP(2),Q(2)
ROP(3),Q(3)
ROP(4),Q(4)
ROP(5),Q(5)

where $Q(i)$ represents the computed quantity associated with the i th penetration rate, $ROP(i)$. The following bit plot files may be saved on disk:

- (1) WOEVROP.DAT contains the weight on bit data computed at each penetration rate (i.e., $Q(1) = WOB$ computed at first specified penetration rate, etc.);
- (2) TRQVROP.DAT contains the drilling torque at each penetration rate;
- (3) SFRVROP.DAT contains the resultant bit side forces at each penetration rate;
- (4) MXVROP.DAT contains the bending moments about the x' -axis at each penetration rate; and
- (5) MYVROP.DAT contains the bending moments about the y' -axis at each penetration rate.

After the bit performance data are written to the selected files, analysis for the initial wear configuration is complete. The program is then ready to consider new wear configurations for the cutters. The program stores the wear ratios computed at the third penetration rate of the five rates specified and uses these values in computing relative cutter wear. This implies that at least three penetration rates must be specified when wear calculations are to be made. For the demonstration analysis, the wear ratios computed at 30 ft/hr were used by the program in computing cutter wear.

In order to calculate new wear configurations for all cutters, the program requires the user to select the soft-rock or hard-rock wear mode and to guide the wear process by specifying a new wearflat area for one of the cutters. For the demonstration analysis, the hard-rock wear mode was selected.

The program then requests the user to specify a new, larger wearflat area for the cutter with the largest wearflat at that point in the analysis. In the case of initially sharp cutters, where all wearflat areas are zero, the program uses the highest-number cutter as the reference cutter (cutter 21 in the demonstration analysis). After the user specifies a new wearflat area for the reference cutter, the program computes the length of hole that the bit must drill in wearing the reference cutter from its current wear configuration to the new specified configuration. (This hole length is based on the third penetration rate specified in the operating conditions input file.) The program then displays the change in hole length and gives the user a chance to change the new wear configuration for the reference cutter. As a result, the user can monitor the cumulative hole length in order to obtain predictions after any given drilling distance. Once the user is satisfied with the new reference cutter wear configuration, the

program computes new wear configurations for all other cutters, based on the wear ratios. It then requests the name of the file where the new wearflat dimensions are to be stored. This file can be used for later reference or for re-starting the program as the initial wear configuration file. If the user does not wish to proceed with the new configuration, the program allows the user to terminate the session.

If the user chooses to continue the session, the program repeats the bit performance calculations for the new wear configuration at all specified penetration rates. This process is repeated as many times as the user specifies, or until the cutter wearflat dimensions grow to the point that the equations developed in Section 3.0 no longer describe the wearflat geometry. The program monitors the wear and will not allow the user to specify a wearflat area that is not valid. For consistent results, the same wear mode should be selected for all wear increments in a given analysis.

Since the wear ratio is a function of the wear configuration of each cutter, small increments in wearflat area growth are recommended. In the early stages of bit wear, increments of 0.005 in² or smaller are recommended. At later stages of wear, increments of 0.010 in² can be used, but the resulting change in drilled borehole length and maximum cutter wear ratios should be monitored to ensure that large changes in these parameters do not occur in any single increment of wear. Larger wear increments than those recommended could lead to significant inaccuracies in the numerical integration routine used for simulating cutter wear, particularly during the early stages of cutter wear. By interactively specifying new wearflat areas, the user can monitor the bit wear, bit performance, and cumulative borehole length. The session can be terminated when the user determines that the bit is worn out, based on either cutter wearflat areas, cutter temperatures, or excess WOB or drilling torque.

For the demonstration analysis, the following wearflat areas were specified for the reference cutter at successive points over the life of the bit: 0.002, 0.010, 0.015, 0.020, 0.025, 0.030, 0.035, 0.040, 0.050, 0.060, 0.070, 0.080, 0.090, 0.100, 0.110, 0.120, 0.130, 0.140, and 0.150 in². The analysis was re-run by specifying increments of 0.001 in² from 0.0 to 0.040 in², and the bit performance predictions were within 2% of those for the larger specified increments in wearflat area for the reference cutter.

4.3 Tabulated Program Output

Part of the output file for the demonstration bit analysis is listed in Appendix G. The program first prints the date and time of the computer run and then the name and contents of the files containing the bit design parameters, wear configurations, and operating conditions.

The computed results are listed next. For each penetration rate requested, the program lists three pages of results. The first of these contains the geometry-dependent results: the cutting order, the cutting height, the location of the center of each cutter wearflat, the cutter wear angle, volume of cut, cross-sectional area of cut, and effective depth of cut for each cutter.

The second page of computed results lists the rock-dependent results: penetrating force, drag force, vertical and radial components of the penetrating force, wearflat temperatures, and wear ratio for each cutter. In cases where a wearflat temperature exceeds the critical level of 350°C, the wear ratio for that cutter is flagged by setting it to a negative value. The program also warns the user at the terminal that one of the cutters experiences thermally-accelerated wear. Wear calculation may continue under such conditions, but the results may not be accurate since a much larger abrasive wear constant is operative under such conditions than under normal wear conditions.

The third page of computed results for each penetration rate contains integrated forces and moments for the bit: WOB, drilling torque, side force in the x' and y' directions, resultant side force, and bending moments about the x' and y' axes.

The results for the demonstration analysis are discussed in the next subsection.

4.4 Discussion of Baseline Analysis Results

The results shown in the output file in Appendix G are summarized in Figures 32-40. These figures were produced by saving appropriate plot files while running PDCWEAR. The data were then edited and formatted for an available graphics program. Similar editing can be done for any graphics program available to the user; or the user could modify the appropriate statements in SUBROUTINE DATPRI of PDCWEAR so that plot data could be output in a format to better suit any available graphics program.

With the baseline bit design used in the demonstration analysis, cutter 15 wore at a higher rate than any other cutter. The growth of this cutter's wearflat area is plotted in Figure 32 as a function of the computed footage drilled by the bit. We designate three points along this curve as reference wear conditions for the bit: "sharp" when all cutter wearflat areas are zero; "worn" when the reference cutter wearflat area is 0.040₂ in²; and "worn out" when the reference cutter wearflat area is 0.100 in². The results indicate that the bit will drill 460 ft before reaching the designated "worn" stage, and it will drill 975 ft before it is worn out.

The distribution of cutter wear for the baseline analysis in each of the designated stages of bit wear is shown in Figure 33. Note that with this design, cutters near but not on gage tend to experience the greatest wear (cutters 13-16). The gage cutters (19-21) wear slightly less than those on the leading face of the bit (cutters 4-6).

Baseline cutter and bit performance parameters in each of the bit wear stages are plotted in Figures 34-40. In Figure 34, the predicted penetrating forces are shown. When the bit is sharp, the penetrating forces tend to decrease from the center of the bit out toward gage. This is caused

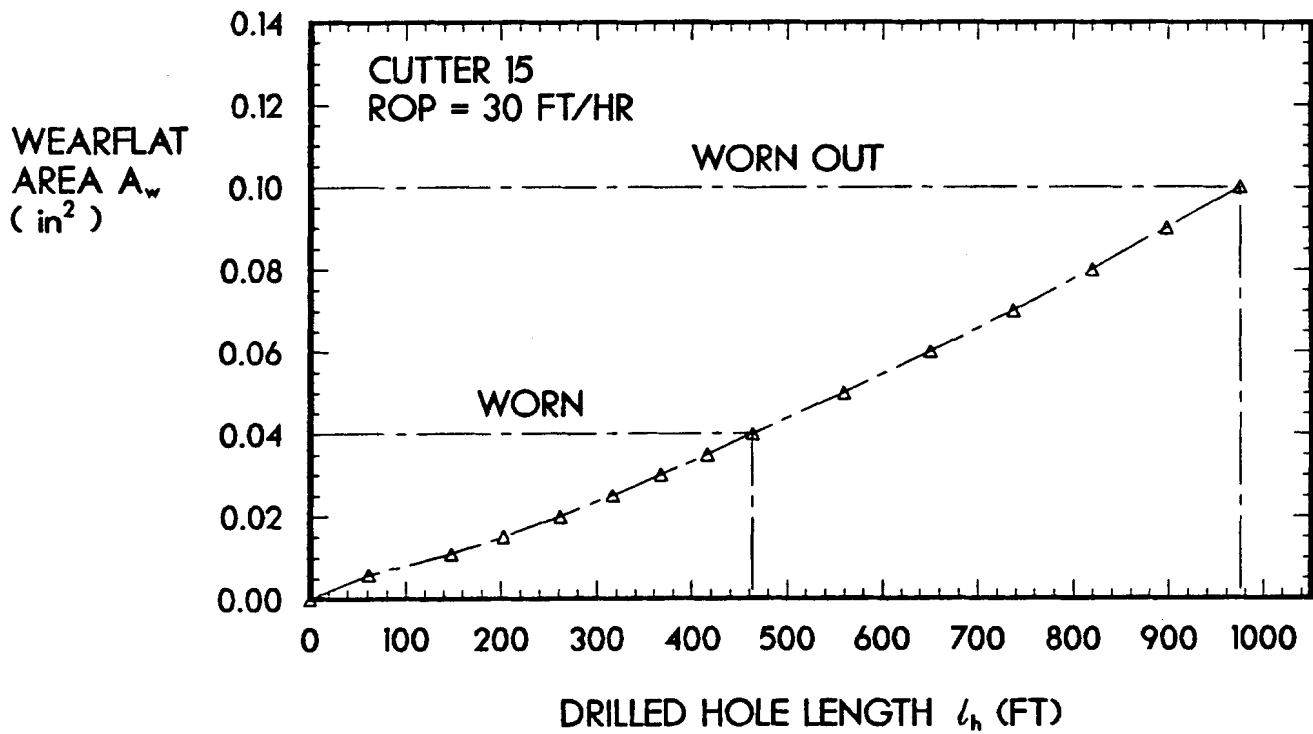


Figure 32 - Predicted wearflat growth of cutter with highest wear rate in the demonstration analysis.

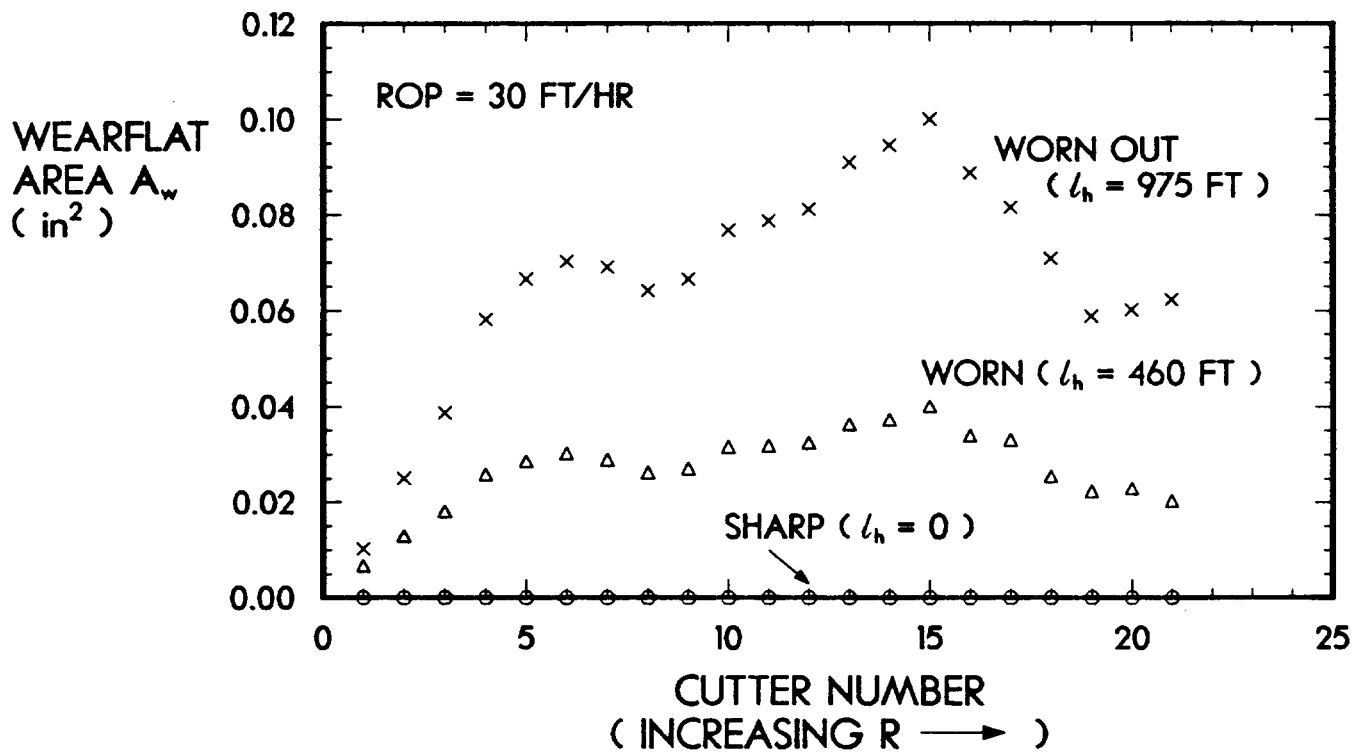


Figure 33 - Predicted wear distribution across bit in the demonstration analysis at designated stages of bit wear.

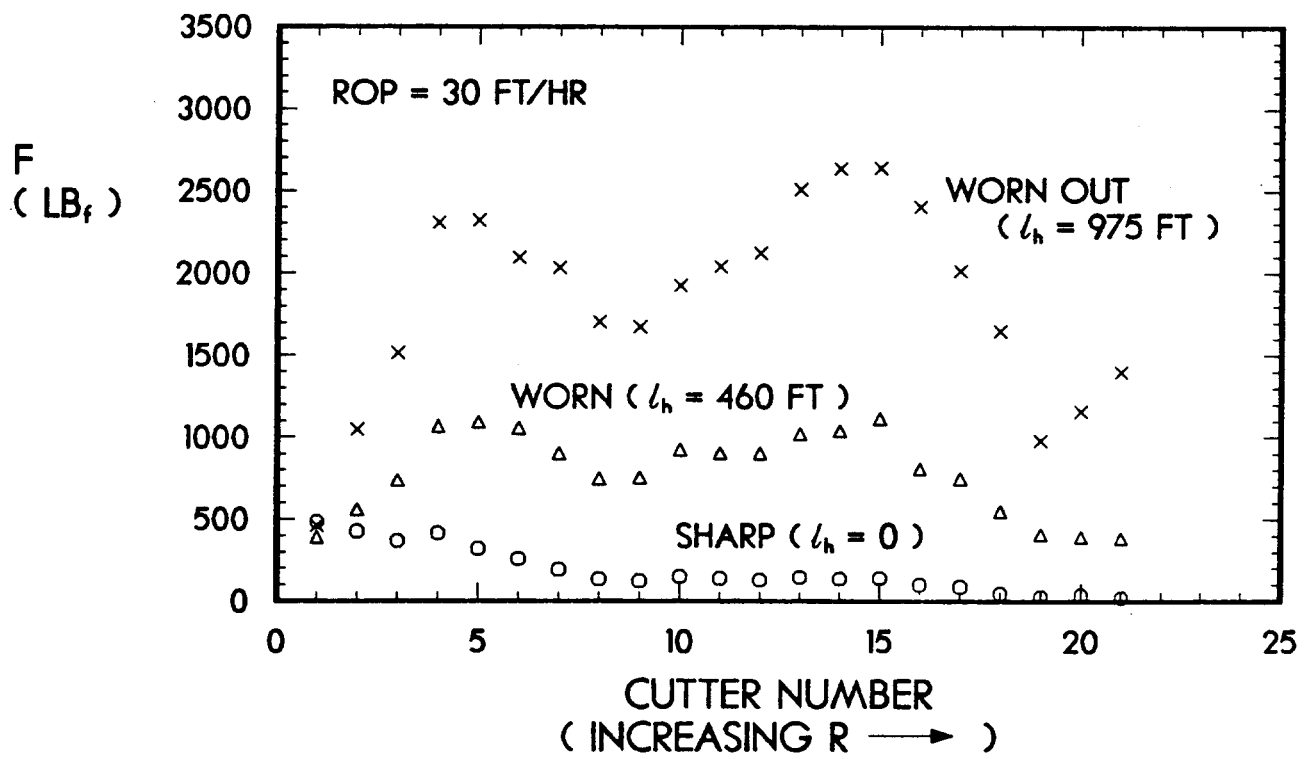


Figure 34 - Predicted cutter penetrating forces in the demonstration analysis.

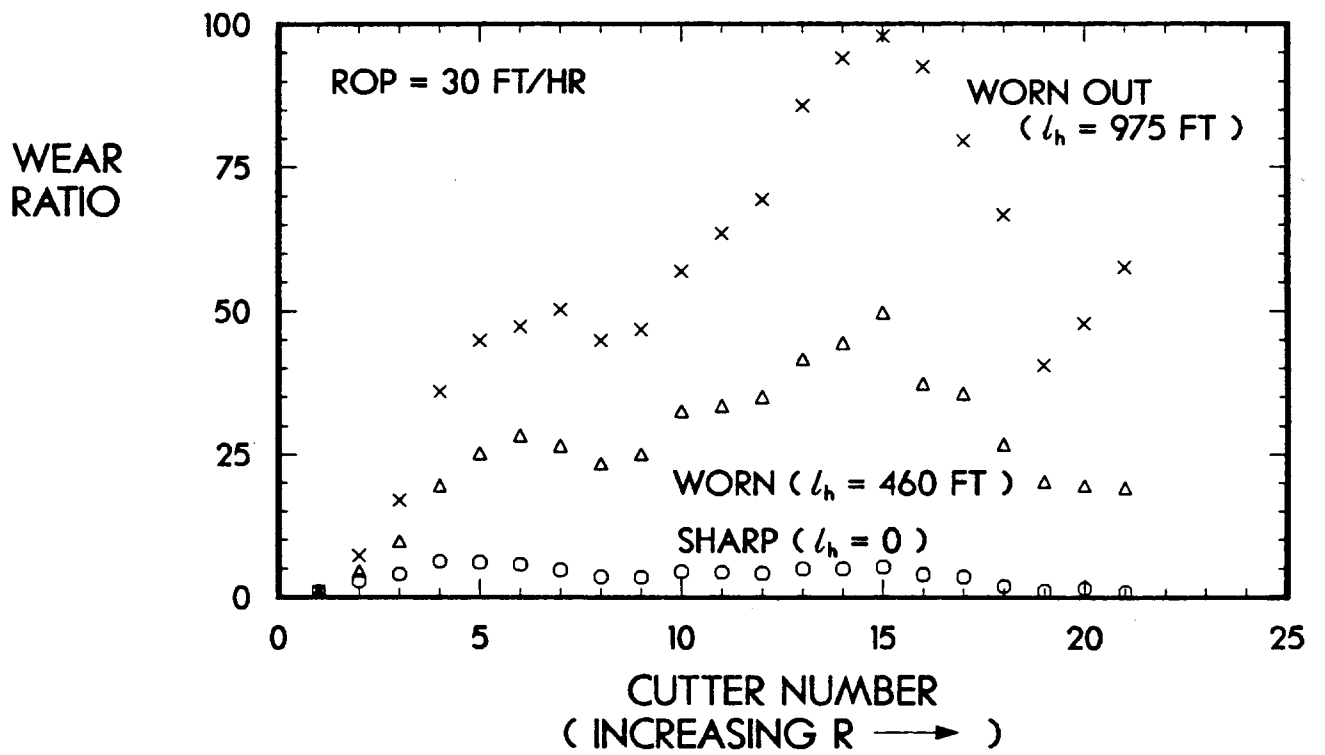


Figure 35 - Predicted cutter wear ratios in the demonstration analysis (wear ratio = 1 for cutter 1 by definition).

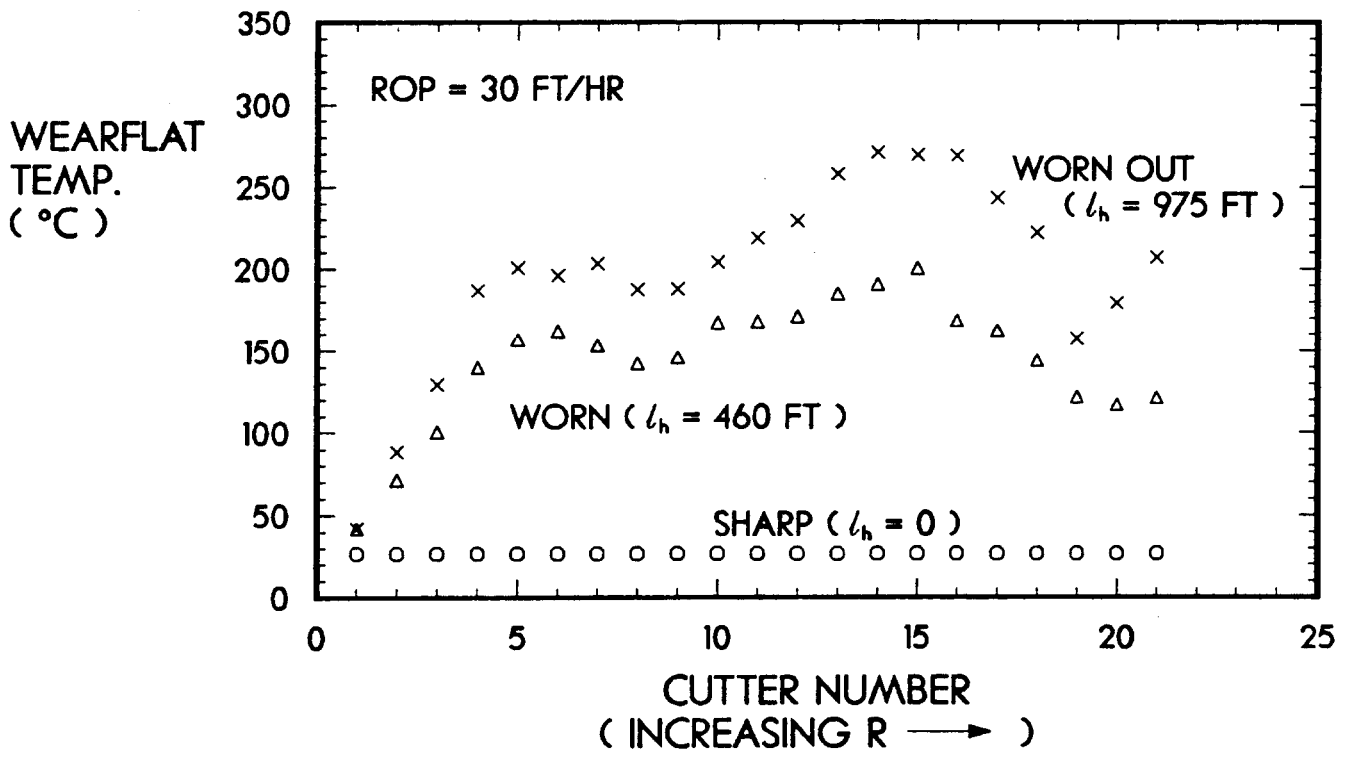


Figure 36 - Predicted cutter wearflat temperatures in the demonstration analysis.

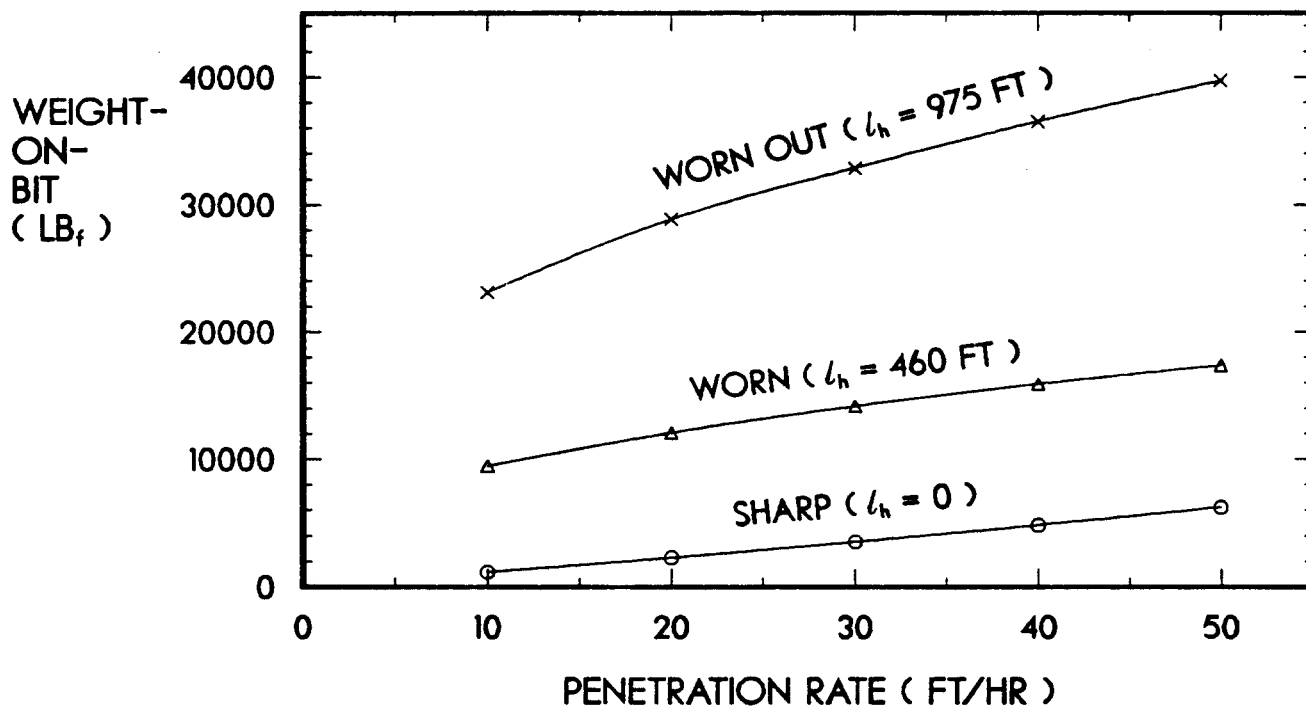


Figure 37 - Predicted WOB at specified penetration rates in the demonstration analysis.

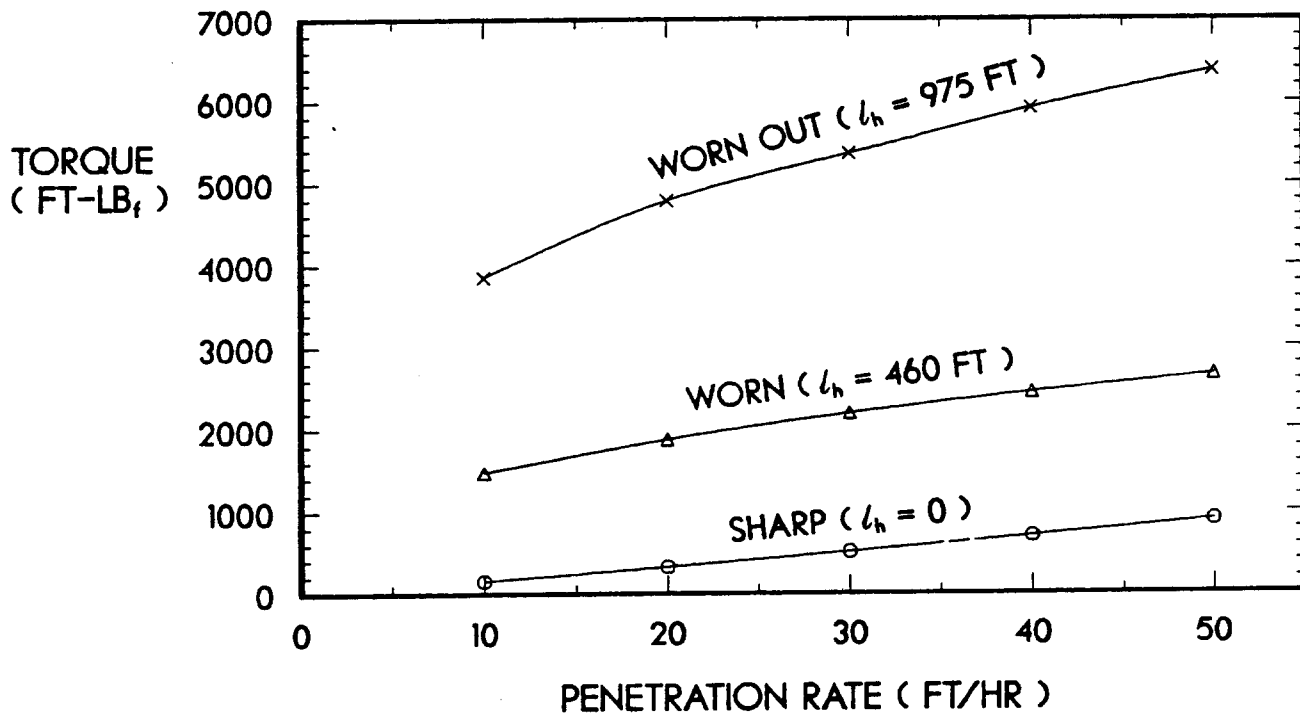


Figure 38 - Predicted drilling torque at specified penetration rates in the demonstration analysis.

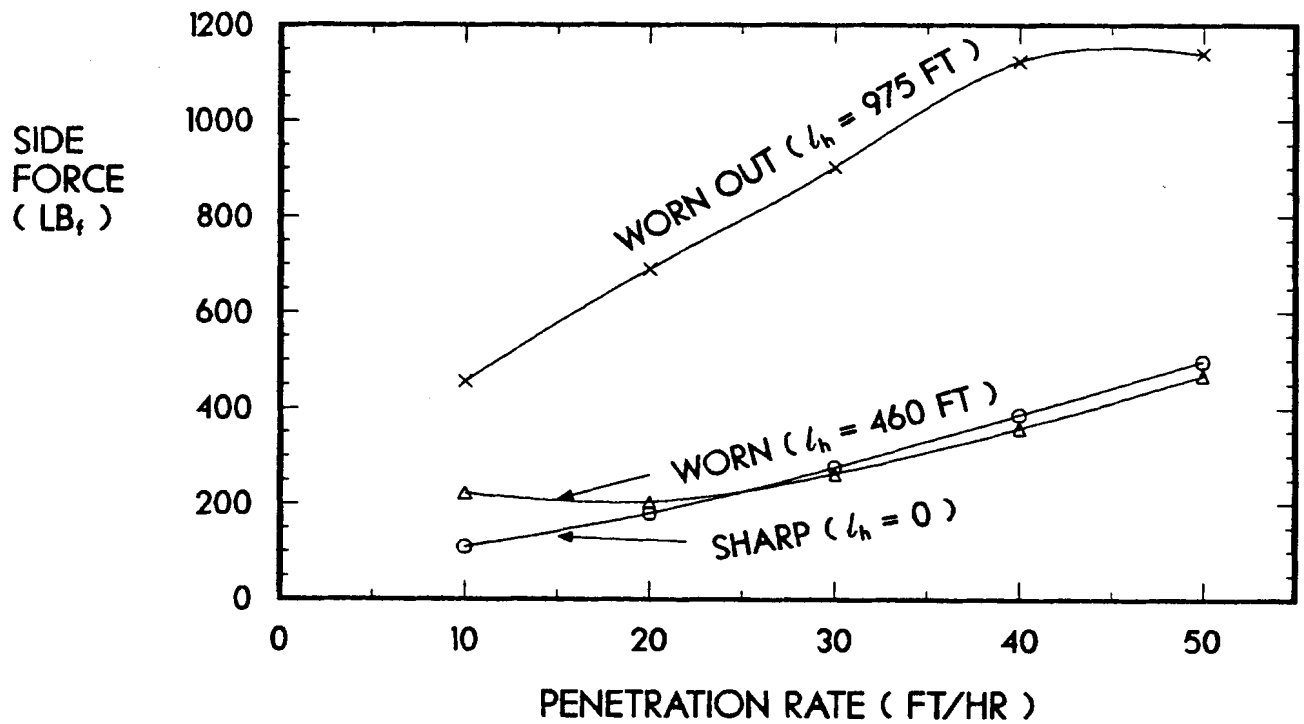


Figure 39 - Predicted resultant bit side force at specified penetration rates in the demonstration analysis.

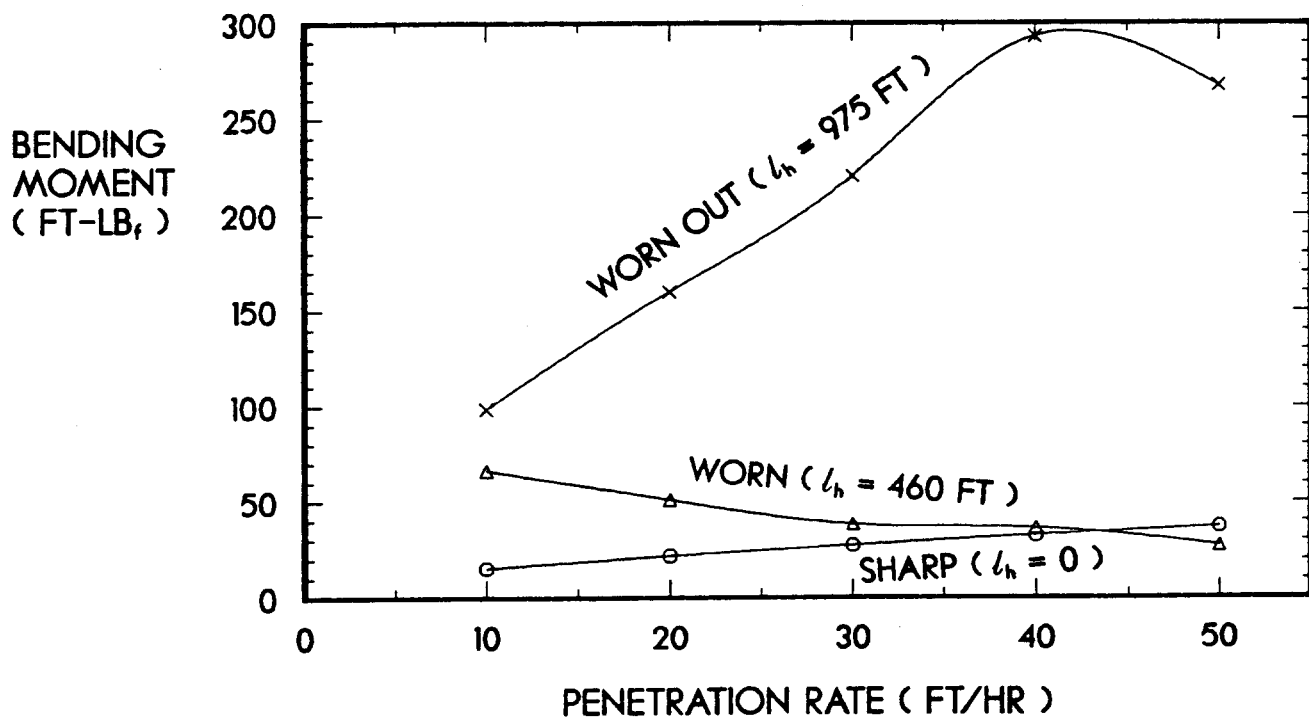


Figure 40 - Predicted resultant bit bending moment at specified penetration rates in the demonstration analysis.

by increased cutter interaction resulting from the closer radial spacing of cutters at increased radial positions on the bit. As the cutters wear, however, the overriding effects of wearflat area cause the penetrating force distribution to change as shown.

The wear ratios resulting from the computed penetrating forces are shown in Figure 35. The integrated effects of the wear ratios at all stages of wear are responsible for the wearflat areas shown in Figure 33.

The computed wearflat temperatures for the baseline analysis are shown in Figure 36. These results indicate that, even when the cutters are severely worn, temperatures are below 350°C and thermally-accelerated wear should not occur. It should be noted, however, that the friction coefficient assumed for this analysis was only 0.07, and the cooling fluid temperature was assumed to be only 80°F. If either of these quantities were higher, which is likely under actual drilling conditions, cutter wearflat temperatures could exceed the critical level, and accelerated wear would occur. Continuing the analysis beyond the designated "worn out" stage indicated that cutter 16 reached the 350°C limit after about 1270 ft of drilling at a penetration rate of 30 ft/hr.

The computed WOB is plotted as a function of ROP in Figure 37. We see a large effect of cutter wear on bit performance. Although the bit requires only 3500 lbf WOB to drill at 30 ft/hr when sharp, it requires nearly ten times that weight to maintain the same ROP when the bit is worn out.

Perhaps an even more compelling indication that the bit is worn out is the excessive drilling torque predicted for this wear condition. As shown in Figure 38, torque increases with cutter wear to levels that conventional drilling practices would not tolerate, resulting in the bit being pulled.

The resultant bit side force predicted for the baseline analysis is shown in Figure 39. This force would develop if the bit were constrained by the walls of the borehole to follow a straight line and to rotate concentrically about its geometric center. In reality, a bit side force would tend to make the bit cut deeper on the side opposite the force, resulting in an oversize hole and eccentric rotation of the bit, or bit wobble. Such imbalance in the bit design is usually undesirable. When worn, the side forces are less than 3% of the WOB. This would seem to suggest that the bit is not greatly unbalanced in the worn condition, but it is not known what levels of side force are significant, especially under dynamic conditions.

Similar comments can be made with respect to the predicted bending moments, shown in Figure 40. (Note that the plotted data are the resultant bending moment, determined by taking the square of the sum of the squares of the bending moments about the x'- and y'-axes.) In the case of bending moment, the drill pipe is capable of providing a reactive torque to prevent excessive tilting of the bit. Again, however, the effects of the bending moment on the dynamic response of the drill string are not known but could be significant.

4.5 Other Program Features

In addition to those already discussed, the program also has the following features:

- 1) The program checks for gaps between cutters where uncut rock could leave the bottomhole pattern such that the bit will not drill. If the program detects such gaps at any point in the wear process, it informs the user and allows the user to terminate the session. Although calculations may continue under such conditions, the results will be uncertain.
- 2) Since the program allows cutters to wear at different rates, it is possible under some conditions that a cutter will reach the point where it no longer contacts the rock. Under these conditions, the program properly predicts zero cutting forces for such a cutter. As a result, the cutter will not wear during the next specified wear increment. Eventually, the wear of surrounding cutters will "catch up" and the cutter will again contact the rock surface and begin to wear.
- 3) The program predicts results similar to the "wearing in" process that has been observed in laboratory bit tests; i.e., weight-on-bit is slightly higher when the cutters are sharp than it is after the cutters have worn slightly. Numerically, this is due to the algorithm that uses the larger of the sharp- or worn-cutter correlation force predictions for a given cutter. When the cutter is slightly worn, the worn-cutter force correlation predicts lower forces than the sharp-cutter correlation, so the sharp cutter correlation is used. For a given penetration rate, however, a slightly worn cutter has a slightly lower effective depth of cut than a sharp cutter. As a result, the cutter forces predicted with a slightly worn cutter at a given penetration rate are lower than those predicted with a sharp cutter at the same penetration rate. Of course as the cutters wear further, the worn-cutter force correlation predicts higher forces than the sharp-cutter correlation, and weight-on-bit increases with cutter wear thereafter.
- 4) Since the program files the new wear configuration for each increment of bit wear, the user can terminate the program at any point and re-start the program by specifying the appropriate file as the initial wear configuration file. It should be noted that re-starting the program sets the cumulative drilled borehole length back to zero. Furthermore, other bit performance predictions will not be precisely the same in a re-start situation as in a continuous run because the number of significant digits stored on disk for the wearflat dimensions is less than that stored in computer memory during a continuous run. In most cases, however, the differences in predicted results are not significant.

5.0 PREDICTED EFFECTS OF DESIGN AND OPERATION ON BIT PERFORMANCE

Now that baseline results have been established for the demonstration analysis, the effects of several important design and operating variables can be assessed. These effects were determined by modifying the bit design and/or operating parameters and repeating the analysis. Results for the modified analyses are illustrated by comparing the performance parameters predicted after drilling the same footage as in the baseline analysis (i.e., 0, 460, and 975 ft).

5.1 Effects of Bit Profile

Perhaps the most obvious of the bit design variables is the bit profile. The profile used in the baseline analysis was relatively flat, with only a 1.0 inch range in cutter longitudinal locations over the 8.5-inch diameter bit. To assess the effects of bit profile, an analysis was performed using the bullet-nose bit design shown in Figure 41. The cutter locations are identical to those of the baseline analysis, except that the longitudinal locations range over 4.0 inches instead of 1.0 inch, and there is no concave portion in the center of the bit.

Shown in Figure 42 are the predicted wearflat areas for the bullet-nose bit. The primary effect of bit profile in this example is to increase wear on most of the cutters, especially those near the nose of the bit (cutters 1-9). This result agrees with field experience, which generally shows that flatter bit profiles are necessary when drilling hard rock, where uneven cutter wear is usually a problem.

Although the bullet-nose bit wears faster, the computed results indicate that in the early stages of drilling, the WOB is lower than that of the baseline analysis, as shown in Figure 43. When plotted in this manner, it is seen that for a given WOB, the bullet-nose bit drills at a much higher ROP than the baseline bit after both have drilled 460 ft of hole. Since the bullet-nose bit wears faster, however, the effects of wearflat area eventually become dominant. After 975 ft of drilling, the bullet-nose bit has become so worn that it drills much slower than the baseline bit design at the same WOB.

The predicted drilling torque for the bullet-nose bit was higher than that for the baseline analysis at all drilled borehole lengths. In the sharp condition, the differences ranged from 8 to 25%, depending on ROP. After 460 ft of drilling, the bullet-nose bit torque was 12 to 17% higher, and after 975 ft, it was 8 to 25% higher. Side forces and bending moments were also more excessive with the bullet-nose bit. This indicates that the sharper the bit profile, the more carefully cutters must be placed in order to balance the bit design.

5.2 Effects of Cutter Placement Density

In this analysis, the number of cutters was reduced from 21 to 15 in order to assess the effects of using a lower cutter placement density. Cutters 8, 10, 12, 14, 16, and 18 were removed from the baseline design, with other cutters remaining in their original positions. The cutters that

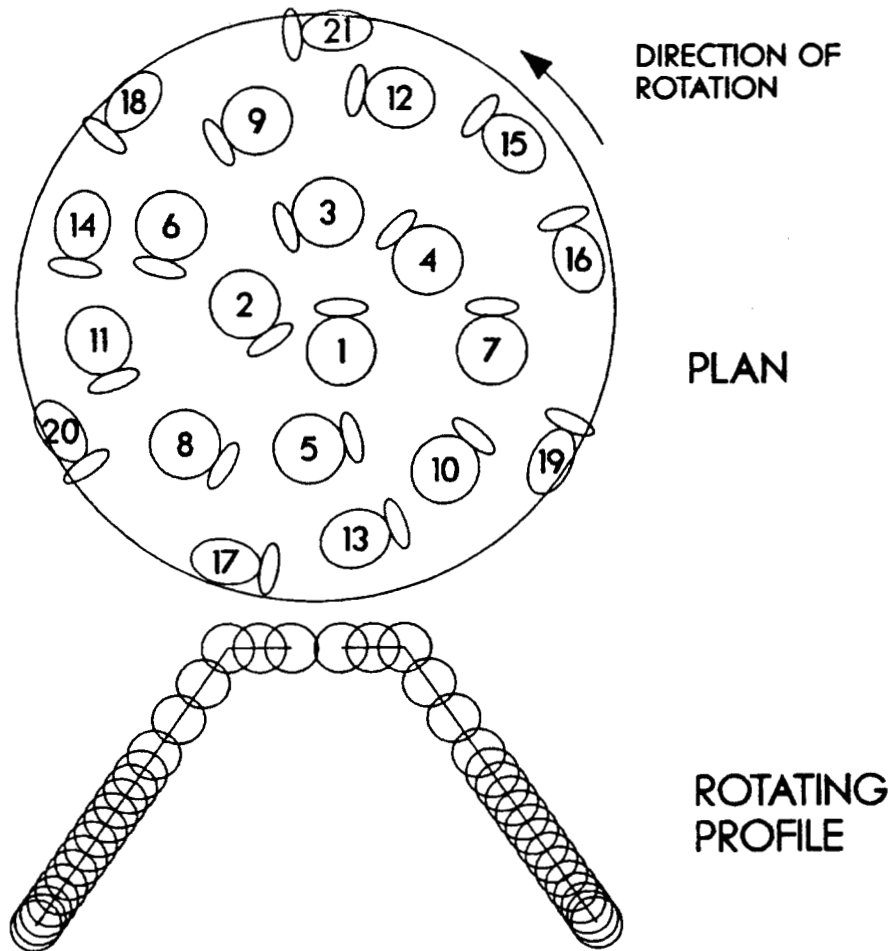


Figure 41 - Schematic of bullet-nose bit design used in modified analysis to illustrate the effects of bit profile.

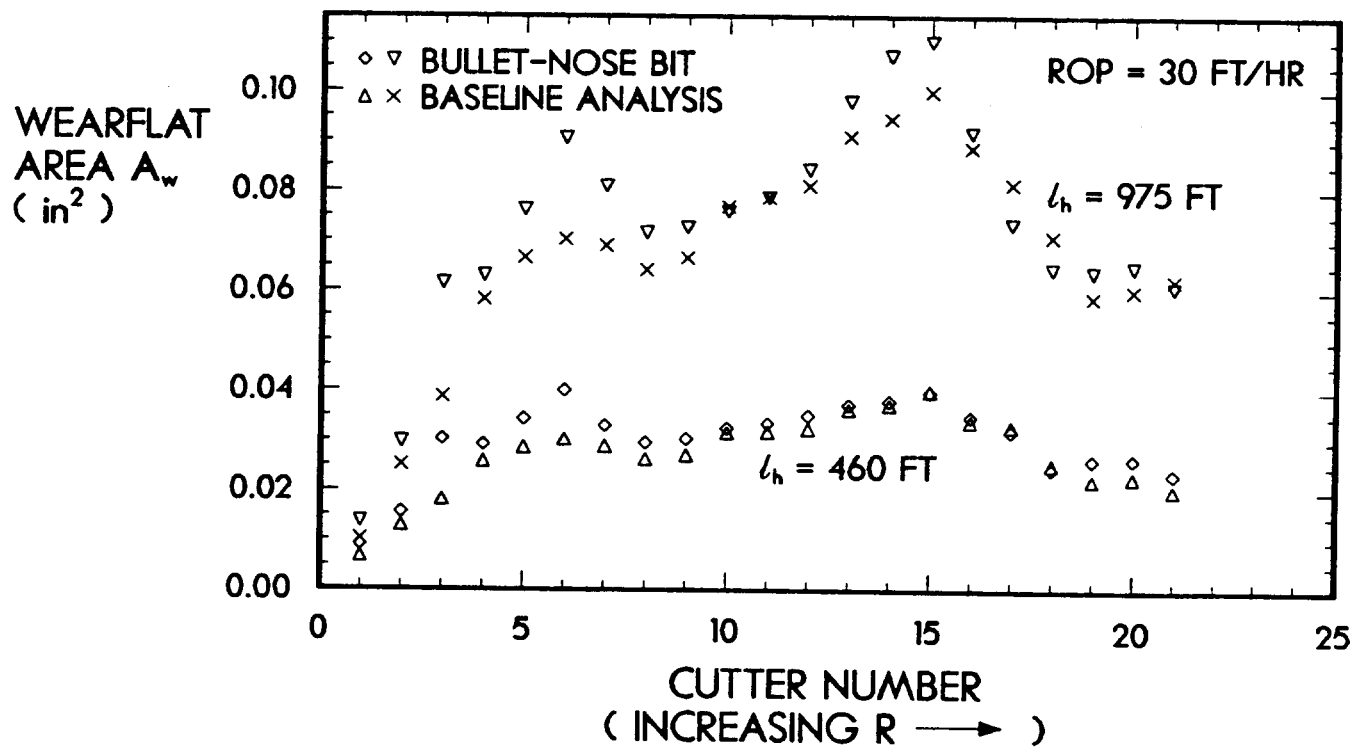


Figure 42 - Predicted cutter wear distribution across bit, showing the effects of bit profile.

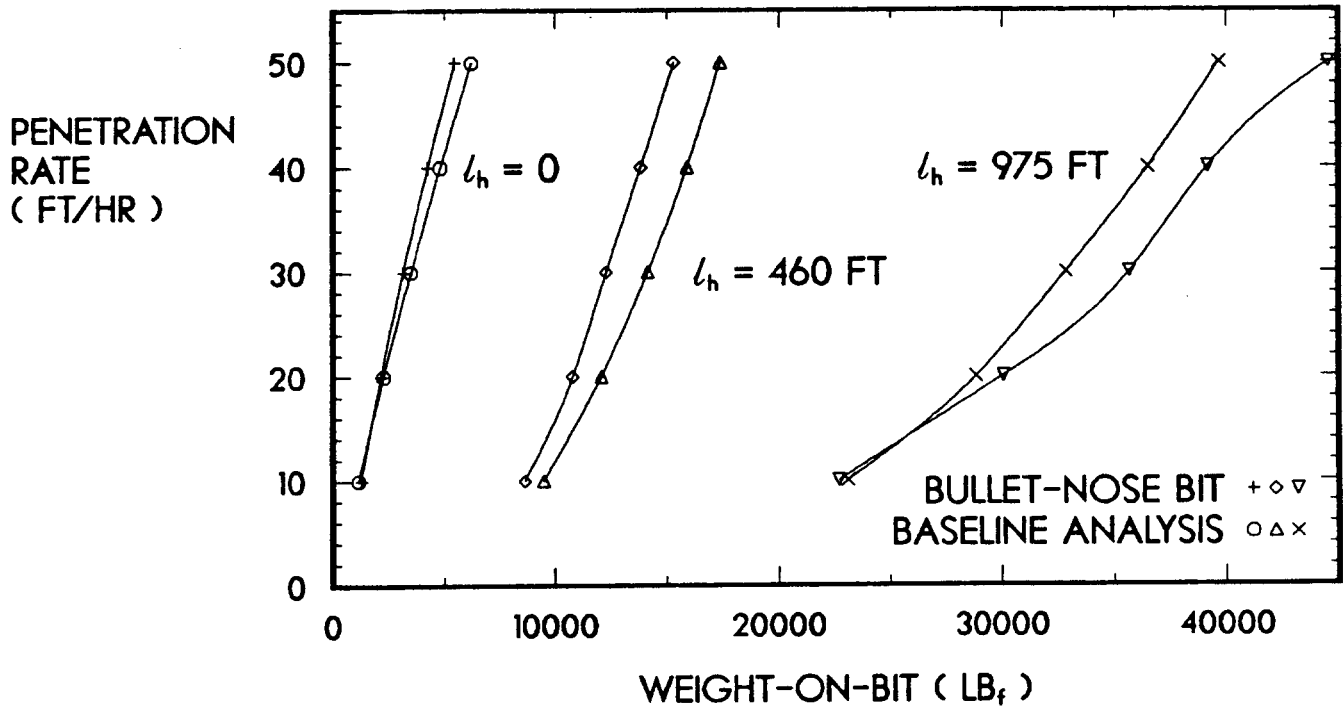


Figure 43 - Specified penetration rate plotted as a function of predicted WOB to illustrate the effects of bit profile.

were removed were so chosen in an effort to maintain balance in the design. The resulting 15-cutter bit design is shown in Figure 44.

In this case, the remaining cutters in the reduced density region (cutters 7-19) experienced greatly increased wear, as shown in Figure 45. This is caused by the reduced interaction and, consequently, higher penetrating forces on these cutters as compared with the baseline analysis. The predicted wearflat cutter temperatures at a ROP of 30 ft/hr indicate that cutter 15 exceeds 350°C after a hole length of 880 ft; thus the cutter-15 wearflat area would actually be even larger than that shown in Figure 45 at 975 ft.

Although the number of cutters used in the two bits is significantly different, the difference in required WOB is relatively small. When the bits are sharp, the 15-cutter bit requires 4 to 7% more WOB. After 475 ft of hole, the 15-cutter WOB is lower by 4 to 8%. By the time both bits have drilled 975 ft, the 15-cutter WOB is 3 to 11% lower. Of course, if the accelerated wear of the cutters that experience thermal wear had been taken into account, the larger wearflat areas for those cutters would have increased the WOB significantly with further drilling after 880 ft. Furthermore, since wear rates increase by 1 to 2 orders of magnitude during this mode of wear, the affected cutters can, for all practical purposes, be considered destroyed. When this happens, the bit may be left in a configuration that will not drill.

These results suggest two ways for defining bit life that may be inherently related under certain conditions. The first is the drilled footage at which thermally-accelerated wear begins on any cutter. In this case, the life of the 15-cutter bit would be 880 ft, and that of the baseline bit would be 1270 ft (at a penetration rate of 30 ft/hr).

Alternatively, we may define the bit life as the drilled footage at which a performance parameter, such as WOB, drilling torque, or bit imbalance, reaches some selected level. In the baseline analysis, we arbitrarily selected a WOB of 40,000 lbf (at 50 ft/hr) as a limit on bit life, based on practical levels for this size bit. This resulted in the WOB-bit life criterion of 33,000 lbf at 30 ft/hr in the baseline analysis. If thermally-accelerated wear occurs, as with the 15-cutter bit, the resulting rapid growth in WOB would cause the bit to more rapidly reach the WOB limit defining bit life. Thus, if the temperature-bit life criterion is reached, it is probable that any practical WOB-bit life criterion will be reached soon thereafter.

In addition to changing the number of cutters, placement density can be modified locally by moving cutters radially and circumferentially. The radial placement of cutters is one of the most important parameters in bit design. To achieve more uniform wear, cutters can be shifted radially to provide a higher placement density in regions of excessive wear and a lower density in regions of low wear.

The circumferential placement of cutters is also important because it affects bit balance during drilling. Excessive side forces can be reduced by shifting cutters circumferentially in the proper directions.

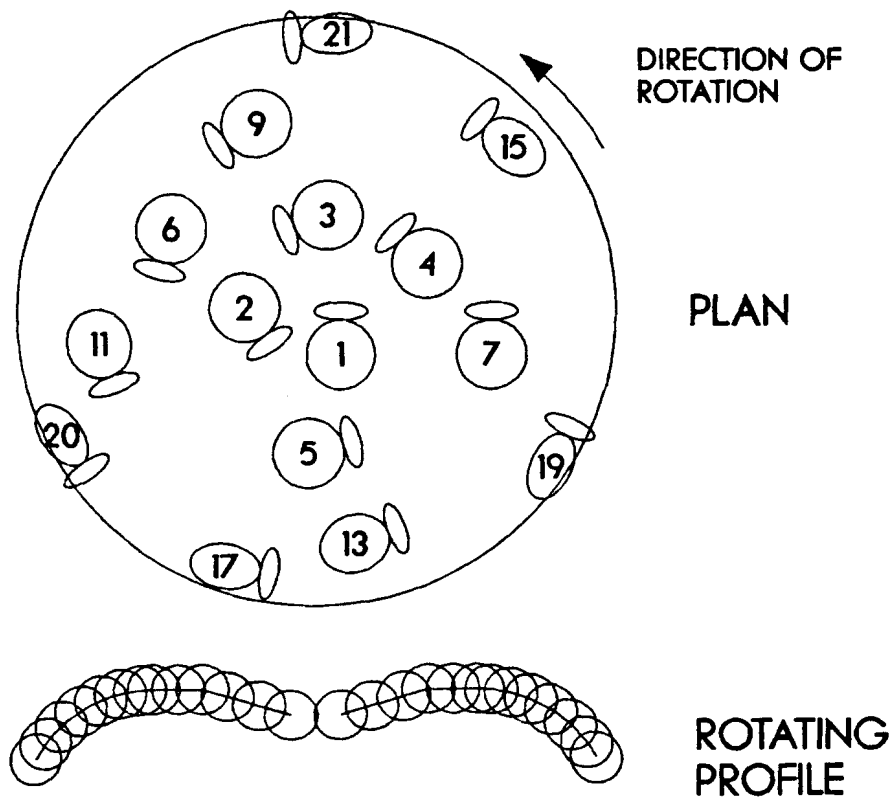


Figure 44 - Schematic of bit design used in modified analysis to illustrate the effects of cutter placement density.

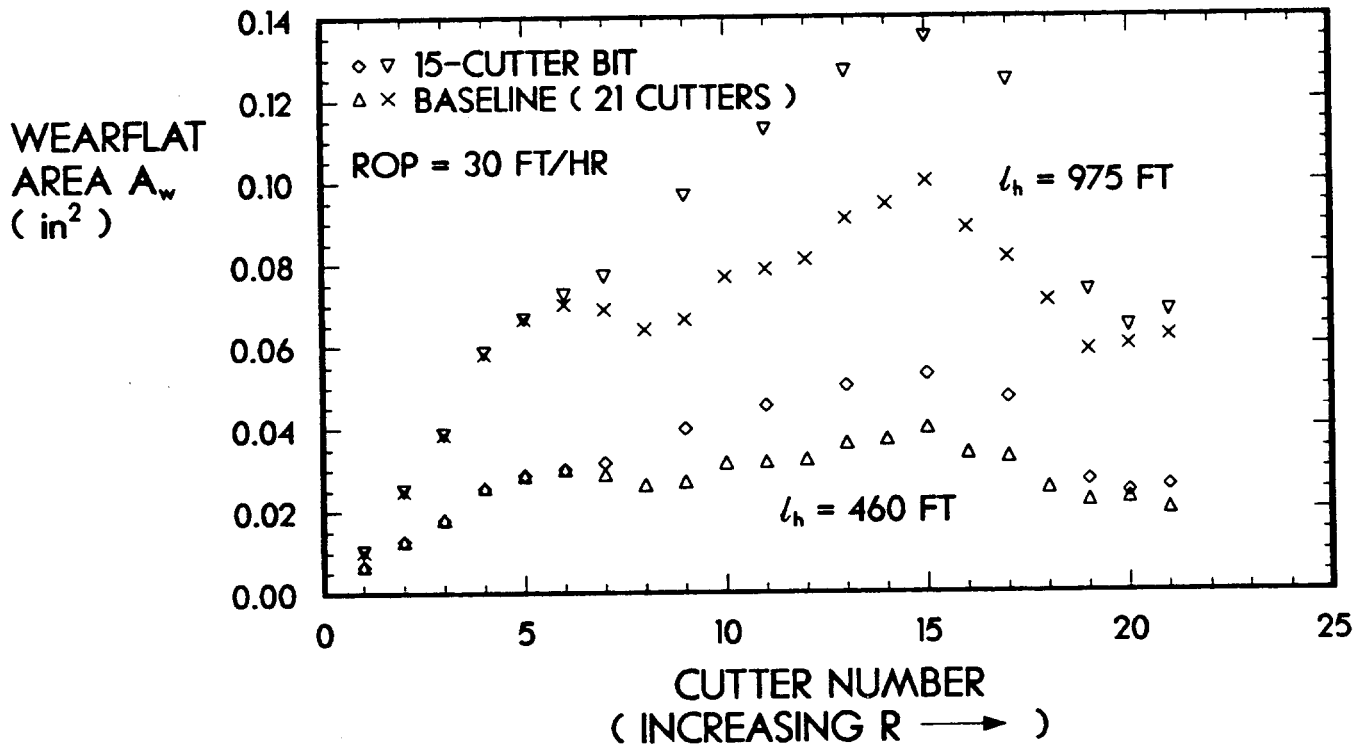


Figure 45 - Predicted cutter wear distribution across bit, showing the effects of cutter placement density.

Circumferential placement also affects individual cutter forces because it determines how the feed rate of the bit is distributed among the cutters (see Eq. 13d).

5.3 Effects of Bit Rotary Speed

For a given penetration rate, the feed rate of the bit (penetration/revolution) decreases as the bit rotary speed is increased (see Eq. 13e). This implies that for a given wear configuration, a selected ROP can be achieved with a lower WOB by increasing rotary speed. To investigate this effect, an analysis was performed by changing the rotary speed in the baseline analysis from 100 to 200 RPM.

The results indicate that when the bit is sharp, the higher rotary speed reduces the WOB requirements by 42 to 54%. Similar reductions in drilling torque were predicted at the higher speed. The lower bit feed rate, however, causes each cutter to travel twice as far in drilling the same length of hole. As a result, the cutters wear faster with respect to footage drilled. This effect is illustrated in Figure 46. Note that all cutters experience increased wear at the higher rotary speed. The wear on cutters 11-18 after 975 ft of hole would be even greater than that shown, because the predicted wearflat temperatures for those cutters exceed 350°C after only 650 to 900 ft.

As a result of the computed wear pattern, the WOB for the higher rotary speed is 11 to 18% higher after 465 ft and 25 to 26% higher after 975 ft of hole. Similar increases in drilling torque were predicted for the higher rotary speed. The conclusion we reach is that, even under conditions where thermal wear effects are not important (e.g. at 460 ft), increased rotary speed is detrimental to bit life and, consequently, to the penetration performance of the bit. This agrees with results obtained in our earlier work [31]. Under conditions where a higher ROP is required, it is better to achieve it by increasing WOB rather than rotary speed.

5.4 Effects of Waterjet Assistance

In the baseline analysis, cutters 13-16 experienced greater wear than the other cutters. In the present modified analysis, the beneficial effects of waterjet assistance are demonstrated by simulating placement of jets in front of those cutters. For these cutters, the single cutter correlation constants measured in the tests with 4500 psi waterjets (Figure 16) were used. This was done by specifying those cutters to be of type B and entering the proper correlation constants into the OPCOND.DAT data file.

Shown in Figure 47 are the computed wear distributions. Waterjet assistance is seen to reduce wear by more than one-half on the assisted cutters. Furthermore, since these cutters do not wear as fast as the adjacent cutters, they remove more rock than they would otherwise remove after a given hole length. As a result, the waterjet-assisted cutters interact more with adjacent cutters, thereby reducing wear on the adjacent cutters as well. This effect is noticeable as far in toward the center of the bit as cutter 3.

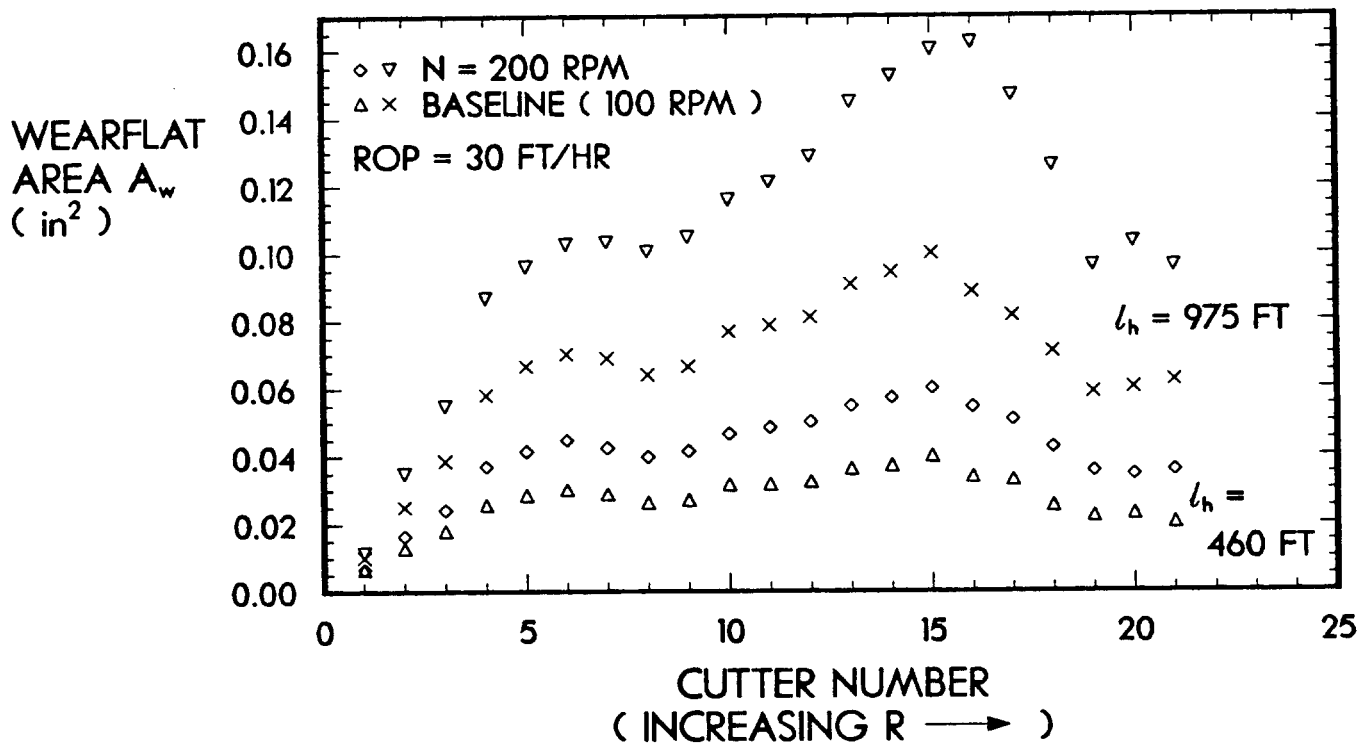


Figure 46 - Predicted cutter wear distribution across bit, showing the effects of rotary speed.

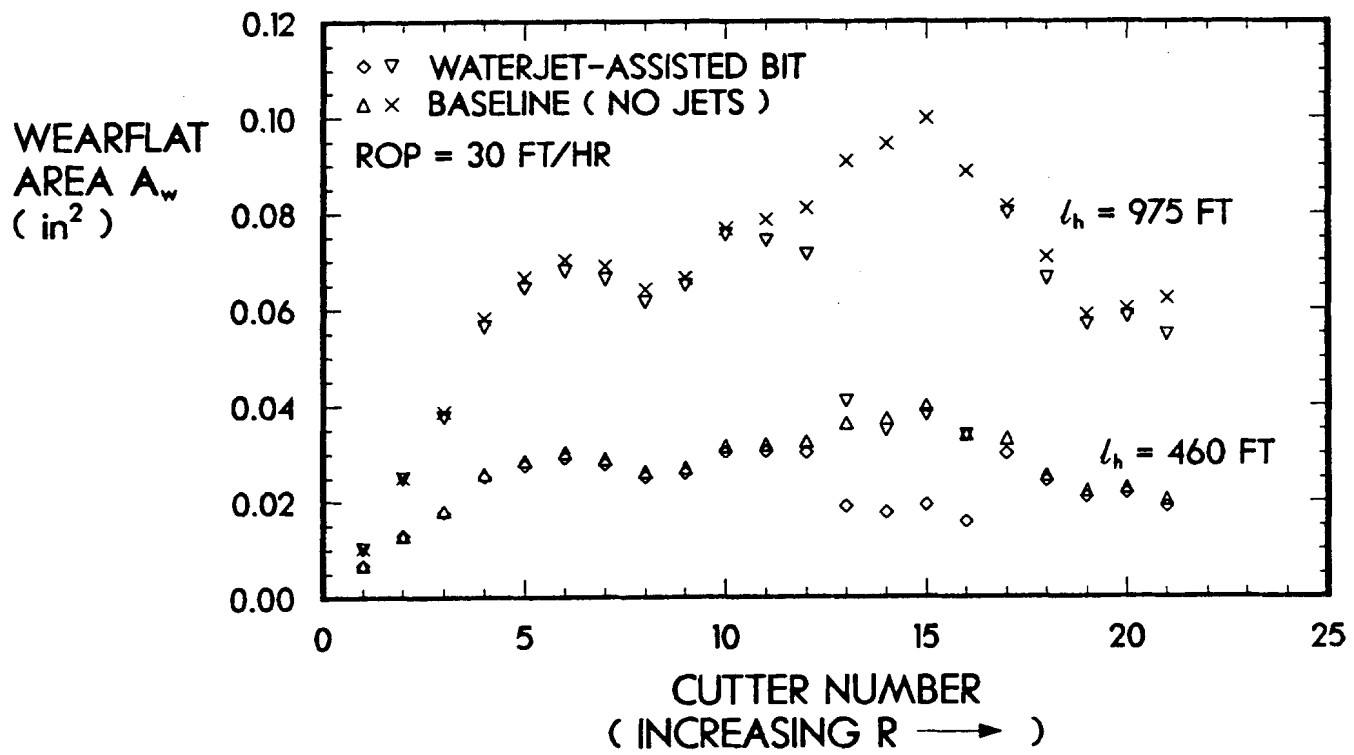


Figure 47 - Predicted cutter wear distribution across bit, showing the effects of waterjet assistance for selected cutters (13-16).

The reduced wear on the bit is responsible for a significant improvement in drilling performance. The WOB required with the jet-assisted bit was computed to be 19 to 23% lower after 460 ft of hole and 23 to 27% lower after 975 ft. Even greater reductions in drilling torque were predicted for the jet-assisted bit: 27 to 33% after 460 ft and 29 to 36% after 975 ft of drilling. If WOB is used as the criterion for declaring the bit worn out, the jet-assisted bit is predicted to have a bit life of 1225 ft, as compared with 975 ft in the baseline analysis. If the onset of thermally-accelerated wear is used as the bit life criterion, the jet-assisted bit drills for 2950 ft, compared with 1220 ft in the baseline analysis.

5.5 Effects of Wear Mode

In this analysis, the soft-rock wear mode was specified to demonstrate the effects on wear patterns and bit performance. Results are shown in Figure 48. After drilling 460 ft, the cutter wearflat areas are up to 30% smaller than those predicted for the hard-rock wear mode assumed in the baseline analysis. Beyond this footage, the difference in wear becomes even more pronounced. After the bit has drilled 975 ft, the wearflat areas in the soft-rock wear mode are up to 63% smaller than those predicted for the hard-rock wear mode.

In the hard-rock wear mode, the wearflat area in contact with the rock is a strong function of the volumetric cutter wear, which in turn is proportional to the cutter penetrating force. Since the wearflat area has a large effect on penetrating force, wear in the hard-rock wear mode tends to occur at an accelerating rate with respect to footage drilled, even in the absence of thermal effects.

The wearflat area in the soft-rock wear mode, however, is not as sensitive to wear volume. In other words, a given increase in dV_w/dL does not produce as large an increase in A_w as it does in the hard-rock^h wear mode. As a result, the wearflat^w area growth rate actually decreases as drilling continues. In this analysis, the maximum predicted wearflat area growth between hole lengths of 460 and 975 ft is only about 34%. This compares with 150% growth in maximum wearflat area in the case of the hard-rock wear mode over the same footage.

The performance parameters in the soft-rock wear mode behave in a similar fashion. The WOB requirements after 460 ft of hole are within 16% of those predicted for the hard-rock wear mode. By the time both bits have drilled 975 ft, however, the bit worn in the soft-rock mode requires 50 to 51% less WOB than that in the hard-rock mode. Similar results were obtained with respect to drilling torque.

Because of the modest wearflat growth, the cutter temperatures in this analysis with the soft-rock wear mode never approach the critical 350°C limit before the cutters are worn to the center of the compacts. When the wear reached this point in the analysis, at 18,666 ft, the calculations were terminated, and the bit was considered worn out. In terms of the WOB-bit life criterion of 33,000 lbf at 30 ft/hr, the bit was predicted to drill

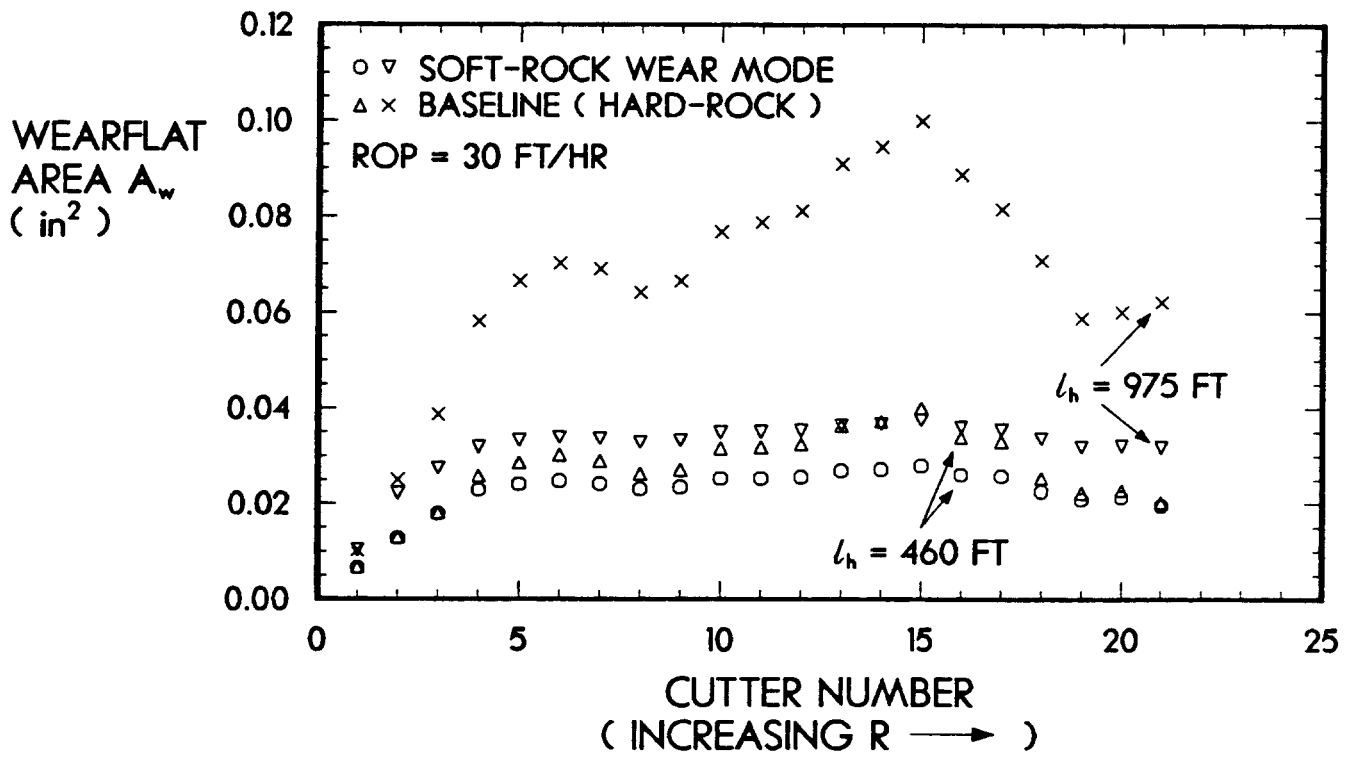


Figure 48 - Predicted cutter wear distribution across bit, showing the effects of wear mode.

over 11,500 ft. It is therefore concluded that significantly greater bit life can be attained when a bit wears in the soft-rock wear mode rather than in the hard-rock wear mode.

5.6 Discussion

The computer code developed in this study predicts that the baseline bit design will drill relatively hard rock at a rate of 10-50 ft/hr and will last for approximately 1000 ft with a WOB of less than 40,000 lbf and a drilling torque of less than 6000 ft-lbf. These and other predicted results appear quite reasonable and are comparable to performance typically achieved with this size bit.

For example, in geothermal drilling tests in the Imperial Valley, California, an 8-3/4" PDC bit drilled 555 ft at an average ROP of 55 ft/hr, with an estimated life of about 1000 ft [17]. The drilled interval contained sandstone, shale, siltstone, and igneous formations. The unconfined compressive strength of the sandstone in this interval was 11,000 psi, about one-half of the Sierra White granite assumed in the present analysis. Under the elevated downhole stresses present in the field test, however, the strength of the sandstone may be comparable to that of the granite at atmospheric pressures. Furthermore, the abrasive wear constant assumed in the demonstration analysis is probably close to the abrasive wear constant of the sandstones drilled in the field tests.

The thermal conditions assumed in the analysis were relatively mild. Downhole cooling fluid temperatures typically exceed 125°F in petroleum drilling and 200°F in geothermal drilling, well above the 80°F assumed in the analysis. Friction coefficients of 0.03-0.20 in water and 0.10-0.32 in air have been measured between PDC cutters and rock. It is therefore possible for the cutter wearflat temperatures to exceed those predicted in the baseline analysis, according to Eq. 31. In that case, thermal wear effects could reduce bit life well below the 1000 ft predicted here.

It has been shown that bit profile can significantly affect bit performance. This is due to the fact that the profile not only affects cutter density and thus interaction, but it also controls the orientation of the cutter penetrating forces. Forces oriented at steep angles, such as those on the side of the bullet-nose bit, contribute directly to cutter wear and bit side forces but have less relative impact on WOB. This explains how a bit design can drill with lower WOB but still experience more rapid wear than a different design.

Nozzles such as those used in the experimental part of this work would produce jets that flow at rates on the order of 12-18 gal/min with nozzle pressure drops of 2000-4500 psi. Since total drilling fluid flow rates of approximately 300 gal/min are typical for this size bit, it appears that up to 16-25 nozzles could be utilized on a single bit to assist PDC cutters. The resulting reduction in cutter forces could extend the applicability of PDC bits to much harder formations and more severe operating conditions. Limitations imposed by space requirements and the tendency for nozzles to plug would need to be overcome, but the potential benefits make the concept attractive.

Bit life in the soft-rock wear mode has been shown to be much greater than that in the hard-rock wear mode. This finding could explain the wide range in bit wear that is sometimes found in formations with apparently similar strengths. If the formation is fractured or has a high percentage of quartz, the probability that the cutters will wear in the hard-rock wear mode is increased, regardless of the apparent strength of the rock. The fact that some PDC bits have experienced bit life as long as 20,000 ft [49], however, is evidence that the soft-rock wear mode is operative under certain conditions.

It should be noted that many of the complex phenomena that contribute to PDC bit wear and performance are by no means completely understood. In this paper, we have developed and used simple models to describe various mechanisms so that the approach can be easily modified as more complete understanding becomes available. PDCWEAR has been written so that different single-cutter force correlations than those developed in this work can be easily substituted if the user so desires.

More work needs to be done to improve understanding of PDC cutting mechanisms. For example, tests should be conducted under elevated fluid and rock stresses to determine how downhole conditions affect these mechanisms. In particular, the effects of ambient pressure on the benefits of waterjet assistance should be investigated.

Finally, the approach developed in this report for predicting PDC bit performance and wear needs to be tested. This could be done by comparing predicted bit performance parameters, such as WOB and drilling torque, with results measured in full-scale PDC bit tests under carefully controlled atmospheric and elevated pressure conditions.

6.0 CONCLUSIONS

- 1) The penetrating force imposed on a worn PDC cutter at a given depth of cut is approximately proportional to the wearflat area in contact with the rock.
- 2) Within the limited range of PDC cutter compact sizes tested (0.5-0.75 inch diameter), the penetrating force is independent of compact diameter. This implies that larger cutters are more efficient in rock removal than smaller ones.
- 3) The penetrating stress required to cut to a given depth with a PDC cutter can be significantly reduced by directing low- to moderate-pressure waterjets onto the rock surface immediately ahead of the cutter. Reductions of 10-15% at 2000 psi nozzle pressure drop and 50-65% reductions at 4500 psi were measured in the present study, which was conducted at atmospheric pressure in granite.
- 4) Two distinct PDC cutter wear modes occur, depending on the type of rock drilled. Soft, plastic rocks tend to wear the flat at an angle with respect to the rock surface, which keeps a smaller area in contact with the rock and the cutter in a sharper condition. Hard, brittle rocks and conditions under which cutter impact loading is prevalent tend to wear the flat parallel to the rock surface, leading to a larger area in contact with the rock and higher cutting forces.
- 5) A method has been developed for using single-cutter data to predict cutter forces and bit performance for arbitrary PDC bit designs. This method is incorporated into the computer code PDCWEAR to make it available for general PDC bit design analysis. The code has been shown to produce reasonable predictions of WOB, drilling torque, and bit life.
- 6) Unless cutter locations are carefully chosen, significant bit side forces and bending moments can develop during drilling. The resulting bit imbalance can cause bit wobble, leading to an overgauge hole and possible bit deviation.
- 7) Bit profile can significantly affect PDC bit performance and wear. It has been shown that bits with sharper profiles tend to initially require less WOB than flat profiles, but sharper profiles wear faster and eventually require greater WOB as drilled borehole length increases.
- 8) The distribution of cutters on a PDC bit can be used as a means for equalizing wear across the bit face. Cutters in regions of low placement density wear faster than those where placement density is high. Within limits, the WOB and torque required to drill at a specified penetration rate is relatively independent of the number of cutters used on the bit. A bit with fewer cutters will, however, wear faster and eventually require greater WOB as drilled borehole length increases.
- 9) Increased bit rotary speed is detrimental to bit life, even under conditions where thermal wear effects are not important. Doubling the

rotary speed from 100 to 200 RPM initially reduces the WOB required to drill at a specified rate, but more rapid wear occurs at the higher speed and eventually leads to greater WOB requirements and lower bit life.

- 10) Waterjet assistance can significantly increase bit life and reduce WOB and drilling torque requirements. Greater than 20% improvements in bit life and 19-36% reductions in WOB and drilling torque are predicted for a design utilizing only four nozzles operating at 4500 psi pressure drop. If space limitations and nozzle plugging problems could be resolved, this technique could be used to significantly extend the range of applicability of PDC bits.

7.0 NOMENCLATURE

A_r	= cross-sectional area of rock removed by cutter (in ²)
ΔA_r	= incremental cross-sectional area of cut (in ²)
A_w	= cutter wearflat area in contact with rock (in ²)
$(A_w)_t$	= total cutter wearflat area (in ²)
b	= $r \cos \beta$ (in)
C_1	= correlation constant in Eq. 3 (psi/in ⁿ¹)
C_2	= correlation constant in Eq. 4 (lbf/in ⁿ²)
c_2	= rock specific heat (Btu/lbm°F)
C_3	= parameter defined in Eq. 14c
C_4	= constant in Eq. 38 (in ¹⁻³ⁿ⁴)
C_5	= constant in Eq. 39 (in ¹⁻²ⁿ⁵)
C_6	= abrasive wear constant (in ² /lbf)
d	= lateral distance between center of test cut and center of previous adjacent cut in single-cutter tests (in)
D	= parameter defined in Eq. 14d and stud diameter (in)
E	= parameter defined in Eq. 14e
f	= thermal response function (°C cm ² /W)
f_r	= bit feed rate (in/rev)
F	= cutter penetrating force (lbf)
F_c	= cutting force, see Eq. 6 (lbf)
F_d	= cutter drag force, see Eq. 6 (lbf)
F_f	= cutter friction force, see Eq. 6 (lbf)
F_r	= radial component of cutter penetrating force (lbf)
F_s	= resultant side force on bit (lbf)
F_v	= longitudinal (vertical) component of cutter penetrating force (lbf)
F'_x	= bit side force in x' direction (lbf)
F'_y	= bit side force in y' direction (lbf)
h	= cutter convective cooling coefficient (Btu/hr ft ² °F)
H	= cutting height of cutter compact center (in)
H'	= longitudinal position of cutter compact center on bit (in)
k_2	= thermal conductivity of rock (Btu/hr ft°F)
l_h	= length of hole drilled (ft)
L	= length of cutter wearflat in contact with rock (in)
L_{max}	= maximum wearflat length contacting rock in soft-rock wear mode (in)
L_t	= total length of cutter wearflat (in)
M	= resultant bit bending moment (ft-lbf)
M'_x	= bit bending moment about x'-axis (ft-lbf)
M'_y	= bit bending moment about y'-axis (ft-lbf)
n_1	= correlation exponent in Eq. 3
n_2	= correlation exponent in Eq. 4
n_4	= exponent in Eq. 38
n_5	= exponent in Eq. 39
n_c	= number of cutters on bit
n_x	= number of Δx elements over which cutter interacts with rock formation
N	= bit rotary speed (rev/min)
Nu	= Nusselt number

Pr = Prandtl number
r = cutter compact radius (in)
 r_w = parameter defined in Eq. 19e (in)
R = radial position of cutter compact center on bit (in)
 Re_D = Reynolds number
ROP = bit rate of penetration (in/min or ft/hr)
 S_c = unconfined compressive rock strength (lbf/in²)
 t_d = thickness of diamond layer on PDC element (in)
T = bit drilling torque (ft-lbf)
 T_f = downhole cooling fluid temperature (°F)
 \bar{T}_w = mean temperature across cutter wearflat (°F or °C)
u = cooling fluid velocity (ft/sec)
V = cutter speed with respect to rock (ft/sec)
 V_r = volume of rock removed by a cutter (in³)
 ΔV_r = incremental volume of cut (in³)
 V_w = cutter wear volume associated with portion of wearflat in contact with rock (in³)
w = width of cutter wearflat at diamond face (in)
 w_c = width of cut (in)
WOB = weight-on-bit (lbf)
WR = cutter wear ratio
x = coordinate along x-axis in hole coordinate system (in)
 Δx = size of element along x-axis (in)
 x' = coordinate along x' -axis in bit coordinate system (in)
 x'_0 = coordinate along x'_0 -axis in cutter coordinate system (in)
 x_0 = coordinate along x_0 -axis in cutter profile coordinate system (in)
 x_{bc} = x-coordinate of the bottom of cut in the center of the cut (in)
 x_{c1} = x-coordinate of first point of contact between cutter and rock (in)
 x_{c2} = x-coordinate of last point of contact between cutter and rock (in)
 x_{w1} = x-coordinate of first end of cutter wearflat width (in)
 x_{w2} = x-coordinate of second end of cutter wearflat width (in)
y = coordinate along y-axis in hole coordinate system (in)
 y' = coordinate along y' -axis in bit coordinate system (in)
z = coordinate along z-axis in hole coordinate system (in)
 z' = coordinate along z' -axis in bit coordinate system (in)
 z_0 = coordinate along z_0 -axis in cutter profile coordinate system (in)
 z'_0 = coordinate along z'_0 -axis in cutter coordinate system (in)
 z_b = z-coordinate of the equivalent bottom of cut at a given x (in)
 z_{bc} = z-coordinate of the bottom of cut in the center of the cut (in)
 z'_{bc} = z' -coordinate of the bottom of cut in the center of the cut (in)
 z_{c1} = z-coordinate of first point of contact between cutter and rock (in)
 z_{c2} = z-coordinate of last point of contact between cutter and rock (in)
 z_{w1} = z-coordinate of first end of cutter wearflat width (in)
 z_{w2} = z-coordinate of second end of cutter wearflat width (in)

β	= cutter backrake angle (deg)
δ	= depth of cut (in)
δ_e	= effective depth of cut (in)
δ_1	= depth of adjacent cut (in)
Δ	= distance from equivalent bottom of cut to rock surface at a given x (in)
Θ	= angular position of cutter compact center on bit (deg)
μ	= friction coefficient between cutter and rock
μ_d	= F_d/F = cutter drag coefficient
μ_f	= cooling fluid viscosity (lbm/ft sec)
ρ_f	= cooling fluid density (lbm/ft ³)
ρ_2	= rock density (lbm/ft ³)
Φ_c	= cutter inclination angle (deg)
Φ_w	= cutter radial wear angle in hole coordinate system (deg)
$(\Phi_w)_o$	= cutter radial wear angle in cutter profile coordinate system (deg)
$(\Phi_w)'_o$	= cutter radial wear angle in cutter coordinate system (deg)
χ_2	= rock thermal diffusivity (ft ² /hr)

subscripts

1	location 1, cutter 1
2	location 2
i	ith Δx element over which cutter interacts with rock formation
j	jth cutter
k	kth cut
() _r	reference cutter
() _o	coordinate expressed in terms of cutter profile coordinate system
()'	coordinate expressed in terms of bit coordinate system
()' _o	coordinate expressed in terms of cutter coordinate system

8.0 ACKNOWLEDGMENT

This work was supported by the U.S. Department of Energy, Geothermal Technologies Division, at Sandia National Laboratories under Contract DE-AC04-76DP00789.

The assistance of David L. Goodwin with the experimental work is gratefully acknowledged.

9.0 REFERENCES

1. Hendrickson, R.R., Winzenried, R.W., and Jones, A.H.: "High-Temperature Seals and Lubricants for Geothermal Rock Bits: Final Report," Sandia National Laboratories Report SAND81-1404, Albuquerque, NM (Sept. 1981).
2. Hibbs, L.E., Jr., Sogolian, G.C., and Flom, D.G.: "Geothermal Compax Drill Bit Development, Final Technical Report," General Electric Corporate Research and Development, prepared for U.S. Dept. of Energy under Contract DE-AC04-76ET27142 (April 1984).
3. Lin, Y.T.: "The Impact of Bit Performance on Geothermal Well Cost," Trans., Geothermal Res. Council (Oct. 1981) 8, 261-66.
4. Carson, C.C. and Lin, Y.T.: "Geothermal Well Costs and Their Sensitivities to Changes in Drilling and Completion Operations," Proc. Intl. Conf. Geothermal Drilling and Completion Tech., Report SAND81-0036C, Sandia Natl. Laboratories, Albuquerque, NM (Jan. 21-23, 1981) 8-1 thru 8-26.
5. Varnado, S.G., Huff, C.F., and Yarrington, P.: "The Design and Use of Polycrystalline Diamond Compact Drag Bits in the Geothermal Environment," paper SPE 8378 presented at the 54th Annual Fall Tech. Conf. and Exhib. of the Soc. of Petr. Engr., Las Vegas, NV, Sept. 23-26, 1979.
6. Varnado, S.G., Huff, C.F., and Yarrington, P.: "Studies Aim at Optimizing Design for PDC Hard-Formation Bits," World Oil (March 1980) 63-70.
7. Pope, L.E.: "Analysis of Failed Stratapax^R-Steel Stud Cutter Elements," Report SAND80-0410, Sandia Natl. Laboratories, Albuquerque, NM (April 1981).
8. Huff, C.F., Ashmore, R.F., and Miller, J.W.: "Single Point Rock Cutting Strength and Fatigue Evaluation of Gas Pressure Diffusion Bonded Stratapax^R," Report SAND77-1962, Sandia Natl. Laboratories, Albuquerque, NM (April 1978).
9. Jellison, J.L.: "Gas Pressure Bonding of Stratapax^R," ASME Paper 77-PET-72 presented at Energy Tech. Conf., Houston, TX, Sept. 18-22, 1977.
10. Huff, C.F., Jellison, J.L., and Varnado, S.G.: "Bonding Technique Attaches Stratapax to Drill Bits," The Oil and Gas Journal (Feb. 19, 1979) 111-114.
11. Middleton, J.N. and Finger, J.T.: "Diffusion Bonding of Stratapax^R for Drill Bits," Report SAND82-2309, Sandia Natl. Laboratories, Albuquerque, NM (January 1983).
12. Huff, C.F., McFall, A.L., and St. Clair, J.A.: "Design of Special Performance Bits Utilizing Synthetic Diamond Cutters," paper SPE 7515 presented at the 53rd Annual Fall Tech. Conf. and Exhib. of the Soc. of Petr. Engr., Houston, TX, Oct. 1-4, 1978.

13. Huff, C.F. and Varnado, S.G.: "Recent Developments in Polycrystalline Diamond Drill Bit Design," Report SAND79-1592C, Sandia Natl. Laboratories, Albuquerque, NM (May 1980); also presented at the 1980 ASME Energy-Source Tech. Conf., New Orleans, LA, Feb. 3-7, 1980.
14. Varnado, S.G., ed.: "Geothermal Drilling and Completion Technology Development Program Annual Progress Report, October 1979-September 1980," Report SAND80-2179, Sandia Natl. Laboratories, Albuquerque, NM (Nov. 1980).
15. Hoover, E.R. and Pope, L.E.: "Failure Mechanisms of Polycrystalline Diamond Compact Drill Bits in Geothermal Environments," Report SAND81-1404, Sandia Natl. Laboratories, Albuquerque, NM (Sept. 1981)
16. Hoover, E.R. and Middleton, J.N.: "Laboratory Evaluation of PDC Drill Bits Under High-Speed and High-Wear Conditions," J. Petr. Tech. (Dec. 1981) 2316-2321.
17. Kelsey, J.R., ed.: "Geothermal Technology Development Program Annual Progress Report, October 1980-September 1981," Report SAND81-2124, Sandia Natl. Laboratories, Albuquerque, NM (Sept. 1982).
18. Heckes, A.A., Meano, W., and Baker, L.E.: "Polycrystalline Diamond Drill Bits for Venezuelan Oil Field Applications," Report SAND82-1963, Sandia Natl. Laboratories, Albuquerque, NM (April 1983).
19. Hibbs, L.E., Jr. and Sogoian, G.C.: "Wear Mechanisms for Polycrystalline Diamond Compacts as Utilized for Drilling in Geothermal Environments-Final Report," Report SAND82-7213, Sandia Natl. Laboratories, Albuquerque, NM (May 1983).
20. Glowka, D.A.: "Thermal Limitations on the Use of PDC Bits in Geothermal Drilling," Trans. Geothermal Res. Council (Aug. 1984) 8, 261-66.
21. Swenson, D.V., Wesenberg, D.L., and Jones, A.K.: "Analytical and Experimental Investigations of Rock Cutting Using Polycrystalline Diamond Compact Drag Cutters," paper SPE 10150 presented at the 56th Annual Fall Tech. Conf. and Exhib. of the Soc. of Petr. Engr., San Antonio, TX, Oct. 5-7, 1981.
22. Ortega, A. and Glowka, D.A.: "Studies of the Frictional Heating of Polycrystalline Diamond Compact Tools During Rock Cutting," Report SAND80-2677, Sandia Natl. Laboratories, Albuquerque, NM (June 1980).
23. Glowka, D.A.: "Optimization of Bit Hydraulic Configurations," Soc. Petr. Engr. J. (Feb. 1983) 21-32.
24. Zeuch, D.H., Swenson, D.V., and Finger, J.T.: "Subsurface Damage Development in Rock During Drag-Bit Cutting: Observations and Model Predictions," Proc. 24th U.S. Symp. on Rock Mech., Texas A&M Univ., College Station, TX, (June 20-23, 1983) 733-742.

25. Swenson, D.V.: "Modeling and Analysis of Drag Bit Cutting," Report SAND83-0278, Sandia Natl. Laboratories, Albuquerque, NM (July 1983).
26. Ortega, A. and Glowka, D.A.: "Frictional Heating and Convective Cooling of Polycrystalline Diamond Drag Tools During Rock Cutting," Soc. Petr. Engr. J. (April 1984) 121-128.
27. Glowka, D.A. and Stone, C.M.: "Thermal Response of Polycrystalline Diamond Compact Cutters Under Simulated Downhole Conditions," Soc. Petr. Engr. J. (April 1985) 143-156.
28. Glowka, D.A.: "Design Considerations for a Hard-Rock PDC Drill Bit," Trans. Geothermal Res. Council (Aug. 1985) 9, 123-128.
29. Glowka, D.A. and Stone, C.M.: "Effects of Thermal and Mechanical Loading on PDC Bit Life," SPE Drilling Engr. (June 1986) 201-214.
30. Zeuch, D.H. and Finger, J.T.: "Rock Breakage Mechanisms with a PDC Bit," paper SPE 14219 presented at the 60th Ann. Tech. Conf. and Exhib. of the Soc. of Petr. Engr., Las Vegas, NV, Sept. 22-25, 1985.
31. Glowka, D.A.: "Implications of Thermal Wear Phenomena for PDC Bit Design and Operation," paper SPE 14222 presented at the 60th Ann. Tech. Conf. and Exhib. of the Soc. of Petr. Engr., Las Vegas, NV, Sept. 22-25, 1985.
32. Glowka, D.A.: "The Use of Single-Cutter Data in the Analysis of PDC Bit Designs," paper SPE 15619 presented at the 61st Annual Tech. Conf. and Exhib. of the Soc. of Petr. Engr., New Orleans, LA, Oct. 5-8, 1986.
33. Lee, M. and Hibbs, L.E., Jr.: "Role of Deformation Twin Bands in the Wear Processes of Polycrystalline Diamond Tools," Wear of Materials, K.C. Ludema, W.A. Glaeser, and S.K. Rhee, eds., ASME (1979) 485-91.
34. Hood, M.: "A Study of Methods to Improve the Performance of Drag Bits Used to Cut Hard Rock," Report 35/77, Chamber of Mines of South Africa (Aug. 1977).
35. Hood, M.: "Cutting Strong Rock with a Drag Bit Assisted by High-Pressure Water Jets," J. South African Inst. Min. Met. (Nov. 1976) 79-90.
36. Dubugnon, O.: "An Experimental Study of Water Assisted Drag Bit Cutting of Rocks," presented at 1st U.S. Water Jet Symp., Golden, CO, April 7-9, 1981.
37. Melaugh, J.F. and Saltzer, J.A.: "Development of a Predictive Model for Drilling Pressurized Shale with Stratapax Blank Bits," presented at ASME Energy Technology Conf., Houston, TX, Jan. 19-22, 1981.
38. Kelsey, J.R., ed: "Geothermal Technology Development Program Annual Progress Report, October 1983-September 1984," Report SAND85-1138, Sandia Natl. Laboratories, Albuquerque, NM (Aug. 1985).

39. Cortes, J. and Besson, A.: "Behavior of Polycrystalline Diamond Compact Cutters While Drilling in Bottomhole Conditions-Field Applications," Proc. Int. Conf. on Geothermal Drilling and Completion Tech., Report SAND81-0036C, Sandia Natl. Laboratories, Albuquerque, NM (Jan. 21-23, 1981) 11-1 thru 11-18.
40. Walker, B., Drilling Research Laboratory, Salt Lake City, UT, private communication, April 1986.
41. Maurer, W.C.: "Bit-Tooth Penetration Under Simulated Borehole Conditions," J. Petr. Tech. (Dec. 1965) 1433-1442.
42. Conn, A.F., Johnson, V.E., Jr., Liu, H.L., and Frederick, G.S.: "Evaluation of Cavitating Jets for Deep-Hole Rock Cutting," Report SAND81-7067, Sandia Natl. Laboratories, Albuquerque, NM (May 1981).
43. Johnson, V.E., Jr., Lindenmuth, W.T., Chahine, G.L., Conn, A.F., and Frederick, G.S.: "Research and Development of Improved Cavitating Jets for Deep-Hole Drilling," Report SAND83-7461, Sandia Natl. Laboratories, Albuquerque, NM (Jan. 1984).
44. Chahine, G.L., Genoux, P.F., Johnson, V.E., Jr., and Frederick, G.S.: "Analytical and Experimental Study of the Acoustics and the Flow Field Characteristics of Cavitating Self-Resonating Water Jets," Report SAND84-7142, Sandia Natl. Laboratories, Albuquerque, NM (Sept. 1984).
45. Chahine, G.L., Genoux, P.F., Liu, H.L., and Johnson, V.E., Jr.: "Analytical and Experimental Study of Self-Resonating Water Jets: Nozzle-Jet and Wall-Jet Interactions," Report SAND86-7124, Sandia Natl. Laboratories, Albuquerque, NM (July 1987).
46. Chahine, G.L., Johnson, V.E., Jr., Kalumuck, K.M., Perdue, T.O., Waxman, D.N., Frederick, G.S., and Watson, R.E.: "Internal and External Acoustics and Large Structures Dynamics of Cavitating Self-Resonating Water Jets," Report SAND86-7176, Sandia Natl. Laboratories, Albuquerque, NM (July 1987).
47. Jones, I.R. and Edwards, D.H.: "An Experimental Study of the Forces Generated by the Collapse of Transient Cavities in Water," J. Fluid Mech. (1960) 7, 596-609.
48. Aronson, E.A., McCaughey, K.G., and Walton, E.L.: "STRATAPAX Computer Program Update," Report SAND82-1087, Sandia Natl. Lab., Albuquerque, NM (Sept. 1982).
49. Gill, C.W. and Martin, J.L.: "Matrix Body PDC Bits Prove Most Cost Effective in the Powder River Basin," paper IADC/SPE 13462 presented at IADC/SPE 1985 Drilling Conference, New Orleans, LA (March 1985) 341-354.
50. Gartling, D.K.: "COYOTE - A Finite Element Computer Program for Nonlinear Heat Conduction Problems," Report SAND77-1332 (Revised), Sandia Natl. Laboratories, Albuquerque, NM (Oct. 1982).

51. Robertson, E.: "Thermal Conductivities of Rocks," USGS Open-File Report 79-356 (1979).

52. Mondy, L. and Duda, L.: "Advanced Wellbore Thermal Simulator GEOTEMP2 User Manual," Report SAND84-0857, Sandia Natl. Laboratories, Albuquerque, NM (Nov. 1984).

APPENDIX A
EXPERIMENTAL SINGLE-CUTTER DATA

TABLE A-1

DESCRIPTION OF CUTTERS USED IN LABORATORY TESTS

CUTTER	A_w (in ²)	w (in)	L (in)	COMPACT DIAMETER (in)	WEARFLAT TYPE *
A	0.016	0.220	0.090	0.50	F
B	0.017	0.240	0.070	0.50	F
C	0.017	0.340	0.050	0.50	F
D	0.020	0.320	0.100	0.75	L
E	0.022	0.220	0.140	0.50	F,L
F	0.030-0.040	0.300-0.320	0.140-0.180	0.50	M,L
G	0.032	0.360	0.130	0.75	L
H**	0.029	0.340	0.120	0.75	L
I	0.040	0.320	0.180	0.50	M
J	0.000	0.000	0.000	0.50	S
K	0.000	0.00	0.00	0.75	S

* F = field-worn; L = laboratory-worn; M = machine ground; S = sharp.

** Cutter H used in waterjet-assisted cuts.

All cutters had a backrake angle of 20°.

TABLE A-2

DRY, NON-INTERACTING CUT TEST DATA FOR BEREA SANDSTONE

CUTTER	A_w (in ²)	w (in)	L (in)	δ (in)	F (lb)	F_d (lb)	F/A_w (psi)	F_d / F
I	0.040	0.320	0.180	0.010	90.1	79.1	2253.	0.88
I	0.040	0.320	0.180	0.010	80.3	68.5	2008.	0.85
I	0.040	0.320	0.180	0.010	82.0	72.3	2050.	0.88
I	0.040	0.320	0.180	0.010	85.4	73.4	2135.	0.86
I	0.040	0.320	0.180	0.010	103.8	94.2	2595.	0.91
I	0.040	0.320	0.180	0.010	125.2	111.6	3130.	0.89
I	0.040	0.320	0.180	0.010	112.0	92.3	2800.	0.82
I	0.040	0.320	0.180	0.010	107.1	98.0	2678.	0.92
I	0.040	0.320	0.180	0.010	124.5	112.6	3113.	0.90
I	0.040	0.320	0.180	0.010	123.3	106.7	3083.	0.87
I	0.040	0.320	0.180	0.010	78.8	73.6	1970.	0.93
I	0.040	0.320	0.180	0.010	80.1	70.4	2003.	0.88
I	0.040	0.320	0.180	0.010	86.9	80.7	2173.	0.93
I	0.040	0.320	0.180	0.020	164.3	150.8	4108.	0.92
I	0.040	0.320	0.180	0.020	146.5	136.4	3663.	0.93
I	0.040	0.320	0.180	0.020	168.0	155.4	4200.	0.92
I	0.040	0.320	0.180	0.020	165.7	151.5	4143.	0.91
I	0.040	0.320	0.180	0.021	172.2	144.5	4305.	0.84
I	0.040	0.320	0.180	0.020	194.5	177.1	4863.	0.91
I	0.040	0.320	0.180	0.020	176.8	162.8	4420.	0.92
I	0.040	0.320	0.180	0.020	175.5	160.5	4388.	0.91
I	0.040	0.320	0.180	0.020	167.9	150.4	4198.	0.90
I	0.040	0.320	0.180	0.020	163.0	149.2	4075.	0.92
I	0.040	0.320	0.180	0.020	172.2	156.9	4305.	0.91
I	0.040	0.320	0.180	0.020	159.9	148.1	3998.	0.93
I	0.040	0.320	0.180	0.021	179.3	159.8	4483.	0.89
I	0.040	0.320	0.180	0.020	173.0	160.4	4325.	0.93
I	0.040	0.320	0.180	0.022	167.6	158.4	4190.	0.95
I	0.040	0.320	0.180	0.021	173.9	162.4	4348.	0.93
I	0.040	0.320	0.180	0.020	175.3	159.9	4383.	0.91
I	0.040	0.320	0.180	0.040	227.4	221.0	5685.	0.97
I	0.040	0.320	0.180	0.040	280.7	263.7	7018.	0.94
I	0.040	0.320	0.180	0.040	272.7	255.8	6818.	0.94
I	0.040	0.320	0.180	0.040	281.2	268.0	7030.	0.95
I	0.040	0.320	0.180	0.039	260.5	246.8	6513.	0.95
I	0.040	0.320	0.180	0.040	243.2	229.8	6080.	0.94
I	0.040	0.320	0.180	0.041	240.1	233.5	6003.	0.97
I	0.040	0.320	0.180	0.040	252.7	241.5	6318.	0.96
I	0.040	0.320	0.180	0.040	252.3	240.9	6308.	0.95
I	0.040	0.320	0.180	0.040	215.3	210.2	5383.	0.98
I	0.040	0.320	0.180	0.040	242.6	229.9	6065.	0.95

TABLE A-2 (CONT'D)

CUTTER	A_w (in ²)	w (in)	L (in)	δ (in)	F (lb)	F_d (lb)	F/A_w (psi)	F_d / F
I	0.040	0.320	0.180	0.040	249.0	235.3	6225.	0.94
I	0.040	0.320	0.180	0.040	255.9	247.8	6398.	0.97
I	0.040	0.320	0.180	0.040	272.9	263.7	6823.	0.97
I	0.040	0.320	0.180	0.040	279.0	268.2	6975.	0.96
I	0.040	0.320	0.180	0.040	237.3	233.6	5933.	0.98
I	0.040	0.320	0.180	0.040	258.6	247.1	6465.	0.96
I	0.040	0.320	0.180	0.040	248.5	233.8	6213.	0.94
I	0.040	0.320	0.180	0.040	230.0	222.3	5750.	0.97
I	0.040	0.320	0.180	0.041	240.5	236.8	6013.	0.98
I	0.040	0.320	0.180	0.041	264.4	249.5	6610.	0.94
I	0.040	0.320	0.180	0.041	226.5	219.5	5663.	0.97
I	0.040	0.320	0.180	0.041	230.0	223.4	5750.	0.97
I	0.040	0.320	0.180	0.042	248.5	239.0	6213.	0.96
I	0.040	0.320	0.180	0.040	235.6	229.6	5890.	0.97
I	0.040	0.320	0.180	0.040	228.4	223.1	5710.	0.98
I	0.040	0.320	0.180	0.041	241.2	229.4	6030.	0.95
I	0.040	0.320	0.180	0.041	264.7	250.0	6618.	0.94
I	0.040	0.320	0.180	0.041	229.9	227.4	5748.	0.99
I	0.040	0.320	0.180	0.060	290.0	285.1	7250.	0.98
I	0.040	0.320	0.180	0.060	285.5	289.3	7138.	1.01
I	0.040	0.320	0.180	0.060	314.3	313.3	7858.	1.00
I	0.040	0.320	0.180	0.060	299.8	301.8	7495.	1.01
I	0.040	0.320	0.180	0.062	289.9	292.0	7248.	1.01
I	0.040	0.320	0.180	0.061	294.4	293.0	7360.	1.00
I	0.040	0.320	0.180	0.061	290.1	286.5	7253.	0.99
I	0.040	0.320	0.180	0.061	312.7	310.8	7818.	0.99
I	0.040	0.320	0.180	0.060	286.2	295.2	7155.	1.03
I	0.040	0.320	0.180	0.080	355.9	365.8	8898.	1.03
I	0.040	0.320	0.180	0.080	379.5	400.0	9488.	1.05
I	0.040	0.320	0.180	0.082	326.3	323.1	8158.	0.99
I	0.040	0.320	0.180	0.080	379.5	400.0	9488.	1.05
I	0.040	0.320	0.180	0.080	319.9	326.1	7998.	1.02
I	0.040	0.320	0.180	0.082	352.7	363.3	8818.	1.03
I	0.040	0.320	0.180	0.082	350.8	383.2	8770.	1.09
I	0.040	0.320	0.180	0.080	366.4	375.5	9160.	1.02
I	0.040	0.320	0.180	0.080	365.2	365.3	9130.	1.00
I	0.040	0.320	0.180	0.080	373.4	371.4	9335.	0.99
I	0.040	0.320	0.180	0.080	362.7	356.8	9068.	0.98
I	0.040	0.320	0.180	0.080	376.3	376.5	9408.	1.00
I	0.040	0.320	0.180	0.100	380.5	410.6	9513.	1.08
I	0.040	0.320	0.180	0.099	410.4	430.2	10260.	1.05
I	0.040	0.320	0.180	0.100	528.1	534.6	13203.	1.01
I	0.040	0.320	0.180	0.100	450.1	469.1	11253.	1.04
I	0.040	0.320	0.180	0.100	451.4	469.6	11285.	1.04

TABLE A-2 (CONT'D)

CUTTER	A_w (in ²)	w (in)	L (in)	δ (in)	F (lb)	F_d (lb)	F/A_w (psi)	F_d/F
I	0.040	0.320	0.180	0.100	427.0	450.0	10675.	1.05
I	0.040	0.320	0.180	0.100	464.9	476.6	11623.	1.03
I	0.040	0.320	0.180	0.100	395.6	417.9	9890.	1.06
I	0.040	0.320	0.180	0.100	479.0	505.8	11975.	1.06
J	0.000	0.000	0.000	0.023	13.3	19.4	---	1.46
J	0.000	0.000	0.000	0.020	16.9	21.7	---	1.28
J	0.000	0.000	0.000	0.022	17.3	21.0	---	1.21
J	0.000	0.000	0.000	0.019	18.6	23.6	---	1.27
J	0.000	0.000	0.000	0.042	60.1	66.0	---	1.10
J	0.000	0.000	0.000	0.041	62.8	75.6	---	1.20
J	0.000	0.000	0.000	0.041	58.1	71.7	---	1.23
J	0.000	0.000	0.000	0.041	57.9	67.5	---	1.17
J	0.000	0.000	0.000	0.080	117.0	143.0	---	1.22
J	0.000	0.000	0.000	0.082	116.0	139.0	---	1.20
J	0.000	0.000	0.000	0.078	128.0	154.0	---	1.20
J	0.000	0.000	0.000	0.060	94.5	110.0	---	1.16
J	0.000	0.000	0.000	0.062	91.3	106.0	---	1.16
B	0.017	0.240	0.070	0.011	45.2	41.7	2659.	0.92
B	0.017	0.240	0.070	0.011	46.9	41.2	2759.	0.88
B	0.017	0.240	0.070	0.011	44.4	39.3	2612.	0.89
B	0.017	0.240	0.070	0.012	39.8	39.0	2341.	0.98
B	0.017	0.240	0.070	0.012	42.8	40.0	2518.	0.93
B	0.017	0.240	0.070	0.013	43.2	37.7	2541.	0.87
B	0.017	0.240	0.070	0.018	58.1	52.4	3418.	0.90
B	0.017	0.240	0.070	0.020	54.5	49.8	3206.	0.91
B	0.017	0.240	0.070	0.020	56.5	51.5	3324.	0.91
B	0.017	0.240	0.070	0.020	58.3	56.2	3429.	0.96
B	0.017	0.240	0.070	0.025	60.5	63.8	3559.	1.05
B	0.017	0.240	0.070	0.043	102.0	106.0	6000.	1.04
B	0.017	0.240	0.070	0.044	102.0	110.0	6000.	1.08
B	0.017	0.240	0.070	0.045	106.0	112.0	6235.	1.06
B	0.017	0.240	0.070	0.043	110.0	116.0	6471.	1.05
B	0.017	0.240	0.070	0.045	102.0	107.0	6000.	1.05
B	0.017	0.240	0.070	0.045	105.0	108.0	6176.	1.03
B	0.017	0.240	0.070	0.043	109.0	113.0	6412.	1.04
B	0.017	0.240	0.070	0.081	176.0	195.0	10353.	1.11
B	0.017	0.240	0.070	0.082	166.0	193.0	9765.	1.16
B	0.017	0.240	0.070	0.082	154.0	169.0	9059.	1.10
B	0.017	0.240	0.070	0.082	138.0	158.0	8118.	1.14
B	0.017	0.240	0.070	0.080	167.0	190.0	9824.	1.14
B	0.017	0.240	0.070	0.083	169.0	198.0	9941.	1.17
C	0.017	0.340	0.050	0.010	46.1	42.7	2712.	0.93
C	0.017	0.340	0.050	0.013	47.4	44.5	2788.	0.94

TABLE A-2 (CONT'D)

CUTTER	A_w (in ²)	w (in)	L (in)	δ (in)	F (lb)	F_d (lb)	F/A_w (psi)	F_d/F
C	0.017	0.340	0.050	0.012	45.9	44.3	2700.	0.97
C	0.017	0.340	0.050	0.012	44.3	46.0	2606.	1.04
C	0.017	0.340	0.050	0.013	46.5	44.5	2735.	0.96
C	0.017	0.340	0.050	0.012	41.7	41.5	2453.	1.00
C	0.017	0.340	0.050	0.012	44.0	42.9	2588.	0.98
C	0.017	0.340	0.050	0.030	95.8	101.0	5635.	1.05
C	0.017	0.340	0.050	0.030	97.9	102.0	5759.	1.04
C	0.017	0.340	0.050	0.030	90.1	96.0	5300.	1.07
C	0.017	0.340	0.050	0.029	93.6	95.0	5506.	1.01
C	0.017	0.340	0.050	0.029	91.2	96.8	5365.	1.06
C	0.017	0.340	0.050	0.029	95.9	93.2	5641.	0.97
C	0.017	0.340	0.050	0.029	97.3	100.0	5724.	1.03
C	0.017	0.340	0.050	0.081	175.0	202.0	10294.	1.15
C	0.017	0.340	0.050	0.081	173.0	205.0	10176.	1.18
C	0.017	0.340	0.050	0.081	159.0	187.0	9353.	1.18
C	0.017	0.340	0.050	0.081	153.0	189.0	9000.	1.24
C	0.017	0.340	0.050	0.081	172.0	204.0	10118.	1.19
C	0.017	0.340	0.050	0.081	164.0	192.0	9647.	1.17
C	0.017	0.340	0.050	0.081	182.0	210.0	10706.	1.15
A	0.016	0.220	0.090	0.023	73.6	72.0	4600.	0.98
A	0.016	0.220	0.090	0.023	74.0	72.4	4625.	0.98
A	0.016	0.220	0.090	0.024	73.8	72.1	4613.	0.98
A	0.016	0.220	0.090	0.023	70.3	68.3	4394.	0.97
A	0.016	0.220	0.090	0.023	74.4	72.4	4650.	0.97
A	0.016	0.220	0.090	0.024	83.9	78.6	5244.	0.94
A	0.016	0.220	0.090	0.023	85.0	79.2	5312.	0.93
A	0.016	0.220	0.090	0.067	133.0	151.0	8313.	1.14
A	0.016	0.220	0.090	0.083	183.0	205.0	11437.	1.12
A	0.016	0.220	0.090	0.083	152.0	177.0	9500.	1.16
A	0.016	0.220	0.090	0.083	157.0	178.0	9813.	1.13
A	0.016	0.220	0.090	0.083	165.0	189.0	10313.	1.15
A	0.016	0.220	0.090	0.083	184.0	201.0	11500.	1.09
A	0.016	0.220	0.090	0.082	170.0	189.0	10625.	1.11
E	0.022	0.220	0.140	0.026	97.9	94.1	4450.	0.96
E	0.022	0.220	0.140	0.024	82.9	80.7	3768.	0.97
E	0.022	0.220	0.140	0.024	87.5	83.8	3977.	0.96
E	0.022	0.220	0.140	0.024	89.2	84.2	4055.	0.94
E	0.022	0.220	0.140	0.024	92.1	85.5	4186.	0.93
E	0.022	0.220	0.140	0.025	98.1	94.2	4459.	0.96
E	0.022	0.220	0.140	0.024	95.7	89.9	4350.	0.94
E	0.022	0.220	0.140	0.085	235.0	259.0	10682.	1.10
E	0.022	0.220	0.140	0.086	224.0	241.0	10182.	1.08
E	0.022	0.220	0.140	0.085	233.0	263.0	10591.	1.13

TABLE A-2 (CONT'D)

CUTTER	A_w (in ²)	w (in)	L (in)	δ (in)	F (lb)	F_d (lb)	F/A_w (psi)	F_d / F
E	0.022	0.220	0.140	0.084	200.0	220.0	9091.	1.10
E	0.022	0.220	0.140	0.084	219.0	235.0	9955.	1.07
E	0.022	0.220	0.140	0.085	214.0	237.0	9727.	1.11
E	0.022	0.220	0.140	0.085	219.0	238.0	9955.	1.09
K	0.000	0.000	0.000	0.021	18.0	24.3	---	1.35
K	0.000	0.000	0.000	0.023	17.0	26.1	---	1.54
K	0.000	0.000	0.000	0.023	16.7	19.2	---	1.15
K	0.000	0.000	0.000	0.020	16.9	23.5	---	1.39
K	0.000	0.000	0.000	0.022	19.6	23.1	---	1.18
K	0.000	0.000	0.000	0.023	17.7	23.7	---	1.34
K	0.000	0.000	0.000	0.021	19.8	24.0	---	1.21
K	0.000	0.000	0.000	0.041	55.5	72.5	---	1.31
K	0.000	0.000	0.000	0.042	51.8	70.5	---	1.36
K	0.000	0.000	0.000	0.042	53.5	69.0	---	1.29
K	0.000	0.000	0.000	0.042	48.2	64.5	---	1.34
K	0.000	0.000	0.000	0.041	53.5	68.0	---	1.27
K	0.000	0.000	0.000	0.041	49.2	68.3	---	1.39
K	0.000	0.000	0.000	0.041	52.1	68.2	---	1.31
K	0.000	0.000	0.000	0.080	109.0	147.0	---	1.35
K	0.000	0.000	0.000	0.080	102.0	142.0	---	1.39
K	0.000	0.000	0.000	0.080	109.0	143.0	---	1.31
K	0.000	0.000	0.000	0.080	97.5	138.0	---	1.42
K	0.000	0.000	0.000	0.080	103.0	141.0	---	1.37
G	0.032	0.360	0.130	0.022	94.9	96.5	2966.	1.02
G	0.032	0.360	0.130	0.021	98.0	97.0	3062.	0.99
G	0.032	0.360	0.130	0.023	94.4	87.9	2950.	0.93
G	0.032	0.360	0.130	0.022	83.6	82.2	2612.	0.98
G	0.032	0.360	0.130	0.023	92.4	94.6	2888.	1.02
G	0.032	0.360	0.130	0.024	95.4	93.6	2981.	0.98
G	0.032	0.360	0.130	0.022	91.2	91.9	2850.	1.01
G	0.032	0.360	0.130	0.041	191.0	196.0	5969.	1.03
G	0.032	0.360	0.130	0.042	188.0	187.0	5875.	0.99
G	0.032	0.360	0.130	0.042	181.0	185.0	5656.	1.02
G	0.032	0.360	0.130	0.041	178.0	184.0	5562.	1.03
G	0.032	0.360	0.130	0.041	182.0	187.0	5687.	1.03
G	0.032	0.360	0.130	0.042	186.0	190.0	5812.	1.02
G	0.032	0.360	0.130	0.081	294.0	319.0	9188.	1.09
G	0.032	0.360	0.130	0.082	280.0	301.0	8750.	1.08
G	0.032	0.360	0.130	0.081	283.0	299.0	8844.	1.06
G	0.032	0.360	0.130	0.081	287.0	313.0	8969.	1.09
G	0.032	0.360	0.130	0.081	297.0	319.0	9281.	1.07

TABLE A-3

DRY, NON-INTERACTING CUT TEST DATA FOR SIERRA WHITE GRANITE

CUTTER	A_w (in ²)	w (in)	L (in)	δ (in)	F (lb)	F_d (lb)	F/A_w (psi)	F_d / F
F	0.034	0.310	0.160	0.011	657.4	423.0	19335.	0.64
F	0.035	0.310	0.165	0.010	553.9	361.0	15826.	0.65
F	0.035	0.310	0.165	0.010	627.1	405.7	17917.	0.65
F	0.035	0.310	0.165	0.010	602.8	389.5	17223.	0.65
F	0.035	0.310	0.165	0.010	591.2	381.7	16891.	0.65
F	0.035	0.310	0.165	0.010	717.7	454.0	20506.	0.63
F	0.035	0.310	0.165	0.010	632.4	412.1	18069.	0.65
F	0.035	0.310	0.165	0.010	789.7	506.3	22563.	0.64
F	0.035	0.310	0.165	0.010	786.9	496.8	22483.	0.63
F	0.035	0.310	0.165	0.010	778.9	509.6	22254.	0.65
F	0.035	0.310	0.165	0.010	782.8	500.0	22366.	0.64
F	0.035	0.310	0.165	0.010	795.3	507.0	22723.	0.64
F	0.035	0.310	0.165	0.010	786.4	502.2	22469.	0.64
F	0.033	0.305	0.155	0.020	737.3	458.0	22342.	0.62
F	0.033	0.305	0.155	0.020	696.4	437.2	21103.	0.63
F	0.033	0.305	0.155	0.020	806.5	500.0	24439.	0.62
F	0.033	0.305	0.155	0.020	740.3	464.7	22433.	0.63
F	0.033	0.305	0.155	0.020	714.5	446.4	21652.	0.62
F	0.033	0.305	0.155	0.020	765.5	485.2	23197.	0.63
F	0.033	0.305	0.155	0.020	771.3	475.3	23373.	0.62
F	0.034	0.310	0.160	0.020	879.4	561.6	25865.	0.64
F	0.034	0.310	0.160	0.020	887.2	544.7	26094.	0.61
F	0.034	0.310	0.160	0.020	896.6	559.5	26371.	0.62
F	0.034	0.310	0.160	0.020	901.8	570.3	26524.	0.63
F	0.034	0.310	0.160	0.020	894.8	546.1	26318.	0.61
F	0.034	0.310	0.160	0.020	921.8	576.0	27112.	0.62
F	0.034	0.310	0.160	0.020	946.9	583.2	27850.	0.62
F	0.034	0.310	0.160	0.037	1220.4	777.3	35894.	0.64
F	0.034	0.310	0.160	0.039	1216.9	783.9	35791.	0.64
F	0.034	0.310	0.160	0.040	1236.2	786.5	36359.	0.64
F	0.034	0.310	0.160	0.040	1242.8	790.5	36553.	0.64
F	0.034	0.310	0.160	0.040	1204.1	798.0	35415.	0.66
F	0.034	0.310	0.160	0.040	1218.7	774.0	35844.	0.64
F	0.036	0.310	0.165	0.038	1418.4	890.6	39400.	0.63
F	0.036	0.310	0.165	0.040	1456.7	916.7	40464.	0.63
F	0.036	0.310	0.165	0.039	1266.9	822.1	35192.	0.65
F	0.036	0.310	0.165	0.038	1372.3	890.4	38119.	0.65
F	0.036	0.310	0.165	0.040	1403.6	905.5	38989.	0.65
F	0.036	0.310	0.165	0.040	1299.8	822.8	36106.	0.63
F	0.036	0.310	0.165	0.057	1484.6	1006.6	41239.	0.68
F	0.036	0.310	0.165	0.060	1356.1	907.8	37669.	0.67

TABLE A-3 (CONT'D)

CUTTER	A_w (in ²)	w (in)	L (in)	δ (in)	F (lb)	F_d (lb)	F/A_w (psi)	F_d / F
F	0.036	0.310	0.165	0.058	1307.7	882.5	36325.	0.67
F	0.036	0.310	0.165	0.060	1346.7	892.6	37408.	0.66
F	0.036	0.310	0.165	0.060	1428.5	931.7	39681.	0.65
F	0.036	0.310	0.165	0.060	1458.9	975.6	40525.	0.67
F	0.036	0.310	0.165	0.063	1518.5	983.3	42181.	0.65
F	0.036	0.310	0.165	0.062	1517.9	1010.8	42164.	0.67
F	0.037	0.315	0.170	0.060	1486.1	953.3	40165.	0.64
F	0.037	0.315	0.170	0.061	1525.7	1002.6	41235.	0.66
F	0.037	0.315	0.170	0.060	1619.2	1050.4	43762.	0.65
F	0.037	0.315	0.170	0.059	1605.0	1037.7	43378.	0.65
F	0.037	0.315	0.170	0.078	1671.4	1140.2	45173.	0.68
F	0.037	0.315	0.170	0.080	1690.4	1147.1	45686.	0.68
F	0.037	0.315	0.170	0.080	1590.8	1070.6	42995.	0.67
F	0.037	0.315	0.170	0.076	1561.5	1054.5	42203.	0.68
F	0.037	0.315	0.170	0.080	1541.5	1041.7	41662.	0.68
F	0.037	0.315	0.170	0.078	1633.1	1083.1	44138.	0.66
F	0.037	0.315	0.170	0.078	1567.4	1053.0	42362.	0.67
F	0.037	0.315	0.170	0.075	1585.9	1068.1	42862.	0.67
F	0.038	0.315	0.170	0.080	1569.2	1075.4	41295.	0.69
F	0.038	0.315	0.170	0.080	1565.5	1050.0	41197.	0.67
F	0.038	0.315	0.170	0.101	1774.5	1216.1	46697.	0.69
F	0.038	0.315	0.170	0.101	1709.7	1201.6	44992.	0.70
F	0.038	0.315	0.170	0.095	1661.3	1147.7	43718.	0.69
F	0.038	0.315	0.170	0.100	1708.5	1166.9	44961.	0.68
F	0.038	0.315	0.170	0.100	1722.1	1200.9	45318.	0.70
F	0.038	0.315	0.170	0.100	1759.2	1231.7	46295.	0.70
F	0.038	0.315	0.170	0.100	1731.9	1206.4	45576.	0.70
F	0.039	0.315	0.175	0.095	1612.6	1138.5	41349.	0.71
F	0.039	0.315	0.175	0.100	1589.1	1124.3	40746.	0.71
F	0.039	0.315	0.175	0.100	1653.3	1172.2	42392.	0.71
J	0.000	0.000	0.000	0.017	31.7	26.3	---	0.83
J	0.000	0.000	0.000	0.015	25.3	16.8	---	0.66
J	0.000	0.000	0.000	0.016	30.4	17.0	---	0.56
J	0.000	0.000	0.000	0.018	29.2	18.8	---	0.64
J	0.000	0.000	0.000	0.013	23.9	16.9	---	0.71
J	0.000	0.000	0.000	0.020	38.0	28.9	---	0.76
J	0.000	0.000	0.000	0.039	131.0	118.0	---	0.90
J	0.000	0.000	0.000	0.039	136.0	120.0	---	0.88
J	0.000	0.000	0.000	0.039	137.0	121.0	---	0.88
J	0.000	0.000	0.000	0.037	136.0	118.0	---	0.87
J	0.000	0.000	0.000	0.061	229.0	217.0	---	0.95
J	0.000	0.000	0.000	0.062	256.0	227.0	---	0.89

TABLE A-3 (CONT'D)

CUTTER	A_w (in ²)	w (in)	L (in)	δ (in)	F (lb)	F_d (lb)	F/A_w (psi)	F_d / F
D	0.020	0.320	0.100	0.023	545.0	360.0	27250.	0.66
D	0.020	0.320	0.100	0.023	568.0	387.0	28400.	0.68
D	0.020	0.320	0.100	0.023	599.0	392.0	29950.	0.65
D	0.020	0.320	0.100	0.023	590.0	396.0	29500.	0.67
D	0.020	0.320	0.100	0.024	610.0	401.0	30500.	0.66
D	0.020	0.320	0.100	0.024	617.0	412.0	30850.	0.67
D	0.020	0.320	0.100	0.024	640.0	418.0	32000.	0.65
D	0.020	0.320	0.100	0.024	619.0	416.0	30950.	0.67
D	0.020	0.320	0.100	0.039	657.0	461.0	32850.	0.70
D	0.020	0.320	0.100	0.040	689.0	475.0	34450.	0.69
D	0.020	0.320	0.100	0.041	669.0	466.0	33450.	0.70
D	0.020	0.320	0.100	0.041	676.0	473.0	33800.	0.70
D	0.020	0.320	0.100	0.041	698.0	481.0	34900.	0.69
D	0.020	0.320	0.100	0.040	699.0	476.0	34950.	0.68
D	0.020	0.320	0.100	0.040	756.0	517.0	37800.	0.68
D	0.020	0.320	0.100	0.042	770.0	511.0	38500.	0.66
D	0.020	0.320	0.100	0.042	770.0	540.0	38500.	0.70
D	0.020	0.320	0.100	0.042	739.0	518.0	36950.	0.70
D	0.020	0.320	0.100	0.042	763.0	526.0	38150.	0.69
D	0.020	0.320	0.100	0.042	741.0	504.0	37050.	0.68
D	0.020	0.320	0.100	0.042	774.0	522.0	38700.	0.67
D	0.020	0.320	0.100	0.042	760.0	519.0	38000.	0.68
D	0.020	0.320	0.100	0.079	855.0	694.0	42750.	0.81
D	0.020	0.320	0.100	0.080	875.0	710.0	43750.	0.81
D	0.020	0.320	0.100	0.079	865.0	694.0	43250.	0.80
D	0.020	0.320	0.100	0.079	926.0	722.0	46300.	0.78
D	0.020	0.320	0.100	0.079	918.0	750.0	45900.	0.82

TABLE A-4

DRY, NON-INTERACTING CUT TEST DATA FOR TENNESSEE MARBLE

CUTTER	A_w (in ²)	w (in)	L (in)	δ (in)	F (lb)	F_d (lb)	F/A_w (psi)	F_d / F
F	0.030	0.300	0.140	0.010	448.2	324.3	14940.	0.72
F	0.030	0.300	0.140	0.010	455.2	322.6	15173.	0.71
F	0.030	0.300	0.140	0.010	442.1	318.0	14737.	0.72
F	0.030	0.300	0.140	0.010	457.1	332.7	15237.	0.73
F	0.030	0.300	0.140	0.010	474.4	350.0	15813.	0.74
F	0.030	0.300	0.140	0.010	527.9	360.6	17597.	0.68
F	0.030	0.300	0.140	0.010	583.0	360.3	19433.	0.62
F	0.030	0.300	0.140	0.010	461.2	336.8	15373.	0.73
F	0.030	0.300	0.140	0.010	447.7	325.0	14923.	0.73
F	0.030	0.300	0.140	0.010	460.1	328.6	15337.	0.71
F	0.030	0.300	0.140	0.010	501.1	354.7	16703.	0.71
F	0.030	0.300	0.140	0.010	509.9	351.2	16997.	0.69
F	0.030	0.300	0.140	0.020	809.6	464.8	26987.	0.57
F	0.030	0.300	0.140	0.020	751.8	459.8	25060.	0.61
F	0.030	0.300	0.140	0.020	768.4	457.0	25613.	0.59
F	0.030	0.300	0.140	0.020	724.8	472.1	24160.	0.65
F	0.030	0.300	0.140	0.020	740.5	474.1	24683.	0.64
F	0.030	0.300	0.140	0.020	758.2	467.9	25273.	0.62
F	0.030	0.300	0.140	0.020	734.6	461.1	24487.	0.63
F	0.030	0.300	0.140	0.020	706.6	449.1	23553.	0.64
F	0.030	0.300	0.140	0.020	723.2	459.0	24107.	0.63
F	0.030	0.300	0.140	0.020	727.0	451.4	24233.	0.62
F	0.030	0.300	0.140	0.020	707.6	431.2	23587.	0.61
F	0.030	0.300	0.140	0.019	761.4	463.8	25380.	0.61
F	0.030	0.300	0.140	0.020	798.3	446.8	26610.	0.56
F	0.030	0.300	0.140	0.018	777.1	452.4	25903.	0.58
F	0.030	0.300	0.140	0.020	673.5	427.3	22450.	0.63
F	0.030	0.300	0.140	0.038	842.0	596.0	28067.	0.71
F	0.030	0.300	0.140	0.037	836.8	574.7	27893.	0.69
F	0.030	0.300	0.140	0.039	854.9	587.4	28497.	0.69
F	0.030	0.300	0.140	0.039	854.3	584.3	28477.	0.68
F	0.030	0.300	0.140	0.038	916.0	574.8	30533.	0.63
F	0.030	0.300	0.140	0.038	865.2	523.5	28840.	0.61
F	0.030	0.300	0.140	0.040	992.2	589.1	33073.	0.59
F	0.030	0.300	0.140	0.039	978.0	573.9	32600.	0.59
F	0.030	0.300	0.140	0.039	1060.7	605.9	35357.	0.57
F	0.030	0.300	0.140	0.039	1060.8	596.3	35360.	0.56
F	0.030	0.300	0.140	0.040	956.2	528.2	31873.	0.55
F	0.030	0.300	0.140	0.040	1143.4	714.2	38113.	0.62
F	0.030	0.300	0.140	0.037	948.8	615.3	31627.	0.65
F	0.030	0.300	0.140	0.040	1025.3	575.9	34177.	0.56

TABLE A-4 (CONT'D)

CUTTER	A_w (in ²)	w (in)	L (in)	δ (in)	F (lb)	F_d (lb)	F/A_w (psi)	F_d / F
F	0.030	0.300	0.140	0.040	996.8	572.7	33227.	0.57
F	0.030	0.300	0.140	0.040	1021.5	557.2	34050.	0.55
F	0.030	0.300	0.140	0.040	1078.9	584.4	35963.	0.54
F	0.030	0.300	0.140	0.040	1106.0	573.0	36867.	0.52
F	0.030	0.300	0.140	0.040	1078.6	578.7	35953.	0.54
F	0.030	0.300	0.140	0.058	1278.6	770.4	42620.	0.60
F	0.030	0.300	0.140	0.060	1107.7	663.1	36923.	0.60
F	0.030	0.300	0.140	0.059	1114.2	683.4	37140.	0.61
F	0.030	0.300	0.140	0.059	1131.7	631.1	37723.	0.56
F	0.030	0.300	0.140	0.060	1174.9	689.6	39163.	0.59
F	0.030	0.300	0.140	0.059	1240.8	738.5	41360.	0.60
F	0.030	0.300	0.140	0.059	1160.3	710.9	38677.	0.61
F	0.030	0.300	0.140	0.060	1202.7	706.5	40090.	0.59
F	0.030	0.300	0.140	0.060	1177.3	704.9	39243.	0.60
F	0.030	0.300	0.140	0.062	1136.2	694.0	37873.	0.61
F	0.030	0.300	0.140	0.059	1300.1	729.7	43337.	0.56
F	0.030	0.300	0.140	0.060	1177.1	694.8	39237.	0.59
F	0.030	0.300	0.140	0.060	1173.4	669.6	39113.	0.57
F	0.030	0.300	0.140	0.060	1200.9	659.6	40030.	0.55
F	0.030	0.300	0.140	0.060	1132.6	630.5	37753.	0.56
F	0.030	0.300	0.140	0.060	1289.4	701.7	42980.	0.54
F	0.030	0.300	0.140	0.060	1336.4	712.9	44547.	0.53
F	0.030	0.300	0.140	0.078	1314.1	822.1	43803.	0.63
F	0.030	0.300	0.140	0.078	1384.3	860.9	46143.	0.62
F	0.030	0.300	0.140	0.077	1156.1	693.2	38537.	0.60
F	0.030	0.300	0.140	0.079	1388.8	862.6	46293.	0.62
F	0.030	0.300	0.140	0.078	1152.4	778.8	38413.	0.68
F	0.030	0.300	0.140	0.078	1420.8	860.4	47360.	0.61
F	0.030	0.300	0.140	0.080	1332.1	812.0	44403.	0.61
F	0.030	0.300	0.140	0.081	1427.6	820.3	47587.	0.57
F	0.030	0.300	0.140	0.080	1138.6	700.0	37953.	0.61
F	0.030	0.300	0.140	0.097	1428.6	980.9	47620.	0.69
F	0.030	0.300	0.140	0.100	1186.0	800.0	39533.	0.67
F	0.030	0.300	0.140	0.100	1259.0	799.9	41967.	0.64
F	0.030	0.300	0.140	0.100	1566.3	984.7	52210.	0.63
F	0.030	0.300	0.140	0.096	1357.7	882.4	45257.	0.65
F	0.030	0.300	0.140	0.100	1341.0	843.2	44700.	0.63
F	0.030	0.300	0.140	0.096	1721.5	1050.9	57383.	0.61
F	0.030	0.300	0.140	0.095	1527.5	923.8	50917.	0.60
F	0.030	0.300	0.140	0.100	1147.4	670.2	38247.	0.58

TABLE A-5

WATERJET-ASSISTED, NON-INTERACTING CUT TEST DATA FOR SIERRA WHITE GRANITE

CUTTER	A_w (in ²)	w (in)	L (in)	δ (in)	F (lb)	F_d (lb)	F/A_w (psi)	F_d/F
NOZZLE PRESSURE DROP - 80 PSI								
H	0.029	0.340	0.120	0.020	846.0	378.0	29172.	0.45
H	0.029	0.340	0.120	0.020	887.0	399.0	30586.	0.45
H	0.029	0.340	0.120	0.020	781.0	341.0	26931.	0.44
H	0.029	0.340	0.120	0.020	744.0	331.0	25655.	0.44
H	0.029	0.340	0.120	0.020	730.0	322.0	25172.	0.44
H	0.029	0.340	0.120	0.020	694.0	314.0	23931.	0.45
H	0.029	0.340	0.120	0.040	958.0	545.0	33034.	0.57
H	0.029	0.340	0.120	0.040	968.0	548.0	33379.	0.57
H	0.029	0.340	0.120	0.040	940.0	533.0	32414.	0.57
H	0.029	0.340	0.120	0.040	925.0	496.0	31897.	0.54
H	0.029	0.340	0.120	0.040	942.0	486.0	32483.	0.52
H	0.029	0.340	0.120	0.040	943.0	517.0	32517.	0.55
NOZZLE PRESSURE DROP - 2000 PSI								
H	0.029	0.340	0.120	0.020	755.0	341.0	26034.	0.45
H	0.029	0.340	0.120	0.020	698.0	314.0	24069.	0.45
H	0.029	0.340	0.120	0.020	687.0	310.0	23690.	0.45
H	0.029	0.340	0.120	0.040	854.0	449.0	29448.	0.53
H	0.029	0.340	0.120	0.040	878.0	461.0	30276.	0.53
H	0.029	0.340	0.120	0.040	835.0	447.0	28793.	0.54
NOZZLE PRESSURE DROP - 4500 PSI								
H	0.029	0.340	0.120	0.020	280.0	151.0	9655.	0.54
H	0.029	0.340	0.120	0.020	211.0	120.0	7276.	0.57
H	0.029	0.340	0.120	0.020	251.0	142.0	8655.	0.57
H	0.029	0.340	0.120	0.040	505.0	271.0	17414.	0.54
H	0.029	0.340	0.120	0.040	461.0	260.0	15897.	0.56
H	0.029	0.340	0.120	0.040	443.0	247.0	15276.	0.56

TABLE A-6

DRY, INTERACTING CUT TEST DATA FOR BEREA SANDSTONE

CUTTER	A_w (in ²)	w (in)	L (in)	d (in)	F (lb)	F_d (lb)	F/A_w (psi)	F_d / F
I	0.040	0.320	0.180	0.150 **	223.0	205.9	5575.	0.92
I	0.040	0.320	0.180	0.200 **	263.8	238.1	6595.	0.90
I	0.040	0.320	0.180	0.200 **	260.9	239.1	6523.	0.92
I	0.040	0.320	0.180	0.300 **	265.7	247.6	6643.	0.93
I	0.040	0.320	0.180	0.400 **	356.7	335.9	8918.	0.94
I	0.040	0.320	0.180	0.400 **	273.3	260.0	6833.	0.95
I	0.040	0.320	0.180	0.450 **	362.4	338.7	9060.	0.93
I	0.040	0.320	0.180	0.450 **	362.7	356.8	9068.	0.98
I	0.040	0.320	0.180	0.500 **	365.3	346.3	9133.	0.95
I	0.040	0.320	0.180	0.500 **	373.8	352.0	9345.	0.94
I	0.040	0.320	0.180	0.500 **	326.3	323.1	8158.	0.99
I	0.040	0.320	0.180	0.500 **	365.2	365.3	9130.	1.00
I	0.040	0.320	0.180	0.500 **	373.4	371.4	9335.	0.99
I	0.040	0.320	0.180	0.600 **	366.4	375.5	9160.	1.02
I	0.040	0.320	0.180	0.050 *	273.3	259.0	6833.	0.95
I	0.040	0.320	0.180	0.100 *	290.3	271.4	7258.	0.93
I	0.040	0.320	0.180	0.150 *	278.0	258.1	6950.	0.93
I	0.040	0.320	0.180	0.200 *	280.8	270.4	7020.	0.96
I	0.040	0.320	0.180	0.250 *	322.6	306.5	8065.	0.95
I	0.040	0.320	0.180	0.300 *	319.7	306.5	7993.	0.96
I	0.040	0.320	0.180	0.300 *	335.9	311.2	8398.	0.93
I	0.040	0.320	0.180	0.350 *	335.9	319.7	8398.	0.95
I	0.040	0.320	0.180	0.400 *	377.6	362.4	9440.	0.96
I	0.040	0.320	0.180	0.500 *	376.7	357.7	9418.	0.95
I	0.040	0.320	0.180	1.000 *	355.9	365.8	8898.	1.03
I	0.040	0.320	0.180	1.000 *	379.5	400.0	9488.	1.05
I	0.040	0.320	0.180	1.000 *	379.5	400.0	9488.	1.05
I	0.040	0.320	0.180	1.000 *	319.9	326.1	7998.	1.02
I	0.040	0.320	0.180	1.000 *	352.7	363.3	8818.	1.03
I	0.040	0.320	0.180	1.200 *	350.8	383.2	8770.	1.09

** Symmetric cutter interaction (two previous adjacent cuts)

* Asymmetric cutter interaction (one previous adjacent cut)

$\delta = 0.080$ inch and $\delta_1 = 0.040$ inch in all cuts (See Figure 9.)

TABLE A-7

DRY, INTERACTING CUT TEST DATA FOR SIERRA WHITE GRANITE

CUTTER	A _w (in ²)	w (in)	L (in)	d (in)	F (lb)	F _d (lb)	F/A _w (psi)	F _d / F
F	0.036	0.310	0.165	0.150 **	1246.7	801.0	34631.	0.64
F	0.036	0.310	0.165	0.200 **	1370.1	887.0	38058.	0.65
F	0.036	0.310	0.165	0.250 **	1381.5	912.0	38375.	0.66
F	0.036	0.310	0.165	0.300 **	1600.6	1020.0	44461.	0.64
F	0.036	0.310	0.165	0.400 **	1557.0	991.0	43250.	0.64
F	0.036	0.310	0.165	0.450 **	1507.6	1005.0	41878.	0.67
F	0.040	0.320	0.180	0.500 **	1740.1	1101.6	43503.	0.63
F	0.037	0.315	0.170	0.500 **	1590.8	1070.6	42995.	0.67
F	0.037	0.315	0.170	0.600 **	1541.5	1041.7	41662.	0.68
F	0.038	0.315	0.170	0.600 **	1569.2	1075.4	41295.	0.69
F	0.034	0.310	0.160	0.050 *	1340.7	822.0	39432.	0.61
F	0.034	0.310	0.160	0.050 *	1210.7	808.0	35609.	0.67
F	0.034	0.310	0.160	0.100 *	1262.9	855.0	37144.	0.68
F	0.034	0.310	0.160	0.150 *	1302.7	850.0	38315.	0.65
F	0.034	0.310	0.160	0.200 *	1483.9	994.0	43644.	0.67
F	0.034	0.310	0.160	0.250 *	1390.9	920.0	40909.	0.66
F	0.034	0.310	0.160	0.300 *	1387.1	928.0	40797.	0.67
F	0.034	0.310	0.160	0.400 *	1480.1	1010.0	43532.	0.68
F	0.038	0.315	0.170	0.800 *	1565.5	1050.0	41197.	0.67
F	0.037	0.315	0.170	0.800 *	1633.1	1083.1	44138.	0.66
F	0.037	0.315	0.170	1.000 *	1690.4	1147.1	45686.	0.68
F	0.037	0.315	0.170	1.000 *	1585.9	1068.1	42862.	0.67
F	0.037	0.315	0.170	1.200 *	1561.5	1054.5	42203.	0.68
F	0.037	0.315	0.170	1.250 *	1567.4	1053.0	42362.	0.67
F	0.037	0.315	0.170	1.250 *	1671.4	1140.2	45173.	0.68

** Symmetric cutter interaction (two previous adjacent cuts)

* Asymmetric cutter interaction (one previous adjacent cut)

$\delta = 0.080$ inch and $\delta_1 = 0.040$ inch in all cuts (See Figure 9.)

APPENDIX B
LISTING OF FORTRAN PROGRAM
PDCWEAR

```

PROGRAM PDCWEAR
C *****
C ISSUED BY SANDIA NATIONAL LABORATORIES
C A PRIME CONTRACTOR TO THE
C UNITED STATES DEPARTMENT OF ENERGY
C *****
C THIS CODE WAS PREPARED IN THE COURSE OF WORK SPONSORED BY THE
C UNITED STATES GOVERNMENT. NEITHER THE UNITED STATES, NOR THE
C THE UNITED STATES DEPARTMENT OF ENERGY, NOR ANY OF THEIR EMPLOYEES,
C NOR ANY OF THEIR CONTRACTORS, SUBCONTRACTORS, OR THEIR EMPLOYEES,
C MAKES ANY WARRANTY, EXPRESS OR IMPLIED, OR ASSUMES ANY LEGAL
C LIABILITY OR RESPONSIBILITY FOR THE ACCURACY, COMPLETENESS, OR
C USEFULNESS OF ANY INFORMATION, APPARATUS, PRODUCT OR PROCESS
C DISCLOSED, OR REPRESENTS THAT ITS USE WOULD NOT INFRINGE PRIVATELY
C OWNED RIGHTS.
C *****
PARAMETER (MXCUT=48)
COMMON /AK/AK
COMMON /COMPOS/RP(MXCUT),AP(MXCUT),RR(MXCUT),HP(MXCUT),
1 BR(MXCUT),MORD(MXCUT),TNAI(MXCUT),AI(MXCUT),
2 HPP(MXCUT),HR(MXCUT),BNOM
COMMON /COMRWK/VR(MXCUT),AR(MXCUT),C3(MXCUT),D(MXCUT),
1 E(MXCUT),XMX(MXCUT),XMN(MXCUT),ZI(MXCUT),SRCX(MXCUT),WK(MXCUT)
COMMON /COMCHA/IDATE,ITIME,BDNAME,RSNAME,WINAME,OCNAME
CHARACTER *11 BDNAME,RSNAME,WINAME,OCNAME
CHARACTER *10 IDATE,ITIME
COMMON /COMIOD/IDTO,IDTI,IDBD,IPRNT,IDWI,IDOC,IDWN
COMMON /COMCON/NC,NRAY,HNOM,FEED,RNOM,EPS,PEDGCT
COMMON /FT/FT50(3,4),FT75(3,4),RL50(3),RL75(3),HL(4),
1 CV50,RV50,CA50,RA50,CV75,RV75,CA75,RA75
C ---- PROGRAM INITIALIZATION
AK=57.29577951
PEDGCT=0.02
CALL DATE(IDATE)
CALL TIME(ITIME)
C ---- OUTPUT DEVICE ASSIGNMENTS
IDTO=6
IDTI=5
IDWI=7
IDOC=8
IDBD=10
IPRNT=20
C ---- THERMAL RESPONSE FUNCTION NUMERICAL DATA
C FT50(I,J)=THERMAL RESPONSE FCT (CM**2-DEG C/W) FOR
C 0.5 INCH DIA. CUTTER AT ITH WEARFLAT LENGTH (RL50(I))
C AND JTH CONV. COOLING COEFF (HL(J)).
C FT75(I,J)=THERMAL RESPONSE FCT FOR 0.75 INCH DIA. CUTTER AT
C ITH WEARFLAT LENGTH (RL75(I)) AND JTH CONV. COOLING
C COEFF. (HL(J)).
RL50(1)=0.0266
RL50(2)=0.148
RL50(3)=0.545
RL75(1)=0.0266
RL75(2)=0.096
RL75(3)=0.148
HL(1)=17.61
HL(2)=176.1
HL(3)=1761.
HL(4)=17610.
FT50(1,1)=0.956
FT50(1,2)=0.170
FT50(1,3)=0.0643
FT50(1,4)=0.0267
FT50(2,1)=5.459
FT50(2,2)=0.896
FT50(2,3)=0.325
FT50(2,4)=0.166
FT50(3,1)=23.48
FT50(3,2)=3.223
FT50(3,3)=0.924
FT50(3,4)=0.540
FT75(1,1)=0.830
FT75(1,2)=0.174
FT75(1,3)=0.0666
FT75(1,4)=0.0263
FT75(2,1)=3.003
FT75(2,2)=0.609
FT75(2,3)=0.234
FT75(2,4)=0.106
FT75(3,1)=4.653
FT75(3,2)=0.913
FT75(3,3)=0.345
FT75(3,4)=0.166

```

```

C ----  CONSTANTS AND EXPONENTS IN WEARFLAT LENGTH VS. WEAR VOLUME
C      AND LENGTH VS. AREA CORRELATIONSa
      CV50=2.94
      RV50=0.40
      CA50=1.59
      RA50=0.68
      CV75=2.72
      RV75=0.40
      CA75=1.38
      RA75=0.68
      WRITE(IDTO,100)
100  FORMAT(' =====//
      1          PROGRAM PDCWEAR'///
      2          PRODUCED BY'/
      3          SANDIA NATIONAL LABORATORIES'/
      4          GEOTHERMAL TECHNOLOGY DEVELOPMENT DIVISION'/
      5          ALBUQUERQUE, NEW MEXICO'//
      6          JUNE 1987'//
      7          ====='//)
      RSNAME=' '
      BDNAME=' '
      WINAME=' '
      OCNAME=' '
      WNNAME=' '
      CALL DRIVER
      END
      SUBROUTINE DRIVER
C ----  THIS SUBROUTINE PERFORMS THE FOLLOWING FUNCTIONS:
C      1) ALLOWS USER TO SPECIFY OUTPUT FILE NAMES
C      2) CALLS INPUT, WHICH READS INPUT DATA FROM FILEC
C      3) SETS UP LOOP TO RUN PROGRAM FOR 5 DIFFERENT ROP'S
C      4) SETS UP LOOP IN PROGRAM TO ITERATE ON CUTTER WEAR ANGLES
C      5) CALLS VACMP, WHICH PERFORMS GEOMETRY CALCULATIONS
C      6) CALLS DATPRI, WHICH PRINTS RESULTS
      PARAMETER (MXCUT=48)
      COMMON /AK/AK
      COMMON /CTWEAR/AWMAX,NCMAX,ASUBWN,MODW,WRA(MXCUT),
1     FAMAX,XBCAMAX,DLH,C6
      COMMON /COMPOS/RP(MXCUT),AP(MXCUT),RR(MXCUT),HP(MXCUT),
1     BR(MXCUT),MORD(MXCUT),TNAI(MXCUT),AI(MXCUT),
2     HPP(MXCUT),HR(MXCUT),BNOM
      PARAMETER (MINRAY=20)
      REAL*8 N1A,N2A,N1B,N2B
      COMMON /COMCON/NC,NRAY,HNOM,FEED,RNOM,EPS,PEDGCT
      COMMON /COMCHA/IDATE,ITIME,BDNAME,RSNAME,WINAME,OCNAME
      CHARACTER *11 BDNAME,RSNAME,WINAME,OCNAME,WNNAME
      CHARACTER *10 IDATE,ITIME
      CHARACTER *20 ROCK
      COMMON /COMIOD/IDTO,IDTI,IDBD,IPRNT,IDWI,IDOC,IDWN
      COMMON /RESULTS/XW1(MXCUT),XW2(MXCUT),WL(MXCUT),
1     YOWORN(MXCUT),ITRAC,ZB(MXCUT),DE(MXCUT),NDE(MXCUT),
2     FP(MXCUT),WOB(5),BMX(5),BMY(5),FR(MXCUT),FV(MXCUT),FX(5),
3     FY(5),TORQ(5),TW(MXCUT),WR(MXCUT),FD(MXCUT),
4     WW(MXCUT),AW(MXCUT),IW1,XC1(MXCUT),XC2(MXCUT),ZC1(MXCUT),
5     ZC2(MXCUT),WA(MXCUT),WAO(MXCUT),ZW1(MXCUT),ZW2(MXCUT),
6     TWMAX(5),WRMAX(5),FWNP(MXCUT),ZBC(MXCUT),XBC(MXCUT),IT1,
7     IC1,IC2,IC3,IC4,IC5,IC6,BF1,BF2,BF3,BF4,BF5,ITYP(MXCUT),IP1,IP2
      COMMON /ROCKDAT/ROCK,RK,RX,FC,DC,DCS,C1A,N1A,C1B,
2     N1B,C2A,N2A,C2B,N2B,TFL,RPM,ROP(5),NROP,IR
      DIMENSION FVL(MXCUT),FRL(MXCUT)
      DIMENSION IWK(MXCUT)
      CHARACTER *1 AIN
C      TRACER "ON" TURNS ON MANY "WRITE" STATEMENTS--USED FOR
C      DEBUGGING
C      TYPE *, 'TURN TRACER ON (Y=1, N=2)'
C      READ(5,4)ITRAC
C4     FORMAT(I1)
      ITRAC=2
      IF(ITRAC.EQ.1)THEN
        OPEN(UNIT=3,NAME='DIAG.DAT',TYPE='NEW')
      ENDIF
C ----  READ INPUT DATA
      CALL INPUT
27     WRITE(IDTO,104)
104    FORMAT('/ DO YOU WISH TO TERMINATE THIS SESSION? (Y,N)')
      CALL READA(M,AIN)
      IF(M.EQ.1.OR.(AIN.NE.'Y'.AND.AIN.NE.'N'))GOTO 27
      IF(AIN.EQ.'Y') CALL STOPP
C ----  NAME OUTPUT DISK FILE
28     WRITE(IDTO,106)
106    FORMAT('/ ENTER NAME OF OUTPUT DISK FILE FOR STORING'
1     ' COMPUTED RESULTS'/
2     '(11 CHAR. OR LESS, INCLUDING .EXTENSION):')

```

```

      READ(IDTI,'(A11)',END=29) RSNAME
      IF(RSNAME.EQ.' ')GO TO 29
      IF(RSNAME.EQ.BDNAME) THEN
        WRITE(IDTO,107)
107   FORMAT(' SAME NAME AS INPUT DATA FILE - NOT ALLOWED')
        GO TO 29
      ENDIF
      IF(RSNAME.EQ.WINAME) THEN
        WRITE(IDTO,108)
108   FORMAT(' SAME NAME AS INITIAL WEAR DATA FILE'
1     ' - NOT ALLOWED')
        GO TO 29
      ENDIF
      IF(RSNAME.EQ.OCNAME) THEN
        WRITE(IDTO,111)
111   FORMAT(' SAME NAME AS OPERATING PARAMETER DATA FILE'
1     ' - NOT ALLOWED')
        GO TO 29
      ENDIF
C ---- OPEN PRINT FILE AND PRINT INPUT DATA
      OPEN(IPRNT,FILE=RSNAME,STATUS='NEW')
      REWIND IPRNT
34   CALL DATPRI(2)
C ---- SET RELATIVE CUTTER RADII, BACKRAKE ANGLE, AND CONV.
C ---- COOLING COEFF. TO ACTUAL VALUES; TRANSPOSE AP AND
C ---- DETERMINE CUTTING ORDER
      DO 38 J=1,NC
      BR(J)=BNOM*BR(J)
      RR(J)=RNOM*RR(J)
      HR(J)=HNOM*HR(J)
      ITYP(J)=1
      IF(HR(J).LT.0.)THEN
        ITYP(J)=2
        HR(J)=-HR(J)
      ENDIF
      AP(J)=360.-AP(J)
      IWK(J)=J
38   TNAI(J)=AP(J)
      CALL RISORT(TNAI,IWK,NC)
      DO 37 J=1,NC
      I=IWK(J)
      MORD(I)=J
37   TNAI(J)=TAN(AI(J)/AK)
C ---- ENTER NRAY
10   WRITE(IDTO,102)
102  FORMAT(' ENTER NRAY')
      CALL READI(M,NRAY)
      IF(M.EQ.1.OR.NRAY.LE.0)GO TO 10
      IC1=0
      IC2=0
      IC3=0
      IC4=0
      IC5=0
      IC6=0
      IB1=0
      IB2=0
      IB3=0
      IB4=0
      IB5=0
      NNW=0
      IT1=0
      IT2=0
      IP1=0
      IP2=0
      IGAP=0
C ---- SET UP LOOP TO RUN PROGRAM FIVE TIMES FOR DIFFERENT
C ---- PENETRATION RATES
800  DO 700 IR=1,NROP
      IW1=0
      FEED=ROP(IR)/RPM/5.
C ---- SET CUTTING HEIGHT AND INITIALIZE RAD. WEAR ANGLES
      DO 40 J=1,NC
      HP(J)=HPP(J)+FEED*AP(J)/360.
      WAO(J)=AI(J)
      FVL(J)=0.
      FRL(J)=0.
40   CONTINUE
C ---- ITERATE ON RADIAL WEAR ANGLES
26   IF(IW1.NE.0)THEN
      IW2=0
      DFRMAX=0.
      DFVMAX=0.
      DO 450 J=1,NC

```

```

IF(FVL(J).EQ.0.)THEN
  IF(IW1.EQ.1)IW2=1
  GO TO 407
ENDIF
DFV=ABS(FV(J)-FVL(J))/FVL(J)*100.
IF(FRL(J).EQ.0.)GO TO 406
DFR=ABS(FR(J)-FRL(J))/FRL(J)*100.
IF(DFR.GT.0.01)IW2=1
406 IF(DFV.GT.0.01)IW2=1
407 FVL(J)=FV(J)
  FRL(J)=FR(J)
  IF(DFR.GT.DFRMAX)DFRMAX=DFR
  IF(DFV.GT.DFVMAX)DFVMAX=DFV
450 CONTINUE
  IF(IW2.EQ.0)GO TO 690
  IF(IW1.GT.30)THEN
    WRITE(5,412)(J,WAO(J),WA(J),J=1,NC)
412 FORMAT(// ' CUTTER OLD WA (DEG.) NEW WA (DEG.)' //
1 (2X,I3,8X,F7.3,9X,F7.3))
411 WRITE(5,410)DFVMAX,DFRMAX
410 FORMAT(/10X,'DFVMAX=',E12.4,' DFRMAX=',E12.4//
1 ' WARNING: RADIAL WEAR ANGLE ALGORITHM DID NOT' //
2 ' CONVERGE AFTER 30 ITERATIONS. CALCULATIONS MAY' //
3 ' CONTINUE, BUT WEAR ANGLE VALUE IS UNCERTAIN.' //
4 ' DO YOU WANT TO CONTINUE? (Y/N)')
    WRITE(IPRNT,462)(J,WAO(J),WA(J),J=1,NC)
462 FORMAT('1'// ' CUTTER OLD WA (DEG.) NEW WA (DEG.)' //
1 (2X,I3,8X,F7.3,9X,F7.3))
    WRITE(IPRNT,463)DFVMAX,DFRMAX
463 FORMAT(/10X,'DFVMAX=',E12.4,' DFRMAX=',E12.4//
1 ' WARNING: RADIAL WEAR ANGLE ALGORITHM DID NOT' //
2 ' CONVERGE AFTER 20 ITERATIONS. CALCULATIONS MAY' //
3 ' CONTINUE, BUT WEAR ANGLE VALUE IS UNCERTAIN.')
    CALL READA(M,AIN)
    IF(M.EQ.1.OR.(AIN.NE.'Y'.AND.AIN.NE.'N'))GOTO 411
    IF(AIN.EQ.'N') CALL STOPP
    GO TO 690
  ENDIF
492 REPF=1.
  IF(IW1.EQ.2.OR.IW1.EQ.3)REPF=.5
  IF(IW1.GE.15)REPF=.5
  DO 550 J=1,NC
    WAO(J)=WAO(J)+(WA(J)-WAO(J))*REPF
550 CONTINUE
  ENDIF
600 LGAP=0
  IW1=IW1+1
  IT1=0
C ---- COMPUTE VOLUMES, AREAS, EFFECTIVE DEPTHS OF CUT, FORCES,
C TEMPERATURES, WEAR RATIOS, AND RADIAL WEAR ANGLES
  CALL VACMP(LGAP)
C ---- TEST FOR GAPS (UNCUT ROCK) BETWEEN CUTTERS
  IF(LGAP.LE.0)GO TO 14
  IF(IGAP.EQ.1)GO TO 14
  WRITE(IDTO,101)LGAP
  WRITE(IPRNT,101)LGAP
101 FORMAT('/ AT LEAST ONE GAP (UNCUT ROCK) NEAR CUTTER ',I3/)
640 WRITE(IDTO,650)
650 FORMAT(' BIT MAY NOT DRILL IN THIS CONFIGURATION.' /
1 ' DO YOU WISH TO CONTINUE? (Y/N)')
  CALL READA(M,AIN)
  IF(M.EQ.1.OR.(AIN.NE.'Y'.AND.AIN.NE.'N'))GO TO 640
  IF(AIN.EQ.'N')CALL STOPP
  IGAP=1
C ---- LOOP BACK TO ITERATE ON WEAR ANGLES
14 GO TO 26
C ---- PRINT COMPUTED RESULTS
690 CALL DATPRI(3)
  CALL DATPRI(4)
  IF(IR.EQ.3)THEN
    AWMAX=0.
    DO 70 J=1,NC
      WRA(J)=WR(J)
      IF(AW(J).GE.AWMAX)THEN
        AWMAX=AW(J)
      NCMAX=J
    ENDIF
70 CONTINUE
    FAMAX=FP(NCMAX)
    XBCAMAX=XBC(NCMAX)
  ENDIF
  IF(IT1.EQ.-1)IT2=-1
700 CONTINUE

```

```

CALL DATPRI(7)
IF(IT2.EQ.-1)THEN
WRITE(IDTO,820)
820  FORMAT(' AT LEAST ONE CUTTER EXPERIENCES THERMALLY-'
1 'ACCELERATED WEAR'/' AT ONE OR MORE OF THE SPECIFIED '
2 'PENETRATION RATES.'/' ADVANCED WEAR CALCULATIONS FOR '
3 'THOSE CUTTERS WILL NOT BE ACCURATE.')
IT2=0
WRITE(IPRNT,822)
822  FORMAT(LX,////)
WRITE(IPRNT,820)
ENDIF
805  WRITE(IDTO,810)
810  FORMAT('/' DO YOU WISH TO REPEAT THE CALCULATIONS'
1 ' WITH MORE ADVANCED CUTTER WEAR ? (Y/N)')
CALL READA(M,AIN)
IF(M.EQ.1.OR.(AIN.NE.'Y'.AND.AIN.NE.'N'))GO TO 805
IF(AIN.EQ.'Y')THEN
CALL CUTWEAR
929  WRITE(IDTO,906)
906  FORMAT(' ENTER NAME OF OUTPUT DISK FILE'
1 ' FOR STORING NEW WEAR CONFIGURATION' /
2 ' (11 CHAR. OR LESS, INCLUDING .EXTENSION):')
READ(IDTI,'(A11)',END=929) WNNAME
IF(WNNAME.EQ.' ')GO TO 929
IF(WNNAME.EQ.BDNAME) THEN
WRITE(IDTO,907)
907  FORMAT(' SAME NAME AS INPUT DATA FILE - NOT ALLOWED')
GO TO 929
ENDIF
IF(WNNAME.EQ.WINAME) THEN
WRITE(IDTO,908)
908  FORMAT(' SAME NAME AS PREVIOUS WEAR DATA FILE'
1 ' - NOT ALLOWED')
GO TO 929
ENDIF
IF(WNNAME.EQ.OCNAME)THEN
WRITE(IDTO,911)
911  FORMAT(' SAME NAME AS OPERATING PARAMETER DATA FILE'
1 ' - NOT ALLOWED')
GO TO 929
ENDIF
IF(WNNAME.EQ.RSNAME)THEN
WRITE(IDTO,912)
912  FORMAT(' SAME NAME AS OUTPUT DISK FILE FOR RESULTS'
1 ' - NOT ALLOWED')
GO TO 929
ENDIF
WINAME=WNNAME
NNW=NNW+1
IDWN=NNW+30
OPEN(IDWN,FILE=WINAME,STATUS='NEW')
CALL DATPRI(9)
CLOSE(IDWN)
210  WRITE(IDTO,220)
220  FORMAT('/' DO YOU WISH TO PROCEED WITH THIS'
1 ' CONFIGURATION? (Y/N) ')
CALL READA(M,AIN)
IF(M.EQ.1.OR.(AIN.NE.'Y'.AND.AIN.NE.'N'))GOTO 210
IF(AIN.EQ.'N') CALL STOPP
GO TO 800
ENDIF
CALL STOPP
END
SUBROUTINE VACMP(LGAP)
C ---- COMPUTES VOLUMES, AREAS, EFFECTIVE DEPTHS OF CUT,
C FORCES AND MOMENTS, WEARFLAT TEMPERATURES, WEAR RATIOS,
C AND WEAR ANGLES
PARAMETER (MXCUT=48)
REAL*8 N1A,N2A,N1B,N2B
COMMON /AK/AK
COMMON /CTWEAR/AWMAX,NCMAX,ASUBWN,MODW,WRA(MXCUT),
1 FAMAX,XBCAMAX,DLH,C6
CHARACTER *20 ROCK
COMMON /COMIOD/IDTO, IDTI, IDBD, IPRNT, IDWI, IDOC, IDWN
COMMON /COMPOS/RP(MXCUT), AP(MXCUT), RR(MXCUT), HP(MXCUT),
1 BR(MXCUT), MORD(MXCUT), TNAI(MXCUT), AI(MXCUT),
2 HPP(MXCUT), HR(MXCUT), BNOM
COMMON /COMRWK/VR(MXCUT), AR(MXCUT), C3(MXCUT), D(MXCUT),
1 E(MXCUT), XMX(MXCUT), XMN(MXCUT), ZI(MXCUT), SRCX(MXCUT), WK(MXCUT)
COMMON /COMCON/NC, NRAY, HNOM, FEED, RNOM, EPS, PEDGCT
COMMON /RESULTS/XW1(MXCUT), XW2(MXCUT), WL(MXCUT),
1 YOWORN(MXCUT), ITRAC, ZB(MXCUT), DE(MXCUT), NDE(MXCUT),

```

```

2 FP(MXCUT),WOB(5),BMX(5),BMY(5),FR(MXCUT),FV(MXCUT),FX(5),
3 FY(5),TORQ(5),TW(MXCUT),WR(MXCUT),FD(MXCUT),
4 WW(MXCUT),AW(MXCUT),IW1,XC1(MXCUT),XC2(MXCUT),ZC1(MXCUT),
5 ZC2(MXCUT),WA(MXCUT),WAO(MXCUT),ZW1(MXCUT),ZW2(MXCUT),
6 TWMAX(5),WRMAX(5),PWNP(MXCUT),ZBC(MXCUT),XBC(MXCUT),IT1,
7 IC1,IC2,IC3,IC4,IC5,IC6,BF1,BF2,BF3,BF4,BF5,ITYP(MXCUT),IP1,IP2
COMMON /ROCKDAT/ROCK,RK,RX,FC,DC,DCS,C1A,N1A,C1B,
2 N1B,C2A,N2A,C2B,N2B,TFL,RPM,ROP(5),NROP,IR
COMMON /FT/FT50(3,4),FT75(3,4),RL50(3),RL75(3),HL(4),
1 CV50,RV50,CA50,RA50,CV75,RV75,CA75,RA75
DIMENSION KT(MXCUT),KXM(MXCUT)
C ---- PEDGCT*RNOM/NRAY IS THE CLOSENESS OF RAY TO EDGE OF CUTTER
DTST=PEDGCT*RNOM/FLOAT(NRAY)
ZMIN=HP(1)-RR(1)
XMIN=RP(1)
XMAX=RP(1)
C ---- COMPUTE CUTTER COEFFICIENTS
TWMAX(IR)=0.
WRMAX(IR)=0.
DO 20 J=1,NC
KXM(J)=J
ZMIN=AMIN1(ZMIN,HP(J)-RR(J))
VR(J)=0.
AR(J)=0.
B=RR(J)*COS(BR(J)/AK)
CSAI=COS(ATAN(TNAI(J)))
SNAI=SIN(ATAN(TNAI(J)))
E(J)=(RR(J)*CSAI)**2+(B*SNAI)**2
D(J)=-CSAI*SNAI*(RR(J)**2-B**2)/(RR(J)*B)
C3(J)=(RR(J)*B)/E(J)
B=SQRT(E(J))-DTST
C ---- XMN(J) AND XMX(J) ARE LOWER AND UPPER LIMITS OF J-TH CUTTER
XMX(J)=RP(J)+B
XMN(J)=AMAX1(0.,RP(J)-B)
IF(ITRAC .EQ. 1)WRITE(3,309)J,XMN(J),XMX(J)
309 FORMAT(' XMN(',I3,')=',F10.5,' XMX(J)=',F10.5)
XMIN=AMIN1(XMIN,XMN(J))
XMAX=AMAX1(XMAX,XMX(J))
CSB=COS(BR(J)/AK)
PWNP(J)=AK*ATAN(TAN(WAO(J)/AK-ATAN(TNAI(J)))/CSB)
SNPWNP=SIN(PWNP(J)/AK)
CSPWNP=COS(PWNP(J)/AK)
RW=(RR(J)**2-(WW(J)/2. )**2)**.5
XBCNP=RW*SNPWNP
ZBCNP=RW*CSPWNP
ZBCN=ZBCNP*CSB
XBC(J)=RP(J)+XBCNP*CSAI+ZBCN*SNAI
ZBC(J)=HP(J)-XBCNP*SNAI+ZBCN*CSAI
XW1N=XBCNP-WW(J)/2.*CSPWNP
ZW1N=ZBCNP+WW(J)/2.*SNPWNP
ZW1N=ZW1N*CSB
XW2N=XBCNP+WW(J)/2.*CSPWNP
ZW2N=ZBCNP-WW(J)/2.*SNPWNP
ZW2N=ZW2N*CSB
XW1(J)=RP(J)+XW1N*CSAI+ZW1N*SNAI
ZW1(J)=HP(J)-XW1N*SNAI+ZW1N*CSAI
XW2(J)=RP(J)+XW2N*CSAI+ZW2N*SNAI
ZW2(J)=HP(J)-XW2N*SNAI+ZW2N*CSAI
DE(J)=0.
NDE(J)=0
XC1(J)=-100.
XC2(J)=-100.
ZC1(J)=-100.
ZC2(J)=-100.
20 CONTINUE
C ---- SET BOUNDS FOR COMPUTATION
ZMIN=ZMIN-10.*FEED
XMN(NC+1)=XMAX+RNOM
KXM(NC+1)=NC+1
C ---- COMPUTE RAY STEP SIZE
DX=RNOM/FLOAT(NRAY)
NX=INT((XMAX-XMIN)/DX+.5)
DX=(XMAX-XMIN)/FLOAT(NX)
X0=XMIN-.5*DX
CALL RISORT(XMN,KXM,NC+1)
K1=1
C ---- LOOP TO COMPUTE Z-VALUES FOR EACH ELEMENT DX
DO 40 NNX=1,NX
X=X0+NNX*DX
XVOL=6.2831853072*X*DX
ZM=ZMIN
LS=0
C ---- FIND CUTTER INTERSECTIONS WITH RAY NORMAL TO X-AXIS

```

```

DO 28 J=1,NC
IF(X.LT.XMN(J))GO TO 28
IF(X.GT.XMX(J))GO TO 28
K=J
K1=J
XR=X-RP(K)
IF((ABS(XR)+DTST)**2.GE.E(K))GO TO 28
XR2=XR**2
SRCX(K)=SQRT(E(K)-XR2)
C ---- COMPUTE UPPER INTERSECTIONS (BASED ON ELLIPTICAL POROFILE)
Z=HP(K)+C3(K)*(D(K)*XR+SRCX(K))
C CHECK TO SEE IF Z SHOULD BE REPLACED WITH Y LOCATION
C OF WEARFLAT ON WORN CUTTER
IF(ITRAC .EQ. 1)WRITE(3,301)K,XW1(K),XW2(K),X
IF(ITRAC .EQ. 1)WRITE(3,302)Z
301 FORMAT(' K= ',I3,' X1= ',F10.5,' X2= ',F10.5,' X= ',F10.5)
302 FORMAT(' Z= ',F10.5)
ZW=ZBC(K)+(XBC(K)-X)*TAN(WAO(K)/AK)
ZB(K)=ZW
IF(ITRAC .EQ. 1)WRITE(3,303)ZW
303 FORMAT(' ZW= ',F10.5)
IF(X .GT. XW1(K) .AND. X .LT. XW2(K))THEN
Z=ZW
GO TO 2
ENDIF
IF(Z.GT.ZW)Z=ZW
2 CONTINUE
IF(Z.LE.ZM)GO TO 28
C ---- Z INTO QUEUE
LS=LS+1
IF(LS.GE.MXCUT) THEN
WRITE(IDTO,1)MXCUT
IF(IPRNT.NE.IDTO)WRITE(IPRNT,1)MXCUT
CALL STOPP
1 FORMAT('/' MXCUT=' ,I6/' MAX NO. OF INTERSECTIONS ' ,
1 'EXCEEDED - INCREASE MXCUT')
ENDIF
ZT(LS)=Z
KT(LS)=K
C ---- REPLACE ZM?
IF((Z-FEED).LE.ZM)GO TO 27
ZM=(Z-FEED)
KM=K
C ---- IS THERE A LOWER INTERS.?
27 ZL=HP(K)+C3(K)*(D(K)*XR-SRCX(K))
IF(ZL.LE.ZM)GO TO 28
LS=LS+1
ZT(LS)=ZL
KT(LS)=-K
28 CONTINUE
C ---- IS THERE A GAP ?
IF(LS.LE.0)THEN
IF(NX.NE.NNX)LGAP=K1
GO TO 40
ENDIF
C ---- SORT ZT IN DECREASING ORDER WHILE CARRYING KT
CALL BRIORT(ZT,KT,LS)
C ---- CUT BACK LS IF POSSIBLE
DO 29 J=1,LS
IF(ZT(J).LE.ZM)GO TO 30
29 CONTINUE
J=LS+1
30 LS=J-1
C ---- PROCESS INTERSECTIONS
MOLE=MXCUT
DO 39 J=1,LS
IF(MOLE.GE.MXCUT)THEN
C ---- AT START OR HOLE
K=KT(J)
ZK=ZT(J)
MOLE=0
GO TO 39
ENDIF
C ---- NO HOLE
M=IABS(KT(J))
IF(MORD(K).LT.MORD(M))GO TO 39
IF(KT(J).LE.0)GO TO 31
C ---- NOT MASKED - CLOSE OFF AND SET NEW K
C ---- COMPUTE INCREMENTAL VOLUME AND AREA OF CUT
VR(K)=VR(K)+XVOL*(ZK-ZT(J))
AR(K)=AR(K)+DX*(ZK-ZT(J))
C ---- COMPUTE INCREMENTAL DEPTH OF CUT
C ---- DMEAN=EFFECTIVE DEPTH OF CUT FOR KTH CUTTER

```

```

C ---- NDMEAN=NUMBER OF SAMPLES IN DETERMINING DMEAN FOR EACH CUTTER
DE(K)=DE(K)*NDE(K)+(ZB(K)-ZT(J))
1 *COS(WAO(K)/AK)
NDE(K)=NDE(K)+1
DE(K)=DE(K)/NDE(K)
IF(XC1(K).EQ.-100.)THEN
XC1(K)=X
ZC1(K)=ZK
ENDIF
XC2(K)=X
ZC2(K)=ZK
IF(ITRAC.EQ.1)WRITE(3,307)XC1(K),ZC1(K),
1 XC2(K),ZC2(K)
307 FORMAT('XC1=' ,F10.5,' ZC1=' ,F10.5,
1 'XC2=' ,F10.5,' ZC2=' ,F10.5)
IF(ITRAC.EQ.1)WRITE(3,304)ZK,J,ZT(J),ZB(K)
304 FORMAT('ZK=' ,F10.5,' ZT(' ,I3,' )=' ,F10.5,' YBOK=' ,F10.5)
IF(ITRAC.EQ.1)WRITE(3,305)K,VR(K),AR(K),DE(K)
305 FORMAT('VR(' ,I3,' )=' ,F10.5,' AR(K)= ' ,F10.5,
1 'DMEAN=' ,F10.5)
ZK=ZT(J)
K=M
GO TO 39
C ---- UNDERCUT
C ---- COMPUTE INCREMENTAL VOLUME AND AREA OF CUT
31 VR(K)=VR(K)+XVOL*(ZK-ZT(J))
AR(K)=AR(K)+DX*(ZK-ZT(J))
C ---- COMPUTE INCREMENTAL DEPTH OF CUT
C ---- DMEAN=EFFECTIVE DEPTH OF CUT FOR KTH CUTTER
C ---- NDMEAN=NUMBER OF SAMPLES IN DETERMINING DMEAN FOR EACH CUTTER
DE(K)=DE(K)*NDE(K)+(ZB(K)-ZT(J))
1 *COS(WAO(K)/AK)
NDE(K)=NDE(K)+1
DE(K)=DE(K)/NDE(K)
IF(XC1(K).EQ.-100.)THEN
XC1(K)=X
ZC1(K)=ZK
ENDIF
XC2(K)=X
ZC2(K)=ZK
IF(ITRAC.EQ.1)WRITE(3,307)XC1(K),ZC1(K),
1 XC2(K),ZC2(K)
IF(ITRAC.EQ.1)WRITE(3,304)ZK,J,ZT(J),ZB(K)
IF(ITRAC.EQ.1)WRITE(3,305)K,VR(K),AR(K),DE(K)
ZK=ZT(J)
C ---- FIND IF HOLE
MOLE=MXCUT
DO 32 L=1,J
I=KT(L)
IF(I.LE.0)GO TO 32
YI=HP(I)+C3(I)*(D(I)*(X-RP(I))-SRCX(I))
IF(YI.GE.ZK.OR.MORD(I).GT.MOLE.OR.I.EQ.K)GO TO 32
M=I
MOLE=MORD(I)
32 CONTINUE
IF(MOLE.EQ.MXCUT)GO TO 39
C ---- NOT A HOLE
K=M
39 CONTINUE
IF(MOLE.EQ.MXCUT)GO TO 40
C ---- FINISH.
C ---- COMPUTE INCREMENTAL VOLUME AND AREA OF CUT
VR(K)=VR(K)+XVOL*(ZK-ZM)
AR(K)=AR(K)+DX*(ZK-ZM)
C ---- COMPUTE INCREMENTAL DEPTH OF CUT
C ---- DMEAN=EFFECTIVE DEPTH OF CUT FOR KTH CUTTER
C ---- NDMEAN=NUMBER OF SAMPLES IN DETERMINING DMEAN FOR EACH CUTTER
DE(K)=DE(K)*NDE(K)+(ZB(K)-ZM)
1 *COS(WAO(K)/AK)
NDE(K)=NDE(K)+1
DE(K)=DE(K)/NDE(K)
IF(XC1(K).EQ.-100.)THEN
XC1(K)=X
ZC1(K)=ZK
ENDIF
XC2(K)=X
ZC2(K)=ZK
IF(ITRAC.EQ.1)WRITE(3,307)XC1(K),ZC1(K),
1 XC2(K),ZC2(K)
IF(ITRAC.EQ.1)WRITE(3,306)ZK,J,ZM,ZB(K)
306 FORMAT('ZK=' ,F10.5,' ZM(' ,I3,' )=' ,F10.5,' YBOK=' ,F10.5)
IF(ITRAC.EQ.1)WRITE(3,305)K,VR(K),AR(K),DE(K)
40 CONTINUE

```

```

C ---- COMPUTE CUTTER FORCES, INCREMENTAL BIT FORCES,
C      TEMPERATURES, WEAR RATIOS, AND RADIAL WEAR ANGLES
      WOB(IR)=0.
      TORQ(IR)=0.
      BMX(IR)=0.
      BMY(IR)=0.
      FX(IR)=0.
      FY(IR)=0.
      DO 1000 J=1,NC
C ---- ***** CUTTER FORCE MODELS (PENETRATING AND DRAG) *****
      TMPFLG=0
      IF(ITYP(J).EQ.1)THEN
        FP(J)=AW(J)*C1A*DE(J)**N1A
        FFS=C2A*DE(J)**N2A
        IF(FPS.GT.FP(J))THEN
          FP(J)=FFS
          TMPFLG=1
        ENDIF
        GO TO 1500
      ENDIF
      FP(J)=AW(J)*C1B*DE(J)**N1B
      FFS=C2B*DE(J)**N2B
      IF(FPS.GT.FP(J))THEN
        FP(J)=FFS
        TMPFLG=1
      ENDIF
1500 FD(J)=FP(J)*DC
      IF(AW(J).EQ.0.)FD(J)=FP(J)*DCS
C ---- *****
C ---- COMPUTE FORCE COMPONENTS, INTEGRATED FORCES, AND
C      INTEGRATED MOMENTS
      SNAP=SIN(AP(J)/AK)
      CSAP=COS(AP(J)/AK)
      FV(J)=-FP(J)*COS(WAO(J)/AK)
      WOB(IR)=WOB(IR)+(-FV(J))
      FR(J)=-FP(J)*SIN(WAO(J)/AK)
      T1=FR(J)*CSAP
      FX(IR)=FX(IR)+T1
      T1=FD(J)*SNAP
      FX(IR)=FX(IR)+T1
      T2=FR(J)*SNAP
      FY(IR)=FY(IR)+T2
      T2=FD(J)*(-CSAP)
      FY(IR)=FY(IR)+T2
      TORQ(IR)=TORQ(IR)+FD(J)*XBC(J)/12.
      T1=FV(J)*XBC(J)*SNAP
      IF(ITRAC.EQ.1)WRITE(3,2000)T1
2000 FORMAT(' T1=',F10.2)
      BMX(IR)=BMX(IR)+T1/12.
      ZBCP=ZBC(J)-FEED*AP(J)/360.
      T1=FD(J)*CSAP*ZBCP
      IF(ITRAC.EQ.1)WRITE(3,2000)T1
      BMX(IR)=BMX(IR)+T1/12.
      T1=-FR(J)*SNAP*ZBCP
      IF(ITRAC.EQ.1)WRITE(3,2000)T1
      BMX(IR)=BMX(IR)+T1/12.
      T2=-FV(J)*XBC(J)*CSAP
      IF(ITRAC.EQ.1)WRITE(3,2001)T2
2001 FORMAT(' T2=',F10.2)
      BMY(IR)=BMY(IR)+T2/12.
      T2=FD(J)*SNAP*ZBCP
      IF(ITRAC.EQ.1)WRITE(3,2001)T2
      BMY(IR)=BMY(IR)+T2/12.
      T2=FR(J)*CSAP*ZBCP
      IF(ITRAC.EQ.1)WRITE(3,2001)T2
      BMY(IR)=BMY(IR)+T2/12.
C --- ***** MODULE TO COMPUTE THERMAL RESPONSE FUNCTION *****
C      (FT) AS FCT. OF CONVECTIVE COOLING (HCONV),
C      WEARFLAT LENGTH (RLWORN) AND CUTTER RADIUS (RR)
2100 CONTINUE
      IF(HR(J).LE.HL(2))THEN
        IH=2
        GO TO 2200
      ENDIF
      IF(HR(J).GE.HL(3))THEN
        IH=4
        GO TO 2200
      ENDIF
      IH=3
2200 IF(WL(J).LE.RL50(2))THEN
      IL=2
      GO TO 2250
    ENDIF

```

```

IL=3
2250 IHM=IH-1
    ILM=IL-1
    FSL=FT50(ILM,IHM)+(HR(J)-HL(IHM))/
    1 (HL(IH)-HL(IHM))*(FT50(ILM,IH)-FT50(ILM,IHM))
    FLL=FT50(IL,IHM)+(HR(J)-HL(IHM))/
    1 (HL(IH)-HL(IHM))*(FT50(IL,IH)-FT50(IL,IHM))
    F50=FSL+(WL(J)-RL50(ILM))/(RL50(IL)-RL50(ILM))*(FLL-FSL)
    IF(WL(J).LE.RL75(2))THEN
        IL=2
        GO TO 2350
    ENDIF
    IL=3
    IHM=IH-1
    ILM=IL-1
2350 FSL=FT75(ILM,IHM)+(HR(J)-HL(IHM))/
    1 (HL(IH)-HL(IHM))*(FT75(ILM,IH)-FT75(ILM,IHM))
    FLL=FT75(IL,IHM)+(HR(J)-HL(IHM))/
    1 (HL(IH)-HL(IHM))*(FT75(IL,IH)-FT75(IL,IHM))
    F75=FSL+(WL(J)-RL75(ILM))/(RL75(IL)-RL75(ILM))*(FLL-FSL)
    FT=F50+(RR(J)-0.26)/(0.375-0.26)*(F75-F50)
    IF(FT.LE.0.)THEN
        WRITE(IDTO,2400)
2400 FORMAT(' COMPUTED THERMAL RESPONSE FCT .LE. 0. '/
    1 ' PLEASE CHECK FOR INCORRECT CUTTER RADIUS OR CONV. COOLING'
    2 ' COEFF. '/ ' CORRECT DATA AND RE-RUN')
    CALL STOPP
    ENDIF
*****
C ---- ***** CUTTER TEMPERATURE MODEL *****
2500 IF(AW(J).EQ.0.)GO TO 2600
    IF(TMPFLG.EQ.1)GO TO 2600
    T1=1.83E-3*FC*FP(J)*FT*XBC(J)*RPM/AW(J)
    T2=1.+0.0147*FT*RK*(XBC(J)*RPM/RX/WL(J))**.5
    TW(J)=(TFL-32.)/1.8+T1/T2
2550 GO TO 2650
2600 TW(J)=(TFL-32.)/1.8
2650 CONTINUE
    IF(TW(J).GT.TWMAX(IR))TWMAX(IR)=TW(J)
C *****
C ---- ***** CUTTER WEAR RATIO MODEL *****
    WR(J)=FP(J)*XBC(J)/FP(1)/XBC(1)
    IF(TW(J).GT.350.)THEN
        WR(J)=-WR(J)
        IT1=-1
    ENDIF
    IF(ABS(WR(J)).GT.ABS(WRMAX(IR)))WRMAX(IR)=WR(J)
C *****
IF(ITRAC.EQ.1)WRITE(3,308)XC1(J),ZC1(J),
    1 XC2(J),ZC2(J)
308 FORMAT(' FINAL: XCONT1= ',F10.5,' ZCONT1= ',F10.5,
    1 ' XCONT2= ',F10.5,' ZCONT2= ',F10.5)
C ---- COMPUTE CUTTER RADIAL WEAR ANGLES
DXC=XC2(J)-XC1(J)
IF(DXC.EQ.0.)GO TO 1000
WA(J)=AK*ATAN(-(ZC2(J)-ZC1(J))/DXC)
1000 CONTINUE
RETURN
END
SUBROUTINE CUTWEAR
PARAMETER (MXCUT=48)
PARAMETER (TD=0.09)
REAL*8 N4,N5
REAL*8 N1A,N2A,N1B,N2B
CHARACTER *20 ROCK
CHARACTER *1 AIN
COMMON /AK/AK
COMMON /RESULTS/XW1(MXCUT),XW2(MXCUT),WL(MXCUT),
    1 YOWORN(MXCUT),ITRAC,ZB(MXCUT),DE(MXCUT),NDE(MXCUT),
    2 FP(MXCUT),WOB(5),BMX(5),BMY(5),FR(MXCUT),FV(MXCUT),FX(5),
    3 FY(5),TORQ(5),TW(MXCUT),WR(MXCUT),FD(MXCUT),
    4 WW(MXCUT),AW(MXCUT),IW1,XC1(MXCUT),XC2(MXCUT),ZC1(MXCUT),
    5 ZC2(MXCUT),WA(MXCUT),WAO(MXCUT),ZW1(MXCUT),ZW2(MXCUT),
    6 TWMAX(5),WRMAX(5),FWNP(MXCUT),ZBC(MXCUT),XBC(MXCUT),IT1,
    7 IC1,IC2,IC3,IC4,IC5,IC6,BF1,BF2,BF3,BF4,BF5,ITYP(MXCUT),IP1,IP2
COMMON /COMPOS/RP(MXCUT),AP(MXCUT),RR(MXCUT),HP(MXCUT),
    1 BR(MXCUT),MORD(MXCUT),TNAI(MXCUT),AI(MXCUT),
    2 HPP(MXCUT),HR(MXCUT),BNOM
COMMON /CTWEAR/AWMAX,NCMAX,ASUBWN,MODW,WRA(MXCUT),
    1 PAMAX,XBCAMAX,DLH,C6
COMMON /COMIOD/IDTO,IDTI,IDBD,IPRNT,IDWI,IDOC,IDWN
COMMON /COMCON/NC,NRAY,HNOM,FEED,RNOM,EPS,PEDGCT
COMMON /FT/FT50(3,4),FT75(3,4),RL50(3),RL75(3),HL(4),

```

```

1 CV50,RV50,CA50,RA50,CV75,RV75,CA75,RA75
COMMON /ROCKDAT/ROCK,RK,RX,FC,DC,DCS,C1A,N1A,C1B,
2 N1B,C2A,N2A,C2B,N2B,TFL,RPM,ROP(5),NR0P,IR
40 WRITE(IDTO,50)
50 FORMAT(' DO YOU WANT HARD-ROCK WEAR MODE (1) /
1 ' OR SOFT-ROCK WEAR MODE (2) ? (1/2)')
CALL READI(M,MODW)
IF(M.EQ.1.OR.(MODW.NE.1.AND.MODW.NE.2))GO TO 40
70 CONTINUE
WRITE(IDTO,100)AWMAX,NCMAX
100 FORMAT(' CURRENT MAXIMUM WEARFLAT AREA IS ',F7.4/
1 ' FOR CUTTER NUMBER ',I3//
2 ' PLEASE ENTER NEW WEARFLAT AREA FOR THIS CUTTER:')
READ(IDTI,*)ASUBWN
C4=CV50+(RR(NCMAX)-0.26)/(0.375-0.26)*(CV75-CV50)
N4=RV50+(RR(NCMAX)-0.26)/(0.375-0.26)*(RV75-RV50)
C5=CA50+(RR(NCMAX)-0.26)/(0.375-0.26)*(CA75-CA50)
N5=RA50+(RR(NCMAX)-0.26)/(0.375-0.26)*(RA75-RA50)
SNB=SIN(BR(NCMAX)/AK)
WLTR=(RR(NCMAX)-(RR(NCMAX)**2-(WW(NCMAX)/2. )**2)**0.5)/SNB
VWR=(WLTR/C4)**(1/N4)
IF(MODW.EQ.1)THEN
WLRN=C5*ASUBWN**N5
WLRNSNB=WLRN*SNB
IF(WLRNSNB.GT.RR(NCMAX))THEN
WRITE(IDTO,259)
259 FORMAT(' SPECIFIED VALUE OF NEW WEARFLAT AREA IS TOO LARGE '
1 ' FOR HARD-ROCK WEAR MODE.'/' PLEASE SPECIFY SMALLER VALUE.')
GO TO 70
ENDIF
VWRN=(WLRN/C4)**(1/N4)
DVW=VWRN-VWR
DLH=DVW*ROP(3)/6.2831853072/XBCAMAX/FAMAX/RPM/C6/60.
110 WRITE(IDTO,120)DLH
120 FORMAT(' TO ATTAIN THIS NEW WEARFLAT AREA, THE BIT MUST DRILL ',
1 ' F8.1,' FEET OF HOLE' /
2 ' SINCE THE LAST WEAR CONFIGURATION. DO YOU WANT TO GO'
3 ' WITH THIS NEW WEARFLAT' /
4 ' AREA FOR THIS CUTTER? (Y/N)' //
4 ' (IF NOT, YOU WILL BE GIVEN A CHANCE TO SPECIFY A'
5 ' DIFFERENT NEW WEARFLAT' /
6 ' AREA FOR THIS CUTTER.)')
CALL READA(M,AIN)
IF(M.EQ.1.OR.(AIN.NE.'Y'.AND.AIN.NE.'N'))GOTO 110
IF(AIN.EQ.'N') GO TO 70
DO 180 J=1,NC
C4=CV50+(RR(J)-0.26)/(0.375-0.26)*(CV75-CV50)
N4=RV50+(RR(J)-0.26)/(0.375-0.26)*(RV75-RV50)
C5=CA50+(RR(J)-0.26)/(0.375-0.26)*(CA75-CA50)
N5=RA50+(RR(J)-0.26)/(0.375-0.26)*(RA75-RA50)
SNB=SIN(BR(J)/AK)
WLT=(RR(J)-(RR(J)**2-(WW(J)/2. )**2)**0.5)/SNB
VW=(WLT/C4)**(1/N4)
VWN=VW+ABS(WRA(J)/WRA(NCMAX))*DVW
WLNSNB=(C4*VWN**N4)*SNB
IF(WLNSNB.GT.RR(J))THEN
WRITE(IDTO,259)
GO TO 70
ENDIF
180 CONTINUE
DO 200 J=1,NC
C4=CV50+(RR(J)-0.26)/(0.375-0.26)*(CV75-CV50)
N4=RV50+(RR(J)-0.26)/(0.375-0.26)*(RV75-RV50)
C5=CA50+(RR(J)-0.26)/(0.375-0.26)*(CA75-CA50)
N5=RA50+(RR(J)-0.26)/(0.375-0.26)*(RA75-RA50)
SNB=SIN(BR(J)/AK)
WLT=(RR(J)-(RR(J)**2-(WW(J)/2. )**2)**0.5)/SNB
VW=(WLT/C4)**(1/N4)
VWN=VW+ABS(WRA(J)/WRA(NCMAX))*DVW
WL(J)=C4*VWN**N4
AW(J)=(WL(J)/C5)**(1/N5)
WW(J)=2.*(RR(J)**2-(RR(J)-WL(J)*SNB)**2)**0.5
200 CONTINUE
GO TO 400
ENDIF
IF(MODW.EQ.2)THEN
AWMAXR=(TD/C5)**(1/N5)
IF(ASUBWN.LE.AWMAXR)THEN
WLTRN=C5*ASUBWN**N5
VWRN=(WLTRN/C4)**(1/N4)
DVW=VWRN-VWR
DLH=DVW*ROP(3)/6.2831853072/XBCAMAX/FAMAX/RPM/C6/60.
140 WRITE(IDTO,120)DLH

```

```

CALL READA(M,AIN)
IF(M.EQ.1.OR.(AIN.NE.'Y'.AND.AIN.NE.'N'))GOTO 140
IF(AIN.EQ.'N') GO TO 70
GO TO 500
ENDIF
DO 250 LIT=1,10000
  WLTRN=TD+LIT*.0005
  AWGUESS=(WLTRN/C5)**(1/N5)-((WLTRN-TD)/C5)**(1/N5)
  IF(AWGUESS.GT.ASUBWN)GO TO 252
250 CONTINUE
  WRITE(IDTO,251)
251 FORMAT(' ERROR IN SOFT-ROCK WEAR MODE PROCEDURE')
  CALL STOPP
252 WLTRN=WLTRN-.00025
  WLTRNS=WLTRN*SNB
  IF(WLTRNS.GT.RR(NCMAX))THEN
    WRITE(IDTO,260)
260 FORMAT(' SPECIFIED VALUE OF NEW WEARFLAT AREA IS TOO LARGE '
1 ' FOR SOFT-ROCK WEAR MODE.'/' PLEASE SPECIFY SMALLER VALUE.')
    GO TO 70
  ENDIF
  VWRN=(WLTRN/C4)**(1/N4)
  DVW=VWRN-VWR
  DLH=DVW*ROP(3)/6.2831853072/XBCAMAX/FAMAX/RPM/C6/60.
130 WRITE(IDTO,120)DLH
  CALL READA(M,AIN)
  IF(M.EQ.1.OR.(AIN.NE.'Y'.AND.AIN.NE.'N'))GOTO 130
  IF(AIN.EQ.'N') GO TO 70
500 DO 270 J=1,NC
  C4=CV50+(RR(J)-0.26)/(0.375-0.26)*(CV75-CV50)
  N4=RV50+(RR(J)-0.26)/(0.375-0.26)*(RV75-RV50)
  C5=CA50+(RR(J)-0.26)/(0.375-0.26)*(CA75-CA50)
  N5=RA50+(RR(J)-0.26)/(0.375-0.26)*(RA75-RA50)
  SNB=SIN(BR(J)/AK)
  WLT=(RR(J)-(RR(J)**2-(WW(J)/2. )**2)**0.5)/SNB
  VW=(WLT/C4)**(1/N4)
  VWN=VW+ABS(WRA(J)/WRA(NCMAX))*DVW
  WLTN=C4*VWN**N4
  IF(WLTN.LE.TD)GO TO 270
  WLTNS=WLTN*SNB
  IF(WLTNS.GT.RR(J))THEN
    WRITE(IDTO,260)
    GO TO 70
  ENDIF
270 CONTINUE
  DO 300 J=1,NC
  C4=CV50+(RR(J)-0.26)/(0.375-0.26)*(CV75-CV50)
  N4=RV50+(RR(J)-0.26)/(0.375-0.26)*(RV75-RV50)
  C5=CA50+(RR(J)-0.26)/(0.375-0.26)*(CA75-CA50)
  N5=RA50+(RR(J)-0.26)/(0.375-0.26)*(RA75-RA50)
  SNB=SIN(BR(J)/AK)
  WLT=(RR(J)-(RR(J)**2-(WW(J)/2. )**2)**0.5)/SNB
  VW=(WLT/C4)**(1/N4)
  VWN=VW+ABS(WRA(J)/WRA(NCMAX))*DVW
  WLTN=C4*VWN**N4
  IF(WLTN.LE.TD)THEN
    WL(J)=WLTN
    AW(J)=(WL(J)/C5)**(1/N5)
    GO TO 290
  ENDIF
  AW(J)=(WLTN/C5)**(1/N5)-((WLTN-TD)/C5)**(1/N5)
  IF(J.EQ.NCMAX)WRITE(5,9998)WLTN,AW(J)
9998 FORMAT(' WLTN=',F8.5,' AW(J)=' ,F8.5)
  WL(J)=TD
290 WW(J)=2.*(RR(J)**2-(RR(J)-WLTN*SNB)**2)**0.5
300 CONTINUE
  ENDIF
400 CONTINUE
  CALL DATPRI(8)
  RETURN
  END
  SUBROUTINE READI(IE,I)
C ---- READ A SINGLE INTEGER ON THE TERMINAL
  COMMON /COMIOD/IDTO, IDTI, IDBD, IPRNT, IDWI, IDOC, IDWN
  IE=1
  READ(IDTI,*,END=2) I
  IE=0
2 RETURN
  END
  SUBROUTINE READA(IE,I)
C ---- READ A SINGLE CHARACTER ON THE TERMINAL
  CHARACTER *1 I
  COMMON /COMIOD/IDTO, IDTI, IDBD, IPRNT, IDWI, IDOC, IDWN

```

```

IE=1
READ(IDTI,1,END=2) I
1  FORMAT(A1)
IE=0
2  RETURN
END
SUBROUTINE STOPP
C ---- TERMINATES PROGRAM, CLOSING OUTPUT DISK FILES
PARAMETER (MXCUT=48)
COMMON /COMIOD/IDTO, IDTI, IDBD, IPRNT, IDWI, IDOC, IDWN
COMMON /RESULTS/XW1(MXCUT), XW2(MXCUT), WL(MXCUT),
1  YOWORN(MXCUT), ITRAC, ZB(MXCUT), DE(MXCUT), NDE(MXCUT),
2  FP(MXCUT), WOB(5), BMX(5), BMY(5), FR(MXCUT), FV(MXCUT), FX(5),
3  FY(5), TORQ(5), TW(MXCUT), WR(MXCUT), FD(MXCUT),
4  WW(MXCUT), AW(MXCUT), IW1, XC1(MXCUT), XC2(MXCUT), ZC1(MXCUT),
5  ZC2(MXCUT), WA(MXCUT), WAO(MXCUT), ZW1(MXCUT), ZW2(MXCUT),
6  TWMAX(5), WRMAX(5), FWNP(MXCUT), ZBC(MXCUT), XBC(MXCUT), IT1,
7  IC1, IC2, IC3, IC4, IC5, IC6, BF1, BF2, BF3, BF4, BF5, ITYP(MXCUT), IP1, IP2
CLOSE(UNIT=3)
CLOSE(IPRNT)
IF(IC1.EQ.1)CLOSE(UNIT=17)
IF(IC2.EQ.1)CLOSE(UNIT=18)
IF(IC3.EQ.1)CLOSE(UNIT=19)
IF(IC4.EQ.1)CLOSE(UNIT=21)
IF(IC5.EQ.1)CLOSE(UNIT=22)
IF(IC6.EQ.1)CLOSE(UNIT=23)
IF(IB1.EQ.1)CLOSE(UNIT=24)
IF(IB2.EQ.1)CLOSE(UNIT=25)
IF(IB3.EQ.1)CLOSE(UNIT=26)
IF(IB4.EQ.1)CLOSE(UNIT=27)
WRITE(IDTO,100)
100  FORMAT(/' PDCWEAR TERMINATED')
STOP
END
SUBROUTINE RISORT(X,Y,N)
C ---- SORTS THE N REALS X IN INCREASING MAGNITUDE,
C ---- CARRYING THE N INTEGERS Y.
INTEGER Y(N),T
REAL X(N)
M = N
201  M = (9*M)/16
IF (M.LE.0) RETURN
M1 = M+1
DO 204 J=M1,N
L = J
I = J-M
202  IF (X(L)-X(I)) 203,204,204
203  S = X(I)
T = Y(I)
X(I) = X(L)
Y(I) = Y(L)
X(L) = S
Y(L) = T
L = I
I = I-M
IF (I-1) 204,202,202
204  CONTINUE
GO TO 201
END
SUBROUTINE BRIORT(X,Y,N)
C ---- SORTS THE N REALS X IN DECREASING MAGNITUDE,
C ---- CARRYING THE N INTEGERS Y.
INTEGER Y(N),T
REAL X(N)
M = N
201  M = (9*M)/16
IF (M.LE.0) RETURN
M1 = M+1
DO 204 J=M1,N
L = J
I = J-M
202  IF (X(L)-X(I)) 204,204,203
203  S = X(I)
T = Y(I)
X(I) = X(L)
Y(I) = Y(L)
X(L) = S
Y(L) = T
L = I
I = I-M
IF (I-1) 204,202,202
204  CONTINUE
GO TO 201

```

```

END
SUBROUTINE INPUT
C ---- READS AND TESTS INPUT DATA
COMMON /COMIOD/IDTO, IDTI, IDBD, IPRNT, IDWI, IDOC, IDWN
COMMON /COMCHA/IDATE, ITIME, BDNNAME, RSNAME, WINAME, OCNAME
CHARACTER *11 BDNNAME, RSNAME, WINAME, OCNAME
CHARACTER *10 IDATE, ITIME
CHARACTER *20 ROCK
PARAMETER (MXCUT=48)
REAL*8 N1A, N2A, N1B, N2B
COMMON /AK/AK
COMMON /CTWEAR/AWMAX, NCMAX, ASUBWN, MODW, WRA(MXCUT),
1 FMAX, XBCAMAX, DLH, C6
COMMON /COMPOS/RP(MXCUT), AP(MXCUT), RR(MXCUT), HP(MXCUT),
1 BR(MXCUT), MORD(MXCUT), TNAI(MXCUT), AI(MXCUT),
2 HPP(MXCUT), HR(MXCUT), BNOM
COMMON /COMRWK/VR(MXCUT), AR(MXCUT), C3(MXCUT), D(MXCUT),
1 E(MXCUT), XMK(MXCUT), XMN(MXCUT), ZT(MXCUT), SRCX(MXCUT), WK(MXCUT)
COMMON /COMCON/NC, NRAY, HNOM, FEED, RNOM, EPS, PEDGCT
COMMON /RESULTS/XW1(MXCUT), XW2(MXCUT), WL(MXCUT),
1 YOWORN(MXCUT), ITRAC, ZB(MXCUT), DE(MXCUT), NDE(MXCUT),
2 FP(MXCUT), WOB(5), BMX(5), BMY(5), FR(MXCUT), FV(MXCUT), FX(5),
3 FY(5), TORQ(5), TW(MXCUT), WR(MXCUT), FD(MXCUT),
4 WW(MXCUT), AW(MXCUT), IW1, XC1(MXCUT), XC2(MXCUT), ZC1(MXCUT),
5 ZC2(MXCUT), WA(MXCUT), WAO(MXCUT), ZW1(MXCUT), ZW2(MXCUT),
6 TWMAX(5), WRMAX(5), PWNP(MXCUT), ZBC(MXCUT), XBC(MXCUT), IT1,
7 IC1, IC2, IC3, IC4, IC5, IC6, BF1, BF2, BF3, BF4, BF5, ITYP(MXCUT), IP1, IP2
COMMON /ROCKDAT/ROCK, RK, RX, FC, DC, DCS, C1A, N1A, C1B,
2 N1B, C2A, N2A, C2B, N2B, TFL, RPM, ROP(5), NROP, IR
CHARACTER *1 AIN
C ---- ENTER BIT DESIGN DATA FROM DISK
IDT=0
MXCUT1=MXCUT-1
10 WRITE(IDTO,101)
101 FORMAT('/ ENTER NAME OF FILE CONTAINING BIT DESIGN DATA'/
1 ' (11 CHAR. OR LESS, INCLUDING .EXTENSION):')
READ(IDTI, 'A11', END=13)BDNAME
IF(BDNAME.EQ.' ')GO TO 10
OPEN(IDBD, FILE=BDNAME, STATUS='OLD')
REWIND IDBD
IDT=1
READ(IDBD, 102, END=200)RNOM, BNOM, HNOM
102 FORMAT(1X, F10.3, 1X, F10.2, 1X, F10.2)
DO 11 NC=1, MXCUT1
READ(IDBD, 119, END=12)I, RP(NC), AP(NC), HPP(NC),
1 AI(NC), RR(NC), BR(NC), HR(NC)
119 FORMAT(1X, I3, 1X, F7.3, 1X, F7.3, 1X, F7.3,
1 1X, F7.3, 1X, F7.3, 1X, F7.3, 1X, F7.3)
11 CONTINUE
NC=MXCUT
READ(IDBD, *, END=12)
GO TO 203
12 NC=NC-1
REWIND IDBD
CLOSE(IDBD, STATUS='KEEP')
13 IF(IDT.EQ.0) THEN
WRITE(IDTO,108)
108 FORMAT(' INPUT DATA HAS NOT YET BEEN ENTERED')
GO TO 10
ENDIF
IF(NC.GT.MXCUT1)GO TO 203
C ---- WANT TO LIST INPUT ON TERM.?
15 WRITE(IDTO,104)NC
104 FORMAT('/ THERE ARE', I4, ' CUTTERS'/
1 ' DO YOU WISH TO LIST THE BIT DESIGN INPUT'
2 ' DATA ON THE TERMINAL? (Y,N)')
CALL READA(M, AIN)
IF(M.EQ.1 OR. (AIN.NE.'Y' AND AIN.NE.'N'))GO TO 15
IF(AIN.EQ.'Y')CALL DATPRI(1)
C ---- TEST BIT DESIGN DATA
40 DO 41 J=2, NC
IF(RP(J).LT.RP(J-1))GO TO 42
41 CONTINUE
C ---- DATA IS IN ORDER
GO TO 45
C ---- DATA IS OUT OF ORDER
42 WRITE(IDTO,118)
118 FORMAT(' CUTTERS ARE NOT ORDERED IN ASCENDING'
1 ' RADIAL POSITION')
WRITE(IDTO,114)
114 FORMAT(' PLEASE CORRECT INPUT DATA FILE(S) AND RE-RUN')
CALL STOPP
45 IF(RNOM.LE.0.)THEN

```

```

121  WRITE(IDTO,121)
    FORMAT(' NOMINAL CUTTER RADIUS .LE. 0. ')
    WRITE(IDTO,114)
    CALL STOPP
    ENDIF
    IF(HNCM.LE.0.)THEN
122  WRITE(IDTO,122)
    FORMAT(' NOMINAL CONV. COOLING COEFF. .LE. 0. ')
    WRITE(IDTO,114)
    CALL STOPP
    ENDIF
    IF(BNCM.LT.0.)THEN
120  WRITE(IDTO,120)
    FORMAT(' NOMINAL BACKRAKE ANGLE .LT. 0. ')
    WRITE(IDTO,114)
    CALL STOPP
    ENDIF
C ---- TEST CUTTERS
    DO 51 J=1,NC
    IF(RP(J).LE.0.)THEN
123  WRITE(IDTO,123)J
    FORMAT(' CUTTER',I3,' RADIAL POSITION .LE. 0. ')
    WRITE(IDTO,114)
    CALL STOPP
    ENDIF
    IF(AP(J).LT.0.)THEN
124  WRITE(IDTO,124)J
    FORMAT(' CUTTER',I3,' ANGULAR POSITION .LT. 0. ')
    WRITE(IDTO,114)
    CALL STOPP
    ENDIF
    IF(AI(J).LE.-90.)THEN
126  WRITE(IDTO,126)J
    FORMAT(' CUTTER',I3,' INCLINATION ANGLE .LE. -90. ')
    WRITE(IDTO,114)
    CALL STOPP
    ENDIF
    IF(AI(J).GE.90.)THEN
127  WRITE(IDTO,127)J
    FORMAT(' CUTTER',I3,' INCLINATION ANGLE .GE. 90. ')
    WRITE(IDTO,114)
    CALL STOPP
    ENDIF
51  CONTINUE
C ---- BIT DESIGN DATA TESTS ARE OK.
C ---- ENTER CUTTER WEAR DATA FROM DISK
    IDT=0
310  WRITE(IDTO,401)
401  FORMAT('/' ENTER NAME OF FILE CONTAINING INITIAL CUTTER'
1 ' WEAR CONFIGURATION' /
2 ' (11 CHAR. OR LESS, INCLUDING .EXTENSION):')
    READ(IDTI,'(A11)',END=313)WINAME
    IF(WINAME.EQ.' ')GO TO 310
    OPEN(IDWI,FILE=WINAME,STATUS='OLD')
    REWIND IDWI
    IDT=1
    DO 311 NCW=1,MXCUT1
    READ(IDWI,419,END=312)I,WL(I),WW(I),AW(I)
419  FORMAT(1X,I3,1X,F10.3,1X,F10.3,1X,F10.4)
311  CONTINUE
312  NCW=NCW-1
    REWIND IDWI
    CLOSE(IDWI,STATUS='KEEP')
313  IF(IDT.EQ.0)THEN
    WRITE(IDTO,108)
    GO TO 310
    ENDIF
    IF(NCW.NE.NC)THEN
    WRITE(IDTO,399)
    WRITE(IDTO,114)
399  FORMAT(' NUMBER OF CUTTERS IN WEAR FILE DOES NOT MATCH' /
1 ' NUMBER OF CUTTERS IN INPUT DATA FILE')
    CALL STOPP
    ENDIF
C ---- WANT TO LIST INPUT ON TERM.?
315  WRITE(IDTO,404)
404  FORMAT(' DO YOU WISH TO LIST THE INITIAL WEAR CONFIGURATION DATA'
2 ' ON THE TERMINAL? (Y,N)')
    CALL READA(M,AIN)
    IF(M.EQ.1.OR.(AIN.NE.'Y'.AND.AIN.NE.'N'))GO TO 315
    IF(AIN.EQ.'Y')CALL DATPRI(5)
C ---- TEST CUTTER WEAR DATA
    DO 351 J=1,NC

```

```

DCT=RNOM*RR(J)*2.
IF(WL(J).LT.0.)THEN
WRITE(IDTO,324)J
324  FORMAT(' CUTTER',I3,' WEARFLAT LENGTH .LT. 0. ')
WRITE(IDTO,114)
CALL STOPP
ENDIF
IF(WW(J).GT.DCT)THEN
WRITE(IDTO,325)J
325  FORMAT(' CUTTER',I3,' WEARFLAT WIDTH .GT. CUTTER DIAMETER')
WRITE(IDTO,114)
CALL STOPP
ENDIF
IF(WW(J).LT.0.)THEN
WRITE(IDTO,326)J
326  FORMAT(' CUTTER',I3,' WEARFLAT WIDTH .LT. 0. ')
WRITE(IDTO,114)
CALL STOPP
ENDIF
AWMAX=WL(J)*WW(J)*1.01
IF(AW(J).GT.AWMAX)THEN
WRITE(IDTO,327)J
327  FORMAT(' CUTTER',I3,' WEARFLAT AREA .GT. WIDTH X LENGTH')
WRITE(IDTO,114)
CALL STOPP
ENDIF
IF(AW(J).LT.0.)THEN
WRITE(IDTO,328)J
328  FORMAT(' CUTTER',I3,' WEARFLAT AREA .LT. 0. ')
WRITE(IDTO,114)
CALL STOPP
ENDIF
351  CONTINUE
C ---- CUTTER WEAR DATA TESTS ARE OK
C ---- ENTER OPERATING PARAMETER DATA FROM DISK
510  WRITE(IDTO,601)
601  FORMAT(/' ENTER NAME OF FILE CONTAINING OPERATING'
1 ' PARAMETER DATA' /
1 ' (11 CHAR. OR LESS, INCLUDING .EXTENSION):')
READ(IDTI,'(A11)')OCNAME
IF(OCNAME.EQ.' ')GO TO 510
OPEN(IDOC,FILE=OCNAME,STATUS='OLD')
REWIND IDOC
READ(IDOC,709)ROCK
709  FORMAT(1X,A20)
READ(IDOC,720)RK
720  FORMAT(1X,F10.3)
READ(IDOC,720)RX
READ(IDOC,720)FC
READ(IDOC,720)DC
READ(IDOC,720)DCS
READ(IDOC,722)C1A
722  FORMAT(1X,E10.4)
READ(IDOC,720)N1A
READ(IDOC,722)C1B
READ(IDOC,720)N1B
READ(IDOC,722)C2A
READ(IDOC,720)N2A
READ(IDOC,722)C2B
READ(IDOC,720)N2B
READ(IDOC,722)C6
READ(IDOC,825)RPM
825  FORMAT(1X,F10.1)
READ(IDOC,825)TFL
READ(IDOC,730)(ROF(I),I=1,5)
730  FORMAT(1X,F10.1,1X,F10.1,1X,F10.1,1X,F10.1,1X,F10.1)
REWIND IDOC
CLOSE(IDOC,STATUS='KEEP')
C ---- WANT TO LIST INPUT ON TERM.?
515  WRITE(IDTO,604)
604  FORMAT(' DO YOU WISH TO LIST THE OPERATING PARAMETER DATA'
1 ' ON THE TERMINAL? (Y/N)')
CALL READA(M,AIN)
IF(M.EQ.1.OR.(AIN.NE.'Y'.AND.AIN.NE.'N'))GO TO 515
IF(AIN.EQ.'Y')CALL DATPRI(6)
C ---- TEST OPERATING PARAMETER DATA
IF(RK.LE.0.)THEN
WRITE(IDTO,724)
724  FORMAT(' ROCK THERMAL CONDUCTIVITY .LE. 0. ')
WRITE(IDTO,114)
CALL STOPP
ENDIF
IF(RX.LE.0.)THEN

```

```

WRITE(IDTO,725)
725  FORMAT(' ROCK THERMAL DIFFUSIVITY .LE. 0.')
WRITE(IDTO,114)
CALL STOPP
ENDIF
IF(FC.LE.0.)THEN
WRITE(IDTO,726)
726  FORMAT(' ROCK-CUTTER FRICTION COEFFICIENT .LE. 0.')
WRITE(IDTO,114)
CALL STOPP
ENDIF
IF(DC.LE.0.)THEN
WRITE(IDTO,727)
727  FORMAT(' WORN CUTTER DRAG COEFFICIENT .LE. 0.')
WRITE(IDTO,114)
CALL STOPP
ENDIF
IF(DCS.LE.0.)THEN
WRITE(IDTO,767)
767  FORMAT(' SHARP CUTTER DRAG COEFFICIENT .LE. 0.')
WRITE(IDTO,114)
CALL STOPP
ENDIF
IF(C1A.LE.0.)THEN
WRITE(IDTO,728)
728  FORMAT(' WORN TYPE A CUTTER CORRELATION CONSTANT C1 .LE. 0.')
WRITE(IDTO,114)
CALL STOPP
ENDIF
IF(N1A.LE.0.)THEN
WRITE(IDTO,729)
729  FORMAT(' WORN TYPE A CUTTER CORRELATION EXPONENT N1 .LE. 0.')
WRITE(IDTO,114)
CALL STOPP
ENDIF
IF(C1B.LT.0.)THEN
WRITE(IDTO,828)
828  FORMAT(' WORN TYPE B CUTTER CORRELATION CONSTANT C1 .LT. 0.')
WRITE(IDTO,114)
CALL STOPP
ENDIF
IF(N1B.LT.0.)THEN
WRITE(IDTO,829)
829  FORMAT(' WORN TYPE B CUTTER CORRELATION EXPONENT N1 .LT. 0.')
WRITE(IDTO,114)
CALL STOPP
ENDIF
IF(C2A.LE.0.)THEN
WRITE(IDTO,758)
758  FORMAT(' SHARP TYPE A CUTTER CORRELATION CONSTANT C2 .LE. 0.')
WRITE(IDTO,114)
CALL STOPP
ENDIF
IF(N2A.LE.0.)THEN
WRITE(IDTO,759)
759  FORMAT(' SHARP TYPE A CUTTER CORRELATION EXPONENT N2 .LE. 0.')
WRITE(IDTO,114)
CALL STOPP
ENDIF
IF(C2B.LT.0.)THEN
WRITE(IDTO,858)
858  FORMAT(' SHARP TYPE B CUTTER CORRELATION CONSTANT C2 .LT. 0.')
WRITE(IDTO,114)
CALL STOPP
ENDIF
IF(N2B.LT.0.)THEN
WRITE(IDTO,859)
859  FORMAT(' SHARP TYPE B CUTTER CORRELATION EXPONENT N2 .LT. 0.')
WRITE(IDTO,114)
CALL STOPP
ENDIF
IF(C6.LE.0.)THEN
WRITE(IDTO,860)
860  FORMAT(' ABRASIVE WEAR CONSTANT C6 .LE. 0.')
WRITE(IDTO,114)
CALL STOPP
ENDIF
IF(RPM.LE.0.)THEN
WRITE(IDTO,731)
731  FORMAT(' BIT ROTARY SPEED .LE. 0.')
WRITE(IDTO,114)
CALL STOPP
ENDIF
ENDIF

```

```

IF(TFL.LE.0.)THEN
WRITE(IDTO,732)
732  FORMAT(' DOWNHOLE COOLING FLUID TEMPERATURE .LE. 0.')
WRITE(IDTO,114)
CALL STOPP
ENDIF
NROP=0
DO 751 I=1,5
IF(NROP.NE.0)GO TO 741
IF(ROP(I).EQ.0.)THEN
NROP=I-1
GO TO 751
ENDIF
IF(I.EQ.1)GO TO 748
IM1=I-1
IF(ROP(I).LE.ROP(IM1))THEN
WRITE(IDTO,733)I,IM1
733  FORMAT(' ROP(',I1,') .LE. ROP(',I1,')')
WRITE(IDTO,734)
734  FORMAT(' PLEASE RE-ORDER ROPS IN ASCENDING ORDER AND RE-RUN')
CALL STOPP
ENDIF
GO TO 751
741  IF(ROP(I).NE.0.) THEN
WRITE(IDTO,742)I
742  FORMAT(' ROP(',I1,') .NE. 0. -- ALL ROPS BEYOND FIRST ZERO'/
1 ' MUST ALSO BE ZERO')
WRITE(IDTO,114)
CALL STOPP
ENDIF
GO TO 751
748  IF(ROP(I).LT.0.) THEN
WRITE(IDTO,749)I
749  FORMAT(' ROP(',I1,') .LT. 0.')
WRITE(IDTO,114)
CALL STOPP
ENDIF
751  CONTINUE
IF(NROP.EQ.0)NROP=5
C ---- OPERATING PARAMETER DATA TESTS ARE OK.
RETURN
200  WRITE(IDTO,201)
201  FORMAT('/ END-OF-FILE WHILE READING INPUT DATA')
CALL STOPP
203  WRITE(IDTO,204)NC,MXCUT1
204  FORMAT('/ NO. OF CUTTERS=',I4,'. MAXIMUM OF ',
1 I4, ' ALLOWED.'/ UPPER LIMIT MAY BE INCREASED BY ADJUSTING '
2 ', 'PARAMETER MXCUT'/' IN ALL SUBROUTINES.')
CALL STOPP
END
SUBROUTINE DATPRI(IND)
C ---- PRINTS DATA ON TERMINAL AND DISK
COMMON /AK/AK
CHARACTER *20 ROCK
COMMON /COMIOD/IDTO, IDTI, IDBD, IPRNT, IDWI, IDOC, IDWN
COMMON /COMCHA/IDATE, ITIME, BDNAME, RSNAME, WINAME, OCNAME
CHARACTER *11 BDNAME, RSNAME, WINAME, OCNAME
CHARACTER *10 IDATE, ITIME
COMMON /COMCON/NC, NRAY, HNOM, FEED, RNOM, EPS, PEDGCT
PARAMETER (MXCUT=48)
REAL*8 N1A, N2A, N1B, N2B
COMMON /CTWEAR/AWMAX, NCMAX, ASUBWN, MODW, WRA(MXCUT),
1 FAMAX, XBCAMAX, DLH, C6
COMMON /COMPOS/ RP(MXCUT), AP(MXCUT), RR(MXCUT), HP(MXCUT),
1 BR(MXCUT), MORD(MXCUT), TNAI(MXCUT), AI(MXCUT),
2 HPP(MXCUT), HR(MXCUT), BNOM
COMMON /RESULTS/XW1(MXCUT), XW2(MXCUT), WL(MXCUT),
1 YOWORN(MXCUT), ITRAC, ZB(MXCUT), DE(MXCUT), NDE(MXCUT),
2 FP(MXCUT), WOB(5), BMX(5), BMY(5), FR(MXCUT), FV(MXCUT), FX(5),
3 FY(5), TORQ(5), TW(MXCUT), WR(MXCUT), FD(MXCUT),
4 WW(MXCUT), AW(MXCUT), IW1, XC1(MXCUT), XC2(MXCUT), ZC1(MXCUT),
5 ZC2(MXCUT), WA(MXCUT), WAO(MXCUT), ZW1(MXCUT), ZW2(MXCUT),
6 TWMAX(5), WRMAX(5), FWNP(MXCUT), ZBC(MXCUT), XBC(MXCUT), IT1,
7 IC1, IC2, IC3, IC4, IC5, IC6, BF1, BF2, BF3, BF4, BF5, ITYP(MXCUT), IP1, IP2
COMMON /ROCKDAT/ROCK, RK, RX, FC, DC, DCS, C1A, N1A, C1B,
2 N1B, C2A, N2A, C2B, N2B, TFL, RPM, ROP(5), NROP, IR
COMMON /COMRWK/VR(MXCUT), AR(MXCUT), C3(MXCUT), D(MXCUT),
1 E(MXCUT), XMX(MXCUT), XMN(MXCUT), ZI(MXCUT), SRCX(MXCUT), WK(MXCUT)
DIMENSION FS(5)
CHARACTER *1 AIN
IO=IDTO
IF(IND.GT.2)GO TO 10
IF(IND.EQ.2)IO=IPRNT

```

```

HL=0.
C ---- PRINT INPUT CONFIGURATION
WRITE(IO,101)IDATE,ITIME,BDNAME
101 FORMAT('1'/' *** INPUT DATA *** ',A10,1X,A10//
1 ' BIT DESIGN DATA FROM FILE ',A11,' :')//
WRITE(IO,100)NC,RNOM,BNOM,HNOM,(J,RP(J),AP(J),HPP(J),
1 AI(J),RR(J),BR(J),HR(J),J=1,NC)
100 FORMAT('/' THERE ARE ',I3,' CUTTERS WITH NOMINAL '
1 'RADIUS =',F8.3,' IN. '//
2 ' NOMINAL BACKRAKE ANGLE =',F8.2,
2 ' DEG. '//
2 ' AND NOMINAL CONVECTIVE COOLING COEFF. =',F8.2,
2 ' BTU/HR-FT**2-F. '//
3 ' RADIAL ANG. LONG. INCL. REL. REL. '
4 ' REL. CONV. '//
5 ' POS. POS. POS. ANGLE RADIUS BACKRAKE'
6 ' COOLING '//
9 ' (IN.) (DEG.) (IN.) (DEG.) ANGLE '
1 ' COEFF. *'//
2 (1X,I3,2X,F7.3,2X,F7.3,2X,F7.3,2X,F7.3,1X,F7.3,1X,F7.3,2X,F7.3))
WRITE(IO,30)
30 FORMAT('///' * NEGATIVE VALUE OF RELATIVE COOLING COEFFICIENT'/'
1 ' DENOTES TYPE B CUTTER. ALL OTHER CUTTERS'
2 ' ARE TYPE A.')
IF(IND.EQ.2)GO TO 500
RETURN
10 GO TO (23,23,23,24,500,600,400,1000,1100),IND
23 WRITE(IPRNT,199)
199 FORMAT('1')
IF(IR.EQ.1)WRITE(IPRNT,110)NRAY
110 FORMAT('///' *** COMPUTED RESULTS ***'// NRAY =',I5)
WRITE(IPRNT,111)ROP(IR),(J,MORD(J),HP(J),XBC(J),ZBC(J),
1 AI(J),WAO(J),VR(J),AR(J),DE(J),J=1,NC)
111 FORMAT('///'
1 ' GEOMETRY-DEPENDENT RESULTS FOR PENETRATION RATE =',F6.2,
2 ' FT/HR'//
3 ' CUTTER CUTTING CUTTING WEARFLAT WEARFLAT CUTTER'
3 ' CUTTER VOLUME AREA'
3 ' EFFECTIVE'//
4 ' ORDER HEIGHT LOCATION LOCATION INCL.'
4 ' WEAR OF OF '
4 ' DEPTH' /
5 ' (IN.) XBC ZBC ANGLE'
5 ' ANGLE CUT CUT '
5 ' OF CUT '//
6 ' (IN.) (IN.) (DEG.)'
6 ' (DEG.) (IN**3/ (IN**2)'
6 ' (IN.)'//
7 20X,' REV )'//
8 (2X,I3,6X,I3,5X,F7.3,3X,F7.3,3X,F7.3,3X,F7.3,2X,F7.3,
1 1X,F7.4,1X,F7.4,1X,F7.4))
RETURN
24 WRITE(IPRNT,112)ROP(IR),(J,VR(J),AR(J),DE(J),FP(J),
2 FD(J),FV(J),FR(J),TW(J),WR(J),J=1,NC)
112 FORMAT('1'///
1 ' ROCK-DEPENDENT RESULTS FOR PENETRATION RATE =',F6.2,
2 ' FT/HR'//
3 1X,'CUTTER VOLUME AREA EFFECTIVE
4 PENETRATING DRAG VERTICAL RADIAL
5 WEARFLAT WEAR'//1X,' OF CUT OF CUT
6 DEPTH OF CUT FORCE FORCE FORCE FORCE
7 TEMPERATURE RATIO'//
8 ' (IN**3/REV) (IN**2) (IN.)
9 (LBF) (LBF) (LBF) (LBF)
1 (DEG. C)')//(2X,I3,5X,
2 F10.4,2X,F10.4,2X,F10.4,3X,F10.1,3X,
3 F10.1,2X,F10.1,3X,F10.1,3X,F10.1,2X,F10.2))
139 WRITE(IPRNT,140)ROCK,ROP(IR)
140 FORMAT('1'///,1X,' INTEGRATED FORCES AND MOMENTS FOR THE FULL'
1 ' BIT:'//,1X,A20,' AT ROP =',3X,F6.1)
WRITE(IPRNT,113)WOB(IR)
113 FORMAT(/,1X,'TOTAL WOB (LBF) =',1X,F8.1)
WRITE(IPRNT,130)TORQ(IR)
130 FORMAT(/,1X,'DRILLING TORQ. (FT-LBF) =',1X,F8.1)
WRITE(IPRNT,118)FX(IR)
118 FORMAT(/,1X,'X SIDE FORCE (LBF) =',1X,F8.1)
WRITE(IPRNT,119)FY(IR)
119 FORMAT(/,1X,'Y SIDE FORCE (LBF) =',1X,F8.1)
FS(IR)=(FX(IR)**2+FY(IR)**2)**.5
WRITE(IPRNT,999)FS(IR)
999 FORMAT(/,1X,'RESULTANT SIDE FORCE (LBF) =',1X,F8.1)
WRITE(IPRNT,131)BMX(IR)
131 FORMAT(/,1X,'B. M. ABOUT X-AXIS (FT-LBF) =',1X,F8.1)

```

```

WRITE(IPRNT,132)BMY(IR)
132 FORMAT(/,1X,'B. M. ABOUT Y-AXIS (FT-LBF) =',1X,F8.1)
WRITE(IO,441)TWMAX(IR)
WRITE(IO,442)WRMAX(IR)
GO TO (250,255,260,265,270),IR
250 WRITE(IO,440)ROCK,ROP(1)
WRITE(IO,413)WOB(1)
WRITE(IO,430)TORQ(1)
WRITE(IO,418)FX(1)
WRITE(IO,419)FY(1)
WRITE(IO,499)FS(1)
WRITE(IO,431)BMX(1)
WRITE(IO,432)BMY(1)
WRITE(IO,441)TWMAX(1)
WRITE(IO,442)WRMAX(1)
GO TO 300
255 WRITE(IO,440)ROCK,ROP(1),ROP(2)
WRITE(IO,413)WOB(1),WOB(2)
WRITE(IO,430)TORQ(1),TORQ(2)
WRITE(IO,418)FX(1),FX(2)
WRITE(IO,419)FY(1),FY(2)
WRITE(IO,499)FS(1),FS(2)
WRITE(IO,431)BMX(1),BMX(2)
WRITE(IO,432)BMY(1),BMY(2)
WRITE(IO,441)TWMAX(1),TWMAX(2)
WRITE(IO,442)WRMAX(1),WRMAX(2)
GO TO 300
260 WRITE(IO,440)ROCK,ROP(1),ROP(2),ROP(3)
WRITE(IO,413)WOB(1),WOB(2),WOB(3)
WRITE(IO,430)TORQ(1),TORQ(2),TORQ(3)
WRITE(IO,418)FX(1),FX(2),FX(3)
WRITE(IO,419)FY(1),FY(2),FY(3)
WRITE(IO,499)FS(1),FS(2),FS(3)
WRITE(IO,431)BMX(1),BMX(2),BMX(3)
WRITE(IO,432)BMY(1),BMY(2),BMY(3)
WRITE(IO,441)TWMAX(1),TWMAX(2),TWMAX(3)
WRITE(IO,442)WRMAX(1),WRMAX(2),WRMAX(3)
GO TO 300
265 WRITE(IO,440)ROCK,ROP(1),ROP(2),ROP(3),ROP(4)
WRITE(IO,413)WOB(1),WOB(2),WOB(3),WOB(4)
WRITE(IO,430)TORQ(1),TORQ(2),TORQ(3),TORQ(4)
WRITE(IO,418)FX(1),FX(2),FX(3),FX(4)
WRITE(IO,419)FY(1),FY(2),FY(3),FY(4)
WRITE(IO,499)FS(1),FS(2),FS(3),FS(4)
WRITE(IO,431)BMX(1),BMX(2),BMX(3),BMX(4)
WRITE(IO,432)BMY(1),BMY(2),BMY(3),BMY(4)
WRITE(IO,441)TWMAX(1),TWMAX(2),TWMAX(3),TWMAX(4)
WRITE(IO,442)WRMAX(1),WRMAX(2),WRMAX(3),WRMAX(4)
GO TO 300
270 WRITE(IO,440)ROCK,ROP(1),ROP(2),ROP(3),ROP(4),ROP(5)
WRITE(IO,413)WOB(1),WOB(2),WOB(3),WOB(4),WOB(5)
WRITE(IO,430)TORQ(1),TORQ(2),TORQ(3),TORQ(4),TORQ(5)
WRITE(IO,418)FX(1),FX(2),FX(3),FX(4),FX(5)
WRITE(IO,419)FY(1),FY(2),FY(3),FY(4),FY(5)
WRITE(IO,499)FS(1),FS(2),FS(3),FS(4),FS(5)
WRITE(IO,431)BMX(1),BMX(2),BMX(3),BMX(4),BMX(5)
WRITE(IO,432)BMY(1),BMY(2),BMY(3),BMY(4),BMY(5)
WRITE(IO,441)TWMAX(1),TWMAX(2),TWMAX(3),TWMAX(4),TWMAX(5)
WRITE(IO,442)WRMAX(1),WRMAX(2),WRMAX(3),WRMAX(4),WRMAX(5)
300 IF(IP1.EQ.0)THEN
IP1=IP1+1
WRITE(IDTO,310)
310 FORMAT(/' DO YOU WANT TO SEND DATA TO CUTTER PLOT FILES? (Y/N)')
CALL READA(M,AIN)
IF(M.EQ.1.OR.(AIN.NE.'Y'.AND.AIN.NE.'N'))GOTO 300
IF(AIN.NE.'Y')GOTO 320
700 WRITE(IDTO,710)
710 FORMAT(/' PENETRATING FORCE VS. CUTTER NUMBER? (Y/N)')
CALL READA(M,AIN)
IF(M.EQ.1.OR.(AIN.NE.'Y'.AND.AIN.NE.'N'))GOTO 700
IF(AIN.EQ.'Y')THEN
IC1=1
OPEN(UNIT=17,NAME='FVSCN.DAT',TYPE='NEW')
ENDIF
715 WRITE(IDTO,720)
720 FORMAT(/' EFFECTIVE DEPTH OF CUT VS. CUTTER NUMBER? (Y/N)')
CALL READA(M,AIN)
IF(M.EQ.1.OR.(AIN.NE.'Y'.AND.AIN.NE.'N'))GOTO 715
IF(AIN.EQ.'Y')THEN
IC2=1
OPEN(UNIT=18,NAME='DEFVSCN.DAT',TYPE='NEW')
ENDIF
725 WRITE(IDTO,730)

```

```

730  FORMAT(/' WEARFLAT TEMPERATURE VS. CUTTER NUMBER? (Y/N)')
      CALL READA(M,AIN)
      IF(M .EQ. 1 .OR. (AIN.NE.'Y'.AND.AIN.NE.'N'))GOTO 725
      IF(AIN.EQ.'Y')THEN
        IC3=1
        OPEN(UNIT=19,NAME='TWVSCN.DAT',TYPE='NEW')
      ENDIF
735  WRITE(IDTO,740)
740  FORMAT(/' WEAR RATIO VS. CUTTER NUMBER? (Y/N)')
      CALL READA(M,AIN)
      IF(M .EQ. 1 .OR. (AIN.NE.'Y'.AND.AIN.NE.'N'))GOTO 735
      IF(AIN.EQ.'Y')THEN
        IC4=1
        OPEN(UNIT=21,NAME='WRVSCN.DAT',TYPE='NEW')
      ENDIF
745  WRITE(IDTO,750)
750  FORMAT(/' ROCK VOLUME VS. CUTTER NUMBER? (Y/N)')
      CALL READA(M,AIN)
      IF(M .EQ. 1 .OR. (AIN.NE.'Y'.AND.AIN.NE.'N'))GOTO 745
      IF(AIN.EQ.'Y')THEN
        IC5=1
        OPEN(UNIT=22,NAME='VRVSCN.DAT',TYPE='NEW')
      ENDIF
755  WRITE(IDTO,760)
760  FORMAT(/' AREA OF CUT VS. CUTTER NUMBER? (Y/N)')
      CALL READA(M,AIN)
      IF(M .EQ. 1 .OR. (AIN.NE.'Y'.AND.AIN.NE.'N'))GOTO 755
      IF(AIN.EQ.'Y')THEN
        IC6=1
        OPEN(UNIT=23,NAME='ARVSCN.DAT',TYPE='NEW')
      ENDIF
      ENDIF
      IF(IC1.EQ.1)WRITE(17,217)BDNAME,WINAME,OCNAME,ROP(IR)
      IF(IC2.EQ.1)WRITE(18,217)BDNAME,WINAME,OCNAME,ROP(IR)
      IF(IC3.EQ.1)WRITE(19,217)BDNAME,WINAME,OCNAME,ROP(IR)
      IF(IC4.EQ.1)WRITE(21,217)BDNAME,WINAME,OCNAME,ROP(IR)
      IF(IC5.EQ.1)WRITE(22,217)BDNAME,WINAME,OCNAME,ROP(IR)
      IF(IC6.EQ.1)WRITE(23,217)BDNAME,WINAME,OCNAME,ROP(IR)
217  FORMAT(A11/,A11/,A11/,F7.2)
      DO 115 J=1,NC
      IF(IC1.EQ.1)WRITE(17,117)J,FP(J)
      IF(IC2.EQ.1)WRITE(18,117)J,DE(J)
      IF(IC3.EQ.1)WRITE(19,117)J,TW(J)
      IF(IC4.EQ.1)WRITE(21,117)J,WR(J)
      IF(IC5.EQ.1)WRITE(22,117)J,VR(J)
      IF(IC6.EQ.1)WRITE(23,117)J,AR(J)
115  CONTINUE
117  FORMAT(I2,',',F12.4)
320  CONTINUE
      RETURN
400  CONTINUE
439  WRITE(IO,440)ROCK,ROP(1),ROP(2),ROP(3),ROP(4),ROP(5)
440  FORMAT('1'///,' INTEGRATED AND SUMMARY DATA FOR THE FULL BIT'/
1    ' AT ALL SPECIFIED PENETRATION RATES * : '//
2    1X,A20,' AT ROP =',3X,F6.1,3X,F6.1,3X,F6.1,3X,F6.1,
3    3X,F6.1/'
4    '
      WRITE(IO,413)WOB(1),WOB(2),WOB(3),WOB(4),WOB(5)
413  FORMAT(/,1X,'TOTAL WOB (LBF)          =' ,1X,F8.1,
1    1X,F8.1,1X,F8.1,1X,F8.1,1X,F8.1)
      WRITE(IO,430)TORQ(1),TORQ(2),TORQ(3),TORQ(4),TORQ(5)
430  FORMAT(1X,'DRILLING TORQ. (FT-LBF)    =' ,1X,F8.1,
1    1X,F8.1,1X,F8.1,1X,F8.1,1X,F8.1)
      WRITE(IO,418)FX(1),FX(2),FX(3),FX(4),FX(5)
418  FORMAT(/,1X,'X SIDE FORCE (LBF)       =' ,1X,F8.1,
1    1X,F8.1,1X,F8.1,1X,F8.1,1X,F8.1)
      WRITE(IO,419)FY(1),FY(2),FY(3),FY(4),FY(5)
419  FORMAT(1X,'Y SIDE FORCE (LBF)        =' ,1X,F8.1,
1    1X,F8.1,1X,F8.1,1X,F8.1,1X,F8.1)
      WRITE(IO,499)FS(1),FS(2),FS(3),FS(4),FS(5)
499  FORMAT(1X,'RESULTANT SIDE FORCE (LBF) =' ,1X,F8.1,
1    1X,F8.1,1X,F8.1,1X,F8.1,1X,F8.1)
      WRITE(IO,431)BMX(1),BMX(2),BMX(3),BMX(4),BMX(5)
431  FORMAT(/,1X,'B. M. ABOUT X-AXIS (FT-LBF) =' ,1X,F8.1,
1    1X,F8.1,1X,F8.1,1X,F8.1,1X,F8.1)
      WRITE(IO,432)BMY(1),BMY(2),BMY(3),BMY(4),BMY(5)
432  FORMAT(1X,'B. M. ABOUT Y-AXIS (FT-LBF) =' ,1X,F8.1,
1    1X,F8.1,1X,F8.1,1X,F8.1,1X,F8.1)
      WRITE(IO,441)TWMAX(1),TWMAX(2),TWMAX(3),TWMAX(4),TWMAX(5)
441  FORMAT(/,1X,'MAX. WEARFLAT TEMP. (DEG. C)=' ,1X,F8.1,
1    1X,F8.1,1X,F8.1,1X,F8.1,1X,F8.1)
      WRITE(IO,442)WRMAX(1),WRMAX(2),WRMAX(3),WRMAX(4),WRMAX(5)
442  FORMAT(1X,'MAX. WEAR RATIO          =' ,1X,F8.2,

```

```

1 1X,F8.2,1X,F8.2,1X,F8.2,1X,F8.2)
IF(IO.EQ.IDTO)THEN
  IO=IPRNT
  GO TO 439
ENDIF
IF(IO.EQ.IPRNT)THEN
  WRITE(IO,460)BDNAME,WINAME,OCNAME
460 FORMAT(///10X,'* BIT DESIGN DATA FROM FILE ',A11/,
1 10X,' CUTTER WEAR CONFIGURATION FROM FILE ',A11/,
2 10X,' OPERATING PARAMETER DATA FROM FILE ',A11)
  IO=IDTO
ENDIF
800 IF(IP2.EQ.0)THEN
  IP2=IP2+1
  WRITE(IDTO,810)
810 FORMAT('/ DO YOU WANT TO SEND DATA TO BIT PLOT FILES? (Y/N)')
  CALL READA(M,AIN)
  IF(M.EQ.1.OR.(AIN.NE.'Y'.AND.AIN.NE.'N'))GOTO 800
  IF(AIN.NE.'Y')GOTO 990
900 WRITE(IDTO,910)
910 FORMAT('/ WOB VS. ROP? (Y/N)')
  CALL READA(M,AIN)
  IF(M.EQ.1.OR.(AIN.NE.'Y'.AND.AIN.NE.'N'))GOTO 900
  IF(AIN.EQ.'Y')THEN
    IB1=1
    OPEN(UNIT=24,NAME='WOBVROP.DAT',TYPE='NEW')
  ENDIF
915 WRITE(IDTO,920)
920 FORMAT('/ DRILLING TORQUE VS. ROP? (Y/N)')
  CALL READA(M,AIN)
  IF(M.EQ.1.OR.(AIN.NE.'Y'.AND.AIN.NE.'N'))GOTO 915
  IF(AIN.EQ.'Y')THEN
    IB2=1
    OPEN(UNIT=25,NAME='TRQVROP.DAT',TYPE='NEW')
  ENDIF
925 WRITE(IDTO,930)
930 FORMAT('/ RESULTANT SIDE FORCE VS. ROP? (Y/N)')
  CALL READA(M,AIN)
  IF(M.EQ.1.OR.(AIN.NE.'Y'.AND.AIN.NE.'N'))GOTO 925
  IF(AIN.EQ.'Y')THEN
    IB3=1
    OPEN(UNIT=26,NAME='SFRVROP.DAT',TYPE='NEW')
  ENDIF
935 WRITE(IDTO,940)
940 FORMAT('/ RESULTANT BENDING MOMENT VS. ROP? (Y/N)')
  CALL READA(M,AIN)
  IF(M.EQ.1.OR.(AIN.NE.'Y'.AND.AIN.NE.'N'))GOTO 935
  IF(AIN.EQ.'Y')THEN
    IB4=1
    OPEN(UNIT=27,NAME='MRVROP.DAT',TYPE='NEW')
  ENDIF
ENDIF
IF(IB1.EQ.1)WRITE(24,980)BDNAME,WINAME,OCNAME
IF(IB2.EQ.1)WRITE(25,980)BDNAME,WINAME,OCNAME
IF(IB3.EQ.1)WRITE(26,980)BDNAME,WINAME,OCNAME
IF(IB4.EQ.1)WRITE(27,980)BDNAME,WINAME,OCNAME
980 FORMAT(A11/,A11/,A11)
DO 965 IR=1,NROP
  IF(IB1.EQ.1)WRITE(24,970)ROP(IR),WOB(IR)
  IF(IB2.EQ.1)WRITE(25,970)ROP(IR),TORQ(IR)
  IF(IB3.EQ.1)WRITE(26,970)ROP(IR),FS(IR)
  IF(IB4.EQ.1)THEN
    BMR=(BMX(IR)**2+BMY(IR)**2)**0.5
    WRITE(27,970)ROP(IR),BMR
  ENDIF
965 CONTINUE
970 FORMAT(F10.2,',',F10.2)
990 CONTINUE
RETURN
500 WRITE(IO,501)WINAME
501 FORMAT('1'/' INITIAL WEAR CONFIGURATION DATA FROM FILE ',
1 A11,':')
WRITE(IO,510)(J,WL(J),WW(J),AW(J),J=1,NC)
510 FORMAT(
1 ' CUTTER WEARFLAT WEARFLAT WEARFLAT /
2 ' LENGTH WIDTH AREA /
3 ' (IN.) (IN.) (IN**2) /
4 (3X,I3,8X,F8.3,6X,F8.3,6X,F8.4))
IF(IND.EQ.2)GO TO 600
RETURN
600 WRITE(IO,601)OCNAME
601 FORMAT('1'/' OPERATING PARAMETER DATA FROM FILE ',
1 A11,':')

```

```

WRITE(IO,610)ROCK,RK,RX,FC,DC,DCS,C1A,
1 N1A,C1B,N1B,C2A,N2A,C2B,N2B,C6,RPM,TFL
610 FORMAT(
1 '
3 '          ROCK TYPE = ',A20/
4 '          ROCK THERMAL CONDUCTIVITY = ',F10.3,' BTU/HR-FT-F'/
5 '          ROCK THERMAL DIFFUSIVITY = ',F10.3,' FT**2/HR'/
6 '          ROCK-CUTTER FRICTION COEFFICIENT = ',F10.3/
7 '          WORN CUTTER DRAG COEFFICIENT = ',F10.3/
8 '          SHARP CUTTER DRAG COEFFICIENT = ',F10.3/
9 '          WORN TYPE A CUTTER CORR. CONSTANT C1 = ',E10.4/
10 '         WORN TYPE A CUTTER CORR. EXPONENT N1 = ',F10.3/
11 '         WORN TYPE B CUTTER CORR. CONSTANT C1 = ',E10.4/
12 '         WORN TYPE B CUTTER CORR. EXPONENT N1 = ',F10.3/
13 '         SHARP TYPE A CUTTER CORR. CONSTANT C2 = ',E10.4/
14 '         SHARP TYPE A CUTTER CORR. EXPONENT N2 = ',F10.3/
15 '         SHARP TYPE B CUTTER CORR. CONSTANT C2 = ',E10.4/
16 '         SHARP TYPE B CUTTER CORR. EXPONENT N2 = ',F10.3/
17 '         ABRASIVE WEAR CONSTANT C6 = ',E10.4,' IN**2/LBF'/
18 '         BIT ROTARY SPEED = ',F10.1,' RPM'/
19 '         DOWNHOLE COOLING FLUID TEMPERATURE = ',F10.1,' F' )
WRITE(IO,620)ROP(1),ROP(2),ROP(3),ROP(4),ROP(5)
620 FORMAT(
1 '          SPECIFIED BIT PENETRATION RATE(S) = ',F10.1,' FT/HR'/
2 4(41X,F10.1/))
RETURN
1000 CONTINUE
HL=HL+DLH
IF(MODW.EQ.1)WRITE(IDTO,1001)ASUBWN,NCMAX,DLH,HL,C6
1001 FORMAT('1/' ***** NEW CUTTER WEAR CONFIGURATION *****//
1 ' OBTAINED BY SPECIFYING HARD-ROCK WEAR MODE'/
2 '   AND NEW WEARFLAT AREA OF ',F7.4/
3 '   FOR CUTTER NUMBER ',I3//
4 ' COMPUTED LENGTH OF HOLE SINCE LAST WEAR CONF. = ',F8.1,' FT'/
5 '   TOTAL LENGTH OF HOLE DRILLED SINCE START = ',F8.1,' FT'/
6 ' (USING ABRASIVE WEAR CONSTANT OF ',E12.4,')'//)
IF(MODW.EQ.2)WRITE(IDTO,1010)ASUBWN,NCMAX,DLH,HL,C6
1010 FORMAT('1/' ***** NEW CUTTER WEAR CONFIGURATION *****//
1 ' OBTAINED BY SPECIFYING SOFT-ROCK WEAR MODE'/
2 '   AND NEW WEARFLAT AREA OF ',F7.4/
3 '   FOR CUTTER NUMBER ',I3//
4 ' COMPUTED LENGTH OF HOLE SINCE LAST WEAR CONF. = ',F8.1,' FT'/
5 '   TOTAL LENGTH OF HOLE DRILLED SINCE START = ',F8.1,' FT'/
6 ' (USING ABRASIVE WEAR CONSTANT OF ',E12.4,')'//)
WRITE(IO,510)(J,WL(J),WW(J),AW(J),J=1,NC)
RETURN
1100 DO 1105 J=1,NC
WRITE(IDWN,1103)J,WL(J),WW(J),AW(J)
1103 FORMAT(1X,I3,1X,F10.3,1X,F10.3,1X,F10.4)
1105 CONTINUE
IF(MODW.EQ.1)WRITE(IPRNT,1001)ASUBWN,NCMAX,DLH,HL,C6
IF(MODW.EQ.2)WRITE(IPRNT,1010)ASUBWN,NCMAX,DLH,HL,C6
WRITE(IPRNT,1110)WINAME
1110 FORMAT(' (THIS CONFIGURATION WAS STORED IN DISK FILE '
1 ,A11,')'//)
WRITE(IPRNT,510)(J,WL(J),WW(J),AW(J),J=1,NC)
RETURN
END

```

APPENDIX C
THERMAL NUMERICAL MODELING OF A 0.75-INCH PDC CUTTER

APPENDIX C

THERMAL NUMERICAL MODELING OF A 0.75-INCH PDC CUTTER

Our earlier work [22,26,27] presented thermal modeling results for PDC cutters with 0.50-inch diameter compacts. Because of the availability of cutters with larger compacts and because of the apparent increased efficiency associated with larger cutters, the models of the earlier work were modified to represent cutters using 0.75-inch diameter compacts.

Three wear configurations were used in this study: mildly worn ($L=0.0266$ inch), moderately worn ($L=0.096$ inch), and severely worn ($L=0.148$ inch) (see Figure 29). In the mildly worn case, the wearflat extends only across the diamond layer; hence, $L=t_d/\cos \beta$. A diamond thickness of 0.025 inch was assumed. In the moderately and severely worn cases, the wearflat extends into the WC-Co compact to which the PDC layer is bonded. The length of the wearflat for each wear configuration is shown in Table C-1 on the next page. The values used for the thermal properties of the cutter materials were the same as those used in the baseline case of our earlier work [27].

Both fully exposed cutters and cutters recessed into the bit body were considered. With the fully exposed cutters, convective cooling boundary conditions were applied to all exposed cutter and bit surfaces. With the recessed cutters, convective cooling along the diamond face was restricted to the lower half of the face, and no convective cooling was provided to the top surfaces of the cutter compact. All surfaces not shown as being convectively cooled in Figure 29 were given an insulating boundary condition. A fixed, uniform heat flux, q , was applied as a boundary condition at the cutter wearflat for a variety of convective cooling coefficients ranging from 17.61 to 1.761×10^4 Btu/hr ft² °F (0.01 to 10.0 W/cm² °C).

As in the earlier studies, a general purpose finite element thermal computer code, COYOTE [50], was used to compute temperature distributions in the cutters. The average temperature computed for the surface node points along the wearflat, \bar{T}_w , was reduced by the assumed cooling fluid temperature, T_f , and divided by the input heat flux to obtain the thermal response of the cutter:

$$f = \frac{\bar{T}_w - T_f}{q} \quad (C-1)$$

Values of f are shown in Table C-1 as a function of the assumed cooling coefficients for both the recessed and fully exposed cutters. Also shown for comparison purposes are the results obtained in Ref. 27 for cutters with a 0.5-inch diameter compact.

TABLE C-1

COMPUTED THERMAL RESPONSE FUNCTION FOR 0.75-INCH AND 0.5-INCH CUTTERS

CF*	Thermal Response Function, f ($^{\circ}\text{C cm}^2/\text{W}$)											
	Mildly Worn ($L=0.027$)				Mod. Worn ($L=0.096$)				Sev. Worn ($L=0.148$)			
	h (Btu/hr ft ² $^{\circ}\text{F}$)				h (Btu/hr ft ² $^{\circ}\text{F}$)				h (Btu/hr ft ² $^{\circ}\text{F}$)			
	17.61	176.1	1761	17610	17.61	176.1	1761	17610	17.61	176.1	1761	17610
1	.830	.174	.067	.026	3.003	.609	.234	.106	4.653	.913	.345	.166
2			.064				.224				.328	
3	.956	.170	.064	.026					5.459	.896	.325	.166

* CF = cutter configuration

1 = 0.75-inch compact cutter recessed

2 = 0.75-inch compact cutter fully exposed

3 = 0.50-inch compact cutter fully exposed (Ref. 27). The length of the "severely worn" wearflat of the 0.75-inch cutter is the same as the length of the "moderately worn" wearflat of the 0.5-inch cutter in Ref. 27. Wearflat length L is in inches.

Note that with the moderate cooling coefficients, the thermal response function for the recessed 0.75-inch cutter is slightly larger than that for the 0.5-inch cutter in cases where a direct comparison is possible. This is caused by the larger mean distance for heat to flow from the wearflat to a cooled surface. For the lower cooling coefficients, however, the thermal response function for the recessed 0.75-inch cutter is lower than that for the 0.5-inch cutter. This is because at very low convective cooling rates, heat transfer is controlled by convection, not conduction, so the larger cooled surface area of the 0.75-inch cutter results in a cooler wearflat. In any case, the difference in thermal response function between the different size cutters is not significant.

The effects of fully exposing the 0.75-inch cutter appear to also be insignificant in that the thermal response function at a given convective cooling coefficient is approximately the same as that for the recessed 0.75-inch cutter. This is due to the fact that most of the heat is convected from the lower half of the diamond face, and cooling the upper half of the face does little to further cool the wearflat. It should be noted, however, that by fully exposing the cutter, the standoff distance between the bit body and the rock surface is increased, thereby reducing fluid velocities and convective cooling coefficients. As a result, a bit with fully exposed 0.75-inch cutters could run significantly hotter than a bit with recessed 0.75-inch cutters at the same drilling fluid flow rate. For this reason, the results for the recessed 0.75-inch cutters are incorporated into PDCWEAR.

APPENDIX D
PDCWEAR INPUT GUIDE

APPENDIX D

PDCWEAR INPUT GUIDE

Three input files are required to run PDCWEAR. These files contain the bit design data, the initial cutter wear configurations, and the operating conditions. The names chosen for these files may be 1 to 11 alphanumeric characters in length, including the file extension. The utility program, FORMAT, may be run interactively by the user to properly format input parameter values and create the required input files. FORMAT produces three files suitable for input to PDCWEAR. These names of these files are selected by the user. A listing of FORMAT is provided in Appendix E.

Bit Design Data File

This file contains data describing the sizes of cutters, their locations in three-dimensional space, their backrake angles, and their convective cooling coefficients. Data is read into PDCWEAR in the following format:

```
      READ(____,102)RNOM,BNOM,HNOM
102  FORMAT(1X,F10.3,1X,F10.2,1X,F10.2)
      READ(____,119)(J,RP(J),AP(J),HPP(J),AI(J),RR(J),BR(J),HR(J),J=1,NC)
119  FORMAT(1X,I3,7(1X,F7.3))
```

where:

RNOM - nominal radius of cutter compact, r_o (inches)
BNOM - nominal cutter backrake angle, β (degrees)
HNOM - nominal cutter convective cooling coefficient, h_o (Btu/hr ft²°F)
RP(J) - radial position of jth cutter, R (inches), see Figure 31
AP(J) - angular position of jth cutter, θ (degrees)
HPP(J) - longitudinal position of jth cutter, H' (inches)
AI(J) - inclination angle of jth cutter, ϕ (degrees)
RR(J) - relative compact radius of jth cutter, r/r_o
BR(J) - relative backrake angle of jth cutter,
HR(J) - relative convective cooling coefficient of jth cutter, h/h_o ;
if positive, jth cutter is a type A cutter; if negative,
jth cutter is a type B cutter;
NC - number of cutters in bit design

Some of these parameters are illustrated in Figure 31.

The radius of the cutter compact affects the cutter profile and thus the effective depth of cut and cutter forces. The compact radius traditionally used in PDC bits is approximately 0.25 inches (0.50-inch diameter compacts). The algorithm used in the code to compute the cross-sectional area of cut, volume of cut, and effective depth of cut for each cutter does not impose any restrictions on the size of the cutters considered. The geometry must simply be that of a circular disk affixed to the bit body at some backrake angle greater than zero (i.e., a negative rake). The algorithms used to compute cutter wearflat temperatures and estimate new wearflat dimensions make use of tabulated data that are accurate only for 0.5 inch and 0.75 inch diameter

compacts. This, in principle, restricts input cutter radii to one-half those values. Calculations for other input radii are done by interpolating or extrapolating on the tabulated data.

The cutter backrake angle defines the degree to which the circular cutter compact profile assumes an elliptical geometry. This angle thus helps define the cutting profile and the resulting cutter forces. In general, a 20° backrake seems to be optimal for hard-rock drilling with PDC cutters [8], while $5-15^\circ$ has been found to minimize cutter forces in softer rocks [8,37]. The input value for the nominal backrake angle must be between 0 and 90° .

The cutter convective cooling coefficient is a function of the hydraulics design of the bit (location and design of fluid ports), the type of drilling fluid, and the flow rate. Shown in Figures D-1 and D-2 are laboratory data obtained in our earlier work [23,27]. Convective cooling coefficients for water flowing past a single instrumented PDC cutter are shown for a uniform flow field and for a low-pressure (80 psi) waterjet flow field. These data are used in Figure D-3 to estimate typical downhole cooling coefficients for a gage cutter on a bit with both air and water cooling. It is seen that coefficients on the order of $1761 \text{ Btu/hr ft}^2 \text{ } ^\circ\text{F}$ ($1.0 \text{ W/cm}^2 \text{ } ^\circ\text{C}$) with water-based drilling muds are typical. With air cooling, coefficients on the order of $88 \text{ Btu/hr ft}^2 \text{ } ^\circ\text{F}$ ($0.05 \text{ W/cm}^2 \text{ } ^\circ\text{C}$) are more common. Effects of fluid port placement, fluid properties, and poor cutter cleaning are discussed in our previous work [23,27].

Because cutter compact radii, backrake angles, and cooling coefficients are not likely to vary significantly over the face of any given bit design, these quantities are entered into the program as relative quantities, i.e. the actual value divided by a nominal value. For instance, if all cutters are assumed identical on a given bit, the parameters RR(J), BR(J), and HR(J) would all be 1.0 for each cutter.

The sign of the relative cooling coefficient is used to identify the type of each cutter. Positive values of the relative cooling coefficients denote type A cutters, which are governed by the penetrating force correlation constants entered for that cutter type in the operating conditions data file. Negative values of the relative cooling coefficient denote type B cutters, which are governed by a separate set of correlation constants entered in the operating conditions data file.

The radial, angular, and longitudinal positions of the cutters are by far the most important design parameters considered by the program. These positions define the center of each cutter compact in the x',y',z' coordinate system (see Figure 31). They determine the cutting profile of the bit and the distribution of cutting loads among the various cutters. The radial position, RP, is the distance in an x',y' plane from the longitudinal (z') axis of the bit to the compact center. Cutters must be entered into the code in ascending

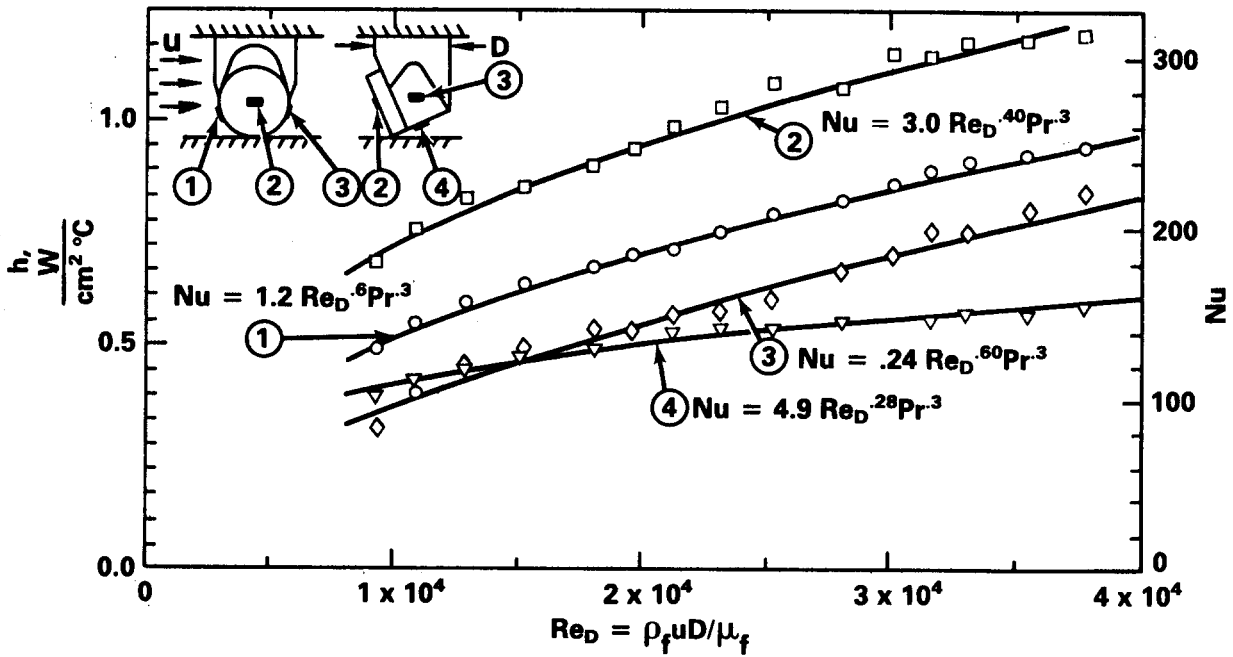


Figure D-1 - Measured heat transfer coefficients for various locations on a stud-mounted 0.5-inch diameter compact cutter due to a uniform flow of water past the cutter (from Ref. 23).

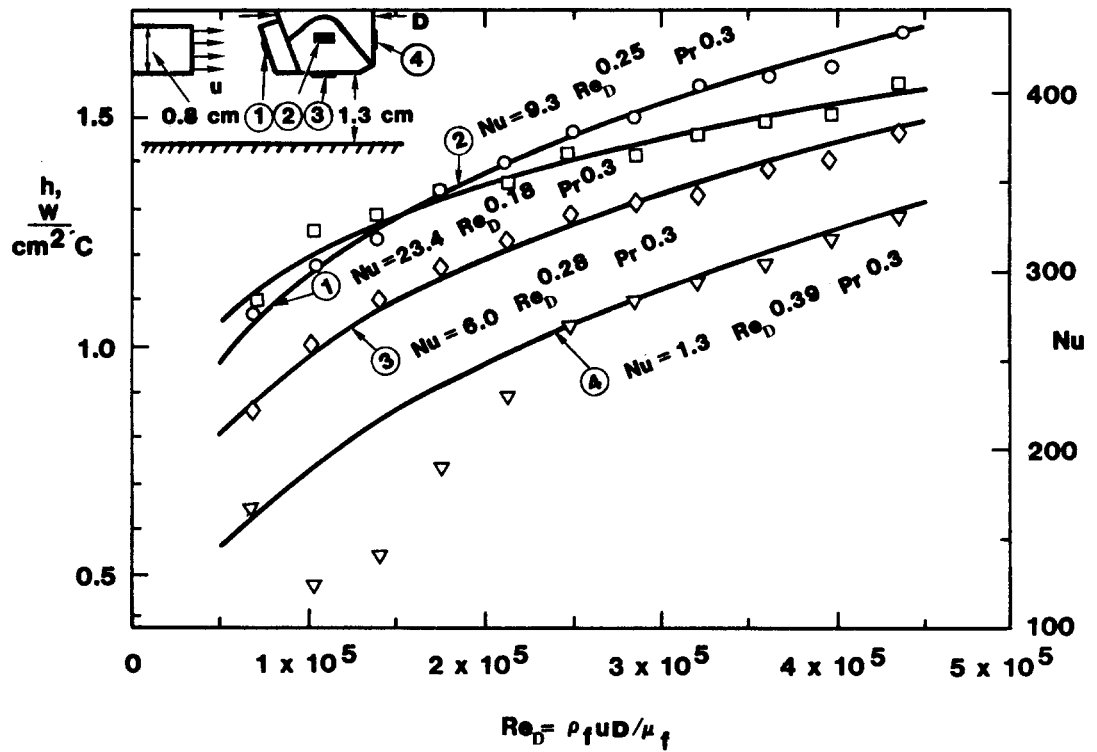


Figure D-2 - Measured heat transfer coefficients for various locations on a stud-mounted 0.5-inch diameter compact cutter due to impingement of a low-pressure (80 psi) waterjet (from Ref. 27).

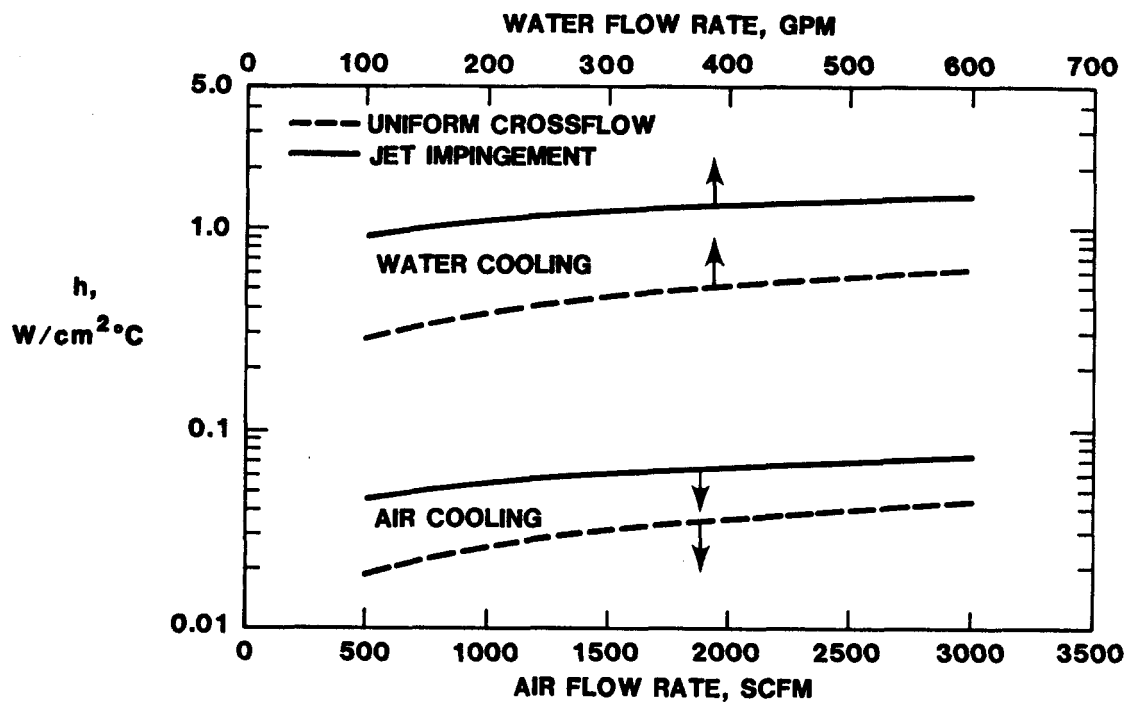


Figure D-3 - Mean PDC cutter heat transfer coefficients under typical air and water drilling conditions (from Ref. 27).

radial order (i.e., increasing RP), although more than one cutter may share the same radial position. The angular position, AP, of the cutter is also measured in an x'-y' plane, counterclockwise from the x'-axis (looking at the face of the bit). The longitudinal position, H', is the distance measured parallel to the z'-axis from the center of the cutter compact to an arbitrary reference plane parallel to the x'-y' axes. It is convenient to make the reference plane pass through the center of one of the cutters (i.e., H'=0 for that cutter). In any case, cutters with positive longitudinal positions are defined as those that lie ahead of the reference plane, in the drilling direction.

The cutter inclination angle, AI, is the angle at which the cutter is mounted on the bit, i.e. the angle between the longitudinal (z') axis of the bit and the minor axis of the elliptical cutter profile. In a stud-mounted bit, this is equivalent to the angle between the longitudinal axis of the bit and the longitudinal axis of the cutter stud. Most cutters are mounted in holes drilled roughly perpendicular to the surface of the bit body; thus the inclination angles are generally described approximately by the bit body profile. Cutters mounted on convex surfaces on the bit body are defined as having positive inclination angles. Concave surfaces are sometimes designed in the PDC bit bodies in the center of the bit to create a cone of rock that helps stabilize the bit while drilling (see, for example, Figure 30). Cutters mounted in such concave regions would generally have negative inclination angles.

In principle, there is no limitation on the number of cutters considered by PDCWEAR. There is a parameter, MXCUT, that is used to dimension arrays in several subroutines for storing cutter-related quantities. This parameter is currently set at 48 and must be increased in size if a larger number of cutters is to be input to the program. To minimize RAM storage requirements while running the program, parameter MXCUT can be reduced to a value equal to the number of cutters on the bit.

Initial Cutter Wear Configuration File

This file describes the cutter wearflats that are to be initially considered by PDCWEAR. The following data are read by the program:

```

      READ(____,419)(J,WL(J),WW(J),AW(J),J=1,NC)
419  FORMAT(1X,I3,1X,F10.3,1X,F10.3,1X,F10.4)

```

where

WL(J) - length of wearflat of jth cutter, L (inches), measured in the center of the wearflat in the direction parallel to cutter travel

WW(J) - width of wearflat of jth cutter, w (inches), measured at the diamond face

AW(J) - wearflat area of jth cutter, A_w (inch²)

These parameters refer to the portion of the wearflat in direct contact with the rock surface being cut.

The algorithms used to compute cutter performance parameters consider the three wear quantities to be independent. The wearflat width affects the cutting profile and thus the cross-sectional area of cut, volume of cut, and

effective depth of cut. The wearflat area defines the cutter penetrating force that develops at a given depth of cut and the frictional heat generated at the cutter/rock interface. The wearflat length is a variable in the wearflat temperature equation, Eq. 31, which predicts an increase in temperature with wearflat length.

The algorithm used to estimate new cutter wear configurations based on computed wear ratios does require the three wearflat dimensions for each cutter to be consistent. For the hard-rock wear mode, Eqs. 38, 39, and 40 relate the wearflat width and length to the wearflat area. For the soft-rock wear mode, Eqs. 45-47 are more relevant (see subsection 3.4). It is important that initial wear configurations for each cutter conform with the appropriate equations if progressive wear calculations are to be made after the initial performance calculations are complete.

Operating Parameter Data File

This file defines the intrinsic drillability of the rock, its thermal properties, the rotary speed of the bit, the downhole cooling fluid temperature, and the penetration rates for which performance calculations are desired. The data are read by the program in the following format:

```

      READ(____,709)ROCK
709  FORMAT(1X,A20)
      READ(____,720)RK
720  FORMAT(1X,F10.3)
      READ(____,720)RX
      READ(____,720)FC
      READ(____,720)DC
      READ(____,720)DCS
      READ(____,722)C1A
722  FORMAT(1X,E10.4)
      READ(____,720)N1A
      READ(____,722)C1B
      READ(____,720)N1B
      READ(____,722)C2A
      READ(____,720)N2A
      READ(____,722)C2B
      READ(____,720)N2B
      READ(____,722)C6
      READ(____,725)N
725  FORMAT(1X,F10.1)
      READ(____,725)TFL
      READ(____,730)(ROP(I),I=1,5)
730  FORMAT(5(1X,F10.1))

```

where

- ROCK - alphanumeric name for the rock associated with the listed values of the below parameters
- RK - thermal conductivity of the rock, k_2 (Btu/hr ft⁰F)
- RX - thermal diffusivity of the rock, χ_2 (ft²/hr)
- FC - friction coefficient between the cutter and the rock, μ

- DC - drag coefficient, μ_d , for worn cutters (see Eq. 5a)
- DCS - drag coefficient, μ_d , for sharp cutters (see Eq. 5a)
- C1A - penetrating stress correlation constant, C_1 , for worn type A cutters (see Eq. 3)
- N1A - penetrating stress correlation exponent, n_1 , for worn type A cutters (see Eq. 3)
- C1B - penetrating stress correlation constant, C_1 , for worn type B cutters (see Eq. 3)
- N1B - penetrating stress correlation exponent, n_1 , for worn type B cutters (see Eq. 3)
- C2A - penetrating force correlation constant, C_2 , for sharp type A cutters (see Eq. 4)
- N2A - penetrating force correlation exponent, n_2 , for sharp type A cutters (see Eq. 4)
- C2B - penetrating force correlation constant, C_2 , for sharp type B cutters (see Eq. 4)
- N2B - penetrating force correlation exponent, n_2 , for sharp type B cutters (see Eq. 4)
- C6 - abrasive wear constant for the cutter material/rock combination (in^2/lbf) (see Eq. 33)
- N - bit rotary speed, N (rev/min)
- TFL - cooling fluid temperature, T_f ($^{\circ}\text{F}$)
- ROP(I) - ith value of the rate of penetration, ROP (ft/hr); up to five values permitted; at least three values required.

The ROCK parameter is used simply to identify the material associated with the listed parameters. An alphanumeric name up to 20 characters in length may be entered here.

The thermal conductivity, RK, and diffusivity, RX, of the rock affect cutter wearflat temperatures because they control the amount of frictional heat generated at the wearflat that the rock absorbs. Typical values for the conductivity range from 0.35 Btu/hr $\text{ft}^{\circ}\text{F}$ for certain shales to over 2.9 Btu/hr $\text{ft}^{\circ}\text{F}$ for anhydrite. Reference [51] contains an extensive compilation of thermal conductivities for most rock types encountered in drilling. The thermal diffusivity is a collection of rock properties:

$$\chi_2 = k_2 / (\rho_2 c_2) \quad , \quad (\text{D-1})$$

where ρ_2 is the rock density and c_2 is the rock specific heat.

The friction coefficient, FC, between the cutter and the rock is one of the most important parameters in the wearflat temperature equation, Eq. 31. This parameter essentially determines what fraction of the cutting power expended by the cutter is converted to frictional heat. Values measured in

the laboratory [19] with four fluid types, four rock types, and two cutting speeds range from 0.03 to 0.31 and are listed in Table D-1.

TABLE D-1
MEASURED PDC/ROCK FRICTION COEFFICIENTS (REF. 19)

ROCK TYPE	CUTTING SPEED (m/s)	FRICTION COEFFICIENT			
		Water	Mud	Diesel	Air
Marble	1	0.20	0.17	0.34	0.33
	5	0.15	0.11	0.13	0.15
Sandstone	1	0.03	0.04	0.05	0.10
	5	0.05	0.04	0.30	0.30
Granite	1	0.09	--	--	0.18
	5	0.05	--	--	0.14
Shale	1	0.09	--	--	0.18
	5	0.06	--	--	0.15

The cutter drag coefficients for sharp and worn cutters have been shown to be functions of rock type and fluid environment (Figures 13, 14, 15, and 17). The drag coefficient is not strongly dependent on depth of cut, so a mean value is all that the program requires. Since the drag coefficient for sharp cutters may be substantially higher than those for worn cutters over the range of interest in depth of cut, the program requires values, DC and DCS, for each of these classes of cutter wear.

Because of the possibility of using waterjet assistance in bit design, different parameters describing the intrinsic drillability are accepted for two types of cutter, type A and type B. The cutter penetrating stress (for worn cutters) and penetrating force (for sharp cutters) correlation constants and exponents for both types (A and B) must be input to the program, although dummy (zero) values may be used for type B cutters if none of the cutters are provided jet assistance. These correlation constants are determined from experimental data, as described previously. In the absence of rock- and environment-specific data for a particular application, the values shown on Figures 10, 11, 12, and 16 may be used for estimating bit performance.

The abrasive wear constant may be determined using single-cutter wear data as described by the equations developed in Ref. 32. In the absence of rock- and environment-specific data for a particular application, the value determined for hard sandstones, $C_6 = 6.89 \times 10^{-13} \text{ in}^2/\text{lbf}$, may be used for estimating bit performance. Since this parameter is used only to calculate the length of hole drilled, the relative performance of different bit designs can be determined by using any non-zero value of C_6 .

The rotary speed of the bit is important because it defines the cutting speeds and thus the frictional heating rate and temperatures of the cutters. Low rotary speeds, 50-200 RPM, are desirable for hard-rock drilling with PDC bits in order to minimize thermal wear effects [20,31]. Downhole turbine speeds up to 1000 RPM may be used successfully if the rock formation is very soft [31]. Cutter forces may be reduced by increasing rotary speed while maintaining a constant penetration rate. Generally, however, the higher speeds tend to increase cutter temperatures more than the lower penetrating stresses reduce them, resulting in higher net temperatures. Also, for a given WOB and drilled borehole length, cutters travel farther abrading against the rock surface when the bit is rotated at a higher speed.

The downhole fluid temperature defines the lowest possible wearflat temperature for the analysis. Downhole fluid temperatures generally exceed 125°F in petroleum drilling and 200°F in geothermal drilling. Computer models have been developed for predicting downhole fluid conditions under a wide variety of conditions [52].

Since knowledge of bit performance over a range of penetration rates is usually desired, the program repeats the calculations at the specified rotary speed for up to five different penetration rates specified by the user. The only requirements on the specified penetration rates is that they be entered in ascending order. Fewer than five penetration rates may be specified by entering zero values in the appropriate data fields after the highest penetration rate specified; however, at least three penetration rates must be specified if cutter wear is to be calculated by the program (the program uses wear ratios computed for the third penetration rate specified). Care should be taken to ensure that the resulting depths of cut do not extend beyond the range for which the cutter stress and force correlation constants and exponents are valid. Practical values for the penetration rate generally range from 5 to 100 ft/hr.

APPENDIX E
LISTING OF FORTRAN PROGRAM FORMAT

```

PROGRAM FORMAT
REAL N1A,N1B,N2A,N2B
CHARACTER *11 INNAME,FRNAME,WDNAME,RKNAME
CHARACTER *20 ROCK
DIMENSION RP(50),AP(50),HPP(50),AI(50),RR(50),
1 BR(50),HR(50),WL(50),WW(50),AW(50)
INNAME=' '
IDISK=10
WDNAME=' '
IDISK7=7
RKNAME=' '
IDISK8=8
WRITE(5,5)
5 FORMAT(' DO YOU WANT TO CREATE BIT DESIGN DATA FILE (Y=1)?')
IFLAG=0
READ(5,*)IFLAG
IF(IFLAG.NE.1)GO TO 305
10 WRITE(5,101)
101 FORMAT(/' ENTER NAME OF FILE TO CONTAIN BIT DESIGN DATA'/
1 ' (11 CHAR. OR LESS, INCLUDING .EXTENSION)')
READ(5,'(A11)')INNAME
IF(INNAME.EQ.' ')GO TO 10
OPEN(IDISK,FILE=INNAME,STATUS='NEW')
WRITE(5,20)
20 FORMAT(' ENTER NOMINAL RADIUS OF CUTTER COMPACTS, RNOM')
READ(5,*)RNOM
WRITE(5,22)
22 FORMAT(' ENTER NOMINAL CUTTER BACKRAKE ANGLE, BNOM')
READ(5,*)BNOM
WRITE(5,25)
25 FORMAT(' ENTER NOMINAL CUTTER CONVECTIVE COOLING COEFFICIENT,'
1 ' HNOM')
READ(5,*)HNOM
WRITE(IDISK,102)RNOM,BNOM,HNOM
102 FORMAT(1X,F10.3,1X,F10.2,1X,F10.2)
WRITE(5,30)
30 FORMAT(' ENTER NUMBER OF CUTTERS, NC')
READ(5,*)NC
DO 11 J=1,NC
WRITE(5,35)J
35 FORMAT(' ENTER RADIAL POSITION, RP, FOR CUTTER ',I3)
READ(5,*)RP(J)
11 CONTINUE
DO 12 J=1,NC
WRITE(5,36)J
36 FORMAT(' ENTER ANGULAR POSITION, AP, FOR CUTTER ',I3)
READ(5,*)AP(J)
12 CONTINUE
DO 13 J=1,NC
WRITE(5,37)J
37 FORMAT(' ENTER LONGITUDINAL POSITION, HPP, FOR CUTTER ',I3)
READ(5,*)HPP(J)
13 CONTINUE
DO 14 J=1,NC
WRITE(5,38)J
38 FORMAT(' ENTER INCLINATION ANGLE, AI, FOR CUTTER ',I3)
READ(5,*)AI(J)
14 CONTINUE
DO 15 J=1,NC
WRITE(5,39)J
39 FORMAT(' ENTER RELATIVE COMPACT RADIUS, RR, FOR CUTTER ',I3)
READ(5,*)RR(J)
15 CONTINUE
DO 16 J=1,NC
WRITE(5,40)J
40 FORMAT(' ENTER RELATIVE BACKRAKE ANGLE, BR, FOR CUTTER ',I3)
READ(5,*)BR(J)
16 CONTINUE
DO 17 J=1,NC
WRITE(5,41)J
41 FORMAT(' ENTER RELATIVE CONVECTIVE HEAT TRANSFER COEFFICIENT,'
1 ' HR, FOR CUTTER ',I3/' (NEGATIVE IF'
1 ' TYPE B CUTTER)')
READ(5,*)HR(J)
17 CONTINUE
DO 18,J=1,NC
WRITE(IDISK,119)J,RP(J),AP(J),HPP(J),AI(J),
1 RR(J),BR(J),HR(J)
119 FORMAT(1X,I3,1X,F7.3,1X,F7.3,1X,F7.3,
1 1X,F7.3,1X,F7.3,1X,F7.3,1X,F7.3)
18 CONTINUE
CLOSE(IDISK,STATUS='KEEP')
305 WRITE(5,306)

```

```

306 FORMAT(' DO YOU WANT TO CREATE WEAR FILE (Y=1)?')
    IFLAG=0
    READ(5,*)IFLAG
    IF(IFLAG.NE.1)GO TO 505
310 WRITE(5,401)
401 FORMAT('/ ENTER NAME OF FILE TO CONTAIN INITIAL CUTTER'
1 ' WEAR CONFIGURATIONS' /
2 ' (11 CHAR. OR LESS, INCLUDING .EXTENSION)')
    READ(5,'(A11)')WDNAME
    IF(WDNAME.EQ.' ')GO TO 310
    OPEN(IDISK7,FILE=WDNAME,STATUS='NEW')
    WRITE(5,30)
    READ(5,*)NC
    DO 311 J=1,NC
    WRITE(5,350)J
350 FORMAT(' ENTER WEARFLAT LENGTH, WL, FOR CUTTER ',I3)
    READ(5,*)WL(J)
311 CONTINUE
    DO 312 J=1,NC
    WRITE(5,351)J
351 FORMAT(' ENTER WEARFLAT WIDTH, WW, FOR CUTTER ',I3)
    READ(5,*)WW(J)
312 CONTINUE
    DO 313 J=1,NC
    WRITE(5,352)J
352 FORMAT(' ENTER WEARFLAT AREA, AW, FOR CUTTER ',I3)
    READ(5,*)AW(J)
313 CONTINUE
    DO 319 J=1,NC
    WRITE(IDISK7,419)J,WL(J),WW(J),AW(J)
419 FORMAT(1X,I3,1X,F10.3,1X,F10.3,1X,F10.4)
319 CONTINUE
    CLOSE(IDISK7,STATUS='KEEP')
505 WRITE(5,506)
506 FORMAT(' DO YOU WANT TO CREATE OPERATING PARAMETER DATA'
1 ' FILE (Y=1)?')
    IFLAG=0
    READ(5,*)IFLAG
    IF(IFLAG.NE.1)GO TO 1000
510 WRITE(5,601)
601 FORMAT('/ ENTER NAME OF FILE TO CONTAIN OPERATING PARAMETER'
1 ' DATA' /' (11 CHAR. OR LESS, INCLUDING .EXTENSION)')
    READ(5,'(A11)')RKNAME
    IF(RKNAME.EQ.' ')GO TO 510
    OPEN(IDISK8,FILE=RKNAME,STATUS='NEW')
    WRITE(5,708)
708 FORMAT(' ENTER ROCK TYPE (NAME)')
    READ(5,'(A20)')ROCK
    WRITE(IDISK8,709)ROCK
709 FORMAT(1X,A20)
    WRITE(5,715)
715 FORMAT(' ENTER ROCK THERMAL CONDUCTIVITY, RK')
    READ(5,*)RK
    WRITE(IDISK8,720)RK
720 FORMAT(1X,F10.3)
    WRITE(5,725)
725 FORMAT(' ENTER ROCK THERMAL DIFFUSIVITY, RX')
    READ(5,*)RX
    WRITE(IDISK8,720)RX
    WRITE(5,728)
728 FORMAT(' ENTER ROCK-CUTTER FRICTION COEFFICIENT, FC')
    READ(5,*)FC
    WRITE(IDISK8,720)FC
    WRITE(5,735)
735 FORMAT(' ENTER DRAG COEFFICIENT, DC, FOR WORN CUTTERS')
    READ(5,*)DC
    WRITE(IDISK8,720)DC
    WRITE(5,736)
736 FORMAT(' ENTER DRAG COEFFICIENT, DCS, FOR SHARP CUTTERS')
    READ(5,*)DCS
    WRITE(IDISK8,720)DCS
    WRITE(5,740)
740 FORMAT(' ENTER PENETRATING STRESS CORRELATION CONSTANT'
1 ' FOR WORN TYPE A CUTTERS, C1A')
    READ(5,*)C1A
    WRITE(IDISK8,825)C1A
825 FORMAT(1X,E10.4)
    WRITE(5,742)
742 FORMAT(' ENTER PENETRATING STRESS CORRELATION EXPONENT'
1 ' FOR WORN TYPE A CUTTERS, N1A')
    READ(5,*)N1A
    WRITE(IDISK8,720)N1A
    WRITE(5,840)

```

```

840 FORMAT(' ENTER PENETRATING STRESS CORRELATION CONSTANT'
1 ' FOR WORN TYPE B CUTTERS, C1B')
  READ(5,*)C1A
  WRITE(IDISK8,825)C1A
  WRITE(5,842)
842 FORMAT(' ENTER PENETRATING STRESS CORRELATION EXPONENT'
1 ' FOR WORN TYPE B CUTTERS, N1B')
  READ(5,*)N1B
  WRITE(IDISK8,720)N1B
  WRITE(5,746)
746 FORMAT(' ENTER PENETRATING FORCE CORRELATION CONSTANT'
1 ' FOR SHARP TYPE A CUTTERS, C2A')
  READ(5,*)C2A
  WRITE(IDISK8,825)C2A
  WRITE(5,747)
747 FORMAT(' ENTER PENETRATING FORCE CORRELATION EXPONENT'
1 ' FOR SHARP TYPE A CUTTERS, N2A')
  READ(5,*)N2A
  WRITE(IDISK8,720)N2A
  WRITE(5,846)
846 FORMAT(' ENTER PENETRATING FORCE CORRELATION CONSTANT'
1 ' FOR SHARP TYPE B CUTTERS, C2B')
  READ(5,*)C2A
  WRITE(IDISK8,825)C2A
  WRITE(5,847)
847 FORMAT(' ENTER PENETRATING FORCE CORRELATION EXPONENT'
1 ' FOR SHARP TYPE B CUTTERS, N2B')
  READ(5,*)N2B
  WRITE(IDISK8,720)N2B
  WRITE(5,754)
754 FORMAT(' ENTER ABRASIVE WEAR CONSTANT, C6')
  READ(5,*)C6
  WRITE(IDISK8,825)C6
  WRITE(5,755)
755 FORMAT(' ENTER BIT ROTARY SPEED, N')
  READ(5,*)RPM
  WRITE(IDISK8,790)RPM
790 FORMAT(1X,F10.1)
  WRITE(5,760)
760 FORMAT(' ENTER DOWNHOLE COOLING FLUID TEMPERATURE, TFL')
  READ(5,*)TFL
  WRITE(IDISK8,790)TFL
  WRITE(5,765)
765 FORMAT(' ENTER BIT PENETRATION RATES, ROP(1), ROP(2), ROP(3),
1 ' ROP(4), AND ROP(5)')
  READ(5,*)ROP1,ROP2,ROP3,ROP4,ROP5
  WRITE(IDISK8,730)(ROP1,ROP2,ROP3,ROP4,ROP5)
730 FORMAT(1X,F10.1,1X,F10.1,1X,F10.1,1X,F10.1,1X,F10.1)
  CLOSE(IDISK8,STATUS='KEEP')
1000 CONTINUE
  END

```

APPENDIX F

LISTING OF PDCWEAR INPUT FILES USED
IN DEMONSTRATION ANALYSIS

TABLE F-1

PDCWEAR INPUT FILE CONTAINING BIT DESIGN DATA
FOR DEMONSTRATION ANALYSIS (BITDES.DAT)

	0.375	20.00	1700.00				
1	0.350	0.000	0.625	-15.000	1.000	1.000	1.000
2	0.800	215.000	0.760	-10.000	1.000	1.000	1.000
3	1.250	110.000	0.895	-5.000	1.000	1.000	1.000
4	1.600	45.000	1.000	-2.000	1.000	1.000	1.000
5	1.950	285.000	1.000	0.000	1.000	1.000	1.000
6	2.300	165.000	1.000	2.000	1.000	1.000	1.000
7	2.495	0.000	0.990	5.000	1.000	1.000	1.000
8	2.635	240.000	0.970	10.000	1.000	1.000	1.000
9	2.775	120.000	0.940	15.000	1.000	1.000	1.000
10	2.915	320.000	0.898	20.000	1.000	1.000	1.000
11	3.055	200.000	0.844	25.000	1.000	1.000	1.000
12	3.195	80.000	0.776	30.000	1.000	1.000	1.000
13	3.335	290.000	0.694	35.000	1.000	1.000	1.000
14	3.475	170.000	0.594	40.000	1.000	1.000	1.000
15	3.615	50.000	0.473	45.000	1.000	1.000	1.000
16	3.735	20.000	0.347	47.500	1.000	1.000	1.000
17	3.835	260.000	0.222	50.000	1.000	1.000	1.000
18	3.915	140.000	0.104	52.500	1.000	1.000	1.000
19	3.975	335.000	0.000	55.000	1.000	1.000	1.000
20	3.975	215.000	0.000	55.000	1.000	1.000	1.000
21	3.975	95.000	0.000	55.000	1.000	1.000	1.000

TABLE F-2

PDCWEAR INPUT FILE CONTAINING INITIAL WEAR CONFIGURATION DATA
FOR DEMONSTRATION ANALYSIS (WEARCF.DAT)

1	0.000	0.000	0.0000
2	0.000	0.000	0.0000
3	0.000	0.000	0.0000
4	0.000	0.000	0.0000
5	0.000	0.000	0.0000
6	0.000	0.000	0.0000
7	0.000	0.000	0.0000
8	0.000	0.000	0.0000
9	0.000	0.000	0.0000
10	0.000	0.000	0.0000
11	0.000	0.000	0.0000
12	0.000	0.000	0.0000
13	0.000	0.000	0.0000
14	0.000	0.000	0.0000
15	0.000	0.000	0.0000
16	0.000	0.000	0.0000
17	0.000	0.000	0.0000
18	0.000	0.000	0.0000
19	0.000	0.000	0.0000
20	0.000	0.000	0.0000
21	0.000	0.000	0.0000

TABLE F-3

PDCWEAR INPUT FILE CONTAINING OPERATING CONDITIONS
FOR DEMONSTRATION ANALYSIS (OPCOND.DAT)

SIERRA WHITE GRANITE

1.300				
0.033				
0.070				
0.550				
0.750				
0.1340E+06				
0.420				
0.3260E+06				
0.930				
0.2550E+05				
1.640				
0.2550E+05				
1.640				
0.6890E-12				
100.0				
80.0				
10.0	20.0	30.0	40.0	50.0

APPENDIX G

PARTIAL PDCWEAR OUTPUT LISTING
FOR DEMONSTRATION ANALYSIS

1

*** INPUT DATA *** 21-MAY-87 10:17:37

BIT DESIGN DATA FROM FILE BITDES.DAT :

THERE ARE 21 CUTTERS WITH NOMINAL RADIUS = 0.375 IN.,
NOMINAL BACKRAKE ANGLE = 20.00 DEG.,
AND NOMINAL CONVECTIVE COEFF. = 1700.00 BTU/HR-FT**2-F.

	RADIAL POS. (IN.)	ANG. POS. (DEG.)	LONG. POS. (IN.)	INCL. ANGLE (DEG.)	REL. RADIUS	REL. BACKRAKE ANGLE	REL. CONV. COOLING COEFF.*
1	0.350	0.000	0.625	-15.000	1.000	1.000	1.000
2	0.800	215.000	0.760	-10.000	1.000	1.000	1.000
3	1.250	110.000	0.895	-5.000	1.000	1.000	1.000
4	1.600	45.000	1.000	-2.000	1.000	1.000	1.000
5	1.950	285.000	1.000	0.000	1.000	1.000	1.000
6	2.300	165.000	1.000	2.000	1.000	1.000	1.000
7	2.495	0.000	0.990	5.000	1.000	1.000	1.000
8	2.635	240.000	0.970	10.000	1.000	1.000	1.000
9	2.775	120.000	0.940	15.000	1.000	1.000	1.000
10	2.915	320.000	0.898	20.000	1.000	1.000	1.000
11	3.055	200.000	0.844	25.000	1.000	1.000	1.000
12	3.195	80.000	0.776	30.000	1.000	1.000	1.000
13	3.335	290.000	0.694	35.000	1.000	1.000	1.000
14	3.475	170.000	0.594	40.000	1.000	1.000	1.000
15	3.615	50.000	0.473	45.000	1.000	1.000	1.000
16	3.735	20.000	0.347	47.500	1.000	1.000	1.000
17	3.835	260.000	0.222	50.000	1.000	1.000	1.000
18	3.915	140.000	0.104	52.500	1.000	1.000	1.000
19	3.975	335.000	0.000	55.000	1.000	1.000	1.000
20	3.975	215.000	0.000	55.000	1.000	1.000	1.000
21	3.975	95.000	0.000	55.000	1.000	1.000	1.000

* NEGATIVE VALUE OF RELATIVE COOLING COEFFICIENT
DENOTES TYPE B CUTTER. ALL OTHER CUTTERS ARE TYPE A.

1

INITIAL WEAR CONFIGURATION DATA FROM FILE WEARCF.DAT :

CUTTER	WEARFLAT LENGTH (IN.)	WEARFLAT WIDTH (IN.)	WEARFLAT AREA (IN**2)
1	0.000	0.000	0.0000
2	0.000	0.000	0.0000
3	0.000	0.000	0.0000
4	0.000	0.000	0.0000
5	0.000	0.000	0.0000
6	0.000	0.000	0.0000
7	0.000	0.000	0.0000
8	0.000	0.000	0.0000
9	0.000	0.000	0.0000
10	0.000	0.000	0.0000
11	0.000	0.000	0.0000
12	0.000	0.000	0.0000
13	0.000	0.000	0.0000
14	0.000	0.000	0.0000
15	0.000	0.000	0.0000
16	0.000	0.000	0.0000
17	0.000	0.000	0.0000
18	0.000	0.000	0.0000
19	0.000	0.000	0.0000
20	0.000	0.000	0.0000
21	0.000	0.000	0.0000

1

OPERATING PARAMETER DATA FROM FILE OPCOND.DAT :

ROCK TYPE = SIERRA WHITE GRANITE
ROCK THERMAL CONDUCTIVITY = 1.300 BTU/HR-FT-F
ROCK THERMAL DIFFUSIVITY = 0.033 FT**2/HR
ROCK-CUTTER FRICTION COEFFICIENT = 0.070
WORN CUTTER DRAG COEFFICIENT = 0.550
SHARP CUTTER DRAG COEFFICIENT = 0.750
WORN TYPE A CUTTER CORR. CONSTANT C1 = 0.1340E+06
WORN TYPE A CUTTER CORR. EXPONENT N1 = 0.420
WORN TYPE B CUTTER CORR. CONSTANT C1 = 0.3260E+06
WORN TYPE B CUTTER CORR. EXPONENT N1 = 0.930
SHARP TYPE A CUTTER CORR. CONSTANT C2 = 0.2550E+05
SHARP TYPE A CUTTER CORR. EXPONENT N2 = 1.640
SHARP TYPE B CUTTER CORR. CONSTANT C2 = 0.2550E+05
SHARP TYPE B CUTTER CORR. EXPONENT N2 = 1.640
ABRASIVE WEAR CONSTANT C6 = 0.6890E-12 IN**2/LBF
BIT ROTARY SPEED = 100.0 RPM
DOWNHOLE COOLING FLUID TEMPERATURE = 80.0 F
SPECIFIED BIT PENETRATION RATE(S) = 10.0 FT/HR
20.0
30.0
40.0
50.0

1

*** COMPUTED RESULTS ***

NRAY = 100

GEOMETRY-DEPENDENT RESULTS FOR PENETRATION RATE = 10.00 FT/HR

CUTTER	CUTTING ORDER	CUTTING HEIGHT (IN.)	WEARFLAT LOCATION XBC (IN.)	WEARFLAT LOCATION ZBC (IN.)	CUTTER INCL. ANGLE (DEG.)	CUTTER WEAR ANGLE (DEG.)	VOLUME OF CUT (IN**3/REV)	AREA OF CUT (IN**2)	EFFECTIVE DEPTH OF CUT (IN.)
1	20	0.645	0.205	0.967	-15.000	-23.149	0.0153	0.0099	0.0521
2	8	0.768	0.694	1.104	-10.000	-16.660	0.0405	0.0090	0.0447
3	14	0.909	1.116	1.237	-5.000	-20.358	0.0558	0.0078	0.0390
4	18	1.018	1.544	1.366	-2.000	-8.296	0.0873	0.0089	0.0437
5	4	1.004	1.954	1.357	0.000	0.609	0.0856	0.0070	0.0336
6	11	1.011	2.276	1.363	2.000	-3.241	0.0823	0.0058	0.0290
7	21	1.010	2.525	1.361	5.000	4.965	0.0658	0.0042	0.0232
8	6	0.977	2.707	1.322	10.000	11.550	0.0551	0.0032	0.0198
9	13	0.953	2.869	1.293	15.000	15.392	0.0578	0.0032	0.0197
10	2	0.900	3.036	1.231	20.000	20.014	0.0645	0.0034	0.0203
11	9	0.853	3.204	1.172	25.000	24.940	0.0665	0.0033	0.0200
12	16	0.792	3.366	1.100	30.000	29.108	0.0672	0.0032	0.0195
13	3	0.698	3.531	0.990	35.000	34.019	0.0742	0.0034	0.0201
14	10	0.605	3.700	0.876	40.000	39.773	0.0757	0.0033	0.0197
15	17	0.490	3.866	0.738	45.000	45.281	0.0775	0.0032	0.0195
16	19	0.366	4.005	0.592	47.500	49.702	0.0637	0.0025	0.0167
17	5	0.228	4.123	0.431	50.000	54.162	0.0559	0.0022	0.0150
18	12	0.116	4.213	0.305	52.500	57.064	0.0412	0.0016	0.0122
19	1	0.001	4.304	0.131	55.000	67.023	0.0162	0.0006	0.0087
20	7	0.008	4.302	0.143	55.000	66.192	0.0174	0.0006	0.0093
21	15	0.015	4.306	0.138	55.000	67.883	0.0152	0.0006	0.0081

1

ROCK-DEPENDENT RESULTS FOR PENETRATION RATE = 10.00 FT/HR

CUTTER	VOLUME OF CUT (IN**3/REV)	AREA OF CUT (IN**2)	EFFECTIVE DEPTH OF CUT (IN.)	PENETRATING FORCE (LBF)	DRAG FORCE (LBF)	VERTICAL FORCE (LBF)	RADIAL FORCE (LBF)	WEARFLAT TEMPERATURE (DEG. C)	WEAR RATIO
1	0.0153	0.0099	0.0521	200.6	150.5	-184.5	78.9	26.7	1.00
2	0.0405	0.0090	0.0447	155.8	116.9	-149.3	44.7	26.7	2.62
3	0.0558	0.0078	0.0390	124.5	93.4	-116.7	43.3	26.7	3.37
4	0.0873	0.0089	0.0437	150.3	112.8	-148.8	21.7	26.7	5.64
5	0.0856	0.0070	0.0336	97.8	73.3	-97.8	-1.0	26.7	4.64
6	0.0823	0.0058	0.0290	76.9	57.6	-76.7	4.3	26.7	4.25
7	0.0658	0.0042	0.0232	53.2	39.9	-53.0	-4.6	26.7	3.26
8	0.0551	0.0032	0.0198	41.1	30.8	-40.3	-8.2	26.7	2.70
9	0.0578	0.0032	0.0197	40.8	30.6	-39.4	-10.8	26.7	2.84
10	0.0645	0.0034	0.0203	42.7	32.1	-40.2	-14.6	26.7	3.15
11	0.0665	0.0033	0.0200	41.8	31.3	-37.9	-17.6	26.7	3.25
12	0.0672	0.0032	0.0195	39.9	29.9	-34.9	-19.4	26.7	3.26
13	0.0742	0.0034	0.0201	41.9	31.4	-34.7	-23.4	26.7	3.59
14	0.0757	0.0033	0.0197	40.7	30.5	-31.3	-26.0	26.7	3.66
15	0.0775	0.0032	0.0195	39.9	29.9	-28.1	-28.4	26.7	3.75
16	0.0637	0.0025	0.0167	30.9	23.2	-20.0	-23.6	26.7	3.00
17	0.0559	0.0022	0.0150	25.9	19.4	-15.2	-21.0	26.7	2.59
18	0.0412	0.0016	0.0122	18.5	13.9	-10.1	-15.5	26.7	1.89
19	0.0162	0.0006	0.0087	10.6	8.0	-4.1	-9.8	26.7	1.11
20	0.0174	0.0006	0.0093	11.9	8.9	-4.8	-10.9	26.7	1.24
21	0.0152	0.0006	0.0081	9.5	7.1	-3.6	-8.8	26.7	0.99

1

INTEGRATED FORCES AND MOMENTS FOR THE FULL BIT:

SIERRA WHITE GRANITE AT ROP =	10.0
TOTAL WOB (LBF) =	1171.1
DRILLING TORQ. (FT-LBF) =	159.1
X SIDE FORCE (LBF) =	1.4
Y SIDE FORCE (LBF) =	-109.0
RESULTANT SIDE FORCE (LBF) =	109.0
B. M. ABOUT X-AXIS (FT-LBF) =	15.3
B. M. ABOUT Y-AXIS (FT-LBF) =	-1.2

1

GEOMETRY-DEPENDENT RESULTS FOR PENETRATION RATE = 20.00 FT/HR

CUTTER	CUTTING ORDER	CUTTING HEIGHT (IN.)	WEARFLAT LOCATION XBC (IN.)	WEARFLAT LOCATION ZBC (IN.)	CUTTER INCL. ANGLE (DEG.)	CUTTER WEAR ANGLE (DEG.)	VOLUME OF CUT (IN**3/REV)	AREA OF CUT (IN**2)	EFFECTIVE DEPTH OF CUT (IN.)
1	20	0.665	0.209	0.988	-15.000	-22.557	0.0309	0.0198	0.0708
2	8	0.776	0.694	1.113	-10.000	-16.561	0.0814	0.0180	0.0639
3	14	0.923	1.120	1.252	-5.000	-19.724	0.1129	0.0157	0.0577
4	18	1.035	1.550	1.384	-2.000	-7.433	0.1741	0.0178	0.0632
5	4	1.008	1.959	1.361	0.000	1.249	0.1714	0.0139	0.0523
6	11	1.022	2.282	1.374	2.000	-2.397	0.1639	0.0115	0.0461
7	21	1.030	2.535	1.380	5.000	6.287	0.1362	0.0086	0.0380
8	6	0.983	2.715	1.327	10.000	12.699	0.1102	0.0065	0.0316
9	13	0.967	2.875	1.305	15.000	16.308	0.1114	0.0062	0.0308
10	2	0.902	3.039	1.232	20.000	20.564	0.1325	0.0070	0.0330
11	9	0.862	3.209	1.179	25.000	25.818	0.1325	0.0066	0.0320
12	16	0.807	3.371	1.112	30.000	30.004	0.1315	0.0062	0.0308
13	3	0.702	3.535	0.992	35.000	34.714	0.1503	0.0068	0.0325
14	10	0.615	3.704	0.883	40.000	40.496	0.1507	0.0065	0.0315
15	17	0.507	3.871	0.750	45.000	46.356	0.1586	0.0065	0.0315
16	19	0.385	4.013	0.602	47.500	51.510	0.1230	0.0049	0.0262
17	5	0.233	4.127	0.431	50.000	55.127	0.1115	0.0043	0.0240
18	12	0.128	4.213	0.317	52.500	57.099	0.0732	0.0028	0.0183
19	1	0.003	4.301	0.140	55.000	65.787	0.0344	0.0013	0.0120
20	7	0.016	4.295	0.165	55.000	63.848	0.0403	0.0015	0.0138
21	15	0.029	4.305	0.156	55.000	67.449	0.0303	0.0011	0.0107

1

ROCK-DEPENDENT RESULTS FOR PENETRATION RATE = 20.00 FT/HR

CUTTER	VOLUME OF CUT (IN**3/REV)	AREA OF CUT (IN**2)	EFFECTIVE DEPTH OF CUT (IN.)	PENETRATING FORCE (LBF)	DRAG FORCE (LBF)	VERTICAL FORCE (LBF)	RADIAL FORCE (LBF)	WEARFLAT TEMPERATURE (DEG. C)	WEAR RATIO
1	0.0309	0.0198	0.0708	331.8	248.9	-306.5	127.3	26.7	1.00
2	0.0814	0.0180	0.0639	280.2	210.2	-268.6	79.9	26.7	2.80
3	0.1129	0.0157	0.0577	237.3	178.0	-223.4	80.1	26.7	3.83
4	0.1741	0.0178	0.0632	275.1	206.3	-272.8	35.6	26.7	6.15
5	0.1714	0.0139	0.0523	202.1	151.5	-202.0	-4.4	26.7	5.70
6	0.1639	0.0115	0.0461	164.1	123.0	-163.9	6.9	26.7	5.40
7	0.1362	0.0086	0.0380	119.5	89.7	-118.8	-13.1	26.7	4.37
8	0.1102	0.0065	0.0316	88.4	66.3	-86.3	-19.4	26.7	3.46
9	0.1114	0.0062	0.0308	84.5	63.4	-81.1	-23.7	26.7	3.50
10	0.1325	0.0070	0.0330	94.8	71.1	-88.7	-33.3	26.7	4.15
11	0.1325	0.0066	0.0320	90.2	67.6	-81.2	-39.3	26.7	4.17
12	0.1315	0.0062	0.0308	84.9	63.7	-73.5	-42.5	26.7	4.13
13	0.1503	0.0068	0.0325	92.6	69.5	-76.1	-52.7	26.7	4.72
14	0.1507	0.0065	0.0315	88.1	66.0	-67.0	-57.2	26.7	4.70
15	0.1586	0.0065	0.0315	87.9	65.9	-60.7	-63.6	26.7	4.91
16	0.1230	0.0049	0.0262	64.8	48.6	-40.3	-50.7	26.7	3.75
17	0.1115	0.0043	0.0240	56.4	42.3	-32.2	-46.3	26.7	3.35
18	0.0732	0.0028	0.0183	36.0	27.0	-19.6	-30.2	26.7	2.19
19	0.0344	0.0013	0.0120	18.1	13.6	-7.4	-16.5	26.7	1.12
20	0.0403	0.0015	0.0138	22.7	17.0	-10.0	-20.4	26.7	1.41
21	0.0303	0.0011	0.0107	14.9	11.2	-5.7	-13.8	26.7	0.93

1

INTEGRATED FORCES AND MOMENTS FOR THE FULL BIT:

SIERRA WHITE GRANITE AT ROP = 20.0
TOTAL WOB (LBF) = 2285.8
DRILLING TORQ. (FT-LBF) = 328.4
X SIDE FORCE (LBF) = -5.8
Y SIDE FORCE (LBF) = -179.6
RESULTANT SIDE FORCE (LBF) = 179.6
B. M. ABOUT X-AXIS (FT-LBF) = 21.6
B. M. ABOUT Y-AXIS (FT-LBF) = -3.3

GEOMETRY-DEPENDENT RESULTS FOR PENETRATION RATE = 30.00 FT/HR

CUTTER	CUTTING ORDER	CUTTING HEIGHT (IN.)	WEARFLAT LOCATION XBC (IN.)	WEARFLAT LOCATION ZBC (IN.)	CUTTER INCL. ANGLE (DEG.)	CUTTER WEAR ANGLE (DEG.)	VOLUME OF CUT (IN**3/REV)	AREA OF CUT (IN**2)	EFFECTIVE DEPTH OF CUT (IN.)
1	20	0.685	0.213	1.010	-15.000	-21.959	0.0465	0.0298	0.0893
2	8	0.784	0.697	1.121	-10.000	-16.169	0.1228	0.0271	0.0825
3	14	0.937	1.124	1.267	-5.000	-19.090	0.1714	0.0238	0.0756
4	18	1.053	1.557	1.402	-2.000	-6.463	0.2605	0.0265	0.0812
5	4	1.013	1.961	1.365	0.000	1.593	0.2575	0.0209	0.0695
6	11	1.033	2.290	1.385	2.000	-1.221	0.2446	0.0171	0.0609
7	21	1.050	2.542	1.399	5.000	7.424	0.2109	0.0133	0.0509
8	6	0.990	2.723	1.331	10.000	14.003	0.1650	0.0097	0.0411
9	13	0.980	2.880	1.317	15.000	17.011	0.1610	0.0089	0.0391
10	2	0.905	3.043	1.233	20.000	21.201	0.2039	0.0107	0.0439
11	9	0.871	3.215	1.185	25.000	26.757	0.1981	0.0098	0.0418
12	16	0.823	3.375	1.126	30.000	30.639	0.1931	0.0091	0.0399
13	3	0.706	3.539	0.993	35.000	35.336	0.2280	0.0103	0.0430
14	10	0.626	3.709	0.889	40.000	41.413	0.2252	0.0097	0.0414
15	17	0.525	3.875	0.762	45.000	47.300	0.2423	0.0100	0.0422
16	19	0.404	4.016	0.616	47.500	52.328	0.1790	0.0071	0.0344
17	5	0.239	4.128	0.435	50.000	55.407	0.1668	0.0064	0.0319
18	12	0.141	4.210	0.333	52.500	56.363	0.0931	0.0035	0.0217
19	1	0.004	4.297	0.149	55.000	64.607	0.0554	0.0021	0.0155
20	7	0.024	4.287	0.189	55.000	61.325	0.0719	0.0027	0.0191
21	15	0.044	4.305	0.171	55.000	67.449	0.0452	0.0017	0.0130

1

ROCK-DEPENDENT RESULTS FOR PENETRATION RATE = 30.00 FT/HR

CUTTER	VOLUME OF CUT (IN**3/REV)	AREA OF CUT (IN**2)	EFFECTIVE DEPTH OF CUT (IN.)	PENETRATING FORCE (LBF)	DRAG FORCE (LBF)	VERTICAL FORCE (LBF)	RADIAL FORCE (LBF)	WEARFLAT TEMPERATURE (DEG. C)	WEAR RATIO
1	0.0465	0.0298	0.0893	485.1	363.8	-449.9	181.4	26.7	1.00
2	0.1228	0.0271	0.0825	426.2	319.6	-409.3	118.7	26.7	2.88
3	0.1714	0.0238	0.0756	369.2	276.9	-348.9	120.8	26.7	4.02
4	0.2605	0.0265	0.0812	414.9	311.2	-412.3	46.7	26.7	6.25
5	0.2575	0.0209	0.0695	321.5	241.1	-321.4	-8.9	26.7	6.10
6	0.2446	0.0171	0.0609	258.7	194.0	-258.7	5.5	26.7	5.74
7	0.2109	0.0133	0.0509	192.9	144.7	-191.3	-24.9	26.7	4.75
8	0.1650	0.0097	0.0411	135.9	101.9	-131.8	-32.9	26.7	3.58
9	0.1610	0.0089	0.0391	125.0	93.8	-119.6	-36.6	26.7	3.49
10	0.2039	0.0107	0.0439	151.6	113.7	-141.3	-54.8	26.7	4.47
11	0.1981	0.0098	0.0418	140.0	105.0	-125.0	-63.0	26.7	4.36
12	0.1931	0.0091	0.0399	129.4	97.1	-111.4	-66.0	26.7	4.23
13	0.2280	0.0103	0.0430	146.2	109.7	-119.3	-84.6	26.7	5.01
14	0.2252	0.0097	0.0414	137.8	103.3	-103.3	-91.1	26.7	4.95
15	0.2423	0.0100	0.0422	142.0	106.5	-96.3	-104.3	26.7	5.33
16	0.1790	0.0071	0.0344	101.5	76.1	-62.0	-80.3	26.7	3.95
17	0.1668	0.0064	0.0319	89.5	67.1	-50.8	-73.7	26.7	3.58
18	0.0931	0.0035	0.0217	47.8	35.8	-26.5	-39.8	26.7	1.95
19	0.0554	0.0021	0.0155	27.4	20.5	-11.7	-24.7	26.7	1.14
20	0.0719	0.0027	0.0191	38.7	29.0	-18.6	-33.9	26.7	1.61
21	0.0452	0.0017	0.0130	20.7	15.5	-7.9	-19.1	26.7	0.86

1

INTEGRATED FORCES AND MOMENTS FOR THE FULL BIT:

SIERRA WHITE GRANITE AT ROP = 30.0
TOTAL WOB (LBF) = 3517.3
DRILLING TORQ. (FT-LBF) = 511.4
X SIDE FORCE (LBF) = -11.0
Y SIDE FORCE (LBF) = -275.8
RESULTANT SIDE FORCE (LBF) = 276.0
B. M. ABOUT X-AXIS (FT-LBF) = 27.2
B. M. ABOUT Y-AXIS (FT-LBF) = -2.5

GEOMETRY-DEPENDENT RESULTS FOR PENETRATION RATE = 40.00 FT/HR

CUTTER	CUTTING ORDER	CUTTING HEIGHT (IN.)	WEARFLAT LOCATION XBC (IN.)	WEARFLAT LOCATION ZBC (IN.)	CUTTER INCL. ANGLE (DEG.)	CUTTER WEAR ANGLE (DEG.)	VOLUME OF CUT (IN**3/REV)	AREA OF CUT (IN**2)	EFFECTIVE DEPTH OF CUT (IN.)
1	20	0.705	0.217	1.032	-15.000	-21.355	0.0624	0.0399	0.1075
2	8	0.792	0.698	1.130	-10.000	-16.084	0.1646	0.0362	0.1004
3	14	0.951	1.128	1.283	-5.000	-18.456	0.2314	0.0320	0.0927
4	18	1.070	1.563	1.421	-2.000	-5.535	0.3462	0.0351	0.0983
5	4	1.017	1.966	1.369	0.000	2.288	0.3440	0.0279	0.0852
6	11	1.043	2.296	1.396	2.000	-0.304	0.3244	0.0226	0.0740
7	21	1.070	2.541	1.419	5.000	7.267	0.2863	0.0180	0.0628
8	6	0.997	2.716	1.340	10.000	12.966	0.2177	0.0127	0.0497
9	13	0.993	2.883	1.329	15.000	17.469	0.2116	0.0117	0.0467
10	2	0.907	3.044	1.235	20.000	21.340	0.2781	0.0146	0.0540
11	9	0.880	3.220	1.191	25.000	27.626	0.2631	0.0130	0.0503
12	16	0.838	3.377	1.140	30.000	30.948	0.2522	0.0119	0.0476
13	3	0.710	3.541	0.996	35.000	35.647	0.3073	0.0139	0.0524
14	10	0.636	3.711	0.898	40.000	41.895	0.2992	0.0129	0.0503
15	17	0.542	3.880	0.775	45.000	48.259	0.3282	0.0135	0.0518
16	19	0.423	4.023	0.626	47.500	53.909	0.2319	0.0092	0.0407
17	5	0.244	4.128	0.440	50.000	55.507	0.2216	0.0086	0.0385
18	12	0.153	4.211	0.345	52.500	56.502	0.1093	0.0041	0.0238
19	1	0.006	4.293	0.159	55.000	63.107	0.0795	0.0030	0.0192
20	7	0.032	4.287	0.197	55.000	61.325	0.1040	0.0039	0.0229
21	15	0.059	4.304	0.188	55.000	67.023	0.0600	0.0022	0.0154

1

ROCK-DEPENDENT RESULTS FOR PENETRATION RATE = 40.00 FT/HR

CUTTER	VOLUME OF CUT (IN**3/REV)	AREA OF CUT (IN**2)	EFFECTIVE DEPTH OF CUT (IN.)	PENETRATING FORCE (LBF)	DRAG FORCE (LBF)	VERTICAL FORCE (LBF)	RADIAL FORCE (LBF)	WEARFLAT TEMPERATURE (DEG. C)	WEAR RATIO
1	0.0624	0.0399	0.1075	657.7	493.3	-612.6	239.5	26.7	1.00
2	0.1646	0.0362	0.1004	587.8	440.9	-564.8	162.9	26.7	2.88
3	0.2314	0.0320	0.0927	515.4	386.6	-488.9	163.2	26.7	4.08
4	0.3462	0.0351	0.0983	567.5	425.6	-564.9	54.7	26.7	6.22
5	0.3440	0.0279	0.0852	448.9	336.7	-448.5	-17.9	26.7	6.19
6	0.3244	0.0226	0.0740	356.7	267.5	-356.7	1.9	26.7	5.74
7	0.2863	0.0180	0.0628	272.5	204.4	-270.3	-34.5	26.7	4.86
8	0.2177	0.0127	0.0497	185.6	139.2	-180.9	-41.6	26.7	3.54
9	0.2116	0.0117	0.0467	167.4	125.6	-159.7	-50.3	26.7	3.39
10	0.2781	0.0146	0.0540	212.4	159.3	-197.9	-77.3	26.7	4.54
11	0.2631	0.0130	0.0503	189.0	141.8	-167.5	-87.7	26.7	4.27
12	0.2522	0.0119	0.0476	172.9	129.7	-148.3	-88.9	26.7	4.10
13	0.3073	0.0139	0.0524	202.6	152.0	-164.7	-118.1	26.7	5.03
14	0.2992	0.0129	0.0503	189.1	141.8	-140.7	-126.3	26.7	4.92
15	0.3282	0.0135	0.0518	198.3	148.7	-132.0	-148.0	26.7	5.40
16	0.2319	0.0092	0.0407	133.5	100.1	-78.6	-107.9	26.7	3.77
17	0.2216	0.0086	0.0385	122.1	91.6	-69.1	-100.6	26.7	3.53
18	0.1093	0.0041	0.0238	55.4	41.6	-30.6	-46.2	26.7	1.64
19	0.0795	0.0030	0.0192	39.1	29.3	-17.7	-34.9	26.7	1.18
20	0.1040	0.0039	0.0229	52.2	39.2	-25.1	-45.8	26.7	1.57
21	0.0600	0.0022	0.0154	27.3	20.5	-10.7	-25.1	26.7	0.82

1

INTEGRATED FORCES AND MOMENTS FOR THE FULL BIT:

SIERRA WHITE GRANITE AT ROP = 40.0
TOTAL WOB (LBF) = 4830.2
DRILLING TORQ. (FT-LBF) = 700.9
X SIDE FORCE (LBF) = -22.4
Y SIDE FORCE (LBF) = -385.2
RESULTANT SIDE FORCE (LBF) = 385.8
B. M. ABOUT X-AXIS (FT-LBF) = 32.6
B. M. ABOUT Y-AXIS (FT-LBF) = 0.1

1

GEOMETRY-DEPENDENT RESULTS FOR PENETRATION RATE = 50.00 FT/HR

CUTTER	CUTTING ORDER	CUTTING HEIGHT (IN.)	WEARFLAT LOCATION XBC (IN.)	WEARFLAT LOCATION ZBC (IN.)	CUTTER INCL. ANGLE (DEG.)	CUTTER WEAR ANGLE (DEG.)	VOLUME OF CUT (IN**3/REV)	AREA OF CUT (IN**2)	EFFECTIVE DEPTH OF CUT (IN.)
1	20	0.725	0.223	1.054	-15.000	-20.436	0.0785	0.0500	0.1255
2	8	0.800	0.700	1.138	-10.000	-15.700	0.2070	0.0454	0.1176
3	14	0.964	1.136	1.299	-5.000	-17.283	0.2928	0.0403	0.1092
4	18	1.087	1.567	1.438	-2.000	-4.914	0.4311	0.0436	0.1143
5	4	1.021	1.971	1.373	0.000	2.998	0.4307	0.0349	0.1001
6	11	1.054	2.305	1.407	2.000	0.984	0.4033	0.0281	0.0860
7	21	1.090	2.536	1.440	5.000	6.468	0.3577	0.0224	0.0731
8	6	1.003	2.712	1.347	10.000	12.272	0.2678	0.0157	0.0571
9	13	1.007	2.879	1.344	15.000	16.851	0.2655	0.0147	0.0544
10	2	0.909	3.039	1.239	20.000	20.555	0.3555	0.0186	0.0638
11	9	0.888	3.215	1.203	25.000	26.741	0.3274	0.0162	0.0583
12	16	0.854	3.378	1.155	30.000	31.103	0.3109	0.0147	0.0545
13	3	0.713	3.539	1.001	35.000	35.251	0.3882	0.0175	0.0613
14	10	0.647	3.713	0.906	40.000	42.280	0.3727	0.0160	0.0581
15	17	0.559	3.887	0.783	45.000	49.869	0.4157	0.0171	0.0604
16	19	0.441	4.028	0.638	47.500	55.083	0.2824	0.0112	0.0466
17	5	0.250	4.131	0.442	50.000	56.180	0.2756	0.0107	0.0445
18	12	0.165	4.210	0.358	52.500	56.401	0.1271	0.0048	0.0259
19	1	0.007	4.286	0.174	55.000	60.979	0.1079	0.0040	0.0235
20	7	0.040	4.287	0.205	55.000	61.325	0.1308	0.0049	0.0262
21	15	0.074	4.303	0.205	55.000	66.604	0.0748	0.0028	0.0178

1

ROCK-DEPENDENT RESULTS FOR PENETRATION RATE = 50.00 FT/HR

CUTTER	VOLUME OF CUT (IN**3/REV)	AREA OF CUT (IN**2)	EFFECTIVE DEPTH OF CUT (IN.)	PENETRATING FORCE (LBF)	DRAG FORCE (LBF)	VERTICAL FORCE (LBF)	RADIAL FORCE (LBF)	WEARFLAT TEMPERATURE (DEG. C)	WEAR RATIO
1	0.0785	0.0500	0.1255	847.3	635.5	-794.0	295.8	26.7	1.00
2	0.2070	0.0454	0.1176	762.2	571.7	-733.8	206.3	26.7	2.83
3	0.2928	0.0403	0.1092	674.8	506.1	-644.3	200.5	26.7	4.06
4	0.4311	0.0436	0.1143	727.1	545.3	-724.5	62.3	26.7	6.04
5	0.4307	0.0349	0.1001	585.5	439.2	-584.7	-30.6	26.7	6.11
6	0.4033	0.0281	0.0860	456.6	342.4	-456.5	-7.8	26.7	5.58
7	0.3577	0.0224	0.0731	349.7	262.3	-347.5	-39.4	26.7	4.70
8	0.2678	0.0157	0.0571	233.1	174.9	-227.8	-49.6	26.7	3.35
9	0.2655	0.0147	0.0544	215.3	161.4	-206.0	-62.4	26.7	3.28
10	0.3555	0.0186	0.0638	279.2	209.4	-261.4	-98.0	26.7	4.50
11	0.3274	0.0162	0.0583	241.3	180.9	-215.5	-108.6	26.7	4.11
12	0.3109	0.0147	0.0545	215.8	161.9	-184.8	-111.5	26.7	3.86
13	0.3882	0.0175	0.0613	261.7	196.2	-213.7	-151.0	26.7	4.91
14	0.3727	0.0160	0.0581	239.5	179.6	-177.2	-161.1	26.7	4.71
15	0.4157	0.0171	0.0604	255.6	191.7	-164.7	-195.4	26.7	5.26
16	0.2824	0.0112	0.0466	167.1	125.3	-95.6	-137.0	26.7	3.57
17	0.2756	0.0107	0.0445	154.6	115.9	-86.0	-128.4	26.7	3.38
18	0.1271	0.0048	0.0259	63.7	47.8	-35.3	-53.1	26.7	1.42
19	0.1079	0.0040	0.0235	54.3	40.7	-26.4	-47.5	26.7	1.23
20	0.1308	0.0049	0.0262	64.8	48.6	-31.1	-56.8	26.7	1.47
21	0.0748	0.0028	0.0178	34.3	25.7	-13.6	-31.5	26.7	0.78

1

INTEGRATED FORCES AND MOMENTS FOR THE FULL BIT:

SIERRA WHITE GRANITE AT ROP =	50.0
TOTAL WOB (LBF)	= 6224.4
DRILLING TORQ. (FT-LBF)	= 898.4
X SIDE FORCE (LBF)	= -34.7
Y SIDE FORCE (LBF)	= -496.5
RESULTANT SIDE FORCE (LBF)	= 497.7
B. M. ABOUT X-AXIS (FT-LBF)	= 36.9
B. M. ABOUT Y-AXIS (FT-LBF)	= 3.3

1

INTEGRATED AND SUMMARY DATA FOR THE FULL BIT
AT ALL SPECIFIED PENETRATION RATES * :

SIERRA WHITE GRANITE AT ROP =	10.0	20.0	30.0	40.0	50.0
TOTAL WOB (LBF)	= 1171.1	2285.8	3517.3	4830.2	6224.4
DRILLING TORQ. (FT-LBF)	= 159.1	328.4	511.4	700.9	898.4
X SIDE FORCE (LBF)	= 1.4	-5.8	-11.0	-22.4	-34.7
Y SIDE FORCE (LBF)	= -109.0	-179.6	-275.8	-385.2	-496.5
RESULTANT SIDE FORCE (LBF)	= 109.0	179.6	276.0	385.8	497.7
B. M. ABOUT X-AXIS (FT-LBF)	= 15.3	21.6	27.2	32.6	36.9
B. M. ABOUT Y-AXIS (FT-LBF)	= -1.2	-3.3	-2.5	0.1	3.3
MAX. WEARFLAT TEMP. (DEG. C)	= 26.7	26.7	26.7	26.7	26.7
MAX. WEAR RATIO	= 5.64	6.15	6.25	6.22	6.11

* BIT DESIGN DATA FROM FILE BITDES.DAT
CUTTER WEAR CONFIGURATION FROM FILE WEARCF.DAT
OPERATING PARAMETER DATA FROM FILE OPCOND.DAT

1

***** NEW CUTTER WEAR CONFIGURATION *****

OBTAINED BY SPECIFYING HARD-ROCK WEAR MODE
AND NEW WEARFLAT AREA OF 0.0020
FOR CUTTER NUMBER 21

COMPUTED LENGTH OF HOLE SINCE LAST WEAR CONF. = 61.3 FT
TOTAL LENGTH OF HOLE DRILLED SINCE START = 61.3 FT
(USING ABRASIVE WEAR CONSTANT OF 0.6890E-12)

(THIS CONFIGURATION WAS STORED IN DISK FILE WCB002.DAT)

CUTTER	WEARFLAT LENGTH (IN.)	WEARFLAT WIDTH (IN.)	WEARFLAT AREA (IN**2)
1	0.021	0.147	0.0022
2	0.033	0.182	0.0041
3	0.037	0.194	0.0049
4	0.045	0.212	0.0064
5	0.044	0.211	0.0063
6	0.043	0.208	0.0061
7	0.040	0.200	0.0055
8	0.036	0.190	0.0046
9	0.035	0.189	0.0045
10	0.039	0.198	0.0053
11	0.039	0.197	0.0052
12	0.038	0.196	0.0051
13	0.041	0.203	0.0056
14	0.041	0.202	0.0056
15	0.042	0.205	0.0058
16	0.037	0.193	0.0049
17	0.036	0.190	0.0046
18	0.028	0.168	0.0032
19	0.023	0.151	0.0024
20	0.026	0.162	0.0029
21	0.020	0.143	0.0020

1

*** COMPUTED RESULTS ***

NRAY = 100

GEOMETRY-DEPENDENT RESULTS FOR PENETRATION RATE = 10.00 FT/HR

CUTTER	CUTTING ORDER	CUTTING HEIGHT (IN.)	WEARFLAT LOCATION XBC (IN.)	WEARFLAT LOCATION ZBC (IN.)	CUTTER INCL. ANGLE (DEG.)	CUTTER WEAR ANGLE (DEG.)	VOLUME OF CUT (IN**3/REV)	AREA OF CUT (IN**2)	EFFECTIVE DEPTH OF CUT (IN.)
1	20	0.645	0.208	0.961	-15.000	-23.149	0.0153	0.0099	0.0465
2	8	0.768	0.697	1.094	-10.000	-16.660	0.0405	0.0090	0.0368
3	14	0.909	1.120	1.226	-5.000	-20.358	0.0558	0.0078	0.0305
4	18	1.018	1.546	1.352	-2.000	-8.296	0.0873	0.0089	0.0337
5	4	1.004	1.954	1.342	0.000	0.609	0.0856	0.0070	0.0249
6	11	1.011	2.277	1.349	2.000	-3.241	0.0823	0.0058	0.0212
7	21	1.010	2.538	1.347	5.000	7.073	0.0649	0.0041	0.0163
8	6	0.977	2.701	1.311	10.000	10.963	0.0557	0.0033	0.0138
9	13	0.953	2.866	1.282	15.000	15.493	0.0575	0.0032	0.0135
10	2	0.900	3.029	1.221	20.000	19.574	0.0642	0.0034	0.0138
11	9	0.853	3.196	1.162	25.000	24.615	0.0666	0.0033	0.0137
12	16	0.792	3.358	1.090	30.000	28.765	0.0669	0.0032	0.0132
13	3	0.698	3.520	0.982	35.000	33.225	0.0750	0.0034	0.0137
14	10	0.605	3.686	0.870	40.000	38.614	0.0755	0.0033	0.0134
15	17	0.490	3.852	0.733	45.000	44.376	0.0779	0.0032	0.0131
16	19	0.366	3.996	0.585	47.500	49.722	0.0621	0.0025	0.0110
17	5	0.228	4.113	0.425	50.000	54.113	0.0576	0.0022	0.0099
18	12	0.116	4.198	0.310	52.500	55.213	0.0370	0.0014	0.0073
19	1	0.001	4.294	0.136	55.000	65.787	0.0143	0.0005	0.0051
20	7	0.008	4.287	0.154	55.000	63.848	0.0160	0.0006	0.0058
21	15	0.015	4.300	0.136	55.000	67.883	0.0227	0.0008	0.0058

1

ROCK-DEPENDENT RESULTS FOR PENETRATION RATE = 10.00 FT/HR

CUTTER	VOLUME OF CUT (IN**3/REV)	AREA OF CUT (IN**2)	EFFECTIVE DEPTH OF CUT (IN.)	PENETRATING FORCE (LBF)	DRAG FORCE (LBF)	VERTICAL FORCE (LBF)	RADIAL FORCE (LBF)	WEARFLAT TEMPERATURE (DEG. C)	WEAR RATIO
1	0.0153	0.0099	0.0465	166.3	91.4	-152.9	65.4	26.7	1.00
2	0.0405	0.0090	0.0368	136.0	74.8	-130.2	39.0	44.8	2.74
3	0.0558	0.0078	0.0305	152.9	84.1	-143.4	53.2	54.5	4.95
4	0.0873	0.0089	0.0337	206.9	113.8	-204.7	29.8	69.9	9.25
5	0.0856	0.0070	0.0249	179.6	98.8	-179.6	-1.9	72.1	10.14
6	0.0823	0.0058	0.0212	161.9	89.1	-161.7	9.2	73.6	10.66
7	0.0649	0.0041	0.0163	129.6	71.3	-128.6	-16.0	69.7	9.51
8	0.0557	0.0033	0.0138	102.5	56.4	-100.6	-19.5	65.4	8.00
9	0.0575	0.0032	0.0135	100.0	55.0	-96.4	-26.7	66.6	8.29
10	0.0642	0.0034	0.0138	116.7	64.2	-110.0	-39.1	71.8	10.22
11	0.0666	0.0033	0.0137	114.5	63.0	-104.1	-47.7	73.1	10.57
12	0.0669	0.0032	0.0132	110.8	61.0	-97.2	-53.3	73.8	10.76
13	0.0750	0.0034	0.0137	124.5	68.5	-104.2	-68.2	78.8	12.67
14	0.0755	0.0033	0.0134	122.4	67.3	-95.6	-76.4	79.9	13.04
15	0.0779	0.0032	0.0131	126.7	69.7	-90.5	-88.6	82.4	14.10
16	0.0621	0.0025	0.0110	98.5	54.2	-63.7	-75.1	75.3	11.37
17	0.0576	0.0022	0.0099	89.0	49.0	-52.2	-72.1	72.9	10.59
18	0.0370	0.0014	0.0073	54.9	30.2	-31.3	-45.1	61.3	6.66
19	0.0143	0.0005	0.0051	34.3	18.8	-14.0	-31.2	52.4	4.25
20	0.0160	0.0006	0.0058	44.5	24.5	-19.6	-39.9	56.8	5.51
21	0.0227	0.0008	0.0058	30.7	16.9	-11.6	-28.5	51.7	3.82

1

INTEGRATED FORCES AND MOMENTS FOR THE FULL BIT:

SIERRA WHITE GRANITE AT ROP = 10.0
TOTAL WOB (LBF) = 2092.0
DRILLING TORQ. (FT-LBF) = 282.4
X SIDE FORCE (LBF) = -7.6
Y SIDE FORCE (LBF) = -97.1
RESULTANT SIDE FORCE (LBF) = 97.4
B. M. ABOUT X-AXIS (FT-LBF) = 9.6
B. M. ABOUT Y-AXIS (FT-LBF) = -1.3

GEOMETRY-DEPENDENT RESULTS FOR PENETRATION RATE = 20.00 FT/HR

CUTTER	CUTTING ORDER	CUTTING HEIGHT (IN.)	WEARFLAT LOCATION XBC (IN.)	WEARFLAT LOCATION ZBC (IN.)	CUTTER INCL. ANGLE (DEG.)	CUTTER WEAR ANGLE (DEG.)	VOLUME OF CUT (IN**3/REV)	AREA OF CUT (IN**2)	EFFECTIVE DEPTH OF CUT (IN.)
1	20	0.665	0.212	0.982	-15.000	-22.557	0.0309	0.0198	0.0652
2	8	0.776	0.698	1.103	-10.000	-16.561	0.0814	0.0180	0.0560
3	14	0.923	1.124	1.241	-5.000	-19.724	0.1129	0.0157	0.0492
4	18	1.035	1.552	1.370	-2.000	-7.433	0.1741	0.0178	0.0530
5	4	1.008	1.958	1.346	0.000	1.249	0.1714	0.0139	0.0433
6	11	1.022	2.288	1.360	2.000	-1.504	0.1638	0.0115	0.0375
7	21	1.030	2.542	1.366	5.000	7.669	0.1357	0.0085	0.0297
8	6	0.983	2.707	1.317	10.000	11.930	0.1105	0.0065	0.0244
9	13	0.967	2.872	1.294	15.000	16.273	0.1092	0.0061	0.0231
10	2	0.902	3.033	1.221	20.000	20.263	0.1335	0.0070	0.0255
11	9	0.862	3.201	1.169	25.000	25.397	0.1320	0.0066	0.0242
12	16	0.807	3.362	1.103	30.000	29.543	0.1292	0.0061	0.0229
13	3	0.702	3.524	0.984	35.000	33.979	0.1527	0.0069	0.0249
14	10	0.615	3.688	0.879	40.000	39.064	0.1500	0.0065	0.0238
15	17	0.507	3.858	0.744	45.000	45.617	0.1604	0.0066	0.0240
16	19	0.385	4.002	0.597	47.500	51.050	0.1189	0.0047	0.0189
17	5	0.233	4.112	0.432	50.000	53.758	0.1153	0.0045	0.0180
18	12	0.128	4.199	0.321	52.500	55.450	0.0617	0.0023	0.0111
19	1	0.003	4.287	0.151	55.000	63.475	0.0374	0.0014	0.0089
20	7	0.016	4.280	0.177	55.000	61.325	0.0452	0.0017	0.0105
21	15	0.029	4.298	0.156	55.000	67.023	0.0354	0.0013	0.0077

1

ROCK-DEPENDENT RESULTS FOR PENETRATION RATE = 20.00 FT/HR

CUTTER	VOLUME OF CUT (IN**3/REV)	AREA OF CUT (IN**2)	EFFECTIVE DEPTH OF CUT (IN.)	PENETRATING FORCE (LBF)	DRAG FORCE (LBF)	VERTICAL FORCE (LBF)	RADIAL FORCE (LBF)	WEARFLAT TEMPERATURE (DEG. C)	WEAR RATIO
1	0.0309	0.0198	0.0652	289.6	159.3	-267.4	111.1	26.7	1.00
2	0.0814	0.0180	0.0560	225.6	124.1	-216.2	64.3	26.7	2.57
3	0.1129	0.0157	0.0492	186.9	102.8	-175.9	63.1	60.8	3.43
4	0.1741	0.0178	0.0530	250.2	137.6	-248.1	32.4	79.1	6.33
5	0.1714	0.0139	0.0433	226.6	124.6	-226.5	-4.9	84.1	7.23
6	0.1638	0.0115	0.0375	205.6	113.1	-205.5	5.4	86.5	7.67
7	0.1357	0.0085	0.0297	166.9	91.8	-165.4	-22.3	82.2	6.92
8	0.1105	0.0065	0.0244	130.1	71.5	-127.2	-26.9	75.9	5.74
9	0.1092	0.0061	0.0231	125.1	68.8	-120.1	-35.1	76.6	5.86
10	0.1335	0.0070	0.0255	150.8	83.0	-141.5	-52.2	85.1	7.46
11	0.1320	0.0066	0.0242	145.5	80.0	-131.4	-62.4	85.8	7.59
12	0.1292	0.0061	0.0229	139.8	76.9	-121.6	-68.9	86.1	7.66
13	0.1527	0.0069	0.0249	160.0	88.0	-132.6	-89.4	93.7	9.19
14	0.1500	0.0065	0.0238	155.6	85.6	-120.9	-98.1	94.4	9.36
15	0.1604	0.0066	0.0240	163.3	89.8	-114.2	-116.7	98.6	10.27
16	0.1189	0.0047	0.0189	123.6	68.0	-77.7	-96.2	87.8	8.07
17	0.1153	0.0045	0.0180	114.4	62.9	-67.6	-92.2	86.1	7.67
18	0.0617	0.0023	0.0111	65.3	35.9	-37.1	-53.8	67.9	4.47
19	0.0374	0.0014	0.0089	43.5	23.9	-19.4	-38.9	59.3	3.04
20	0.0452	0.0017	0.0105	56.9	31.3	-27.3	-49.9	65.2	3.97
21	0.0354	0.0013	0.0077	34.8	19.1	-13.6	-32.0	55.0	2.44

1

INTEGRATED FORCES AND MOMENTS FOR THE FULL BIT:

SIERRA WHITE GRANITE AT ROP = 20.0
TOTAL WOB (LBF) = 2757.4
DRILLING TORQ. (FT-LBF) = 359.6
X SIDE FORCE (LBF) = 34.2
Y SIDE FORCE (LBF) = -135.1
RESULTANT SIDE FORCE (LBF) = 139.3
B. M. ABOUT X-AXIS (FT-LBF) = 5.4
B. M. ABOUT Y-AXIS (FT-LBF) = 1.0

1

GEOMETRY-DEPENDENT RESULTS FOR PENETRATION RATE = 30.00 FT/HR

CUTTER	CUTTING ORDER	CUTTING HEIGHT (IN.)	WEARFLAT LOCATION XBC (IN.)	WEARFLAT LOCATION ZBC (IN.)	CUTTER INCL. ANGLE (DEG.)	CUTTER WEAR ANGLE (DEG.)	VOLUME OF CUT (IN**3/REV)	AREA OF CUT (IN**2)	EFFECTIVE DEPTH OF CUT (IN.)
1	20	0.685	0.216	1.004	-15.000	-21.959	0.0465	0.0298	0.0836
2	8	0.784	0.700	1.111	-10.000	-16.169	0.1228	0.0271	0.0745
3	14	0.937	1.128	1.256	-5.000	-19.090	0.1714	0.0238	0.0669
4	18	1.053	1.558	1.388	-2.000	-6.463	0.2605	0.0265	0.0709
5	4	1.013	1.961	1.351	0.000	1.593	0.2575	0.0209	0.0602
6	11	1.033	2.301	1.371	2.000	0.331	0.2446	0.0171	0.0514
7	21	1.050	2.530	1.388	5.000	5.854	0.2112	0.0133	0.0423
8	6	0.990	2.702	1.324	10.000	11.213	0.1623	0.0095	0.0330
9	13	0.980	2.870	1.308	15.000	15.989	0.1603	0.0089	0.0313
10	2	0.905	3.035	1.223	20.000	20.638	0.2051	0.0108	0.0359
11	9	0.871	3.204	1.177	25.000	25.797	0.1967	0.0098	0.0333
12	16	0.823	3.365	1.117	30.000	30.073	0.1890	0.0090	0.0311
13	3	0.706	3.525	0.987	35.000	34.235	0.2308	0.0104	0.0348
14	10	0.626	3.692	0.886	40.000	39.797	0.2228	0.0096	0.0327
15	17	0.525	3.862	0.757	45.000	46.464	0.2465	0.0102	0.0340
16	19	0.404	4.008	0.607	47.500	52.640	0.1703	0.0068	0.0253
17	5	0.239	4.113	0.436	50.000	54.053	0.1728	0.0067	0.0251
18	12	0.141	4.200	0.332	52.500	55.718	0.0821	0.0031	0.0141
19	1	0.004	4.283	0.161	55.000	62.026	0.0642	0.0024	0.0130
20	7	0.024	4.280	0.185	55.000	61.325	0.0743	0.0028	0.0140
21	15	0.044	4.297	0.174	55.000	66.497	0.0504	0.0019	0.0104

1

ROCK-DEPENDENT RESULTS FOR PENETRATION RATE = 30.00 FT/HR

CUTTER	VOLUME OF CUT (IN**3/REV)	AREA OF CUT (IN**2)	EFFECTIVE DEPTH OF CUT (IN.)	PENETRATING FORCE (LBF)	DRAG FORCE (LBF)	VERTICAL FORCE (LBF)	RADIAL FORCE (LBF)	WEARFLAT TEMPERATURE (DEG. C)	WEAR RATIO
1	0.0465	0.0298	0.0836	435.7	239.7	-404.1	162.9	26.7	1.00
2	0.1228	0.0271	0.0745	360.6	198.3	-346.4	100.4	26.7	2.69
3	0.1714	0.0238	0.0669	302.1	166.1	-285.4	98.8	26.7	3.63
4	0.2605	0.0265	0.0709	332.6	182.9	-330.4	37.4	26.7	5.52
5	0.2575	0.0209	0.0602	260.2	143.1	-260.1	-7.2	92.6	5.43
6	0.2446	0.0171	0.0514	234.7	129.1	-234.7	-1.4	95.2	5.75
7	0.2112	0.0133	0.0423	193.5	106.4	-192.5	-19.7	90.8	5.21
8	0.1623	0.0095	0.0330	147.8	81.3	-145.0	-28.7	82.6	4.25
9	0.1603	0.0089	0.0313	142.3	78.3	-136.8	-39.2	83.5	4.35
10	0.2051	0.0108	0.0359	174.3	95.8	-163.1	-61.4	94.2	5.63
11	0.1967	0.0098	0.0333	166.4	91.5	-149.8	-72.4	94.3	5.68
12	0.1890	0.0090	0.0311	158.9	87.4	-137.6	-79.6	94.3	5.69
13	0.2308	0.0104	0.0348	184.0	101.2	-152.1	-103.5	103.8	6.90
14	0.2228	0.0096	0.0327	177.9	97.9	-136.7	-113.9	104.2	6.99
15	0.2465	0.0102	0.0340	189.0	103.9	-130.2	-137.0	109.9	7.77
16	0.1703	0.0068	0.0253	139.8	76.9	-84.8	-111.1	95.9	5.97
17	0.1728	0.0067	0.0251	131.5	72.3	-77.2	-106.5	95.0	5.76
18	0.0821	0.0031	0.0141	72.1	39.7	-40.6	-59.6	72.2	3.23
19	0.0642	0.0024	0.0130	50.9	28.0	-23.9	-44.9	64.8	2.32
20	0.0743	0.0028	0.0140	64.2	35.3	-30.8	-56.3	70.2	2.93
21	0.0504	0.0019	0.0104	39.3	21.6	-15.7	-36.1	58.7	1.80

1

INTEGRATED FORCES AND MOMENTS FOR THE FULL BIT:

SIERRA WHITE GRANITE AT ROP = 30.0
TOTAL WOB (LBF) = 3477.8
DRILLING TORQ. (FT-LBF) = 424.0
X SIDE FORCE (LBF) = 22.3
Y SIDE FORCE (LBF) = -181.7
RESULTANT SIDE FORCE (LBF) = 183.0
B. M. ABOUT X-AXIS (FT-LBF) = 14.9
B. M. ABOUT Y-AXIS (FT-LBF) = -1.5

GEOMETRY-DEPENDENT RESULTS FOR PENETRATION RATE = 40.00 FT/HR

CUTTER	CUTTING ORDER	CUTTING HEIGHT (IN.)	WEARFLAT LOCATION XBC (IN.)	WEARFLAT LOCATION ZBC (IN.)	CUTTER INCL. ANGLE (DEG.)	CUTTER WEAR ANGLE (DEG.)	VOLUME OF CUT (IN**3/REV)	AREA OF CUT (IN**2)	EFFECTIVE DEPTH OF CUT (IN.)
1	20	0.705	0.219	1.025	-15.000	-21.355	0.0624	0.0399	0.1018
2	8	0.792	0.701	1.120	-10.000	-16.084	0.1646	0.0362	0.0923
3	14	0.951	1.132	1.271	-5.000	-18.456	0.2314	0.0320	0.0838
4	18	1.070	1.565	1.406	-2.000	-5.535	0.3462	0.0351	0.0879
5	4	1.017	1.965	1.355	0.000	2.288	0.3440	0.0279	0.0756
6	11	1.043	2.305	1.382	2.000	0.978	0.3243	0.0226	0.0641
7	21	1.070	2.526	1.408	5.000	5.174	0.2814	0.0177	0.0529
8	6	0.997	2.697	1.332	10.000	10.423	0.2143	0.0126	0.0412
9	13	0.993	2.864	1.323	15.000	15.108	0.2145	0.0119	0.0394
10	2	0.907	3.027	1.228	20.000	19.397	0.2804	0.0147	0.0458
11	9	0.880	3.200	1.187	25.000	25.169	0.2588	0.0128	0.0413
12	16	0.838	3.368	1.131	30.000	30.550	0.2490	0.0118	0.0387
13	3	0.710	3.528	0.989	35.000	34.702	0.3096	0.0140	0.0438
14	10	0.636	3.696	0.894	40.000	40.488	0.2956	0.0127	0.0408
15	17	0.542	3.864	0.772	45.000	47.062	0.3356	0.0139	0.0433
16	19	0.423	4.012	0.621	47.500	53.500	0.2191	0.0087	0.0308
17	5	0.244	4.115	0.439	50.000	54.588	0.2267	0.0088	0.0312
18	12	0.153	4.201	0.344	52.500	55.796	0.1049	0.0040	0.0172
19	1	0.006	4.278	0.172	55.000	60.467	0.0938	0.0035	0.0170
20	7	0.032	4.280	0.193	55.000	61.325	0.1004	0.0038	0.0171
21	15	0.059	4.296	0.191	55.000	66.109	0.0657	0.0024	0.0126

1

ROCK-DEPENDENT RESULTS FOR PENETRATION RATE = 40.00 FT/HR

CUTTER	VOLUME OF CUT (IN**3/REV)	AREA OF CUT (IN**2)	EFFECTIVE DEPTH OF CUT (IN.)	PENETRATING FORCE (LBF)	DRAG FORCE (LBF)	VERTICAL FORCE (LBF)	RADIAL FORCE (LBF)	WEARFLAT TEMPERATURE (DEG. C)	WEAR RATIO
1	0.0624	0.0399	0.1018	601.8	331.0	-560.5	219.1	26.7	1.00
2	0.1646	0.0362	0.0923	512.6	281.9	-492.5	142.0	26.7	2.72
3	0.2314	0.0320	0.0838	437.3	240.5	-414.8	138.5	26.7	3.75
4	0.3462	0.0351	0.0879	472.5	259.9	-470.3	45.6	26.7	5.60
5	0.3440	0.0279	0.0756	369.4	203.2	-369.1	-14.7	26.7	5.50
6	0.3243	0.0226	0.0641	281.8	155.0	-281.7	-4.8	26.7	4.92
7	0.2814	0.0177	0.0529	212.6	117.0	-211.8	-19.2	97.1	4.07
8	0.2143	0.0126	0.0412	162.1	89.2	-159.5	-29.3	87.9	3.31
9	0.2145	0.0119	0.0394	156.7	86.2	-151.3	-40.8	89.1	3.40
10	0.2804	0.0147	0.0458	193.1	106.2	-182.1	-64.1	101.4	4.43
11	0.2588	0.0128	0.0413	182.2	100.2	-164.9	-77.5	100.7	4.42
12	0.2490	0.0118	0.0387	174.1	95.8	-150.0	-88.5	100.9	4.44
13	0.3096	0.0140	0.0438	202.7	111.5	-166.6	-115.4	111.7	5.42
14	0.2956	0.0127	0.0408	195.3	107.4	-148.6	-126.8	111.8	5.47
15	0.3356	0.0139	0.0433	209.2	115.1	-142.5	-153.2	118.9	6.12
16	0.2191	0.0087	0.0308	152.0	83.6	-90.4	-122.2	102.0	4.62
17	0.2267	0.0088	0.0312	144.1	79.3	-83.5	-117.5	101.6	4.49
18	0.1049	0.0040	0.0172	78.6	43.2	-44.2	-65.0	76.3	2.50
19	0.0938	0.0035	0.0170	57.0	31.4	-28.1	-49.6	69.4	1.85
20	0.1004	0.0038	0.0171	69.9	38.4	-33.5	-61.3	74.0	2.27
21	0.0657	0.0024	0.0126	42.7	23.5	-17.3	-39.0	61.4	1.39

1

INTEGRATED FORCES AND MOMENTS FOR THE FULL BIT:

SIERRA WHITE GRANITE AT ROP =	40.0
TOTAL WOB (LBF) =	4363.2
DRILLING TORQ. (FT-LBF) =	494.2
X SIDE FORCE (LBF) =	14.2
Y SIDE FORCE (LBF) =	-253.3
RESULTANT SIDE FORCE (LBF) =	253.7
B. M. ABOUT X-AXIS (FT-LBF) =	24.0
B. M. ABOUT Y-AXIS (FT-LBF) =	-0.1

GEOMETRY-DEPENDENT RESULTS FOR PENETRATION RATE = 50.00 FT/HR

CUTTER	CUTTING ORDER	CUTTING HEIGHT (IN.)	WEARFLAT LOCATION XBC (IN.)	WEARFLAT LOCATION ZBC (IN.)	CUTTER INCL. ANGLE (DEG.)	CUTTER WEAR ANGLE (DEG.)	VOLUME OF CUT (IN**3/REV)	AREA OF CUT (IN**2)	EFFECTIVE DEPTH OF CUT (IN.)
1	20	0.725	0.225	1.047	-15.000	-20.436	0.0785	0.0500	0.1198
2	8	0.800	0.703	1.128	-10.000	-15.700	0.2070	0.0454	0.1095
3	14	0.964	1.140	1.288	-5.000	-17.283	0.2928	0.0403	0.1003
4	18	1.087	1.569	1.424	-2.000	-4.914	0.4311	0.0436	0.1038
5	4	1.021	1.970	1.359	0.000	2.998	0.4307	0.0349	0.0904
6	11	1.054	2.305	1.393	2.000	0.984	0.4004	0.0279	0.0762
7	21	1.090	2.520	1.429	5.000	4.313	0.3506	0.0220	0.0627
8	6	1.003	2.694	1.339	10.000	9.974	0.2637	0.0155	0.0484
9	13	1.007	2.861	1.337	15.000	14.600	0.2675	0.0148	0.0468
10	2	0.909	3.026	1.230	20.000	19.149	0.3576	0.0188	0.0554
11	9	0.888	3.196	1.198	25.000	24.547	0.3229	0.0160	0.0491
12	16	0.854	3.365	1.148	30.000	30.014	0.3127	0.0148	0.0462
13	3	0.713	3.530	0.991	35.000	35.002	0.3898	0.0176	0.0524
14	10	0.647	3.696	0.904	40.000	40.622	0.3679	0.0159	0.0484
15	17	0.559	3.867	0.786	45.000	47.573	0.4252	0.0175	0.0521
16	19	0.441	4.016	0.634	47.500	54.658	0.2677	0.0106	0.0360
17	5	0.250	4.112	0.449	50.000	53.811	0.2780	0.0108	0.0369
18	12	0.165	4.196	0.362	52.500	54.653	0.1271	0.0048	0.0201
19	1	0.007	4.273	0.181	55.000	59.131	0.1265	0.0047	0.0212
20	7	0.040	4.280	0.201	55.000	61.325	0.1263	0.0047	0.0202
21	15	0.074	4.295	0.207	55.000	65.912	0.0795	0.0029	0.0146

1

ROCK-DEPENDENT RESULTS FOR PENETRATION RATE = 50.00 FT/HR

CUTTER	VOLUME OF CUT (IN**3/REV)	AREA OF CUT (IN**2)	EFFECTIVE DEPTH OF CUT (IN.)	PENETRATING FORCE (LBF)	DRAG FORCE (LBF)	VERTICAL FORCE (LBF)	RADIAL FORCE (LBF)	WEARFLAT TEMPERATURE (DEG. C)	WEAR RATIO
1	0.0785	0.0500	0.1198	785.2	431.9	-735.8	274.2	26.7	1.00
2	0.2070	0.0454	0.1095	677.9	372.9	-652.7	183.5	26.7	2.70
3	0.2928	0.0403	0.1003	586.9	322.8	-560.4	174.4	26.7	3.78
4	0.4311	0.0436	0.1038	620.9	341.5	-618.6	53.2	26.7	5.51
5	0.4307	0.0349	0.0904	495.4	272.5	-494.7	-25.9	26.7	5.52
6	0.4004	0.0279	0.0762	374.2	205.8	-374.2	-6.4	26.7	4.88
7	0.3506	0.0220	0.0627	271.4	149.3	-270.6	-20.4	26.7	3.87
8	0.2637	0.0155	0.0484	177.4	97.6	-174.7	-30.7	26.7	2.70
9	0.2675	0.0148	0.0468	168.3	92.6	-162.9	-42.4	93.7	2.72
10	0.3576	0.0188	0.0554	221.5	121.8	-209.2	-72.7	26.7	3.79
11	0.3229	0.0160	0.0491	195.9	107.8	-178.2	-81.4	106.2	3.54
12	0.3127	0.0148	0.0462	187.6	103.2	-162.4	-93.8	106.5	3.57
13	0.3898	0.0176	0.0524	218.5	120.2	-179.0	-125.3	118.4	4.36
14	0.3679	0.0159	0.0484	209.7	115.4	-159.2	-136.6	118.1	4.38
15	0.4252	0.0175	0.0521	226.1	124.3	-152.5	-166.9	126.4	4.94
16	0.2677	0.0106	0.0360	162.3	89.3	-93.9	-132.4	107.1	3.69
17	0.2780	0.0108	0.0369	154.7	85.1	-91.3	-124.8	107.0	3.60
18	0.1271	0.0048	0.0201	83.9	46.1	-48.5	-68.4	79.6	1.99
19	0.1265	0.0047	0.0212	62.5	34.4	-32.1	-53.7	73.5	1.51
20	0.1263	0.0047	0.0202	75.0	41.2	-36.0	-65.8	77.5	1.81
21	0.0795	0.0029	0.0146	45.4	25.0	-18.5	-41.4	63.6	1.10

1

INTEGRATED FORCES AND MOMENTS FOR THE FULL BIT:

SIERRA WHITE GRANITE AT ROP = 50.0
TOTAL WOB (LBF) = 5405.5
DRILLING TORQ. (FT-LBF) = 575.2
X SIDE FORCE (LBF) = -3.6
Y SIDE FORCE (LBF) = -340.4
RESULTANT SIDE FORCE (LBF) = 340.4
B. M. ABOUT X-AXIS (FT-LBF) = 33.4
B. M. ABOUT Y-AXIS (FT-LBF) = 2.1

1

INTEGRATED AND SUMMARY DATA FOR THE FULL BIT
AT ALL SPECIFIED PENETRATION RATES • :

SIERRA WHITE GRANITE AT ROP =	10.0	20.0	30.0	40.0	50.0
TOTAL WOB (LBF)	= 2092.0	2757.4	3477.8	4363.2	5405.5
DRILLING TORQ. (FT-LBF)	= 282.4	359.6	424.0	494.2	575.2
X SIDE FORCE (LBF)	= -7.6	34.2	22.3	14.2	-3.6
Y SIDE FORCE (LBF)	= -97.1	-135.1	-181.7	-253.3	-340.4
RESULTANT SIDE FORCE (LBF)	= 97.4	139.3	183.0	253.7	340.4
B. M. ABOUT X-AXIS (FT-LBF)	= 9.6	5.4	14.9	24.0	33.4
B. M. ABOUT Y-AXIS (FT-LBF)	= -1.3	1.0	-1.5	-0.1	2.1
MAX. WEARFLAT TEMP. (DEG. C)	= 82.4	98.6	109.9	118.9	126.4
MAX. WEAR RATIO	= 14.10	10.27	7.77	6.12	5.52

* BIT DESIGN DATA FROM FILE BITDES.DAT
CUTTER WEAR CONFIGURATION FROM FILE WCB002.DAT
OPERATING PARAMETER DATA FROM FILE OPCOND.DAT

1

***** NEW CUTTER WEAR CONFIGURATION *****

OBTAINED BY SPECIFYING HARD-ROCK WEAR MODE
AND NEW WEARFLAT AREA OF 0.0100
FOR CUTTER NUMBER 4

COMPUTED LENGTH OF HOLE SINCE LAST WEAR CONF. = 86.2 FT
TOTAL LENGTH OF HOLE DRILLED SINCE START = 147.6 FT
(USING ABRASIVE WEAR CONSTANT OF 0.6890E-12)

(THIS CONFIGURATION WAS STORED IN DISK FILE WCB010.DAT)

CUTTER	WEARFLAT LENGTH (IN.)	WEARFLAT WIDTH (IN.)	WEARFLAT AREA (IN**2)
1	0.030	0.173	0.0035
2	0.045	0.212	0.0064
3	0.051	0.225	0.0078
4	0.060	0.245	0.0100
5	0.060	0.244	0.0099
6	0.060	0.244	0.0099
7	0.057	0.238	0.0091
8	0.052	0.227	0.0080
9	0.052	0.227	0.0080
10	0.057	0.239	0.0093
11	0.057	0.239	0.0092
12	0.057	0.238	0.0092
13	0.061	0.247	0.0102
14	0.061	0.247	0.0103
15	0.064	0.252	0.0108
16	0.057	0.239	0.0092
17	0.056	0.236	0.0089
18	0.044	0.210	0.0063
19	0.038	0.195	0.0050
20	0.042	0.205	0.0058
21	0.034	0.185	0.0043

DISTRIBUTION

DISTRIBUTION:
DOE/TIC-4500-UC-66c (400)

Thomas Ahrens
Seismological Laboratory 252-21
California Institute of Technology
Pasadena, CA 91125

Tom Anderson
Drilling Fluid Consultants
17726 SW Overlook Ln.
Lake Oswego, OR 97034

Chuji Araki
Geothermal Energy Research &
Development Co., LTD
Kyodo Bldg.
11-7, Kabuto-Cho, Nihonbashi
Chuo-Ku, Tokyo. 103, Japan

C. Arkinson
Imperial College of Science &
Technology
Dept. of Mathematics
Huxley Bldg.
Queen's Gate, London SW7 2BZ
England

Dr. J. J. Azar
Tulsa University Drilling
Research Projects
Petroleum Engineering Dept.
North Campus Drill Bldg.
2450 Marshall
Tulsa, OK 74110

Bill Baker
Smith Tool
P.O. Box C-19511
Irvine, CA 92713

Jerry Baird
Jordan, Apostol, Ritter
Associates, Inc.
Administrative Building 7
Davisville, RI 02854

John Barr
NL Hycalog
15112 Morales Rd.
P.O. Box 60747
Houston, TX 77205

John Barr
NL Hycalog
Oldends Lane
Industrial Estate,
Stonehouse, Gloucester
England GL10 3RQ

Ken Bigelow
Norton Christensen, Inc.
Diamond Technology Center
2532 South 3270 West
Salt Lake City, UT 84119

Ed Bingman
Shell Oil Co.
Two Shell Plaza
P.B. Box 2099
Houston, TX 77001

Alan Black
Drilling Research Laboratory
University Research Park
400 Wakara Way
Salt Lake City, UT 84108

Mike Bockleie
Diamond Technology Center
2532 South 3270 West
Salt Lake City, UT 84119

Gerold R. Boyle
Anco Diamond Composites Corp.
545 5th Ave.
New York, NY 10017

Ben Bradford
Dowell
P.O. Box 2710
Tulsa, OK 74102

Jim Bresee
U.S. Dept. of Energy
Geothermal Technologies Division
Forrestal Bldg., CE-324
1000 Independence Ave., SW
Washington, DC 20585

Kirk Brownell
The Robbins Co.
Box 97027
Kent, WA 98031

John Bunting
US Synthetic Corp.
365 South Mountain Way
Orem UT 84057

Trevor Burgess
Anadrill Schlumberger
200 Macco Blvd.
Sugarland, TX 77478

Dr. Georges Chahine
Tracor Hydronautics, Inc.
7210 Pindell School Rd.
Laurel, MD 20810

Curtis Cheatham
Shell Oil Co.
Two Shell Plaza
P.B. Box 2099
Houston, TX 77001

John Cheatham
Rice University
Mechanical Engineering Dept.
P.O. Box 1892
Houston, TX 77001

Weng-Kwen Chia
Smith Tool Co.
P.O. Box C-19511
Irvine, CA 92713

David Clark
Conoco Production Research
P.O. Box 1267
Ponca City, OK 74603

Dr. Andrew F. Conn
Tracor Hydronautics, Inc.
7210 Pindell School Rd.
Laurel, MD 20810

Craig Cooley
Norton Christensen, Inc.
Diamond Technology Center
2532 South 3270 West
Salt Lake City, UT 84119

George Cooper
Schlumberger Cambridge Research
P.O. Box 153
Cambridge CB2 3BE
England

Jim Combs
Geothermal Resources Int'l., Inc.
1825 S. Grant, Suite 900
San Mateo, CA 94402

Brett Davies
Huddy International
Suite 304
7061 S. University Blvd.
Littleton, CO 80122

Ken Davis
Davis/Hicks Drill Bits
P.O. Box 7906
Midland, TX 79703

Mike Daylong
Magnum Tools, Inc.
230 Bushnell, Suite #3
San Antonio, TX 78212

Mahlon Dennis
Stratabit
600 Kenrick, Suite A1
Houston, TX 77060

Roderic Deyo
Norton Christensen, Inc.
Diamond Technology Center
2532 South 3270 West
Salt Lake City, UT 84119

Larry Diamond
Smith Dyna-Drill
P.O. Box C-19576
Irvine, CA 92713

Benny G. DiBona
Drilling Research Laboratory
University Research Park
400 Wakara Way
Salt Lake City, UT 84108

John Dismukes
Exxon Research & Engineering Co.
Route 22 East
Clinton Township
Annandale, NJ 08801

Harold Doiron
Reed Tool Co.
7000 Hollister, Suite 200
Houston, TX 77040

Jim Dupstadt
Dresser Mining Services
& Equipment Div.
P.O. Box 24647
Dallas, TX 75224

Edward Efsic
Stratabit
600 Kenrick, Suite A1
Houston, TX 77060

Ian Faulkner
CRA Limited
55 Collins St.
Melbourne, Australia 3000

Rubin Feenstra
Shell Research B.V.
Volmerlaan 6
2288 GD Rijswijk ZH
The Netherlands

John E. Fontenot
NL Petroleum Services
P.O. Box 60087
Houston, TX 77205

Scott Forrest
Smith Tool
P.O. Box C-19511
Irvine, CA 92713

James Friant
The Robbins Co.
Box 97027
Kent, WA 98031

Dr. Melvin Friedman
Center for Technophysics
and Dept. of Geology
College Station, TX 77843

Daniel Garcia
Tulsa University Drilling
Research Projects
Petroleum Engineering Dept.
North Campus Drill Bldg.
2450 Marshall
Tulsa, OK 74110

Michel Geradin
Institut de Mecanique
21 Rue E. Solvay
4000 Liege, Belgium

Malcolm Goodman
EnerTech Engineering &
Research Co.
2600 Southwest Freeway
Suite 300
Houston, TX 77098

Beverly Geller
Infoplosion
512 Sunderland Rd.
Teaneck, NJ 07666

George Ghushn
BDM Corp.
16300 Christensen Rd.
Suite 315
Seattle, WA 98188

Louis Hibbs, Jr.
General Electric Co.
P.O. Box 8, Bldg. K-1
Schenectady, NY 12301

Gerold Hebert
Dresser Security
P.O. Box 667
Scott, LA 70583

Washan Ho
NL Industries
3000 North Belt
Houston, TX 77032

Larry Hoberock
Amoco Production Company
Research Center
P.O. Box 591
Tulsa, OK 74102

Dr. Michael Hood
University of California
Dept. of Materials Science &
Minerals Engineering
Berkeley, CA 94720

Stuart Hoenig
Dept. of Electrical Engineering
University of Arizona
Tuscon, AZ 85721

Jessie Holster
Exxon Production Research
P.O. Box 2189
Houston, TX 77001

Hsin Huang
Norton Christensen, Inc.
Diamond Technology Center
2532 South 3270 West
Salt Lake City, UT 84119

Dr. Virgil E. Johnson, Jr.
Tracor Hydronautics, Inc.
7210 Pindell School Rd.
Laurel, MD 20810

Bernard Kear
Exxon Research and Engineering Co.
Clinton Township
Route 22 East
Annandale, NJ 08801

Jim Kingsolver
Smith Tool
P.O. Box C-19511
Irvine, CA 92713

Jack Kolle'
FlowDril Corporation
21414 - 68th Ave. So.
Kent, WA 98032

George A. Kolstad
U.S. Dept. of Energy
Office of Basic Energy Sciences
GPN Bldg., G-226
Washington, DC 20585

Doug Kridler
Valdiamont
3935 Research Park
Ann Arbor, MI 48104

Ergun Kuru
Petroleum Engineering Dept.
Louisiana State University
Baton Rouge, LA 70830

James Langford
Security Division
Dresser Industries
P.O. Box 2467
Dallas, TX 75224

B. J. Livesay
Livesay Consultants
2616 Angell Ave.
San Diego, CA 92122

Harvey E. Mallory
P.O. Box 54696
Tulsa, OK 74155

John Marsh
BDM Corp.
1801 Randolph Rd SE
Albuquerque, NM 87106

Ed Martin
Mobil Research &
Development Corporation
Dallas Research Laboratory
13777 Midway Rd.
Dallas, TX 75224

Steve Mathis
Exxon Production Research
P.O. Box 2189
Houston, TX 77001

Larry Matson
Stratabit
600 Kenrick, Suite A1
Houston, TX 77060

William Maurer
Maurer Engineering, Inc.
10301 NW Freeway
Suite 202
Houston, TX 77018

Alan McFall
NL Petroleum Services
P.O. Box 60087
Houston, TX 77205

Frank McCaffery
Chevron Oil Research
P.O. Box 446
La Habra, CA 90631

John Melaugh
Melaugh Associates, Ltd.
2651 E. 21st St.
Tulsa, OK 74114

Keith Millheim
Amoco Production Company
Research Center
P.O. Box 591
Tulsa, OK 74102

John Minge'
Sohio
4440 Warrensville Ctr. Rd.
Cleveland, OH 44128

Stuart Moffitt
Reed Tool Co.
7000 Hollister, Suite 200
Houston, TX 77040

Roland Mottershead
CRA Limited
55 Collins St.
Melbourne, Australia 3000

Joe Neudecker
Los Alamos National Laboratory
Mail Stop 777
Los Alamos, NM 87545

Robert Nicholson
Well Production Testing, Inc.
P.O. Box 69
Carlsbad, CA 92008

Paul Pastusek
Reed Tool Co.
7000 Hollister, Suite 200
Houston, TX 77040

Gene Polk
P. O. Box 280
Sandia Park, NM 87047

Lew Pratsch
U.S. Dept. of Energy
Geothermal Technologies Division
Forrestal Bldg., CE-324
1000 Independence Ave., SW
Washington, DC 20585

Steve Pye
Union Geothermal Division
Union Oil Co. of California
Union Oil Center
461 S. Boylston
Los Angeles, CA 90017

Robert Radtke
Tracor, Inc.
Deerbrook Plaza
9810 FM 1960 By-pass
Suite 270-K
Humble, TX 77338

Marshall Reed
U.S. Dept. of Energy
Geothermal Technologies Division
Forrestal Bldg., CE-324
1000 Independence Ave., SW
Washington, DC 20585

Troy Reed
Conoco Production Research
P.O. Box 1267
Ponca City, OK 74603

Jim Reichman
FlowDril Corporation
21414 - 68th Ave. So.
Kent, WA 98032

Roger Rinaldi
Resource Technology, Inc.
4555 South Harvard
Tulsa, OK 74135

David Rowley
Drilling Research Laboratory
University Research Park
400 Wakara Way
Salt Lake City, UT 84108

John C. Rowley
Los Alamos National Laboratory
Mail Stop 462
Los Alamos, NM 87545

Bill Schwinkendorf
BDM Corp.
1801 Randolph Rd SE
Albuquerque, NM 87106

Adel Sheshtawy
Tri-Max Corp.
P.O. Drawer 1285
Norman, OK 73070

Bill Short, Jr.
Short Cuts, Inc.
9714 Lanward
Dallas, TX 75238

Alan Sinor
Amoco Production Company
Research Center
P.O. Box 591
Tulsa, OK 74102

David Sitler
GE Specialty Materials
P.O. Box 568
Worthington, OH 43085

Dwight Smith
Halliburton
Drawer 1431
Duncan, OK 73533

David Sommers
University of Missouri-Rolla
Rock Mechanics Facility
Rolla, MO 65401

Steve Southland
Stratabit
600 Kenrick, Suite A1
Houston, TX 77060

Al Sutko
Conoco Production Research
P.O. Box 1267
Ponca City, OK 74603

Malcolm Taylor
NL Hycalog
15112 Morales Rd.
P.O. Box 60747
Houston, TX 77205

George P. Tennyson
DOE/ALO
P.O. Box 5400
Albuquerque, NM 87115

Mike Thigpen
Stratabit
600 Kenrick, Suite A1
Houston, TX 77060

Martin Thompson
Schlumberger Cambridge Research
P.O. Box 153
Cambridge CB2 3BE
England

Tom Turner
Phillips Petroleum Company
Geothermal Operations
655 East 4500 South
Salt Lake City, UT 84107

D. B. Uthus
U.S. Dept. of Energy
Div. of Oil, Gas, and Shale Technology
FE-33
Washington, DC 20545

Bruce Walker
Drilling Research Laboratory
University Research Park
400 Wakara Way
Salt Lake City, UT 84108

Tom Warren
Amoco Production Company
Research Center
P.O. Box 591
Tulsa, OK 74102

Dennis Williams
Specialty Materials Dept.
General Electric Co.
5325 Huntley Rd.
Worthington, OH 43085

1521 C. M. Stone
3141 S. A. Landenberger (5)
3151 W. L. Garner (3)
5267 J. R. Kelsey
6200 V. L. Dugan
6227 A. A. Heckes
6240 R. K. Traeger
6241 J. C. Dunn (15)
6241 J. F. Finger
6242 A. Ortega
6300 R. W. Lynch
6310 T. O. Hunter
6314 J. R. Tillerson
6314 D. A. Glowka (30)
6314 T. E. Hinkebein
7864 D. L. Goodwin
8024 P. W. Dean
9242 L. M. Ford